DOCTOR OF PHILOSOPHY

Development and Evaluation of NI-P-PTFE Based Nano-Composite Coatings for Medical Devices

Gou, Jian

Award date:
2015

Mechanical & Electronic Engineering

School of Science & Engineering

DEVELOPMENT AND EVALUATION OF NI-P-PTFE BASED NANO-COMPOSITE COATINGS FOR MEDICAL DEVICES

Jian Gou

A Thesis Submitted to University of Dundee, in Fulfilment of the Requirements for the Degree of Doctor of Philosophy (Ph.D.)

September 2015

DECLARATION

I hereby declare that the following thesis is of my own composition, that it is a true record of work completed by myself and that it has not previously been accepted for a higher degree at this University or any other institution of learning.

……

Jian Gou

CERTIFICATE

I certify that Jian Gou has performed the research described in this thesis under my supervision and has fulfilled the conditions of the relevant Ordinance and Regulations of the University of Dundee, so that she is qualified to submit for the Degree of Doctor of Philosophy.

……..

Dr. Qi Zhao
Division of Mechanical & Electronic Engineering

ACKNOWLEDGEMENTS

First of all, I would like to express my deepest gratitude to my supervisor Dr. Qi Zhao for his kind guidance, encouragement, suggestions throughout my reseach work. I also would like to thank Dr. Qi Zhao, Prof. Guiling Ning, Prof. Ping Dong and China scholarship council to give me this great opportunity to study in the University of Dundee and give me financial supports.

I would like to thank the technicians in the division of Mechanical Engineering at the University of Dundee for helping me make the sample and maintain laboratory equipment. And I also want to thank my supervisor's research group including Miss Xueju Su, Mr. Wei Song, Mr. Kai Fu, Mr. Chenghuo Shang, Mr Dawei Ren and Mr Shuai Zhang for their help and company.

Finally, I would like to thank my mother and my father. Thanks for their encouragement, support and love during my PhD study in the UK.

Jian Gou

ABSTRACT

Medical device-associated infections and corrosion behaviour of medical devices always impose considerable inconvenience and distress to patients and place a substantial economic burden on health care systems. The aim of this research is to solve this problem by developing a new coating which can reduce bacterial adhesion and slow down the corrosion behaviour efficiently.

In this study, two kinds of Ni-P-PTFE based coatings including Ni-P-PTFE-ZrO_2 and Ni-P-PTFE-ZrO_2-TiO_2 were developed by electroless plating technique. The assays of bacterial adhesion and removal were conducted on nano-composite Ni-P-PTFE-ZrO_2 and Ni-P-PTFE-ZrO_2-TiO_2 coatings to see whether or not they have the capability of effectively resisting bacterial adhesion or reducing adhered bacteria. The anticorrosive properties of these Ni-P-PTFE based coatings were also investigated by electrochemical test.

In the assay of bacterial adhesion and removal, two different bacteria were used including *Escherichia coli* and *Staphylococcus aureus.* The Ni-P-PTFE-ZrO_2 and Ni-P-PTFE-ZrO_2-TiO_2 coatings prepared with the different concentrations of PTFE, ZrO_2 and TiO_2 showed that the concentrations had significant influence on the bacterial adhesion and removal using a dipping process. The effect of surface free energy and its components of the coatings on the performance of bacterial adhesion and removal were also investigated. Extended DLVO theory also explained why some coatings adhered less bacteria than others by analysing total interaction energy between bacteria and the coatings. While in the corrosion test, open circuit potential, polarization resistance (Rp), corrosion current density (Icorr), and corrosion rate (CR) were obtained by measuring the open circuit potential and anodic, cathodic tafel plots of Ni-P-PTFE-ZrO_2 and Ni-P-PTFE-ZrO_2-TiO_2 coatings to evaluate their anticorrosive performances.

In conclusion, the new nano-composite Ni-P-PTFE-ZrO_2 and Ni-P-PTFE-ZrO_2-TiO_2 coatings showed the better capability of resisting bacterial adhesion and reducing adhered bacteria after dipping process than Ni-P and Ni-P-PTFE coatings and also have better anticorrosive property than Ni-P and Ni-P-PTFE coatings. These two new coatings have great potential to be used in the medical device market.

NOMENCLATURE

Latin Letters

A	Hamaker constant, surface area
A_{131}	Hamaker constant between particles 1 across medium 3
A_{132}	Hamaker constant between particle 1 and surface 2 across medium 3
E	Electrical potential
F	Faraday number
F_d	Drag force
G	Gibbs interaction energy
h	Coating thickness
H	Distance
H_0	Minimum equilibrium distance of interaction = 0.157 nm
I	Current density
K	Unit of thermodynamic temperature
k_B	Boltzmann constant
n	The number of electrons
P	Pressure
R	Microbial radius
R_p	Polarization resistance
t	Coating time
T	Temperature

U Dipping speed

V Volume

Greek letters

γ^{AB} Polar or acid-base component of surface free energy

γ^{d} Apolar component of surface free energy

γ^{LW} Lifshitz-van der Waals component of surface free energy

γ^{p} Polar component of surface free energy

γ_s Solid surface energy

γ_{sl} Solid-liquid interfacial energy

γ^{-} Electron-donating parameter of the acid-base component

γ^{+} Electron-accepting parameter of the acid-base component

ε Permittivity, 6.95×10^{-10}

ε_0 Permittivity of vacuum, 8.85×10^{-12}

ε_r Relative permittivity or dielectric constant

θ Contact angle

μ Viscosity

λ Correction length of molecules in a liquid

ζ Zeta potential

π_e Spread pressure

τ_w Shear stress

ρ Fluid or solid density

β_A Anodic Tafel constant

β_C Cathodic Tafel constant

Abbreviation

CFU	Colonies Forming Units
CR	Corrosion rate
DLVO	Derjaguin–Landau–Verwey–Overbeek
mm/a	Millimetre per year
E. coli	Escherichia coli
PTFE	Polytetrafluoroethylene
rpm	Revolutions per minute
S. aureus	Staphylococcus aureus
TSA	Tryptone Soya Agar
TSB	Tryptone Soya Broth

CONTENTS

List of Figures

List of Tables

1 LITERATURE REVIEW

1.1 Medical Device-Associated Problems

1.1.1 Medical Device-Associated Infections

1.1.1.1 Impact of Medical Device-associated Infections

Over the past half century, medical devices and implants have become an indispensable part of the health care system. For example totally internal medical devices such as artificial hip, artificial knee, prosthetic heart valves, intravascular catheters and hearing aids, as well as partially internal medical devices such as dental implants and bone fracture pin have been ubiquitously used. The number of primary arthroplasties is increasing constantly worldwide. By 2030, compared with the number registered in 2005, the estimated number of primary total hip arthroplasties is to reach 572000 with an increase of 174% and the number of primary total knee arthroplasties will reach 3.48 million, an increase of 673% (Montanaro, Speziale et al. 2011). While for the UK, the 7th Annual Report from The National Joint Registry (NJR) for England and Wales show more than 905000 procedures registered, which make the NJR to be the largest registry of its kind in the world and the number of knee replacement was 77545 in 2009, which was recorded on the NJR. (Montanaro, Speziale et al. 2011). For other European country such as Germany, the number of medical devices annually used are over 2.5 million (Mack, Becker et al. 2004). In the United states, the number of urinary catheters annually used in the USA is about 23 million and approximately 25% of patients need the insertion of a urinary catheter during their treatment in the hospital (Chaiban, Hanna et al. 2005). High market demand for medical devices and advances in the manufacture of synthetic biomaterials contribute to the explosive growth in

the value of the biomaterial market which is more than $300 billion US dollars and the rate of increase is predicted to be 20% per year (Simchi, Tamjid et al. 2011).

Unfortunately, insertion or implantation of medical devices into the body is always associated with a significant risk of foreign body-related infections such as local infections and bloodstream infections (von Eiff, Jansen et al. 2005). For local infections, although orthopedic implants have a relatively lower risk of bacterial infection, for instance, the infection rate after total joint replacement surgery is predicted to be in the range of 0.5-5%, the consequences are still very serious because the number of patients with such orthopaedic implants is enormous (Campoccia, Montanaro et al. 2006). For severe infections of such orthopaedic implants, the surgical debridement with retention of implants and chemotherapy with full spectrum antibiotics sometimes are not effective enough to resolve infection issues. Implant removal and replacement may have been the last option to eradicate severe infections, and one single occurrence of infected arthroplasty is estimated to cost over $50000 and the rate of recidivation and implant replacement is also up to 10% (Campoccia, Montanaro et al. 2006). Compared with total joint replacement, the infection rate of the use of external fixators such as bone fracture fixation pins is much higher than the total joint replacement. It has been reported that the infection rate of pin tract infection range from 11-100% (Sims and Saleh 2000, Schalamon, Petnehazy et al. 2007), although the criteria for the diagnosis of pin tract infection are different. It is very painful and distressing for patients when they suffer from repeated infections, and once the bone (osteomyelitis) is infected, it is almost impossible to eradicate infections and threatens the success of the treatment (Campoccia, Montanaro et al. 2006). Compared with local infections, catheter-related bloodstream infections are also a significant problem in both developing and developed countries. More than 500000 catheter-related bloodstream infections occur each year

in the USA and the attributable mortality rate is up to 25% and the related extra cost is roughly $28000 per case(Charville, Hetrick et al. 2008). Besides, according to a report of The International Nosocomial Infection Control Consortium (INICC) which collects the data from 43 countries including 503 intensive care units in Latin America, Asia, Africa and Europe from January2007 to December 2012, the pooled rates of catheter-related bloodstream infections is 4.9 per 1000 central line-days. And the extra cost per infection is an estimated $4888 to $11591(Chen, Dai et al. 2014, Rosenthal, Maki et al. 2014). Overall, although medical devices are widely used to restore the quality of life, medical device-associated infections impose considerable inconvenience and distress to patients and place a substantial economic burden on health care systems.

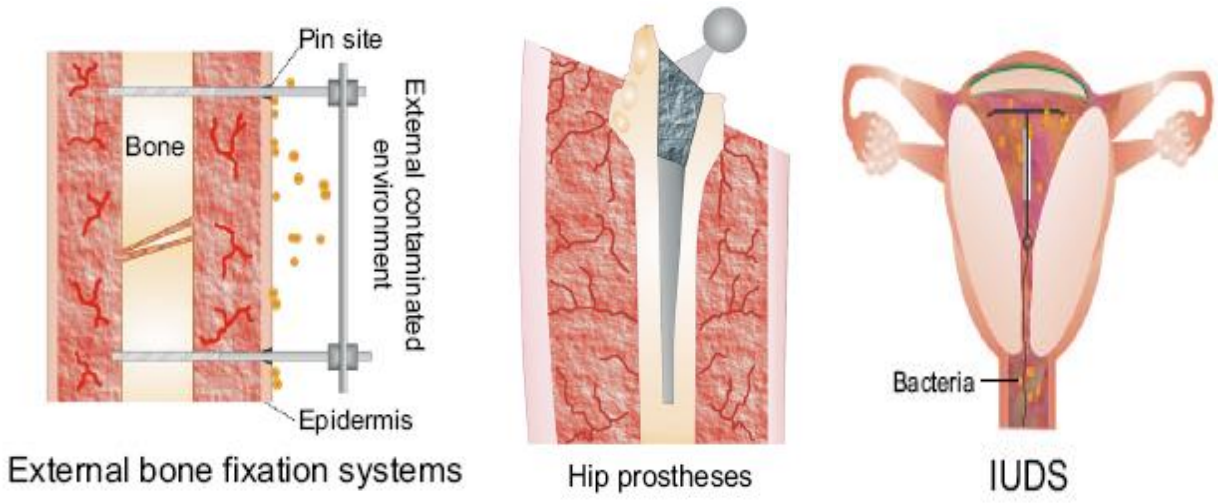

Figure 1. 1 Examples of medical devices with different anatomic location (Davide and Carla 2013)

1.1.1.2 Pathogenesis of Medical Device-associated Infection

Bacteria are usually considered a ubiquitous life form existing in the world. And there are two types of bacterial living states: planktonic and sessile (Ubbink and Schär-Zammaretti 2007, Garrett, Bhakoo et al. 2008). It is widely accepted that bacteria are more likely to attach to the solid surface in contact with liquids as a sessile population, and it is estimated that the number of bacteria in terms of sessile populations is 1000 to 10000 times larger than planktonic ones in any given environment (Davies 2000).

Bacterial attachment to the surface will lead to the formation of biofilms. Inappropriate formation of biofilms causes a lot of problems, for example, biofilms lead to pipe corrosion and blockage of filtration equipment in the oil industry, while for hospital-related infection especially those related to medical devices or implantations, bacterial adhesion onto the surface and subsequent formation of a biofilm can lead to the failure of surgery or implantation of medical devices(Walker and Marsh 2004, Garrett, Bhakoo et al. 2008, Xu and Siedlecki 2012).

Implanting medical devices into the body will lead to an increased susceptibility to infections. It was reported by Elek and Conen in 1957 that patients with suture can be infected by 10^4 times fewer bacteria than those without suture (Elek and Conen 1957, Daghighi, Sjollema et al. 2013). Normally, bacteria such as *S. aureus*, easily found in the nasopharynx and on our skin, are obstructed by mucous membranes and the skin, and rarely cause infection (Harris and Richards 2006). However, when these barriers are breached due to surgery or insertion of medical devices into the body, these bacteria have the opportunity to enter the underlying tissue to attach to the foreign body. Once bacteria adhere on the surface of a foreign body, they have the capability of forming a thick and multi-layered biofilm leading to the medical device-associated infection (Simões, Simões et al. 2010).

The contamination sources mostly come from small numbers of bacteria from the patient's skin or mucous membranes during the surgical implantation of the medical device. Sometimes bacteria from the clinical staff or contaminated surgical equipment also contribute to the medical device-associated infections. *E.coli*, *staphylococci*, *Pseudomonas aeruginosa* and *Candida species* are diagnosed to be common bacteria, particularly *Staphylococci* is considered to be a major organism associated with medical device-associated infections(Katsikogianni and Missirlis 2004, von Eiff, Jansen et al. 2005). Overall the medical device associated infections increase public concern and drive many researches and investigations with respect to pathogenic mechanism, promoting a further understanding of the process of bacterial adhesion and formation of biofilm.

1.1.1.2.1 Bacterial Attachment to the Surface of Medical Devices

Figure 1.3 shows processes of biofilm formation. And bacterial attachment is a significant step in the pathogenesis of medical device-associated infections. However, it is still elusive to elucidate the mechanism with respect to bacterial attachment to a surface. And the dominating factors involved are also quite complex because the effect of the surface properties of the bacteria, and the physical and chemical properties of implants on bacterial attachment to medical devices is enormous(Abu-Lail and Camesano 2006).

Generally, bacteria in terms of planktonic are firstly transported to the surface of medical devices by physical forces such as Brownian motion, van der Waals attraction forces, surface electrostatic force, hydrophobic interactions, diffusion, sedimentation due to gravitational force and convective mass transport or by bacterial appendages such as flagella. These physical

interactions can be further categorized as long-range interactions and short-range interactions (An and Friedman 1998, Katsikogianni and Missirlis 2004, Garrett, Bhakoo et al. 2008).

The long-range interactions happen when a bacteria penetrates the hydrodynamic boundary layer into an overall non-specific attraction area where the distances between bacteria and surfaces are about 20 nm, and van der Waals forces of attraction and electrostatic repulsion begin to interplay (An and Friedman 1998, Katsikogianni and Missirlis 2004). Due to most of substratum and bacteria being negatively charged, with distances between bacteria and substratum being closer, electrostatic repulsion forces as a function of distance dominate the interactions which prevent bacteria approaching to the substratum (Walker and Marsh 2004). At this stage, all the interactions are weak and reversible, which means the bacteria can still exhibit Brownian motion and can be removed very easily by their own motility or fluid shear forces (Marshall 1986).

Subsequently, when the distances between bacteria and substratum surface come into less than 5 nm, the various short-range interactions become effective, such as hydrogen bonding, ionic and dipole interactions and hydrophobic interactions (Katsikogianni and Missirlis 2004, Palmer, Flint et al. 2007). The weak and reversible attachment becomes much stronger and irreversible. In the transition of bacterial reversible attachment to irreversible attachment, the surface structures of the bacterial cell begin to play a role on specific interaction between bacteria and substratum. For instance, bacterial nanofibers, such as Pili and flagella as typical cell appendages with lengths from hundreds of nanometers to several micrometers and diameters from several nanometers to tens of nanometers could tether a bacteria body to substratum by piercing the energy barrier due to their small radii, which will be described later in the XDLVO theory (Garrett, Bhakoo et al. 2008). In addition, surface-associated proteins also mediate the bacterial initial attachment to the

substratum. For example, SSP-1 and SSP-2, as *Staphylococcal* surface proteins, existing on fimbria-like appendages were reported to be involved in bacterial initial adhesion (Veenstra, Cremers et al. 1996). Bap also play an important role not only in intercellular adhesion and biofilm formation, but also in the initial attachment of *S. aureus* to an abiotic surface (Cucarella, Solano et al. 2001). Aside from proteins, polysaccharides such as lipopolysaccharide and exo-polysaccharides also have a function for bridging between the cell and substratum (Walker and Marsh 2004, Hori and Matsumoto 2010).

Actually, bacterial adhesion is a more complicated process. Apart from the fact that the direct interaction between bacteria and naked surface of the medical device plays a significant role in the early age of bacterial adhesion, there are also other important factors such as environmental factors, which also affect bacterial adhesion. For example, when a medical device is implanted into a human body and exposed to physiological fluids, it will be covered quickly with serum and connective tissue proteins such as fibronectin, fibrinogen, laminin, collagen and so on, which may be considered as specific receptors for colonising bacteria (von Eiff, Jansen et al. 2005, Campoccia, Montanaro et al. 2013). And these host proteins not only mediate bacterial adhesion by binding to substratum and altering the physicochemical property of foreign body surface, but also interact with bacterial adhesins which were described as ”microbial surface components recognizing adhesive matrix molecules”(MSCRAMMAs) anchored to the cell wall (Montanaro, Speziale et al. 2011, Campoccia, Montanaro et al. 2013). For example, Fibronectin is recognized for its capability of mediating the bacterial adhesion of *S. aureus* to the surface of medical devices due to the specific interaction between receptorial proteins possessed by S. aureus and host protein. This specific ligand- and receptor- like interaction changes the surface

physicochemical characteristics of bacteria and eventually promotes *S. aureus* adhesion to substratum (An and Friedman 1998, Montanaro, Speziale et al. 2011).

1.1.1.2.2 Formation of Biofilm

Once bacteria initially adhere to the surface of the foreign body, the cell proliferation and intercellular adhesion are involved (von Eiff, Jansen et al. 2005), which is also described as exponential growth phase. The number of bacteria dispersed over the surface increase rapidly, and these adhered bacteria spread outward and upward from the attachment point to develop into a mature and complex biofilm (Garrett, Bhakoo et al. 2008).

In general, there are several bacterial behaviours contributing to development of biofilm. First of all, the redistribution of attached bacteria by surface motility is one of the important factors in developing biofilms. For instance, for Gram-negative bacteria such as *Pseudomonas aeruginosa* and *Escherichia coli,* flagella and pili both play an important role in bacterial surface colonization (Hall-Stoodley and Stoodley 2002). However, for non-motile bacteria such as staphylococci, surface motility is not prerequisite to form biofilm. In *S. epidermidis*, excretion of polysaccharide intercellular adhesin (PIA) is responsible for intercellular adhesion, and *Bap,* as a biofilm-associated protein, was also detected to enhance intercellular adhesion and accumulation in multilayered cell clusters for *Staphylococcus aureus* (Cucarella, Solano et al. 2001, Hall-Stoodley and Stoodley 2002).

In addition, binary division of attached bacteria has an enormous effect on microcolony formation, which is described as a formation of discrete cell clusters. Most of these microcolonies are arranged in a horizontal mode in the biofilms, but they may also form vertical arrays (Garrett, Bhakoo et al. 2008) and when these microcolonies grow in size and hold together,

it is called macrocolonies. There are two types of structures of macrocolonies, one of which consists of mushroom-like towers contributing to the penetration of nutrients to bacteria deep within a biofilm (Garrett, Bhakoo et al. 2008). Another structure, flat structure, is also one of the basic structures in the biofilm. In the process of the formation of macrocolonies, extracellular polymeric substances (EPS) will be responsible for binding cells within macrocolonies and extracelluar DNA and dead cell debris also exist in these macrocolonies (Monds and O'Toole 2009, Percival, Malic et al. 2011). Figure show the whole process of biofilm formation:

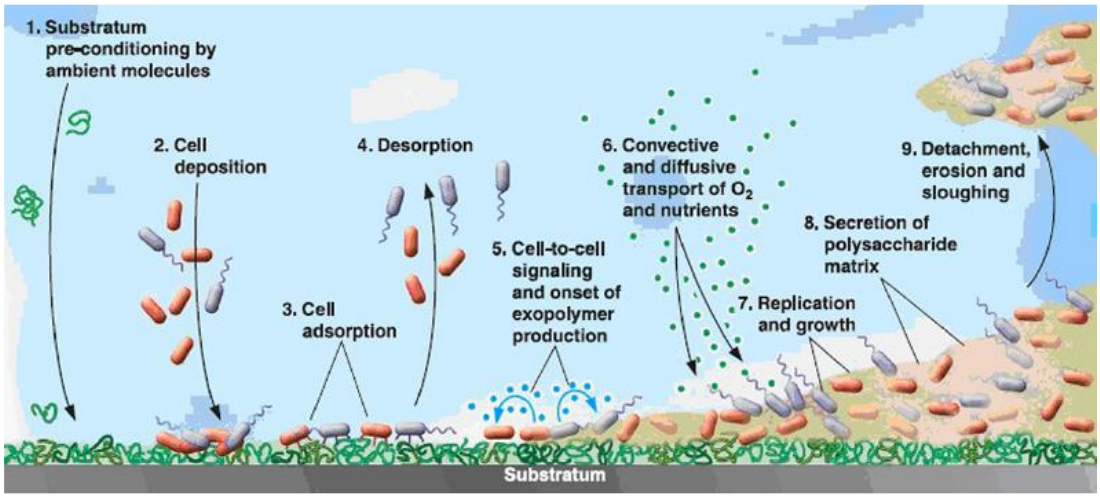

Figure 1. 2 Developmental model of biofilm formation (Breyers and Ratner 2004)

The bacteria in the microcolonies show distinct gene expression compared with planktonic counterparts, and it has been reported that once bacteria come into contact with a surface, the gene expression will be regulated (Walker and Marsh 2004). For example, extracellular polymeric substances (EPS) including polysaccharide, nucleic acids, lipids and proteins are excreted by Bacterial cells in biofilm microcolonies (Tsuneda, Aikawa et al. 2004).This slime-like matrix accounting for 50–90% of the total organic carbon of the biofilm(Walker and Marsh 2004) not only is responsible for cohesion of bacteria and bacterial adhesion to substratum but

also acts as a barrier to protect microorganisms in the biofilm against adverse conditions (Simões, Simões et al. 2010). 75-89% of the biofilm EPS composition consists of proteins and polysaccharides (Simões, Simões et al. 2010), and polysaccharides, as a best-studied component of EPS, has a significant role in maintaining the mechanical stability of biofilm (Hall-Stoodley and Stoodley 2002, Simões, Simões et al. 2010).

Besides, quorum sensing plays an important role in biofilm development (von Eiff, Jansen et al. 2005). Bacteria are considered to have the ability to sense and respond to changing environments by modulating gene expression to adapt to external environments. Quorum sensing, as an intercellular signalling, is normally associated with a range of important microbial activities based on auto-induction (Simões, Simões et al. 2010), such as the regulation of virulence factors, EPS synthesis and development of complex mushroom structures (Hall-Stoodley and Stoodley 2002, Simões, Simões et al. 2010). For example, in *S. aureus* the quorum sensing system, the accessory gene regulator (agr) locus, was activated during the transition from exponential growth phase to the stationary growth phase, which contributes to the biofim-associated infections (von Eiff, Jansen et al. 2005). In addition, when medical devices are implanted into different positions in human bodies, the environmental condition of the implantations is different, including the PH values, temperature and hydrodynamics. And the quorum sensing of the biofilm system will make a corresponding adjustment according to the specific implanted conditions which lead to the diversity in the real biofilm development (Garrett, Bhakoo et al. 2008, Campoccia, Montanaro et al. 2013).

Finally, with the formation of mature biofilm, individual cells may detach and macrocolonies may dissolve from biofilm due to nutrient depletion, shear force, quorum sensing and so on. And

the detached bacteria return to the planktonic phase and begin a new developmental cycle (Walker and Marsh 2004, Monds and O'Toole 2009).

Overall, the bacterial adhesion, growth and final formation of biofilm on the implanted surface play a significant role in medical devices-associated infections. Once a mature biofilm is established, the host defence mechanisms usually seem to have no capability of eliminating the bacteria from the infected medical devices due to the protection of biofilm (von Eiff, Jansen et al. 2005, Campoccia, Montanaro et al. 2010). And it has been reported that the bacteria within biofilm are up to 1000 times more tolerant to antibiotics treatment in contrast to planktonic bacteria (Song, Kong et al. 2011).

1.1.2 Medical Device Corrosion

1.1.2.1 Problem of Medical Device Tribocorrosion

Corrosion is a ubiquitous process that has an enormous effect on almost every aspect of our lives from petrochemical plants in the field of petroleum industry, infrastructures such as bridges and buildings (Shipilov and Le May 2006, Kelley and Untereker 2013) to human beings ourselves. For example, the teeth of human beings suffer from mechanical wear and corrosion (Barbour and Rees 2005), and it is very easy to find out that surface destruction and erosion of natural teeth are very common among elderly people. Besides, long period and extensive abrasion and wear of hip joints or knee joints in the presence of potentially corrosive body fluids (Ryu and Shrotriya 2013) also lead to damage of the joint especially for athletes and elderly people. Therefore, on the one hand, medical devices can make a great contribution to replacing those damaged natural organs such as a hip joint or teeth and so on to maintain the quality of lives of human beings (Ratner, Hoffman et al. 2004, Yan, Neville et al. 2010). However, on the other hand, these implanted

medical devices can also suffer from the same wear and corrosion issues as natural teeth or knees do (Ratner, Hoffman et al. 2004, Pezzotti and Yamamoto 2014).

In the field of medical devices, tribocorrosion is one of the most important properties of medical device coatings in aspects of tribology and corrosion resistance (Mathew, Kerwell et al. 2014). The tribology of implanted medical devices in human bodies is affected by many factors such as the load, frequency and the surface property of the medical devices that are in touch, while for corrosion, it is an electrochemical response for medical devices which are implanted into human bodies and surrounded by local tissues and body fluids (Mathew, Kerwell et al. 2014). Tribocorrosion research draws increasing attention from scientists and engineers, especially for development of orthopaedic, oral, maxillofacial implantable medical devices such as dental implants, maxillomandibular fixation plates and screws, total hip joint replacement, knee joint replacement and so on, all of which suffer more from mechanical wear and body fluids corrosion (Ingham and Fisher 2000, Mercuri 2007, Huber, Reinisch et al. 2009, Meslemani and Kellman 2012, Mathew, Kerwell et al. 2014).

The effect of the tribocorrosion of medical devices in human bodies is enormous. The corrosion process of medical devices in body fluids and mechanical movements of implants against each other will lead to the release of metal ions or some particles from the medical devices. This will cause adverse tissue responses and postimplantation complications such as inflammation, necrosis, and osteolysis (Ryu and Shrotriya 2013), which is another main reason to lead to the failure of implantation of medical devices.

Like contact allergy in our daily life, there are about 4000 substances listed and proven to cause contact allergy, and 15-20 percent of the population of Europe have to take care of at least one allergen (Reclaru, Ziegenhagen et al. 2014). Similar to contact allergy, most people are also

sensitive to the released metal ions or particulate debris in the body, and the reason is that the released metal ions or particulate debris will lead to many adverse physiological effects, such as cytotoxicity, genotoxicity, metal sensitivity and so on (Sargeant and Goswami 2006, Sargeant and Goswami 2007, Valero Vidal and Igual Muñoz 2013), especially when the metals have several valences. For example, the metal ions such as Fe^{3+}, $Co^{2+,}$ Cr^{3+}can interact with albumin to form the metal-binding protein. A typical example of tribocorrosive phenomena in the oral environment is associated with dental implants. In dentistry, titanium material is one of the favourite candidates as dental implants and it has been found to release titanium particles around the gingival sulcus and peri-implant tissues due to the process of corrosion and wear which may lead to bone resorption (Abey, Mathew et al. 2011, Mathew, Abbey et al. 2012, Mathew, Kerwell et al. 2014).

Furthermore, the release of metal ions also has an effect on cells which is far from the releasing location where medical devices are implanted through body fluids transportation (Valero Vidal and Igual Muñoz 2013). For instance, when a hip prosthesis is implanted into a human body, releasing metallic components and ions from the hip prosthesis not only lead to the increase of the metal ions near implants which induce metallosis such as the black coloration of the surrounding tissue (Rocha, Oliveira et al. 2013), but they can also be detected in other organs such as kidney, liver and body fluids, which is harmful for the host health condition (Urban, Jacobs et al. 2000).

Besides, the corrosion and mechanical wear also will lead to the reduction of the mechanical strength of medical devices (Ryu and Shrotriya 2013), especially those which have to bear the weight of the human body such as a total hip joint.

Last but not least, one of the neglected reasons leading to the failure of the implantation of medical devices is the welds corrosion. Usually, more attention will be paid to the anticorrosive property of the bulk coatings; however, weld corrosion is more susceptible to the failure of implantations, because compounds in weld zones are complex and components in this zone are usually different from these in bulk coatings. For some anticorrosive coatings, metal oxide film acts as an efficient protective layer against corrosion behaviours. However, sometimes the metal oxide protective film cannot be formed in a weld zone due to an inert gas protection during the welding process, which means that although bulk coatings have excellent anticorrosive properties, the corrosion rate of weld zones may be much higher than that of bulk coatings. And a rapid corrosion rate can lead to the damage of the medical device. For example, the working life of an implanted pacemaker, whose coating is usually considered to be 250 μm thick, is expected to be 10 to 20 years. However, if the corrosion rate is as high as 12.5 μm/year, then this pacemaker will be out of order quickly and threaten people's life. Overall, the qualified coatings of medical devices need to meet great corrosion resistance and great mechanical properties (Kelley and Untereker 2013).

1.1.2.2 Mechanism of Corrosion

Corrosion is an oxidative process, a physicochemical interaction between the material and the environment it is surrounded by. The oxidative process means the material will lose electrons to become a new chemical compound, and according to the physical law, the electric quantity should be balanced in a whole system, which means that there is also a reduction reaction as a corresponding interaction (Kelley and Untereker 2013). And this is the essence of the corrosion process. Every electrochemical corrosion cell must have four basic components: 1, the anode, where the materials are corroded, 2, the cathode, which provides the sites for the reduction

reaction, 3, the electrolyte for the ionic conduction, 4, the electrical connection between the anode and the cathode to allow electrons to flow between them.

There are many forms of corrosion, such as uniform corrosion, galvanic corrosion, pitting corrosion, crevice corrosion and so on. Uniform corrosion, as a prevalent corrosion, is defined as a uniform, regular erosion of metal on the surface, which means the corrosive environment should corrode all parts of exposed surfaces and the surface itself should be compositionally uniform. The equipment found in chemical industries usually suffer from uniform corrosion, especially when it is exposed to atmospheric conditions or acid conditions. Compared with uniform corrosion, another corrosion is termed as pitting corrosion. Pitting corrosion is a localized non-uniform corrosion and it is unpredictable in comparison with uniform corrosion. Pitting corrosion is usually observed as a tiny spot, and these deep pits sometimes can isolate the transport between the bulk solution and the liquid in the pit, which will accelerate the corrosion rate and the high ratio of pits in the coatings can cause significant change of mechanical strength of the material and material penetration. Galvanic corrosion is a kind of corrosion which does not depend on the traditional oxidant (O_2) as a driving force to induce the corrosion behaviour as uniform corrosion and pitting corrosion do. When any two different metals with different corrosion potentials E_{corr} are coupled in the presence of a corrosive electrolyte, the corrosion will happen at the more positive one. That explains why the corrosion phenomena preferentially happen near the weld where two dissimilar metals are connected.

Every corrosion behaviour can be explained by thermodynamics. The principal driving force of corrosion behaviours is the change of Gibbs energy ΔG, which means that the products that the material and environment produce will lead to the alteration of Gibbs energy ΔG. and, if the reaction is spontaneous, ΔG for the process must be negative, which means Gibbs energy in the

final state of the reaction should be lower than that in the initial state after corrosion behaviours. And there is a fundamental relationship between ΔG and electrochemical potential E^{0}_{cell} which is(Sørensen, Kiil et al. 2009):

$$\Delta G = -n \cdot F \cdot E^{0}_{Cell} \quad (1)$$

$$E^{0}_{Cell} = E^{0}_{Ox} + E^{0}_{Red} \quad (2)$$

Where n is the number of electrons exchanged in the reaction and F is a Faradays constant. E is overall electrical equilibrium potential and the negative (-) in the equation (1) means that overall electrical equilibrium potential E has a negative effect on the change of Gibbs energy ΔG and E is determined by two standard potentials of anodic and cathodic half-cell reaction in the process of corrosion.

Therefore, according to the potential of anodic and cathodic half-cell reaction, we can calculate the total change of Gibbs energy ΔG. For example, if the overall electrical equilibrium potential E^{0}_{cell} for one corrosive reaction is positive, according to the equation (1), ΔG is negative, which means the corrosive reaction is thermodynamically favoured (Sørensen, Kiil et al. 2009).

Although thermodynamic studies make a great contribution to the judgement of the possibility of corrosion behaviours on implanted medical devices, the real corrosion rate of reaction is influenced by other factors such as metal oxide film, for example, a metal oxide film usually is considered as a protective film to prevent corrosion behaviours, and the change of Gibbs energy ΔG of reaction between aluminum and water is negative (ΔG=-241.5kJ/mol), which means that the corrosion reaction should be spontaneous and easily happens; however, the real situation of

corrosion behaviours is that with the formation of a tough layer of aluminium oxides, the corrosion rate is very low (Sørensen, Kiil et al. 2009).

Besides, tribology also exerts an enormous influence on real corrosion rates. As mentioned above, the formation of mental oxide film can prevent corrosion behaviours effectively. However, when this kind of metal oxide layer is removed by rubbing, the corrosion rate will increase dramatically. Medical devices such as dental implants and hip prostheses, all suffer from this issue (Ryu and Shrotriya 2013). For example, titanium material as a material for dental implants can form a passive oxide layer which can prevent corrosion behaviours effectively. However once this oxide layer is damaged by fretting or wear, it may lead to the increase of corrosion rate in actual applications (Rocha, Oliveira et al. 2013).

Furthermore, the environmental factors, such as PH value, oxygen levels and proteins in body fluid, also exert an enormous effect on the process of corrosion (Rocha, Oliveira et al. 2013). For instance, compared with other orthodontic appliances, dental implants are prone to suffer from the corrosive attack, due to the exposure to the more corrosive oral environment including variable PH value and immersion in saliva (Mathew, Abbey et al. 2012)

1.2 Prevention Strategy

1.2.1 Prevention Strategy Against Medical Device-Associated Infection

1.2.1.1 General Considerations

As mentioned above, nowadays more and more patients rely on the assistance of medical devices to restore their normal life. However, the implantation of medical devices often results in associated infections due to bacterial adherence and colonization on the surface of medical devices. Thus, in order to reduce this incidence of infection, scientists always try to find different

strategies or methods to synthesize and develop the coating endowed with better antibacterial properties to decrease medical device-associated infections.

Since the middle of the 19th Century, people have found out that the noble metal Ag could be used for indwelling catheters in gynaecology (Sims 1869); however, people did not have a clear direction to choose antibacterial materials but, instead, relied on empirical experience, because at that time people did not know the exact reasons for infections (Raspe, von Münchhausen et al. 1954). The advancement of microbiology and the discovery of the first disinfectants at the end of 19th century promoted the development of antibacterial biomaterial, such as the invention of the first antibiotic releasing biomaterial in the 1940s (Silverman 1949, Raspe, von Münchhausen et al. 1954). Especially in recent years, the requirement for the use of medical devices has increased dramatically. And the interest of scientists to develop and synthesize better anti-infective coatings has been aroused due to enormous markets for medical devices. A great number of papers are published on this topic every year and a wide range of strategies and approaches have been adopted to achieve different antibacterial coatings, which depend on specific locations where medical devices are implanted (Campoccia, Montanaro et al. 2013).

1.2.1.2 Antibiotic Releasing Coatings

1.2.1.2.1 Conventional Organic and Inorganic Coatings

The idea of combination of antibiotic and medical device is considered an effective way to decrease medical device-associated infections. Compared with conventional systemic drug therapy to prevent implantation infections, the combination of antibiotic and medical device has numerous acknowledged advantages. Firstly, the strategy of local antibiotic release could control the release concentration of antibiotic from the surface of medical devices. Secondly, the

antibiotic can be transported directly to the specific site, which is more effective than conventional approach. Finally, releasing time is much longer with the lower dose of antibiotics on the surface of medical devices compared with systemic drug therapy (Wu and Grainger 2006).

Nowadays, antibiotic releasing coatings have been widely used in the field of medical devices, such as musculoskeletal and orthopaedics-related devices (Zilberman and Elsner 2008). And there are a wide range of antibiotics loaded into these coatings such as vancomycin, tobramycin, cefamandol, cephalothin, carbenicillin, amocicillin, gentamicin and so on (Stigter, Bezemer et al. 2004). In the antibiotic carrier systems, one of the most frequently used carriers for the antibiotics is polymethylmethacrylate (PMMA) (Teupe, Meffert et al. 1992).

Since 1970, the innovative idea of using polymethylmethacrylate (PMMA) beads as a carrier releasing antibiotics in bone cement to prevent local medical devices-associated infections was introduced in the literature (Buchholz and Engelbrecht 1970), and the gentamicin-loaded PMMA beads were commercially available in Europe in 1977 (Giamarellos-Bourboulis 2000), and it has been widely accepted as a way to reduce the medical device-associated infection for nearly four decades especially bone infection such as osteomyelitis (Wu and Grainger 2006, Zilberman and Elsner 2008).

Although PMMA has good properties such as good biocompatibility and rapid release of antibiotics (Giamarellos-Bourboulis 2000), PMMA is not biodegradable, which means that it is necessary to operate secondary surgery to remove the PMMA material before new bone can regenerate in the defect (Zilberman and Elsner 2008), and the releasing rate of antibiotics is relative lower due to its unbiodegradable property. Therefore a great number of biodegradable polymeric carriers are found such as PLGA, PLA, poly (d.l-lactic acid) (PDLLA), PEG and so on, which can contribute to releasing larger quantities of antibiotics and longer release periods at

controllable rates, and they have no need to conduct a device-removal operation (Ali, Zhong et al. 1993, Zilberman and Elsner 2008, Simchi, Tamjid et al. 2011). According to Price and co-workers research, 20 wt% of antibiotic gentamicin loaded biodegradable PLGA orthopaedic coatings have the ability to prevent more than 99% of bacterial adhesion over 24 hours compared with uncoated samples (Ali, Zhong et al. 1993). Besides, natural polymeric carriers such as collagen (Prabu, Dharmaraj et al. 2006, Shanmugasundaram, Sundaraseelan et al. 2006) and chitosan (Aoyagi, Onishi et al. 2007, Rossi, Marciello et al. 2007), are also very attractive candidates due to their great biocompatibility, lower price and promotion of cell growth (Zilberman and Elsner 2008).

Besides, inorganic materials such as Synthetic hydroxyapatite (HAP) and calcium phosphates also draw increasing interest due to their intrinsic non-toxicity, high biocompatibility and the ability to support the growth of new bone tissue and promotion of bone-tissue integration (Hench 1991, Martins, Goissis et al. 1998). A great number of experiments have been conducted in vitro and in vivo to prove their great properties as mentioned above; also the results of antibiotic-loaded HAP against bacterial infection and releasing rate of antibiotic present its promising perspective as an excellent coating for medical devices (Stigter, Bezemer et al. 2004, Duan, Fan et al. 2005, Alt, Bitschnau et al. 2006, Chai, Hornez et al. 2007).

1.2.1.2.2 Nanostructured Coatings

In recent decades, with the advancement of nanotechnology and development of nanomaterials, a great number of new nanostructured materials have been synthesized. For antibiotic releasing coatings, compared with conventional coatings as mentioned above, nanostructured coatings possess better properties such as better chemical stability and better control of release kinetics (Simchi, Tamjid et al. 2011). And different shapes of nanostructured materials such as nanotube,

nano core-shell, nanocomposite coatings are designed to meet different demands according to the specific functions which the medical coatings play.

As we know, HAP is a great candidate to be an antibiotic carrier, and when HAP was fabricated into a form of core-shell nano-structure to cover antibiotics, which has been reported to have better properties. For example, the core-shell structure can provide longer time to release antibiotics (70% release after 20 hours) (Xu, Tanaka et al. 2007) compared with conventional HAP based antibiotic-releasing coatings (70% release after 10hours on average) (Stigter, Bezemer et al. 2004). Besides, nano-diamond based antibiotic-releasing coatings draw scientists' interest to be an alternative promising material for medical devices (Simchi, Tamjid et al. 2011). For example, the diamond-based coatings exhibited a stable and continuous release of antibiotics for at least 1 month, which is much better than the HAP based nano-structure coating (Lam, Chen et al. 2008) and the result of the cytotoxicity and anti-inflammatory response of nano-diamond based coatings in vivo is very satisfactory (Huang, Pierstorff et al. 2008). In addition, TiO_2 nanotubes also have gained significant attention because TiO_2 nanotubes not only act as an antibiotics carrier, but they also have a positive effect on growth of cells around coatings due to the favourable nano-scale roughness (Simchi, Tamjid et al. 2011). Furthermore, the amount of antibiotics-release can be controlled via tailoring the diameter and length of nanotubes. For example, the same diameter of nanotubes with 1 μm in length release twice less antibiotics than the amount of antibiotics from 5 μm nanotubes. A similar trend is obtained for nanotubes with the same length but different diameters (Peng, Mendelsohn et al. 2009).

Overall, developing antibiotic releasing coatings for medical devices is an effective approach to prevent medical device-associated infections by releasing antibiotics locally at the site of

implantation. Compared with systemic drug therapy, it is more efficient to resist local bacterial infections and decrease the side effects of parenteral antibiotics (Simchi, Tamjid et al. 2011).

1.2.1.2 Anti-biofouling Nanostructured Surfaces and Coatings

Nature always is one of the most important teachers for human beings; there are countless inspirations originating from nature which benefit human beings. Especially in the last hundred years, with the development of science and technology, the inspiration from nature can be transformed into products quickly, which draws more attention from scientists and engineers from multidisciplinary fields to investigate and learn from nature and to gain inspiration from nature (Hasan, Crawford et al. 2013). In the field of biomimetics, through billions years of evolution by nature, a wide range of natural surfaces such as shark skin, insect wings, plant leaves and so on are found to be of multiple integrated functions including low-adhesive, superhydrophobic, self-cleaning and other properties, which are considered to have the capability of preventing bacterial adhesion (Barthlott and Neinhuis 1997, Liu and Jiang 2011). For example, the surface of cicada wings can effectively prevent the adhesion of *Pseudomonas aeruginosa* due to the pattern of nanopillars, which not only makes the surface hydrophobic but could also penetrate all the bacteria to death and change the morphology of the bacteria (Ivanova, Hasan et al. 2012). Besides, the surface of taro leaves also have the ability to resist bacterial adhesion as a result of the nanostructure feature of the surface which traps the air between nanostructures to keep the surface superhydrophobic (Ma, Sun et al. 2011). Overall, the nanostructure of these natural surfaces contribute to the excellent property of resisting bacterial fouling. Scientists are inspired by the characteristics of these natural surfaces with the result that more and more nanostructured surfaces and coatings are synthesized and tested and applied in medical devices to prevent medical device-associated infections.

A great number of coatings and surfaces are synthesized by mimicking the similar nanoscale pattern of natural anti-adhesive surfaces, and most of biomimetic hierarchical micro-or nano-structured surfaces or coatings can be prepared by the two-step replication process. For example, the microstructure of the shark-skin surface can be synthesized by using PDMA as template of counter-shape of shark skin, which can be seen in figure 1.3 (Liu and Li 2012). Similar methods could also be applied to prepare coatings with similar nanostructure of rice leaves, lotus leaves and so on (Gao, Liu et al. 2009). Apart from the fact that a great number of coatings are indirectly prepared by the template of natural surfaces, nanostructured surfaces or coatings with different sizes and shapes including grooves, columns, protrusions and so on can also be prepared by the aid of physical and chemical fabrication technologies (Anselme, Davidson et al. 2010).

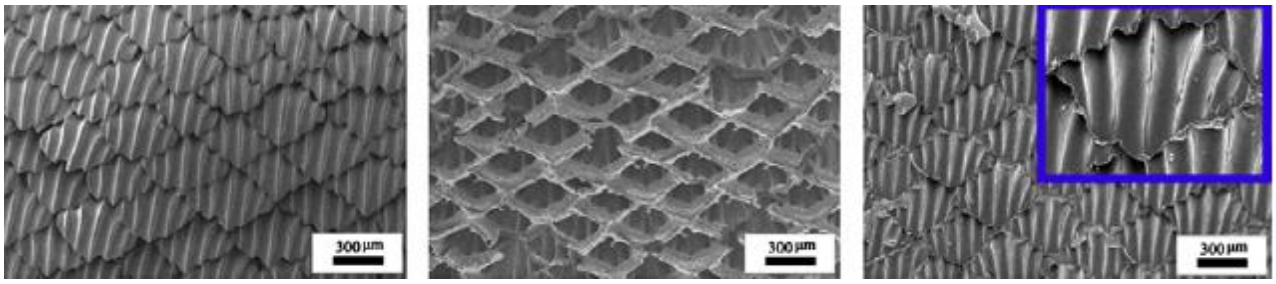

(a) A real shark skin (b) PDMS negative replica (c) Shark skin replica

Figure 1. 3 The SEM images of the shark-skin surface and the surfaces of PDMS sheets prepared via micro-replication.(Liu and Li 2012)

Basically, there are two types of nano- or microfabrication techniques, one of which is topographical patterning. For example, photolithography, as a silicon patterning technique, is widely used particularly in the electronics industry due to its capability of creating structures of any desired shape rapidly and reproducibly at the sub-micron level (Anselme, Davidson et al.

2010), which can also be used to prepare coatings with different nanostructures to examine the effect of nanostructures on bacterial adhesion. However, the resolution of the pattern is limited by the wavelength of the light to allow the size of feature to 50nm. Compared with the method of photolithography, the method of electron beam, which is limited by wavelength of electrons, can achieve higher resolution of surface structures to be as low as 15nm (Blättler, Huwiler et al. 2006). Apart from the technique of lithography, scientists also make use of spaces between the copolymer micelles to prepare nanostructured surfaces, and different nanostructures can be obtained by changing the polymer blocks and solvents (Wen, Chung et al. 2006). Besides, nanostructured surfaces of coatings can be prepared by polymer demixing method according to the incompatibility of two polymers (Dalby, Pasqui et al. 2004). Furthermore, metallic oxidation, nanophase, gradients and similar methods are also applied to the preparation of coatings (Anselme, Davidson et al. 2010).

Another type of patterning is chemical patterning. In contrast to topographical patterning, the chemical patterning is the modification of chemistry at a micro- or nanoscale. Different methods, such as micro-contact printing, transfer from topography, LB film and so on, are widely used to obtain nanoscale chemical modification of coatings (Anselme, Davidson et al. 2010). Actually, it is usually difficult to separate the topographical patterning from chemical patterning, because these two types of surface patterning combined with each other most of the time (Anselme, Davidson et al. 2010).

In recent years, a large number of nanostructured coatings and surfaces have been prepared and present great properties of resisting bacteria adhesion. For example, the nanostructured surface of polyurethane with ordered arrays of pillars was found to have the ability to effectively reduce the adhesion of *staphylococcal* strains (Xu and Siedlecki 2012). Nano-structured silicon wafers, with

gold protrusions in form of dots and lines prepared by combined techniques of topographical patterning and chemical patterning, also present great properties of resisting the adhesion of *E. coli* and *S. aureus* (Komaromy, Li et al. 2012). Besides, titanium surfaces with nano-scale roughness not only result in a decrease of bacterial attachment such as *Staphylococcus aureus*, *Pseudomonas aeruginosa*, but it also has a significant effect on promoting formation of bone tissue (Puckett, Taylor et al. 2010), which is very important for biocompatibility of implanted medical devices. And the similar contributions of nano-structured coatings to enhancing multiple osteoblast behaviours are also reported (Biggs, Richards et al. 2009, Zhao, Mei et al. 2010).

1.2.1.3 Anti-adhesive and Anti-bacterial Coatings

1.2.1.3.1 Silver Based Coatings

In recent centuries, silver, as one of the most significant antimicrobial agents, has been extensively used for the treatment of burns and preventing infections (Rai, Yadav et al. 2009). For example, in the 18th century, silver nitrate was used for the treatment of venereal diseases, perianal abscesses and so on (Kawahara, Tsuruda et al. 2000). And a certain concentration of silver nitrate was also found to be effective to treat fresh burns in the 19th Century (Castellano, Shafii et al. 2007). Since then, Scientists have never stopped researching the potential properties and applications of silver and related silver salts.

The mechanism of the antibacterial property of silver can be attributed to the fact that the silver and silver ion will bond to thiol groups in proteins and enzymes in the bacterial cell wall and cell membrane to change the metabolism of bacteria and the structure of the bacterial cell wall. Besides, silver ion also could directly penetrate into the bacterial cell to make a DNA molecule lose its replication ability, all of which will lead to the inhibition of bacterial growth and the

death of bacteria. Figure 1.4 show the Mechanisms of toxicity of nanoparticles (NPs) against bacteria. (Kim, Kuk et al. 2007, Shao and Zhao 2010, Simchi, Tamjid et al. 2011). In the field of pharmaceutical products and medical devices, a great number of advantages of Ag have been found out to make it an excellent material, including its broad spectrum biocides (Lara, Garza-Trevino et al. 2011), no toxicity to human cells in given concentrations (Rojas, Slunt et al. 2000) and avoiding to develop bacterial resistance (Simchi, Tamjid et al. 2011). In recent decades, due to considerable advantages of silver and advancement of synthesis of nanomaterials, a great number of coatings of medical devices are prepared by incorporating nanoparticle silver into different substrates. And a series of Ag based organic composite coatings present high efficiency in resisting bacterial adhesion, such as Ag-polyvinylpyrrolidone (PVP) (Nishino and Kanno 2008), Ag- polyethylene glycol (PEG) (Ragaseema, Unnikrishnan et al. 2012), Ag-polypropylene (PP) (Wu, Lee et al. 2012) ,Ag-PTFE (Zhao, Liu et al. 2005) and so on, all of which not only prevent bacterial adhesion by altering the physicochemical property of coatings including hydrophobicity, roughness and surface free energy, but also reduce the aggregation of Ag nanoparticle to maintain high antibacterial function due to the affinity of the functional group of polymers for the Ag nanoparticle.

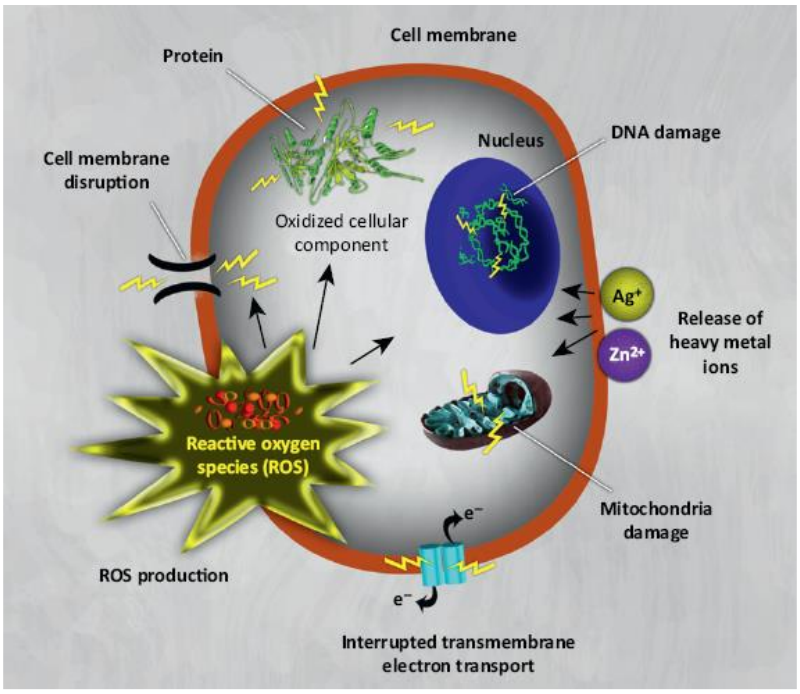

Figure 1. 4 Mechanisms of toxicity of nanoparticles (NPs) against bacteria. (Hajipour, Fromm et al. 2012) .

However, when Ag-polymer coatings are implanted into human bodies, sometimes the mechanical strength cannot meet the requirement for load-bearing implants due to high shear forces between bones and implant surfaces (Simchi, Tamjid et al. 2011). Also the strong affinity of functional group of polymers for the Ag nanoparticles sometimes restricts the release of silver ions which lead to the failure of experiments in vivo (Masse, Bruno et al. 2000). Therefore, there is another trend to prepare Ag based inorganic coatings to improve the mechanical property of the coatings and pursue the balance between highly efficient antibacterial actions and good biocompatibility. Different coatings such as Ag- hydroxyapatite (HA) (Chen, Liu et al. 2006), Ag-diamond like carbon (DLC) (Schwarz, Hauser-Gerspach et al. 2011), Ag-Ni-P (Shao and Zhao 2010), Ag-TiO_2 (Shao and Zhao 2010), and so on have been prepared, which present good antibacterial behaviours and great potential to be a candidate material for medical devices.

However, a long debate still exists about the biocompatibility of Ag. There are some papers which show the result to demonstrate the nontoxicity of Ag to the cells (Wen, Lin et al. 2007, Guzman, Dille et al. 2012), but some papers present controversial results. For example, the Ag nanoparticle was found out to be toxic on C18-4 cell which is a cell line with spermatogonial stem cell characteristics and the cytotoxicity enhanced with the increase of concentration of silver nanoparticles (Braydich-Stolle, Hussain et al. 2005). Therefore, controlling release of Ag at a relative low concentration to reduce cytotoxic risks is one of the toughest issues in designing Ag-based coatings implanted into human bodies, especially for the Ag in the form of nanoparticle (Albers, Hofstetter et al. 2013). Although the efficient antibacterial concentration of Ag can reach a very low point, when the medical device was implanted into human bodies surrounded by physical fluids, it is difficult to control the real release concentration of nanoparticle Ag or Ag ions and to balance the biocompatibility and antibacterial property of nanoparticle Ag based coatings.

1.2.1.3.2 Ceramic Based Coatings

Silica based materials are considered traditional ceramic which is prepared from natural raw material such as clay, and most traditional ceramic materials are widely used as porcelain, sanitary ware , pottery and so on. Compared with traditional silica based ceramic material, advanced ceramics such as titanium dioxide, zirconium dioxide and so on are of higher quality and purity which attract dramatic attention because of their good mechanical, optical, chemically inert and biocompatibility properties and the application of these advanced ceramic materials is mainly focused on biomedical and bioengineering fields such as medical device coatings, bioreactors, chromatographic support and so on (Riedel and Chen 2011, Treccani, Yvonne Klein et al. 2013).

1.2.1.3.2.1 TiO_2 Based Coatings

Titanium, as a rare metal, was first discovered in 1790, and is one of the most important metals in many fields, such as aerospace and military industry (Liu, Chu et al. 2004). Especially in recent decades, the oxide of titanium (TiO_2) and TiO_2 based materials are extensively used in medical device fields such as artificial hip joints, artificial teeth, artificial heart valves, artificial vascular stents and so on (Liu, Chu et al. 2004) due to its excellent biocompatibility, corrosion resistance, mechanical properties and antibacterial capability which is one of the most important factors in preventing the failure of implantation of medical devices.

The mechanism of the antibacterial property of TiO_2 is due to photocatalytic reactions. With the irradiation of ultraviolet, the surface of the TiO_2 coatings will produce hydroxyl radicals and superoxide ions due to the reaction between the atmospheric water, oxygen and pairs of electrons and holes on the TiO_2 surface, which is generated by the photon energy of ultraviolet, and these hydroxyl radicals and superoxide ions contribute to its antibacterial properties (Mills and Le Hunte 1997). Besides, surface properties of TiO_2 coatings can be altered by ultraviolet radiation, for example, the surface contact angle of water can be decreased dramatically which is also considered to play a role in resisting bacterial adhesion (Aita, Hori et al. 2009).

A series of TiO_2 based composite materials with good antibacterial properties and biocompatibility are prepared for the coating of medical devices. For example, when TiO_2 materials were used as major component of coatings, pure TiO_2 coatings with different roughness (Wu, Zitelli et al. 2011), different nano-structrure of TiO_2 such as nanotube (Cui, Gao et al. 2012) and TiO_2 utilized as a carrier to load nano-Ag particles (Zhao, Wang et al. 2011) , Zn particles (Hu, Zhang et al. 2012) and so on, which present excellent antibacterial properties and

biocompatibility. While adding a small amount of nanoparticle TiO_2 into other coatings also can enhance the antibacterial property and biocompatibility compared with original coatings, such as Ni-P-PTFE based coatings (Liu and Zhao 2011), DLC based coatings (Marciano, Lima-Oliveira et al. 2009) and other polymer coatings such as Polypropylene (Bahloul, Médis et al. 2012), all of which not only maintain the original property of resisting bacterial adhesion but also enhance the antibacterial effectiveness.

1.2.1.3.2.2 ZrO_2 Based Coatings

Zirconia (ZrO_2) is the oxide of element Zr, which locates at the same group in the periodic table of elements with Ti (IV B), which means that there are some similar properties in these two elements and their oxides. For example, ZrO_2 is also of excellent mechanical property, biocompatibility and resisting bacterial adhesion property (Buczynski, Kory et al. 2003, Scarano, Piattelli et al. 2004, Depprich, Zipprich et al. 2008). Therefore, Zirconia (ZrO_2) is also considered one of most significant ceramics materials in modern technology (Muñoz, Gallego et al. 2006). It is widely used in industrial applications such as catalyst, fuel cells, gas sensing and so on, due to excellent wear resistance and good chemical inertness (Harvey, Diefenbach et al. 1999, Kreuer 2003, Muñoz, Gallego et al. 2006). Besides, ZrO_2 is bioinert, together with its good mechanical property, good biocompatibility and great anticorrosion property, which leads to its wide biomedical application in orthopaedic applications (Treccani, Yvonne Klein et al. 2013), such as femoral heads for total hip replacement and dental restoration and so on (Piconi, Maccauro et al. 2003, Chevalier, Deville et al. 2004, Treccani, Yvonne Klein et al. 2013). Besides, a great number of researches about the comparison between TiO_2 and ZrO_2 have been conducted in medical device applications. For example, features of osseointegration of ZrO_2 and

TiO_2 show similar good bone response (Thomsen, Larsson et al. 1997, Depprich, Zipprich et al. 2008), and both of them show great biocompatibility (Jum'ah, Beekmans et al. 2012). Furthermore, the property of resisting the adhesion of bacteria of TiO_2 and ZrO_2 was compared, which shows that the zirconia coatings present superior effect to titanium coatings on resisting bacterial adhesion especially after coatings with saliva pellicle. The mechanism of zirconia in reducing bacterial adhesion is related to the surface free energy and indirect influence on the adhesion of certain types of proteins on the Zirconia coatings which prevent bacterial adhesion as mentioned above (Al-Radha, Dymock et al. 2012). Due to its similar property with TiO_2 and its white colour which can meet the aesthetic requirement for patients in dental restoration, ZrO_2 material was considered a good candidate to replace TiO_2 especially in the field of dentistry (Jum'ah, Beekmans et al. 2012).

1.2.1.4 Others

1.2.1.4.1 Ni-P Based Coatings

Electroless coating was considered a revolutionary method of coating technique, which was first developed to coat inner walls of tubes during the World War II (Sudagar, Lian et al. 2013). And after that, a series of electroless deposition coatings were developed such as nickel-tungsten, nickel-phosphorus, nickel –boron alloys and so on (Gao, Du et al. 2007, Srinivasan, Meenakshi et al. 2010, Sudagar, Lian et al. 2013). In recent years, electroless plating has drawn increasing attention due to some of its distinctive properties including their excellent corrosion resistance, high hardness, fast plating rate and so on (Sahoo and Das 2011), which lead to its application in the fields of engineering, surface science such as coatings of medical devices (Domenech, Lima et al. 2003, Wang, Vora et al. 2004). Although there are many metals such as nickel, copper, gold and so on chosen to be deposited by electroless plating technique, 95% of production of

industrial electroless platings are electroless nickel-phosphorus or nickel- boron coatings and the use of electroless nickel-phosphorus coatings has increased steadily in the last ten years (Sudagar, Lian et al. 2013). When electroless nickel-phosphorus coating evolved into a mature subject of research, in order to achieve the better properties of Ni-P coatings such as higher lubricity and hardness, anti-wear properties, different nanoparticles were incorporated into Ni-P based composite coatings. For example, Ni-P-SiC can be developed by co-depositing the hard particles SiC into the Ni-P coatings which can increase wear resistance and hardness of the coatings compared with Ni-P coatings (Dong, Chen et al. 2009). Similarly, doping PTFE (poly tetra fluoro ethylene) into Ni-P coatings makes the new coating anti-adhesive with lower friction and good corrosion resistance, due to the low coefficient of friction and extremely low surface free energy (18.6 mN/m) of the PTFE (Zhao, Liu et al. 2002, Zhao 2004). Due to the anti-adhesive property of Ni-P-PTFE coatings, researchers from biological engineering fields also found that the Ni-P-PTFE has excellent property of resisting bacterial adhesion (Zhao, Liu et al. 2002, Zhao 2004), and the better property of resisting bacterial adhesion of the coatings is prepared by adding nanoparticles of TiO_2 into Ni-P-PTFE coatings which present excellent capability of resisting bacteria (Liu and Zhao 2011), which, in turn, make Ni-P-PTFE coatings ideal to apply to medical devices.

1.2.1.4.2 DLC Based Coatings

Diamond-like carbon (DLC) coating is known as a black amorphous material and the carbon-carbon bonds include two forms such as sp^2 and sp^3, which are not like crystalline diamond with only one form of carbon-carbon bond (sp^3). Due to the sp^2 form of carbon-carbon bonds which is the same as graphite, the DLC coating has an extremely smooth surface and low friction (Dearnaley and Arps 2005). In recent years, the DLC is used as a base material which is doped

with different elements such as DLC-Si, DLC-F, DLC-Cr, DLC-Ag, DLC-TiO_2 and so on (Zhao, Liu et al. 2007, Marciano, Lima-Oliveira et al. 2009, Su, Zhao et al. 2010, Schwarz, Hauser-Gerspach et al. 2011, Jelinek, Kocourek et al. 2015), all of which not only can keep the original property of the bare DLC due to the amorphous phase of bare DLC, but also can enhance the anti-fouling and other properties of the DLC coatings (Hauert 2003). For instance, the addition of element F into DLC coatings can reduce bacterial attachment and increase bacterial removal rate by changing the surface free energy of the coatings (Su, Zhao et al. 2010). Besides, the corrosion resistance, wear resistance, excellent haemocompatibility and its antibacterial properties contribute to biological application of DLC coatings into commercial cardiovascular implants such as artificial heart valves and stents (Hauert 2003).

In conclusion, in order to solve medical device-associated infections, different strategies were adopted to develop different coatings or material. because it has been a very difficult task to find out one coating or material which can be used as a perfect material to solve all the medical device associated problems, advantages and disadvantages of different strategies or coatings are listed in the table 1.1. And ceramic material such as TiO_2 and ZrO_2 are not only biocidal but also anti-adhesive, which can be considered as a potential material to be further developed.

Table 1. 1 Advantages and disadvantages of different strategies against medical device-associated infections

Strategy	Developed coatings	Advantages	Disadvantages
Releasing Antibiotics	Conventional carrier material: PMMA, PLGA, PLA, PDLLA collagen, chitosan etc. Nanostructured carrier material: HAP (core-shell), nano-diamond TiO_2(tube)	Compared with systemic drug therapy, antibiotic releasing coatings can control the release concentration of antibiotic and the antibiotic can be transported directly to the specific site and decrease the side effects of parenteral antibiotics	It is easy to lead to the bacterial drug resistance especially in the body environments with low concentration of antibiotics.
Bionic Structure	Shark-skin, rice leaves, lotus leaves etc. shaped surfaces by two-step replication process. Nanostructured surfaces with different sizes and shapes including grooves, columns, protrusions by topographical patterning and chemical patterning technique, such as nano-structured polyurethane and silicon wafers with gold protrusions	Bionic structure coatings have similar property as natural surfaces such as excellent anti-adhesive, superhydrophobic self-cleaning in natural environment	When this type of coatings are immersed in the body fluids, conditioning film covered on the surface immediately lead to lower efficiency of antibacterial property
Anti-adhesive and anti-bacterial composition	1, Silver based coatings 2, Ceramic based coatings such as TiO_2 and ZrO_2 based coatings, 3, Ni-P based coatings and DLC coatings	1, Silver based coatings have excellent antibacterial property 2, TiO_2 and ZrO_2 based coatings have excellent antibacterial and anti-adhesive property 3，Ni-P based coatings and DLC coatings have good antibacterial property	1, toxicity of Ag to C18-4 cell and poor non-stick property 2 TiO_2 and ZrO_2 based coatings do not have special disadvantages 3 Ni-P based coatings and DLC coatings are not biocidal or have low efficiency to kill bacteria

1.2.2 Anticorrosive Coatings

Since the corrosion process happens on the interface between medium and material, the basic strategy of preparing anticorrosive coatings is to directly or indirectly prevent or slow the medium from eroding the material. There are three basic approaches to prepare anticorrosive coatings, which can be classified into inhibitive coatings, sacrificial coatings and barrier coatings (Sørensen, Kiil et al. 2009). The mechanism of both inhibitive coatings and sacrificial coatings against corrosion relies on the release of ions to slow corrosive behaviours. For example, inhibitive coatings need to release ions and react with the substrate to form a protective layer when the coating is permeated by moisture (Alibakhshi, Ghasemi et al. 2013), and sacrificial coatings need to sacrifice a more active material to protect the major material (Schaefer and Miszczyk 2013). These two kind of coatings are widely used in the industrial fields. However, the release of ions from implanted medical devices has a detrimental effect on the human body leading to the failure of implantation as mentioned above. Therefore, barrier protection is considered as a main strategy to prevent corrosive behaviours in the field of medical devices. The mechanism of barrier coatings is to prevent the aggressive species such as liquids, gases, ions and so on to permeate the coatings and directly corrode substrates(Sørensen, Kiil et al. 2009). And the ionic impermeability of the barrier coatings also plays a significant role on anticorrosive behaviours, because this impermeability means that the whole corrosive circuit is cut off by barrier coatings or the current between anode and cathode is limited to a very small value.

Different organic, inorganic, ceramic, metallic alloys and composite materials are used to prepare anticorrosive coatings of medical devices (Sørensen, Kiil et al. 2009, Blaiszik, Kramer et al. 2010, GAO, LI et al. 2012). Inorganic oxide materials such as SiO_2, TiO_2, ZrO_2, ZnO, SiC

(Gu, Ma et al. 2012, Sonawane, Bhanvase et al. 2012, Li, Ma et al. 2013, Grari, Dhouibi et al. 2015, Wu, Zhou et al. 2015) and organic material such as epoxy, polyaniline, polypyrrole, polythiophene and so on are widely used as anticorrosion coatings (de Leon and Advincula 2015). Different series of metallic alloys such as NiTi, $Zn_xMg_yAl_2O_4$, Ni-P based coatings also present great anticorrosive properties (Zhao and Liu 2005, Veselý and Kalendova 2008, Fadlallah, El-Bagoury et al. 2014), as does carbon material like DLC coatings and graphene coatings which also can resist corrosive behaviours effectively (Choi, Lee et al. 2008, Liu, Hua et al. 2015).

Nowadays, hybrid coatings draw more and more attention of engineers and researchers, because they not only present their own advantages, but also can overcome their own drawbacks. For example, for organic and inorganic hybrid coatings, most inorganic materials can react with metal substrates and enhance the strength of adhesion between coatings and substrates, which is the drawback of pure organic coatings (Seok, Kim et al. 2006). While organic particles can contribute to the mechanical flexibility and toughness of hybrid coatings (Hofacker, Mechtel et al. 2002), and adding organic particles into inorganic coatings could improve impermeability of aggressive species such as liquids, gases, ions and so on to prevent corrosion behaviours. This is because organic particles is considered to have the capability of filling the pores between inorganic particles in inorganic coatings especially when they are prepared by sol-gel method, which is one of the prevalent methods to prepare anticorrosion coatings (Sørensen, Kiil et al. 2009).

In conclusion, from the literature review above, we can see that there are a lot of strategies to deal with medical device associated infections and medical device corrosion. Ceramic material such as TiO_2 and ZrO_2 not only show great capability of antibacterial and anti-adhesive property

but also are widely used to prevent corrosive behaviour especially combining with polymer to form organic and inorganic hybrid coatings.

2 Aim and Objectives

In this study, in order to solve the medical device-associated infections and medical device corrosion, I try to develop a new coating which has great capability of resisting bacterial adhesion and preventing corrosive behaviours effectively. I expect this kind of coating can be considered as a potential candidate to apply into medical devices to effectively reduce medical device-associated infections and corrosive behaviours.

Zr and Ti locate at the same group in the periodic table of elements (IV B), and their oxide ZrO_2 and TiO_2 are both extensively used in medical device fields due to their excellent biocompatibility, corrosion resistance, mechanical properties and antibacterial capability as we mentioned in literature review chapter. Ni-P-PTFE coatings were used as the matrix, which has been proven that they are of anti-adhesive property and corrosion resistance property due to the addition of PTFE, which have low coefficient of friction and surface free energy (Zhao, Liu et al. 2002, Zhao 2004). Based on the idea of addition of PTFE into Ni-P coating to enhance its anti-adhesive and corrosion resistance property, New coatings are designed by adding nanoparticle ZrO_2 and TiO_2 into the Ni-P-PTFE matrix. And the organic and inorganic hybrid coatings are attempted to enhance the property of anti-bacterial adhesion and corrosion resistance. First type of novel coating is Ni-P-PTFE-ZrO_2. ZrO_2, which has been widely used in orthopaedic applications, was added to Ni-P-PTFE coatings to enhance its antibacterial property, biocompatibility and great anticorrosion property (Treccani, Yvonne Klein et al. 2013). Second type of novel coating is Ni-P-PTFE-ZrO_2-TiO_2. As we mentioned in literature review, TiO_2 material is widely used in the medical device markets, and its excellent properties such as antibacterial capability, biocompatibility, corrosion resistance and mechanical properties contribute to medical devices having higher safety and longer working life when implanted in

human bodies. In recent years, some new coatings are developed by incorporating nanoparticle TiO_2 into other coatings which help to enhance the property of new coatings such as antibacteiral property, anticorrosion property, mechanical property and so on (Thomsen, Larsson et al. 1997, Depprich, Zipprich et al. 2008, Ionita, Grecu et al. 2011, Cui, Gao et al. 2012). Therefore, Ni-P-PTFE-ZrO_2-TiO_2 coatings are designed by adding nanoparticle TiO_2 into Ni-P-PTFE-ZrO_2 coatings to further enhance the antibacterial property and anticorrosion property.

By a series of assays of bacterial adhesion and removal, and electrochemical corrosion experiments, I hope that two types of novel developed Ni-P-PTFE-ZrO_2 and Ni-P-PTFE-ZrO_2-TiO_2 coatings can be proved to prevent bacterial adhesion effectively and protect medical devices from corrosive behaviours.

3 CHARACTERISTIC OF COATINGS

3.1 Thickness of coatings

There are several method which can be used to measure the thickness of coatings, such as non-destructive methods (e.g. micrometer measurement) and destructive methods (e.g. cross-sectioning measurement).

In this study, the thickness of Ni-P, Ni-P-PTFE, Ni-P-PTFE-ZrO_2 and Ni-P-PTFE-ZrO_2-TiO_2 coatings was measured with a micrometer with accuracy of 1 μm. and the thickness of prepared coatings mentioned above were in the range of 23-48 μm depending on deposition time and bath composition.

3.2 Surface free energy and Contact angle of coatings

Surface free energy (SFE) is one of the most important parameters to evaluate physico-chemical property of substances. In this study, surface free energy of prepared coatings such as Ni-P, Ni-P-PTFE, Ni-P-PTFE-ZrO_2 and Ni-P-PTFE-ZrO_2-TiO_2 coatings were also measured to evaluate their surface physico-chemical property. SFE is produced on the interface between different phases or different substances, where different phase or substances such as air, liquid and solid contact each other. Due to different cohesive forces of different substances, there exists an unbalanced force field on the interface between different substances or phases, which contributes to the production of SFE. The surface free energy (γ_s) of solid substance is usually defined as the change of the total surface energy (G) by altering per surface area (A) at constant temperature (T), pressure (P) and moles (n) (Good 1992, Chaudhury 1996):

$$\gamma_S = (\delta G / \delta A)_{T,P,n} \qquad (3.1)$$

Contact angle measurement is a kind of wetting characteristics of solid surface. The contact angle can be measured by testing the angle between solid/liquid interface and liquid/vapour interface, which can be seen in figure 3.1.

From figure 3.1, we can see that θ represents the contact angle; γ_{SL} represents the interfacial tensions between solid and liquid; γ_{LV} (γ_L) represents the interfacial tensions between liquid and vapour; (or γ_S) represents the interfacial tensions between solid and vapour. And when these three interfacial tensions balanced on the interface, the liquid drop will keep stable, and static contact angle will be measured. Surface free energy of prepared coatings mentioned above can be calculated by measuring their surface contact angle (CA) by placing a drop of liquid on the surface of coatings, which will be introduced in section 3.2.3.

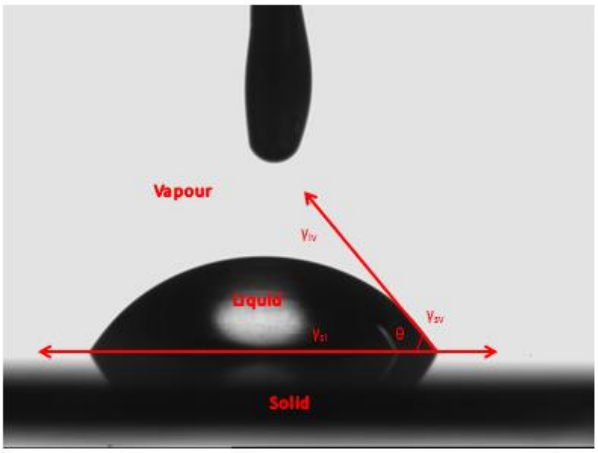

Figure 3.1 contact angle

3.2.1 Calculation of surface free energy

3.2.1.1 Young's equation

In 1805, Thomas Young first argued that the contact angle of a liquid can be considered as mechanical equilibrium of a drop resting on a solid surface at the three-phase boundary (Young 1805) and it is shown as following equation:

$$\gamma_{LV}\cos\theta = \gamma_{SV} - \gamma_{SL} \quad (3.2)$$

However, in 1937, Bangham and Razouk (1937) pointed out vapour adsorption on the solid surface should be considered for the young's equation, and there was a new term which should be added into the Young's equation called the spreading pressure where $\gamma_S = \gamma_{SV} + \pi_e$. If the spreading pressure is neglected, the Young equation is modified as (Girifalco and Good 1957):

$$\gamma_L\cos\theta = \gamma_S - \gamma_{SL} \quad (3.3)$$

In Young's equation, $\gamma_L$and $cos\theta$ both can be measured, and if the solid-liquid interfacial energy γ_{SL}can be represented or expressed in term of the γ_L or γ_S, solid surface free energy γ_S can be calculated.

One of the methods which can help to solve this problem is proposed by Fowkes who first put forward the surface component approach in 1962 (Fowkes 1962, Fowkes 1964, Fowkes, McCarthy et al. 1980). Fowkes divided the total surface energy into two parts, dispersive part and non-dispersive part. The first part resulted from the molecular interactions due to London forces and the second is due to all non-London forces:

$$\gamma = \gamma^d + \gamma^p \quad (3.4)$$

He proposed the following relation for solid/liquid interacting by only dispersion force interaction.

$$\gamma_{SL} = \gamma_S + \gamma_L - 2\sqrt{\gamma_S^d \cdot \gamma_L^d} \quad (3.5)$$

Combing the Yong's equation, the following expression is obtained:

$$\gamma_L(1 + \cos\theta) = 2\sqrt{\gamma_S^d \gamma_L^d} \quad (3.6)$$

Although Fowkes only considered dispersive interactions between solid and liquid, Fowkes approach still has a significant effect on calculation of γ_S later. For example, van Oss Acid-Base approach use the similar form to express γ_{SL}^{LW} with Lifshitz-van der Waals apolar component, which can be seen in equation4.8, and van Oss Acid-Base Approach is widely accepted and used for calculating surface free energy right now.

3.2.1.2 Van Oss Acid-Base Approach

Van Oss et al. divided the total surface free energy of a solid into two components, Lifshitz-van der Waals apolar component (γ_i^{LW})and Lewis acid/base polar component (γ_i^{AB}) in 1986(Van Oss, Good et al. 1986).

$$\gamma_i = \gamma_i^{LW} + \gamma_i^{AB} \quad (3.7)$$

The apolar part γ^{LW}, follows the Fowkes treatment (equation 3.5) (Van Oss, Good et al. 1986, Van Oss, Chaudhury et al. 1987, Van Oss, Chaudhury et al. 1988, Van Oss 1993, Van Oss 2006)

$$\gamma_{SL}^{LW} = \left(\sqrt{\gamma_S^{LW}} - \sqrt{\gamma_L^{LW}}\right)^2 \tag{3.8}$$

The acid-base polar component γ_i^{AB} can be further subdivided into an electron donor γ_i^- and an electron acceptor γ_i^+ subcomponent. γ_i^{AB} can be expressed as following equation:

$$\gamma_i^{AB} = 2\sqrt{\gamma_i^+ \gamma_i^-} \tag{3.9}$$

Unlike the LW interactions, which are mathematically symmetrical, the acid/base interactions are essentially asymmetrical. For a polar substance. the electron acceptor and the electron donor parameters are quite different. At the solid-liquid interface the electron acceptors of solid will interact with the electron donors of liquid, and vice versa. Van Oss expressed the acid/base interaction in the following equation:

$$\gamma_{SL}^{AB} = 2\left(\sqrt{\gamma_S^+} - \sqrt{\gamma_L^+}\right)\left(\sqrt{\gamma_S^-} - \sqrt{\gamma_L^-}\right) \tag{3.10}$$

For a binary system like the solid-liquid interface the total free energy of interaction is

$$\gamma_{SL}^{Total} = \left(\sqrt{\gamma_S^{LW}} - \sqrt{\gamma_L^{LW}}\right)^2 + 2\left(\sqrt{\gamma_S^+} - \sqrt{\gamma_L^+}\right)\left(\sqrt{\gamma_S^-} - \sqrt{\gamma_L^-}\right) \tag{3.11}$$

or

$$\gamma_{SL} = \gamma_S + \gamma_L - 2(\sqrt{\gamma_S^{LW} \cdot \gamma_L^{LW}} + \sqrt{\gamma_S^+ \cdot \gamma_L^-} + \sqrt{\gamma_S^- \cdot \gamma_L^+}) \tag{3.12}$$

Combining this with Equation 3.3, the following equation is obtained:

$$\gamma_L \cdot (1+\cos\theta) = 2(\sqrt{\gamma_S^{LW} \cdot \gamma_L^{LW}} + \sqrt{\gamma_S^{+} \cdot \gamma_L^{-}} + \sqrt{\gamma_S^{-} \cdot \gamma_L^{+}}) \quad (3.13)$$

In order to determine the surface free energy components (γ_S^{LW}) and parameters γ_s^+ and γ_s^- of a solid, the contact angle must be measured by dropping three different liquids with known surface tension components ($\gamma_L^{LW}, \gamma_L^+, \gamma_L^-$), and two of them must be polar liquid, which means γ_L^+ and γ_L^- should not be zero for two tested liquids.

3.2.2 Equipment for contact angle measurement

In this study surface contact angles of prepared coatings were obtained by using a sessile drop method with a Dataphysics OCA-20 contact angle analyser. This instrument consists of a CCD video camera with a resolution of 768×576 pixel and up to 50 images per second, multiple dosing/micro-syringe units and a temperature controlled environmental chamber, as shown in figure 3.2. The drop image was processed by an image analysis system, which calculated both the left and right contact angles from the shape of the drop with an accuracy of ± 0.1 °. Three test liquids were used as a probe for surface free energy calculations: distilled water, diiodomethane (Sigma) and ethylene glycol (Sigma). The data for surface tension components of the test liquids are given in table 3.1

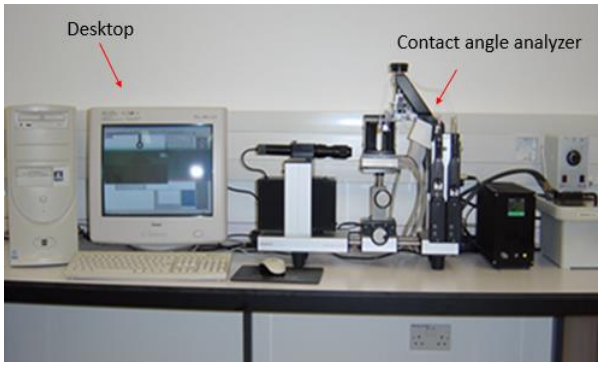

Figure 3.2 Dataphysics OCA-20 contact angle analyzer

In this study, the static contact angles of water, diiodomethane and ethylene glycol on prepared coatings including Ni-P, Ni-P-PTFE, Ni-P-PTFE-ZrO_2 and Ni-P-PTFE-ZrO_2-TiO_2 coatings were measured at 25 ℃ by the sessile drop technique and analysed by using Dataphysics OCA-20 contact angle analyzer. The samples were ultrasonically cleaned in acetone, ethanol and deionized water in sequence for 5 minutes before contact angle measurement.

Table 3.1 Test liquids and their surface tension components (Good 1992)

Surface tension data (mJ/m^2)	γ_L	γ_L^{LW}	γ_L^+	γ_L^-
Water, H_2O	72.8	21.8	25.5	25.5
Diiodomethane,CH_2I_2	50.8	50.8	0.0	0.0
Ethylene glycol,$C_2H_6O_2$	48.0	29.0	1.9	47.0

3.2.3 Surface free energy of coatings

As mentioned above, three different liquids including water, diiodomethane and ethylene glycol were dropped on the surface of coatings to measure their static contact angles, which will build up equations to calculate surface free energy and its component of prepared coatings by van Oss acid-base approach, besides these surface free energy components also can be used in extended DLVO theory to calculate the interaction energy between bacteria and prepared coatings in some liquid solution and explain bacterial preference to attachment to certain kind of coatings.

Table 3.2, 3.3 and 3.4 show the data of contact angle and the total surface free energy and its components of prepared coatings including Ni-P, Ni-P-PTFE, Ni-P-PTFE-ZrO_2 and Ni-P-PTFE-ZrO_2-TiO_2. Table 3.2 show data of Ni-P and Ni-P-PTFE coatings PTFE1 means Ni-P-PTFE coating prepared by 8ml/L PTFE; PTFE2 means Ni-P-PTFE coating prepared by 12ml/L. Table 3.3 shows data of Ni-P-PTFE-ZrO_2 coatings prepared by three different concentration of ZrO_2 including 0.625 g/L(Low), 1.25 g/L(Medium) and 1.875 g/L(High) and two different concentration of PTFE including 8ml/L and 12ml/L(P1 and P2) and coating P1ZrL means that coating prepared by 8ml/L PTFE(P1) and low concentration 0.625g/L of ZrO_2(ZrL) . Table 3.4 shows data of Ni-P-PTFE-ZrO_2-TiO_2 coatings prepared by three different concentration of TiO_2 including 0.4 g/L(Low), 0.8 g/L(Medium) and 1.2 g/L(High), two different concentration of PTFE including 8ml/L and 12ml/L(P1 and P2) and three different concentration of ZrO_2 including 0.625 g/L(Low), 1.25 g/L(Medium) and 1.875 g/L(High) and coating P1ZrLTiL means that coating prepared by 8ml/L PTFE(P1), low concentration 0.625g/L of ZrO_2(ZrL) and low concentration 0.4g/L TiO_2(TiL).

According to table 3.2, 3.3 and 3.4, we can see that compared with Ni-P coating, other coatings such as Ni-P-PTFE, Ni-P-PTFE-ZrO_2 and Ni-P-PTFE-ZrO_2-TiO_2 coatings have larger water contact angle and diiodomethane contact angle, but have less surface free energy ranging from 12.48 mJ/m^2 to 35.61 mJ/m^2. Ni-P-PTFE-ZrO_2 coatings have least surface free energy ranging from 12.48 mJ/m^2 to 27.21mJ/m^2. From the aspect of surface free energy component, Ni-P-PTFE-ZrO_2-TiO_2 coatings have larger γ^{LW} and γ^- than Ni-P-PTFE-ZrO_2 coatings especially for Ni-P-PTFE-ZrO_2-TiO_2 prepared by 8ml/L PTFE. For γ^+, all the coating did not show big differences each other, but Ni-P-PTFE-ZrO_2-TiO_2 coatings prepared by 12ml/L PTFE show larger γ^+ than those prepared by 8ml/L PTFE. Besides the surface free energy component of Ni-P-PTFE as a basic coating have a significant effect on the surface free energy component of Ni-P-PTFE based coatings especially for Ni-P-PTFE-ZrO_2-TiO_2 coatings. For example, Ni-P-PTFE coating 2 prepared by low concentration of PTFE have larger γ^{LW} and γ^- than Ni-P-PTFE coating 3 prepared by high concentration of PTFE, which leads to the larger γ^{LW} and γ^- of Ni-P-PTFE-ZrO_2-TiO_2 prepared by 8ml/L PTFE than that prepared by 12ml/L PTFE.

Table 3.2 Contact Angle and Surface Energy Components of Ni-P and Ni-P-PTFE Coatings

name	chemistry			Contact angle, θ			Surface free energy (mJ/m^2)				
	Ni-P & Ni-P-PTFE			θ^{di}	θ^{eg}	θ^{w}	γ^{LW}	γ^{+}	γ^{-}	γ^{AB}	γ^{TOT}
	$NiSO_4$(g/L)	NaH_2PO_2(g/L)	PTFE(ml/L)								
Ni-P	25	15	0	44.±1.2	60.±1.0	61.5±0.7	37.55	0.00	32.38	0.00	37.55
PTFE 1	25	15	8	76.8±2.0	75.2±0.4	88.6±1.8	19.18	0.30	7.78	3.08	22.26
PTFE 2	25	15	12	91.2±0.8	78.7±2.2	118.±3.5	7.68	2.96	4.63	7.41	15.09

Table 3.3 Contact Angle and Surface Energy Components of Ni-P-PTFE-ZrO_2 Coatings

name	chemistry		Contact angle, θ			Surface free energy (mJ/m^2)				
	Ni-P-PTFE-ZrO_2		θ^{di}	θ^{eg}	θ^{w}	γ^{LW}	γ^{+}	γ^{-}	γ^{AB}	γ^{TOT}
	PTFE(ml/L)	ZrO_2(g/L)								
P1ZrL	8	0.625	92.1±0.6	88.3±0.3	112.9±1.0	11.81	0.68	0.17	0.67	12.48
P1ZrM	8	1.250	91.2±0.8	78.7±2.2	118.±3.5	12.19	2.75	0.00	0.00	12.19
P1ZrH	8	1.875	86.4±0.6	77.3±1.3	109.±2.0	14.37	1.63	0.01	0.21	14.58
P2ZrL	12	0.625	82.5±0.9	75.2±1.1	95.1±1.0	16.21	0.68	4.08	3.33	19.58
P2ZrM	12	1.250	78.7±0.3	75.8±1.7	104.3±1.6	18.19	0.79	0.36	1.07	19.25
P2ZrH	12	1.875	72.1±1.3	60.6±2.8	83.6±1.6	21.73	1.04	7.23	5.48	27.21

Table 3.4 Contact Angle and Surface Energy Components of Ni-P-PTFE-ZrO_2-TiO_2 Coatings

name	chemistry			Contact angle, θ			Surface free energy (mJ/m^2)				
	Ni-P-PTFE-ZrO_2-TiO_2			θ^{di}	θ^{eg}	θ^{w}	γ^{LW}	γ^{+}	γ^{-}	γ^{AB}	γ^{TOT}
	PTFE (ml/L)	ZrO_2 (g/L)	TiO_2 (g/L)								
P1ZrLTiL	8	0.625	0.4	72.2±1.5	63.9±0.3	72.9±0.6	21.67	0.22	20.84	4.23	25.90
P1ZrLTiM	8	0.625	0.8	63.0±0.8	67.1±1.3	76.6±1.3	26.79	0.00	17.04	0.00	26.79
P1ZrLTiH	8	0.625	1.2	65.6±1.8	65.1±1.3	80.0+±0.5	25.38	0.10	12.17	2.22	27.60
P1ZrMTiL	8	1.250	0.4	67.4±1.1	64.8±0.1	85.1±1.4	24.36	0.33	7.24	3.10	27.45
P1ZrMTiM	8	1.250	0.8	61.0±0.9	59.7±0.7	79.5±0.9	28.02	0.23	9.96	3.01	31.02
P1ZrMTiH	8	1.250	1.2	60.0±0.8	63.1±0.2	80.8±1.0	28.592	0.06	10.07	1.57	30.17
P1ZrHTiL	8	1.875	0.4	57.4±0.8	59.9±1.2	75.3±1.1	30.08	0.03	14.33	1.39	31.48
P1ZrHTiM	8	1.875	0.8	59.3±0.7	58.4±1.0	53.8±0.5	29.00	0.00	42.11	0.00	29.00
P1ZrHTiH	8	1.875	1.2	47.6±0.1	59.6±0.5	77.4±0.1	35.61	0.00	10.68	0.00	35.61
P2ZrLTiL	12	0.625	0.4	86.6±0.2	59.8±0.7	88.4±1.3	14.25	5.69	2.35	7.32	21.57
P2ZrLTiM	12	0.625	0.8	83.2±1.9	53.7±1.0	94.0±0.4	15.89	9.22	0.00	0.00	15.89
P2ZrLTiH	12	0.625	1.2	87.1±0.1	55.1±0.8	97.6±1.2	14.72	8.56	0.00	0.00	14.72
P2ZrMTiL	12	1.250	0.4	77.5±0.9	58.4±0.2	92.7±0.5	18.79	4.88	0.42	2.88	21.67
P2ZrMTiM	12	1.250	0.8	81.0±0.4	67.8±0.2	101.8±0.8	16.99	3.82	0.00	0.00	16.99
P2ZrMTiH	12	1.250	1.2	72.0±0.9	58.6±0.5	94.7±0.2	21.76	3.88	0.11	1.32	23.08
P2ZrHTiL	12	1.875	0.4	62.2±0.7	51.5±0.3	81.4±1.5	27.33	1.21	5.57	5.18	32.51
P2ZrHTiM	12	1.875	0.8	67.5±1.2	58.2±0.7	95.4±0.4	24.30	1.82	0.40	1.70	26.00
P2ZrHTiH	12	1.875	1.2	58.3±0.4	50.1±0.4	64.5±1.0	29.60	0.26	22.82	4.88	34.45

4 METHODS OF TESTING COATINGS

4.1 Assays of Bacterial Adhesion and Removal

4.1.1 Types of Bacteria

There are two types of bacterial strains including gram-positive and gram-negative bacteria. The structure, compositions and functions of the cell wall are different between these two kinds of bacteria. For gram-positive bacteria, the cell wall consists of a 20-50nm thick rigid layer of peptidoglycan on top of cytoplasmic membrane and teichoic acids exist within the layer of peptidoglycan, which is the unique component of the gram-positive bacteria. For gram-negative bacteria, the cell wall is much more complex, which comprises the layer of peptidoglycan which is much thinner (about 1-2nm) and contains two layers of phospholipid membranes including an inner cytoplasmic membrane and an outer membrane covering the surface membrane; the unique component for the gram-negative bacteria are lipopolysaccharides, which exist on the outer membranes and have the capability of increasing the negative charge of cell membranes and contribute to the structural integrity and viability of the bacteria (Hajipour, Fromm et al. 2012).

In this study, the assays of bacterial adhesion and removal were conducted at the Biological and Nanomaterials Lab, University of Dundee. The bacteria involved in the experiments including gram-negative *Escherichia coli ATCC 25922* and gram-positive *staphylococcus aureus ATCC 25923*. Both of them are common bacteria which could cause medical device-associated infections. *Escherichia coli* are typically rod-shaped bacteria which are about 2.0 μm long and 0.25–1.0 μm in diameter. The optimal growth of *E.coli* occurs at 37ºC. On the other hand, *staphylococcus aureus* are sphere-shaped and are about 0.5−1.5 μm in diameter.

4.1.2 Bacterial Culture

Escherichia coli and *staphylococcus aureus* were originally collected by clinical isolation and then the strains were subcultured and stored in TSB solution (Tryptone Soya Broth, Oxoid®, UK) containing 15% glycerol as frozen stock at -80ºC. For bacterial assays, bacteria need to be cultured from a stationary phase. Firstly, agar plates TSA (Tryptone Soya Agar) were streaked out with a sterile loop after dipping in the stored bacterial solution and then the agar plates TSA were incubated overnight at 37ºC. Secondly, one colony was taken from the agar plate and inoculated in 5-10ml TSB solution and grown statically overnight at 37ºC. Thirdly, five hundred microliters were taken from the previous solution and mixed with 100ml TSB solution in a conical flask and grown in a shaker incubator for 3-5 hours at 37ºC with the speed of 200rpm and the rough concentration of bacteria (CFU) can be obtained by the value of OD_{600}. This should be checked every 30minutes after 2 hours of bacterial incubation to make sure that the value of OD corresponds to mid-exponential phase of bacteria. Finally, strains were harvested by centrifuge for 5 minutes with 4500rpm at -4ºC and after the bacteria were washed once again by sterile distilled water, the bacteria were resuspended in NaCl solution (0.9%) to ensure that the final concentration was 10^6 CFU/ml. The components of TSB and TSA are given in table 5.1.

Table 4.1 components of TSB and TSA

	components	Quantity(g/L)
TSA	Pancreatic digest of casein	17
	Papaic digest of soybean meal	3
	Sodium chloride	5
	Di-basic potassium phosphate	2.5
	Glucose	2.5
TSB	Tryptone	15
	Soya peptone	5
	Sodium chloride	5
	Agar	15

4.1.3 Growth Curve of Bacteria

Once bacterial strains are nourished in the TSB solutions, the size and number of the cell will increase, and there are associations between the logarithm of the cell number and incubation time, which can be plotted as the growth curve of bacteria and according to the growth curve, the growth of bacteria can be divided into four phases.

The first phase is lag phase. Bacteria strains will not have cell division behaviours which means that the number of bacterial strains does not increase in this phase; however, the size of cells will

increase and the enzyme production will be secreted. This phase will last from 1 hour to several days depending on the type of bacteria and environment such as temperature, medium and so on.

The second phase is the exponential or logarithmic phase. During this phase, the number of bacteria increases dramatically. Usually one cell will be divided into 2 cells, and the number of bacteria will reach to maximum at the end of this stage.

The third phase is the stationary phase. The number of total bacteria remains constant for the whole phase due to the similar rate of death and increase of bacteria.

The last phase is the death phase, which means that the number of viable bacteria decreased exponentially and growth rate is much less than death rate at this stage.

In this study, the bacteria in the logarithmic phase were used for bacterial adhesion and removal assays because they are more active and vigorous in this phase and experiment results are more reliable.

4.1.4 Assays Procedure of Bacterial Adhesion and Removal

4.1.4.1 Assay of Bacterial Adhesion

In this study, 10^6 CFU/ml of *Escherichia coli* and *staphylococcus aureus* suspension were prepared respectively. In order to test property of prepared coatings against bacterial adhesion, every coating with 5 other replicate coatings were immersed in a tank containing 100 ml bacterial suspension for 2 hours at 37 ^{o}C. After 2 hours, each coating was taken out by sterile forceps from the tank and dipped into sterile distilled water twice to remove residual bacterial suspension and some loosely attached bacteria. And then the number of bacteria adhered on the coating were counted by fluorescence microscope method.

4.1.4.2 Assay of Bacterial Removal

The purpose of assays of bacterial removal is to examine the adhesive strength between bacteria and prepared coatings, which is very significant to development of biofilm. The assay was conducted by using a dipping device which was designed by Zhao et al. (2008). As the figure 5.1 shows, the detailed process of the assay is that the dipping device can move the coating sample up and down 20 times into the water at constant 0.03 m/s speed (at a shear stress of 0.014N/m^2, which can be seen in equation 4.1) at 37^{o}C, and the shear stress from the interface between coatings and water leads to the removal of weakly adhered bacteria on the coating. The number of remaining attached bacteria and original attached bacteria on the coating can be counted by fluorescence microscope and the removal percentage can also be calculated. And the shear stress τ_w that acts on coatings can be calculated by the following equation (Zhao, Liu et al. 2008):

$$\tau_w = \frac{F_d}{b \times L} \tag{4.1}$$

$$F_d = \pm 0.646 b \sqrt{\rho \mu L U^3} \tag{4.2}$$

In equation 4.1, b and L represent the width of the coating and the depth of water which the coating is dipped in (0.075 m). ρ and μ represent density and viscosity of water which is 1000kg/m^3 and 0.6947 ×10^{-3} Pa s (37^{o}C). F_d is drag force which can be calculated by equation 4.2, where U is the dipping speed (0.03m/s).

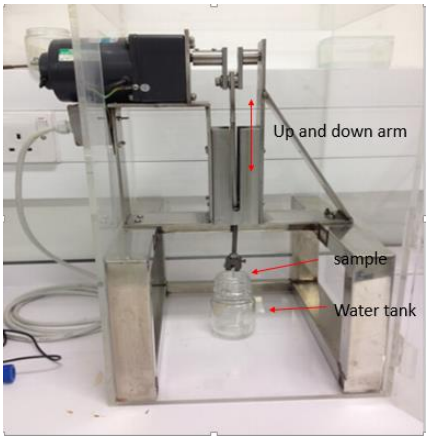

Figure 4.1 Dipping Device

4.1.5 Cell Counting Methods

There are a wide selection of methods to count the number of bacteria. For example, indirect methods such as dry weight calculation, turbidity and spectrophotometric method can calculate the number of bacteria by the relation between physical parameters and the amount of bacteria. Another strategy is direct method. There are two common direct methods including viable plate counts method and microscope method. Although there are advantages and disadvantages for indirect methods and direct methods, for our assays of bacterial adhesion and removal, direct methods are more suitable due to their accuracy.

4.1.5.1 Viable Plate Counts Methods

Viable plate is one of most significant methods to count bacteria. This method needs to collect the total bacteria adhered on the surface and disperse it into sterile water to become bacterial suspension. And then a certain volume of bacterial suspension was taken and incubate on TSA agar plate to count the number of bacteria. The detailed procedure is to dilute this certain volume of bacterial suspension to be 10^{-1}, 10^{-2}, 10^{-3} of original concentration of bacterial suspension, until the bacteria can be clearly counted on the agar plate. The optimal plates should present 30-

300 colonies, because if the number of colonies is less than 30, it is not suitable for statistical reasons. When the number is larger than 300, it is difficult to count the number accurately and it is also rather ineffective. Although the viable plate counts method can obtain accurate number of bacteria or Colony Forming Unites (CFU)/ cm^2, there are some drawbacks. The first one is that only viable bacteria can be incubated to be a colony on the TSA agar plate, which means that this method cannot count the dead bacteria on the surface, which is also very significant to development of biofilm and medical device-associated infections. The second one is that this counting method is not very effective. It needs to take 1-2 days to get results of bacterial assays. Therefore, the viable plate counts method is not first choice for assays of bacterial adhesion and removal in this study. However, in this study, viable plate counts method made a great contribution to plotting growth curves of different bacteria and to building up the relationship between value of OD_{600} and concentration of bacteria, which is very important to obtain bacteria at the logarithmic phase as mentioned above.

4.1.5.2 Fluorescence Microscope Methods

Compared with viable plate counts methods, Fluorescence microscope method is highly effective and can obtain the results of bacterial assays immediately. Besides, Fluorescence microscope methods can count both alive and dead bacteria by staining bacteria with fluorescent dyes, which can be observed by a fluorescence microscope.

In this study, we use the fluorescence microscope method to calculate the number of bacteria (CFU/cm^2) on the surface. With the help of LIVE/DEAD *BacLight* bacterial viability kit, the colours of the stained alive and dead bacteria look different when they were observed by fluorescence microscope. The reason is that the kit includes two kinds of nucleic acid stains and they are SYTO 9 and propidium iodide. SYTO 9 stain can penetrate most membranes, while

propidium iodide stain usually cannot permeate membranes of live cells but damaged or dead membrane. Which means propidium iodide can only stain the dead bacteria. When bacteria are stained by these two nucleic acids, with the aid of fluorescent light emitted from fluorescence microscope, the colour of viable bacteria is green and the colour of dead bacteria is red. The detailed procedures of counting bacterial by fluorescence microscope method can be concluded as followed:

Firstly, after assays of bacterial adhesion or removal as mentioned above, 5ul of SYTO 9 and propidium iodide were used to stain the bacteria at different areas of the coating respectively. With the help of coverslip, the stained area of SYTO 9 and propidium iodide can both reach to 1 square centimeter. And after staining for 15min in the dark environment, the stained bacteria can be observed by fluorescence microscope.18 fields of each coating were chosen and observed to count live and dead bacteria (9 fields for alive bacteria and 9 fields for dead bacteria) and the final number of bacteria will be the mean value of 9 fields.

In our lab, a BX41 Olympus Fluorescence Microscope with QICAM High-Performance Digital CCD Camera and Image-pro Plus software was used to count the bacteria on the surface of coatings, and the number of bacteria on each chosen field of surface can be accurately counted manually or automatically with the help of *Image Pro Plus* software.

4.2 Anticorrosion Assays

As mentioned in the literature review part, corrosion is a ubiquitous process and the effect of corrosive behaviour of implanted medical devices in the human body is enormous. For example, the release of metal ions or particles from the medical devices due to corrosive behaviour not only can cause adverse tissue responses and postimplantation complication, but also it can reduce

the working life of medical devices. Overall, it is very significant to test the anticorrosive property of coatings used for medical devices.

4.2.1 Classification of Anticorrosive Assays

Basically, there are two types of methods to evaluate anticorrosive capability of materials. One is testing in vivo. For example the medical device can be implanted into the body of animals such as rabbits. By blood test, pathological examination and X-ray examination to evaluate the anticorrosive property of medical devices (Hou, Li et al. 2014). One of the advantages is the environment where the medical devices implanted is similar to that in human body, which means the result of anticorrosive evaluation of coatings is more convincing. However, this kind of assays in vivo needs long period of time to obtain the results.

Another type of test is conducted in vitro. This kind of assays are often conducted in a simulated environment for better reproducibility. And according to different requirements, there are several methods used for testing anticorrosive property of materials in the lab such as electrochemical test, planned-interval test (weight-loss) and so on. And in this study, the anticorrosive property of a series of Ni-P-PTFE-ZrO_2 and Ni-P-PTFE-ZrO_2-TiO_2 coatings are tested by electrochemical corrosion method because it produces the results more quickly than other laboratory test. The entire polarization curve which show anodic and cathodic behaviour of the coating in a specific solution requires just only minutes to a few hours.

4.2.2 Electrochemical Corrosion Test

4.2.2.1 Three-Electrode Electrochemical Corrosion System

In this study, potentiostatic polarization scan is used for electrochemical test. The device we use to examine the anticorrosive property of Ni-P-PTFE-ZrO_2 and Ni-P-PTFE-ZrO_2-TiO_2 coatings is three-electrode system which is shown in figure 4.2. Three-electrode electrochemical corrosion system consists of working electrode, auxiliary electrode and reference electrode. From figure 4.2, we can see that these three electrodes immerse into electrolyte solutions and connect with an electronic device called a potentiostat to form a test cell. The function of each electrode can be concluded as followed: the working electrode is the anode of the cell and connect to the specimen which needs to be tested, which means that corrosion reactions happened on this electrode and the coupon corrodes and goes into solution in the form of metal ions; while cathode reactions happen on the auxiliary electrode. At the cathode, some reducible species in the electrolyte adsorbs and picks up electrons, although the cathode itself does not react. Reference electrode is used as a reference electrode potential for polarization of the other two.

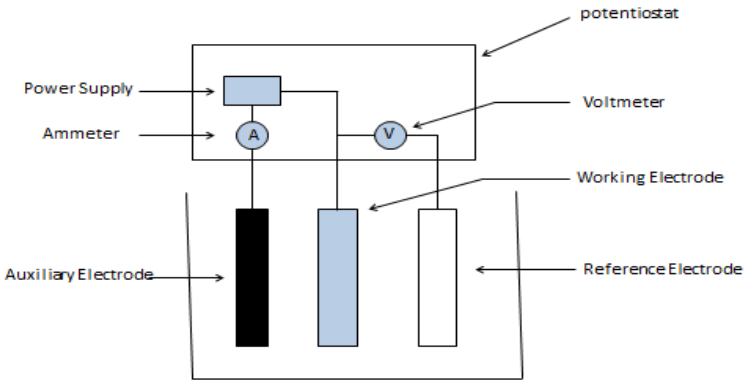

Figure 4.2 Three-electrode polarization circuit

In this assays, Ni-P-PTFE-ZrO_2 and Ni-P-PTFE-ZrO_2-TiO_2 coatings are working electrode. While Pt and SCE were the auxiliary and reference electrodes respectively. Working electrode and auxiliary electrode Platinum (Pt) immersed directly in the NaCl electrolyte solution. While reference electrode the Saturated Calomel Electrode (SCE) connect to the cell via the salt bridge probe to ensure the reference electrode cannot be contaminated to affect the reference potential. The tests were performed at room temperature (25^oC). And the test started after 15min preheat of the system.

4.2.2.2 Measurement of Open Circuit Potential and Potentiodynamic Polarization Plot

Measurement of open circuit potential and potentiodynamic polarization are conducted. The open circuit potential of working electrode was measured and plotted as a function of time. The tests last for about 2-3 hours. The open circuit potential is the reflection of the thermodynamic stability of material. While during the measurement of potentiodynamic polarization, the tafel polarization curve can be achieved, which consist of cathodic polarization curve and anodic polarization curve, which can be seen in the figure 4.3. The reason of producing cathodic polarization curve and anodic polarization curve is that the potentiostat monitors the potential of the coupon compared with the reference electrode. And if the potential is not the desired value set on the instrument, the potentiostat will change the cell current between working electrode and auxiliary electrode to bring the potential to the desired value, and the potential and resulting current are recorded. And with the potential increasing slightly, the tafel polarization curve are drawn, According to tafel polarization curve the corrosion potential (E_{corr}), polarization resistance (R_p), corrosion current density (I_{corr}), and corrosion rate (CR) can be obtained.

The corrosion potential (E_{corr}) and corrosion current density (I_{corr}) can be directly obtained by tafel polarization curve. As figure 4.3 shows, when cathodic polarization curve and anodic

polarization curve intersect, the corresponding potential is E_{corr} and I_{corr} can be obtained by superimpose a straight line along the linear portion of the anodic and cathodic curve and extrapolate it through E_{corr}. And according to the slope of the straight line fitting to the tafel polarization curve, anodic Tafel constant (β_A) and cathodic Tafel constant (β_C) can be obtained.

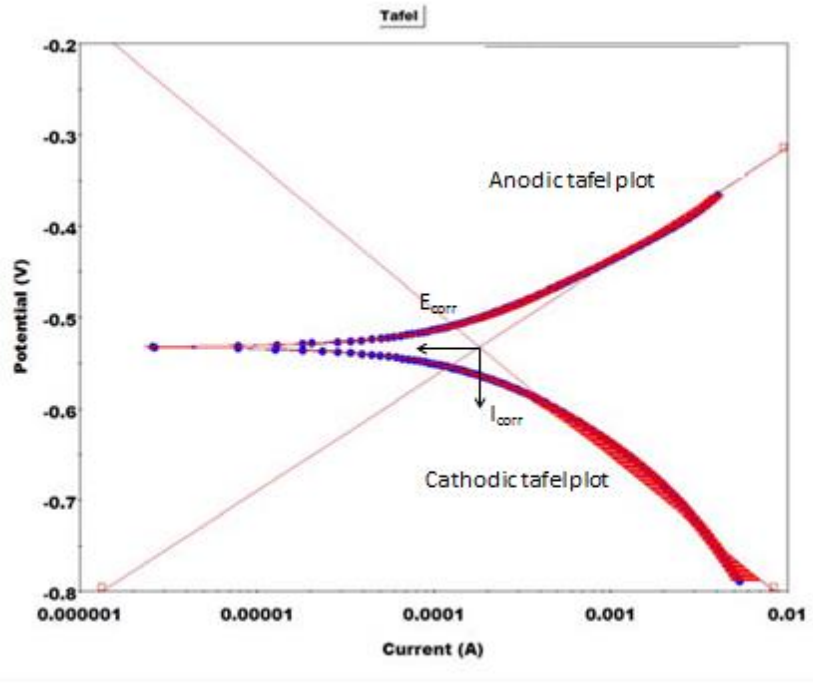

Figure 4.3 Anodic and Cathodic Tafel Plots

I_{corr} is very important parameter, which can be related to the rate of the electrochemical reaction, since it is a measure of the number of electrons that flow in a given period of time. Once I_{corr}, anodic Tafel constant (β_A) and cathodic Tafel constant (β_C) has been determined, polarization resistance (R_p) can be calculated by the following equation (RYU and SHROTRIYA 2013):

$$R_p = \frac{\beta_A \beta_C}{2.3 I_{corr}(\beta_A + \beta_C)} \quad (4.3)$$

R_P value not only can provide quantitative information as corrosion current and corrosion rate do, it also can contribute to assessing the relative ability of a material to resist corrosion if samples

have equal surface area and the materials with the highest R_P have the highest corrosion resistance.

5 PREPARATION OF Ni-P-PTFE BASED NANOCOMPOSITE COATINGS

5.1 Deposition Mechanisms of Electroless Ni-P-PTFE-ZrO_2 and Ni-P-PTFE-ZrO_2-TiO_2 coatings

Ni-P-PTFE based coatings including Ni-P-PTFE, Ni-P-PTFE-ZrO_2, Ni-P-PTFE-ZrO_2-TiO_2 and Ni-P-PTFE-TiO_2 are prepared by the electeroless plating technique. The detailed procedure of synthetizing these coatings above can be briefly described as follows: firstly, a thin Ni layer was plated on the stainless steel sheets in the activation steps which will be introduced below; secondly, Ni-P coatings were synthetized to form a sub-layer by the electroless plating technique, which would enhance the strength of adhesion between substrates and electroless coatings, because the preparation of coatings from the thin Ni layer to Ni-P coatings to Ni-P-PTFE based coatings is much better acting as a gradient process compared with the preparation of coatings directly from Ni layer to Ni-P-PTFE based coatings. After the preparation of Ni-P coatings, a series of Ni-P-PTFE based coatings including Ni-P-PTFE, Ni-P-PTFE-ZrO_2 and Ni-P-PTFE-ZrO_2-TiO_2 are prepared by co-depositing nanoparticle PTFE, ZrO_2, TiO_2 into Ni-P matrix. Figure 5.1 shows the preparation procedure of electroless Ni-P-PTFE based coatings.

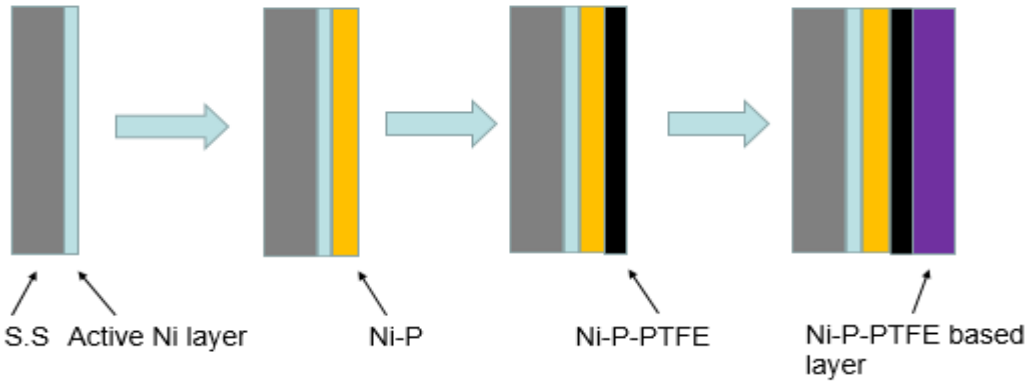

Figure 5. 1 Preparation procedure of electroless Ni-P-PTFE based coatings

In this study, for the preparation of Ni-P-PTFE based coatings, the nickel ions in the electroless plating solution are reduced by atomic hydrogen which is generated by hypophosphite, and elemental phosphorus was also generated during this reaction, which contributes to the generation of Ni-P coatings (Brenner and Riddell 1946). During this procedure, nickel sulfate ($NiSO_4$ $6H_2O$) is used as the nickel source; hypophosphite is used as a reducing agent; elemental nickel acts as a catalyst, which is firstly deposited in stainless steel sheets during the activation step which is a significant step before preparing Ni-P coatings by the electroless plating technique. Finally a Ni-P sub-layer was prepared on the stainless steel sheets and Ni-P-PTFE coatings will be developed based on this Ni-P coating. The mechanism of Ni-P and Ni-P-PTFE based coatings is shown by following five steps of chemical reactions (Brenner and Riddell 1946):

Firstly, atomic hydrogen was generated by the reaction between water and hypophosphite. The atomic hydrogen is absorbed at the catalytic surface:

$$H_2PO_2^- + H_2O \xrightarrow{catalytic} HPO_3^{2-} + H^+ + 2\,[H] \qquad (5.1)$$

It is also argued that the formation of atomic hydrogen is due to the dehydrogenation of the hypophosphite ion during formation of the metaphosphite ion (Gutzeit G, 1959):

$$H_2PO_2^- \xrightarrow{catalytic} PO_2^- + 2\,[H] \qquad (5.2)$$

This is followed by the formation of an orthophosphite molecule and a hydrogen ion (Brenner and Riddell 1946):

$$PO_2^- + H_2O \rightarrow HPO_3^{2-} + H^+ \qquad (5.3)$$

Secondly, nickel ions are reduced by the absorbed atomic hydrogen and generated on the stainless steel sheet:

$$Ni^{2+} + 2[H] \rightarrow Ni^{0} + 2H^{+} \quad (5.4)$$

During the process of reduction of nickel ions, hydrogen gas will be produced on the stainless steel sheet, which is due to the recombination of two atomic hydrogen atoms:

$$2\,[H] \rightarrow (H + H) \rightarrow H_2 \quad (5.5)$$

Thirdly, the reaction between hypophosphite and atomic hydrogen results in the formation of elemental phosphorus:

$$H_2PO^{2-} + [H] \rightarrow H_2O + OH^{-} + P^{0} \quad (5.6)$$

Fourthly, Nickel and phosphorus were codepositted on the stainless steel to form Ni-P coatings.

$$Ni + P \rightarrow Ni\text{-}P \quad (5.7)$$

Finally, different particles such as Nickel, phosphorus, ZrO_2, TiO_2 and PTFE codeposit on the Ni-P matrix.

$$Ni + P + PTFE \rightarrow Ni\text{-}P\text{-}PTFE \quad (5.8)$$

$$Ni + P + PTFE + ZrO_2 \rightarrow Ni\text{-}P\text{-}PTFE\text{-}ZrO_2 \quad (5.9)$$

$$Ni + P + PTFE + ZrO_2 + TiO_2 \rightarrow Ni\text{-}P\text{-}PTFE\text{-}ZrO_2\text{-}TiO_2 \quad (5.10)$$

ZrO_2, TiO_2, PTFE particles with surfactant will be codeposited into the Ni-P matrix in the following three different ways:

The first way is physical adsorption: ZrO_2, TiO_2 and PTFE particles in the solution diffuse onto the active catalytic surface by intermolecule force.

The second way is chemical adsorption: ZrO_2, TiO_2 and PTFE particles directly adsorb to the active substrate by chemical covalent bond force.

The third way is electrostatic adsorption: different particles such as ZrO_2, TiO_2 and PTFE particles with different charge also will have electrostatic interaction with the Ni-P matrix.

5.2 Preparation of Electroless Ni-P-PTFE-ZrO_2 and Ni-P-PTFE-ZrO_2-TiO_2 Coatings

In this study, Ni-P, Ni-P-PTFE and Ni-P-PTFE based coatings including Ni-P-PTFE-ZrO_2 and Ni-P-PTFE-ZrO_2-TiO_2 are prepared on 316L stainless steel sheet. The size of the sheet is 25mm×25mm×1mm, and before the coatings are prepared by electroless plating technique, pre-treatment procedure of the coatings needs to be completed, which are listed in table 5.1.

As table 5.1 shows, pre-treatment procedure includes four basic steps. The first one is alkaline cleaning and the function of this step is to remove the ester compounds on the surface of stainless steel sheets. The composition of alkaline cleaning solution used in this study is shown in table 5.2. After the immersion of sheets in the alkaline solution at 80^oC for 10min, the sheets need to be cleaned by deionised water at room temperature.

Table 5.1 Pretreatment procedures of Ni-P-PTFE based electroless coatings

Procedures	Bath composition and operating conditions
Alkaline cleaning	NaOH: 20-35 g/l; Na_3PO_4: 25-35 g/l; Na_2CO_3: 25-30 g/l; Na_2SiO_3: 5-10 g/l; 60-80 ℃; 5-10 min.
Rinsing	H_2O; room temperature
Electrocleaning	NaOH : 20-35 g/l; Na_3PO_4: 25-35 g/l; Na_2CO_3: 25-30 g/l; Na_2SiO_3: 5-10 g/l; room temperature; 2-3 min; voltage: 5-7 V.
Rinsing	H_2O; room temperature
Pickling	HCl (30%):H_2O=1:1; room temperature, 0.5-1 min.
Activation	$NiCl_2 \cdot 6H_2O$:200-400 g/l; HCl (30%):75-200 ml/l; anode plates: Ni; current density: 2~3 A/dm^2; room temperature; 1-3 min.

Next step is electrocleaning. The detailed procedure for this step can be described as follows: the sheet used to prepare Ni-P-PTFE based coatings and another two stainless steel plates are immersed in the alkaline solution. They connect with DC power supply and form an electrolytic cell as shown in Figure 5.2. The sheet used for preparing the coating is connected to an anode and another two stainless steel plates are connected to cathodes. The content of the electrocleaning solution is the same as that of alkaline cleaning solution, which can be seen in table 5.2. The purpose of the electrocleaning is to further clean the sheet, and this step is conducted under direct current voltage (about 5 V) at room temperature for 3 min, followed by deionised water.

Table 5.2 Compostion of Alkaline Cleaning Solution

Component	concentration
NaOH	20~25 g/l
Na_3PO_4	25-35g/l
Na_2CO_3	20-30g/l
Na_2SiO_3	5~10g/l

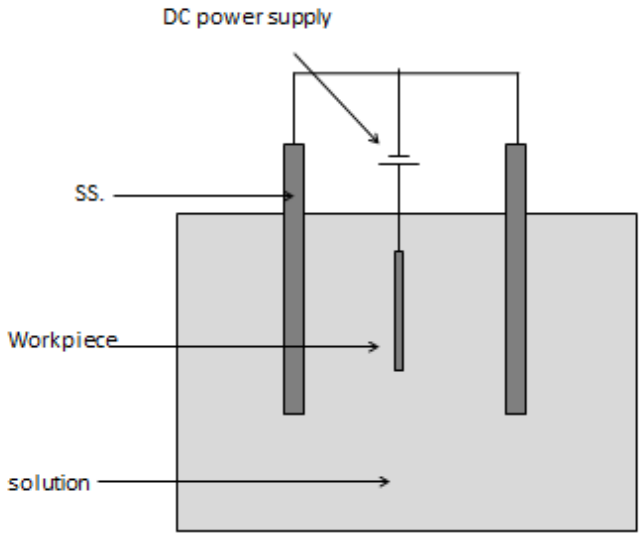

Figure 5. 2 Schematic drawing of cathodic eletrocleaning device

The third step is pickling, the oxidized film can be removed in this step, and the time of pickling should be controlled to about 1min because the time should ensure that the oxidized film is removed and the surface of the sheet should not be exceedingly eroded by hydrochloric acid solution.

The final step is activation. The reason to conduct activation of the surface of the sheet is that stainless steel is an inert metal and activation is necessary to make sure that the reaction of the electroless plating can be conducted quickly when the sheet is immersed in the electroless plating solution under 85^{o}C. During the activation step, a thin layer of elemental Ni can be generated on the surface of the stainless steel sheet. As we mentioned above, Ni^{2+} was reduced by atomic hydrogen to generate Ni-P coatings, but atomic hydrogen was generated by the reaction between water with hypophosphite with the help of catalysis, and elemental Ni itself is a catalyst during preparing Ni-P-PTFE based coating, which means that this elemental Ni layer can accelerate the initial reaction between Ni ions and reduction agents. It also can ensure that the reaction between Ni ions and reduction agents can happen on the surface of the sheet, and the strength of adhesion between stainless steel and Ni-P coatings is strong enough to avoid peeling.

Similar as the procedure of alkaline cleaning, the sheet and another two nickel plates immersed in activation solution and connect with DC power supply to form an electrolytic cell; however, the sheet used for preparing coatings should be connected to the cathode and the two stainless steel plates are connected to the anode to ensure both sides of the sheet can deposit the thin layer of Ni, which is shown in figure 5.3. The composition of the activation solution used in this study is shown in table 5.3. After activation, the sheet was rinsed with deionized water at room temperature and transferred them into electroless plating solution immediately.

Table 5.3 Composition of Activation Solution

Component	Concentration
$NiCl_2 \cdot 6H_2O$	200~400 g/l
HCl (30%)	75~200ml/l

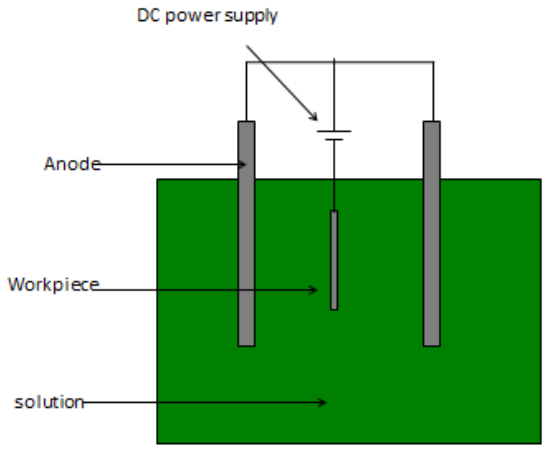

Figure 5. 3 Schematic drawing of activation device

5.3 Bath Composition of Electroless Ni-P-PTFE-ZrO_2 and Ni-P-PTFE-ZrO_2-TiO_2 coatings

The composition of electroless plating solution which is used to prepare Ni-P and Ni-P-PTFE based coatings is shown in table 5.4 including the source of Nickel, reducing agent, complexing agent and buffering agent.

For the nickel source, there are several sources of nickel which can be chosen, such as nickel sulfate, nickel chloride, nickel hypophosphite (Ni $(H_2PO_2)_2$) and nickel acetate. In this study nickel sulfate ($NiSO_4 \cdot 6H_2O$) is used as nickel source. The reason is that chloride anion of nickel chloride has a negative effect on the anticorrosive property of prepared Ni-P-PTFE based coatings and the drawback of nickel acetate is the lower rate of Ni in mass compared with nickel

Table 5.4 Bath composition and operating conditions for electroless Ni-P and Ni-P-PTFE based nano-composite coating

Composition	Ni-P	Ni-P-PTFE	Ni-P-PTFE-ZrO_2	Ni-P-PTFE-ZrO_2-TiO_2
$NiSO_4$ $6H_2O$ (g/L)	25	25	25	25
$Na_3C_6H_5O_7$ H_2O (g/L)	15	15	15	15
NaH_2PO_2 H_2O (g/L)	15	15	15	15
CH_3COONa (g/L)	15	15	15	15
PTFE (ml/L)	0	8-12ml/L	8-12ml/L	8-12ml/L
ZrO_2 (g/L)	0	0	0.625-1.875	0.625-1.875
TiO_2 (g/L)	0	0	0	0.4-1.2
Temperature(^oC)	85	85	85	85
PH	4.8	4.8	4.8	4.8
Stirring(rpm)	0	60	60	60

sulfate. Although $Ni(H_2PO_2)_2$ is the best candidate to be the source of nickel because no other elements are brought into Ni-P coatings, the price is much higher than other nickel salts which makes it to be second choice. Therefore, nickel sulfate ($NiSO_4$ $6H_2O$) was used in this research, and the molecular mass of $NiSO_4$ $6H_2O$ is 262.86g/mol.

For reducing agent, there are many reducing agents which have been commercially used such as sodium hypophosphite, amino boranes, sodium borohydride and hydrazine (Sudagar, Lian et al. 2013). Compared with boron and hydrazine, sodium hypophosphite costs less but reduces more

nickel ion. For example, 1kg sodium hypophosphite can reduce 200g nickel, and efficiency is as high as 37% (Mallory 1974). Besides, Ni-P coatings reduced by hypophosphite have better corrosion resistance property compared with Ni-B coatings which are reduced by sodium borohydride (Sudagar, Lian et al. 2013).

Complexing agents are also necessary in the process of electroless plating of Ni-P and Ni-P-PTFE based coatings. They play a key role in preventing the decomposition of electroless plating solution and ensure the reaction only happens on the catalytic surface. And in this study Sodium citrate ($Na_3C_6H_5O_7$ $2H_2O$) is used as the complexing agent. For Ni-P-PTFE based coatings, the quality of the coating including roughness, porosity and internal stress, relies on the stable plating solution. Sodium citrate not only can slow the decrease of pH value, but it also can prevent the precipitation of nickel salts and decrease the concentration of free nickel by coordinating to the nickel ion or free nickel with its polydentate ligands to form chelate rings, which have an enormous effect on stability of the plating solution.

As mentioned above, hydrogen ion was produced during the electroless plating of Ni-P-PTFE based coatings, which means that the pH value will decrease with the increase of plating time and the instability of the electroless plating solution will lead to the failure of preparation of Ni-P-PTFE based coatings. Therefore the role of buffering agents is to minimize the change of pH value and keep the stability of the electroless plating solution. In this study, Sodium citrate ($Na_3C_6H_5O_7$ $2H_2O$) also can make some contribution to maintaining the pH value of the electroless plating solution, however it mainly acts as a complexing agent. Buffering agents usually contain a mixture of weak acid or weak alkali and their salt. In this study, sodium acetate (CH_3COONa) is used as a buffering agent.

5.4 Materials and Equipment for Electroless Plating

The sheet for preparing Ni-P-PTFE based coatings was stainless steel 316L plates (Goodfellow Company, UK). The composition of the stainless steel includes iron 69%, chromium 18%, nickel 10%, molybdenum 3%, and the density is 7.96 g/cm^3. The chemicals used for preparing Ni-P-PTFE based coatings were from the Sigma-Aldrich company, UK and Fisher Company, UK. For example, nanoparticle ZrO_2 and TiO_2 were bought from Aldrich, with particle size of 100nm and 25 nm respectively. And 60 wt % PTFE emulsion was obtained from Aldrich, with a particle size in the range of 0.05-0.5μm.

6 EXPERIMENTAL RESULTS AND DISCUSSION

6.1 Assays of Bacterial Adhesion and Removal

In this part, bacterial adhesion and removal assays are conducted on two different kinds of Ni-P-PTFE based nano-composite coatings including Ni-P-PTFE-ZrO_2 and Ni-P-PTFE-ZrO_2-TiO_2 coatings to investigate the adhesive strength of bacteria to different coatings and their capability of resisting bacterial adhesion. Two different bacteria including gram-negative *Escherichia coli* and gram-positive *staphylococcus aureus* are used in the assays of bacterial adhesion and removal. Besides, the effect of total surface free energy and its components of the coating on bacterial adhesion and removal were also investigated.

6.1.1 Ni-P-PTFE-ZrO_2 Coatings

In this study, a series of Ni-P-PTFE-ZrO_2 coatings were prepared with different content of PTFE and ZrO_2 by altering the concentration of PTFE and ZrO_2 in the electroless plating solution. And there were three different concentrations of ZrO_2 including 0.625 g/L, 1.25 g/L and 1.875 g/L and two different concentrations of PTFE including 8ml/L and 12ml/L used to prepare 6 different coatings to test them whether or not to have the capability of resisting bacterial adhesion effectively and removing adhered bacteria easily. As mentioned above, bacterial adhesion play a key role in development of biofilm and medical device associated infection. And the strength of bacterial attachment on the coatings have a significant effect on controlling and removing adhered bacteria. Therefore in this part, we conduct bacterial adhesion and removal assays to evaluate prepared Ni-P-PTFE-ZrO_2 coatings.

The bath composition and operating conditions for electroless Ni-P-PTFE-ZrO_2 nano-composite coatings is given in table 3.4. ZrO_2 nano-powder was brought from Aldrich, and the particle size of ZrO_2 is less than 100 nm. Detailed information of different coatings such as coating 1-9 are shown in table 4.2 and 4.3. Experimental procedure of bacterial adhesion and removal are introduced in section 5.4.1. The assay of bacterial adhesion such as *Escherichia coli* and *Staphylococcus aureus* on the Ni-P-PTFE-ZrO_2 was investigated by immersing the coatings in the bacterial suspension of 10^6 cells/ml for 2h at 37 ^oC.

6.1.1.1 Effect of ZrO_2 on Bacterial Adhesion and Removal

In this part, capability of Ni-P-PTFE-ZrO_2 coatings against bacterial adhesion and removing adhered bacteria on the coating are presented from Figure 6.1 to Figure 6.6.

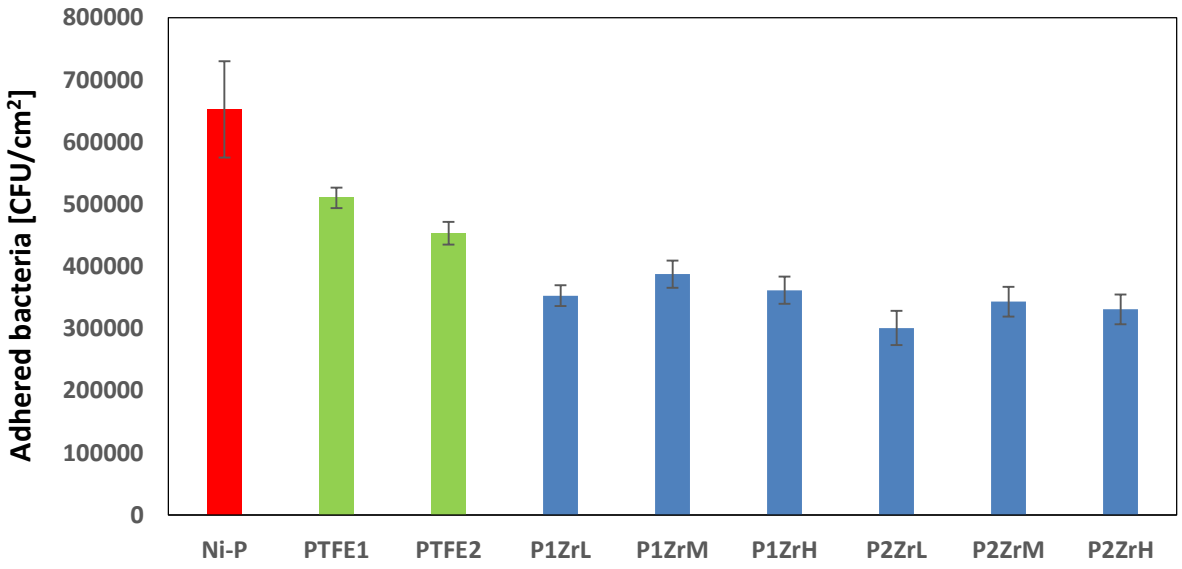

Figure 6.1 Adhesion of *Escherichia coli* on Ni-P-PTFE-ZrO_2 coatings

Figure 6.1 indicates that Ni-P-PTFE-ZrO_2 coating performed better capability against *E. coli* adhesion compared with Ni-P and Ni-P-PTFE coatings. Compared with Ni-P and Ni-P-PTFE

coatings, the number of *E. coli* adhesion on the Ni-P-PTFE-ZrO_2 coatings (CFU/cm^2) was 54.1% -59.4% of Ni-P coating and 69.2%-76.0% and 66.4%-75.7% of Ni-P-PTFE coatings which were prepared by low concentration of PTFE (8ml/L) and high concentration of PTFE (12ml/L) respectively. The results demonstrates addition of nanoparticle ZrO_2 have a positive effect on resisting bacterial adhesion. And coatingP1ZrL and coatings P2ZrL which were prepared by low concentration of ZrO_2 (0.625 g/L) present better performance against adhesion of *E. coli.*

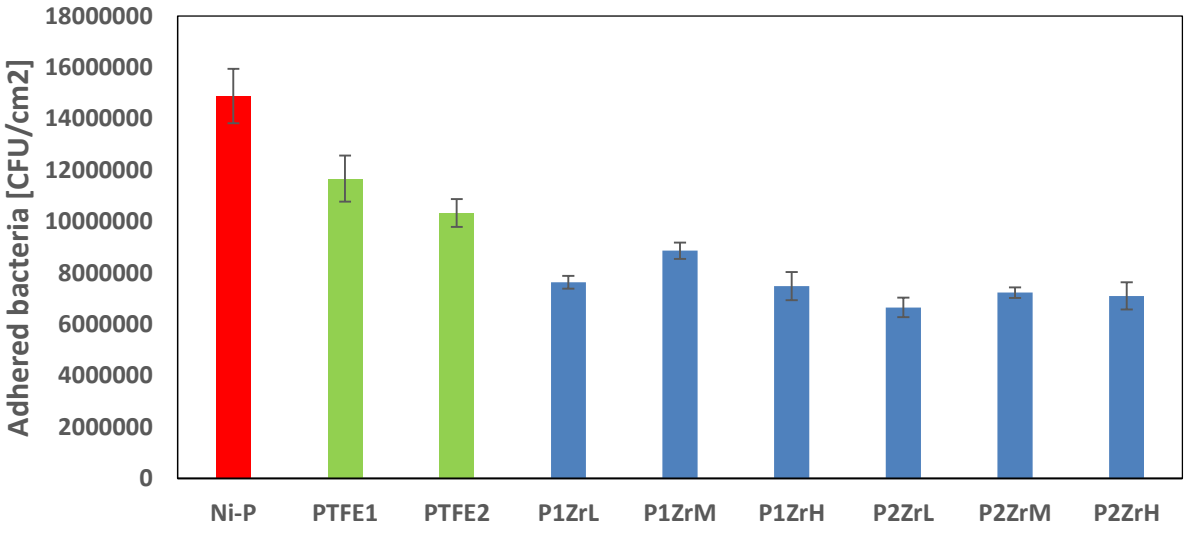

Figure 6.2 Adhesion of *Staphylococcus aureus* on Ni-P-PTFE-ZrO_2 coatings

Figure 6.2 shows that the result of Ni-P-PTFE-ZrO_2 coatings against *Staphylococcus aureus* adhesion of Compared with Ni-P and Ni-P-PTFE coatings, the number of bacterial adhesion on the Ni-P-PTFE-ZrO_2 coatings (CFU/cm^2) was 44.7%-51.3% of Ni-P coating, 64.1%-76.0% and 64.4%-70.0% of Ni-P-PTFE coatings which are prepared by low concentration of PTFE (8ml/L) and high concentration of PTFE (12ml/L) respectively. Similar as the result from figure 6.1, Figure 6.2 demonstrates addition of nanoparticle ZrO_2 plays a significant role in resisting

bacterial adhesion. And coating P1ZrL and coating P2ZrL which were prepared with 0.625 g/L of ZrO_2 present better performance against adhesion of *staphylococcus aureus.*

In conclusion, Ni-P-PTFE-ZrO_2 coatings prepared by low concentration of ZrO_2 (0.625g/L) have better capability of resisting bacterial adhesion such as *E. coli* and *S. aureus* adhesion. And it can be explained by the effect of total surface free energy of Ni-P-PTFE-ZrO_2 coatings on number of adhered bacteria, which is shown in figure 6.7 and 6.18. Beside, in chapter 7, according to XDLVO theory, we simulated the procedure of bacterial adhesion on the coating, and it also can explain why coating P1ZrL and coating P2ZrL adhered less bacteria by analysing total interaction energy between bacteria and coatings.

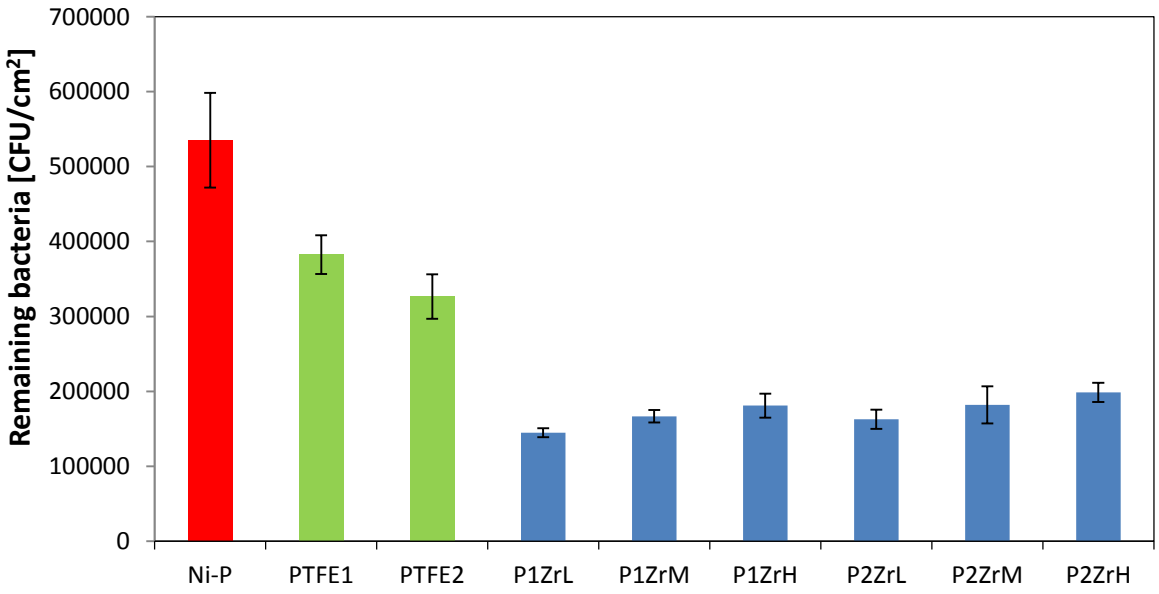

Figure 6.3 Remaining *Escherichia coli on* Ni-P-PTFE-ZrO_2 coatings after dipping process

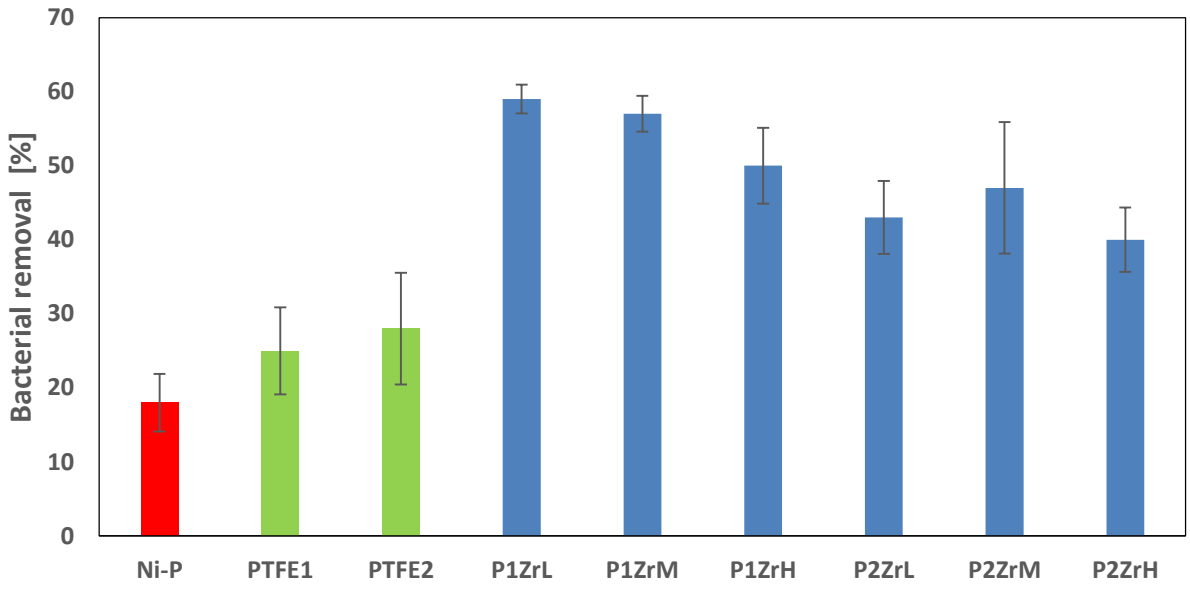

Figure 6.4 removal percentage of *Escherichia coli from* Ni-P-PTFE-ZrO_2 coatings after dipping process

Figure 6.3 and Figure 6.4 show the results of bacterial removal assays. It can be seen from Figure 6.3 that Ni-P-PTFE-ZrO_2 coatings prepared by higher concentration of ZrO_2 remained larger number of *Escherichia coli* cells on the Ni-P-PTFE-ZrO_2 coatings after dipping process, which means the strength of bacterial adhesion is larger. Coating P1ZrL which is prepared by 8ml/L PTFE and 0.625g/L ZrO_2 remains least number of *E. coli*. Compared with Ni-P coating, and Ni-P-PTFE coatings prepared by low (8ml/L) and high (12ml/L) concentration of PTFE, the remaining number of bacteria on the coating P1ZrL was 26.0% of Ni-P, 36.8% and 44.3% of Ni-P-PTFE coatings respectively.

While Figure 6.4 shows the removal percentage of *Escherichia coli* from Ni-P-PTFE-ZrO_2 coatings after dipping process. Ni-P-PTFE-ZrO_2 coatings show higher bacterial removal percentage than Ni-P and Ni-P-PTFE coatings, Coating P1ZrL still has the highest removal percentage of adhered *E. coli*. Compared with Ni-P coatings and Ni-P-PTFE coatings whose

removal percentage are 18%, 25% and 28% respectively, while the removal percentage of coating P1ZrL is 59%.

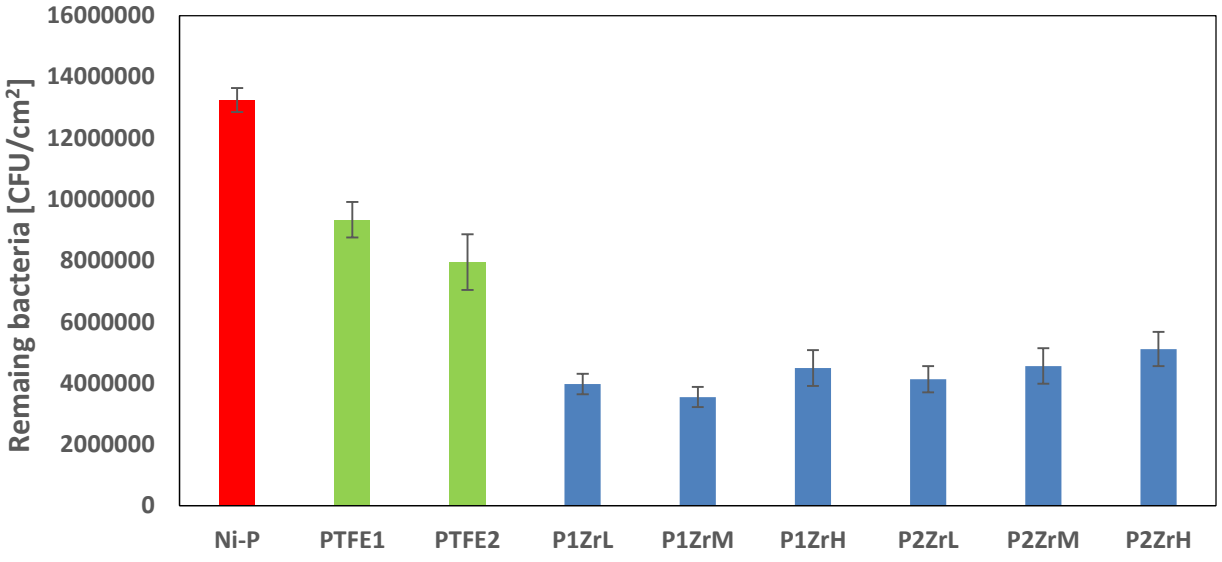

Figure 6.5 Remaining *Staphylococcus aureus* cells on Ni-P-PTFE-ZrO_2 coatings after dipping process

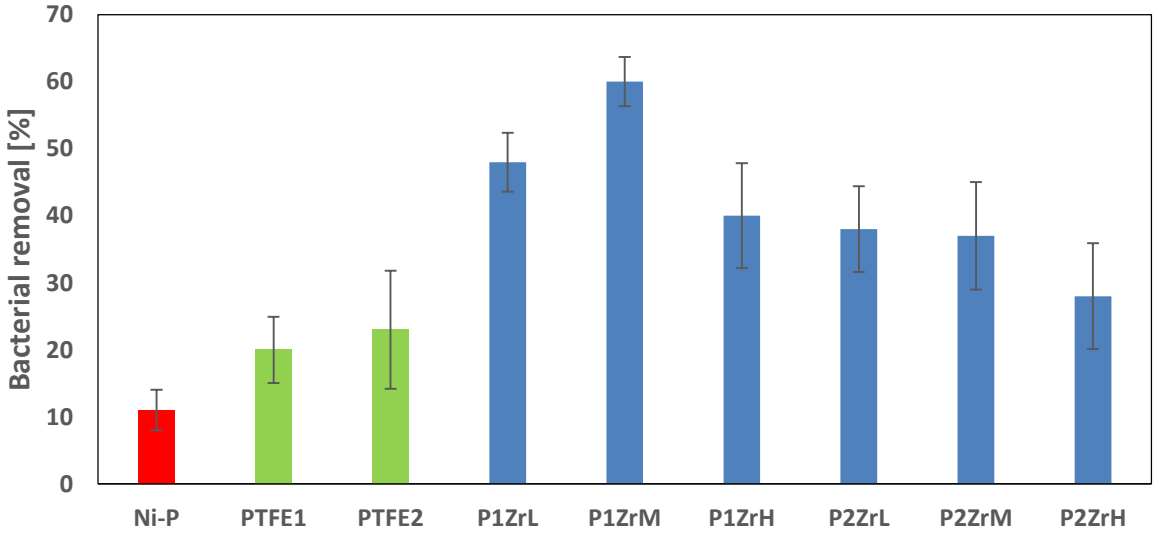

Figure 6.6 removal percentage of *Staphylococcus aureus from* Ni-P-PTFE-ZrO_2 coatings after dipping process

Figure 6.5 shows that remaining *staphylococcus aureus* cells on the Ni-P-PTFE-ZrO_2 coatings after dipping process have an increasing trend when Ni-P-PTFE-ZrO_2 coatings were prepared by higher concentration of ZrO_2.coating P1ZrM which is prepared by 8ml/L PTFE and 1.25 g/L ZrO_2 shows better results than other coatings. Compared with Ni-P coating, and Ni-P-PTFE coatings with low (8ml/L) and high (12ml/L) concentration of PTFE, the remaining number of *S. aureus* on thecoating P1ZrM was 26.8% of Ni-P, 38.0% and 44.6% of Ni-P-PTFE coatings respectively.

While Figure 6.6 presents the removal rate of *staphylococcus aureus* from Ni-P-PTFE-ZrO_2 coatings after dipping process. Andcoating P1ZrM also has higher removal rate of bacteria Compared with Ni-P coatings and Ni-P-PTFE coatings whose removal percentage are 11%, 20% and 23% respectively, the removal rate ofcoating P1ZrM is as high as 60%.

In conclusion, in the assay of *E. coli* and *S. aureus* removal,coating P1ZrL and 5 prepared by low concentration of PTFE (8ml/L) and low concentration of ZrO_2 (0.625g/L and 1.25g/L) present less remaining bacteria and larger removal rate using a dipping process. The reason is thatcoating P1ZrL and 5 have less value of surface free energy component γ^{LW} and total surface free energy than other coatings. The relationship of total surface free energy vs. remaining bacteria, γ^{LW} vs. remaining bacteria and total surface free energy vs. bacteria removal rate can be seen in figure 6.8-6.10 and 6.12-6.14.

6.1.1.2 Effect of PTFE on Bacterial Adhesion and Removal

The effect of PTFE on *Escherichia coli* and *Staphylococcus aureus* adhesion and removal on the Ni-P-PTFE-ZrO_2 coatings are shown in figure 6.1-6.6. From Figure 6.1, we can conclude that Ni-P-PTFE-ZrO_2 coating prepared by high concentration of PTFE (12ml/L) can resist adhesion

of *E. coli* better than those prepared by low concentration (8ml/L), which might be explained by the effect of surface free energy on bacterial adhesion. Ni-P-PTFE-ZrO_2 coatings prepared by 12ml/L PTFE are approach optimal antibacterial adhesion surface free energy between 20 and 30mJ/m^2, which had been investigated by Zhao et al. (Liu and Zhao 2005), and Figure 6.7 shows the relationship between surface free energy of Ni-P-PTFE-ZrO_2 and number of adhered *E. coli*. Besides, from table 3.3, we can see that Ni-P-PTFE-ZrO_2 coatings prepared by 12ml/L PTFE have larger value of surface free energy component γ^-, which also have a significant effect on reducing bacterial adhesion (Liu and Zhao 2011). Similar results for effect on *S. aureus* adhesion can be seen in Figure 6.2. Ni-P-PTFE-ZrO_2 prepared by higher concentrate of PTFE have better capability of resisting adhesion of *staphylococcus aureus*.

As seen in Figure 6.3, it shows the effect of PTFE on number of remaining *E. coli* on Ni-P-PTFE-ZrO_2 coatings using a dipping process. Compared with effect of PTFE on bacterial adhesion, less number of *E. coli* (CFU/cm^2) remains on Ni-P-PTFE-ZrO_2 coatings which is prepared by low concentration of PTFE (8ml/L) after dipping process, which is the opposite effect of PTFE on bacterial adhesion. And the reason for this result can be explained that less total surface free energy and surface free energy component γ^{LW} may have more effect on strength of bacterial adhesion than γ^-, which lead to less bacterial remaining on Ni-P-PTFE-ZrO_2 coatings (8ml/L). And the relationship between remaining bacteria on the coatings and surface free energy component can be seen in figure 6.9 to 6.12. Similar result can be seen in Figure 6.5, which also shows that Ni-P-PTFE-ZrO_2 coatings prepared by low concentrate of PTFE (8ml/L) will remain less *staphylococcus aureus* on Ni-P-PTFE-ZrO_2 coatings.

6.1.1.3 Effect of surface free energy of Ni-P-PTFE-ZrO_2 coatings on bacterial adhesion and removal

In order to investigate the effect of total surface free energy and its component on bacterial adhesion and removal. The relationship between total surface free energy vs bacterial adhesion, total surface free energy vs remaining bacteria, surface free energy component γ^{LW} vs. remaining bacteria, total surface free energy vs bacterial removal percentage are shown in Figure 6.7-6.14.

As shown in Figure 6.7 and 6.11, there exists a correlation between bacterial adhesion and total surface free energy of Ni-P-PTFE-ZrO_2 coatings. According to Figure 6.7, when the surface free energy of coatings was approximately 20-25mJ/m^2, the number of *E. coli* attached to the coating reached to minimum. And similar results for *S. aureus* can be seen in Figure 6.11. There also exists an optimal surface free energy at about 20-25mJ/m^2, where the number of bacterial adhesion is minimal. And it is consistent with the conclusion of Baier and Zhao et al, which verifies that surface free energy between 20 and 30mJ/m^2 is optimal to resist bacterial adhesion (Zhao 2004). The correlation coefficient R^2 values for number of *E. coli* and *S. aureus* versus surface free energy of Ni-P-PTFE-ZrO_2 coatings are 0.6569 and 0.7041 respectively.

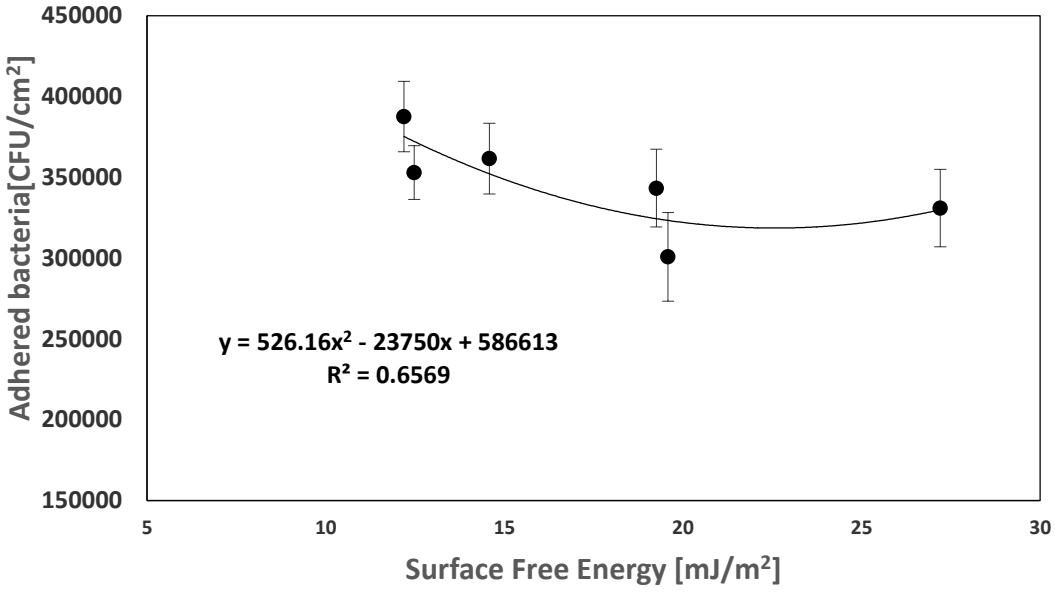

Figure 6.7 Effect of Surface Free Energy of Ni-P-PTFE-ZrO_2 coatings on the adhesion of *Escherichia coli*

Figure 6.8 and Figure 6.12 show the relationship between total surface free energy and remaining number of *E. coli* and *S. aureus* on the Ni-P-PTFE-ZrO_2 coatings respectively. In these two figures, remaining bacterial number (CFU/cm^2) was positively correlated with total surface free energy, which means that the strength of adhered bacteria to Ni-P-PTFE-ZrO_2 coatings increased with total surface free energy increasing. The correlation coefficient R^2 for remaining number of *E. coli* and *S. aureus* versus surface free energy of Ni-P-PTFE-ZrO_2 coatings were 0.5123 and 0.7121 respectively.

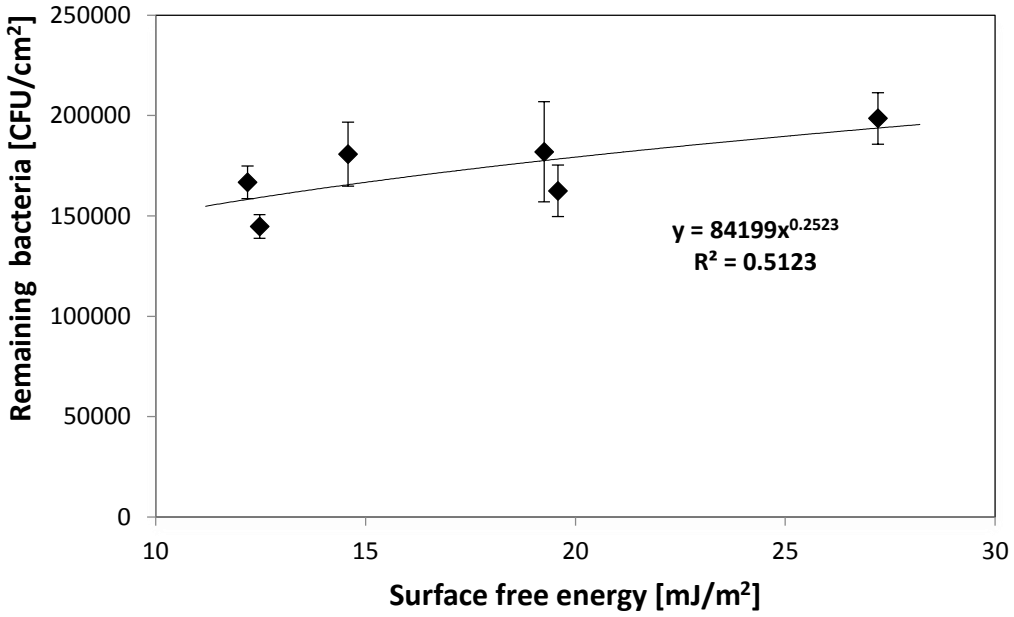

Figure 6.8 Effect of Surface Free Energy of Ni-P-PTFE-ZrO_2 coatings on the remaining *Escherichia coli* cells

The effect of γ^{LW} of Ni-P-PTFE-ZrO_2 coatings on remaining number of *Escherichia coli* and *Staphylococcus aureus* is also investigated, which can be seen in the Figure 6.9 and Figure 6.13. The number of remaining *Escherichia coli* and *staphylococcus aureus* increased with values of γ^{LW} of Ni-P-PTFE-ZrO_2 coatings increasing, which is similar as the result of correlation between remaining bacterial adhesion and surface free energy which can be seen in Figure 6.8 and Figure 6.12. The correlation coefficient R^2 for number of remaining *E. coli* and *S. aureus* versus γ^{LW} were 0.6817 and 0.7862 respectively.

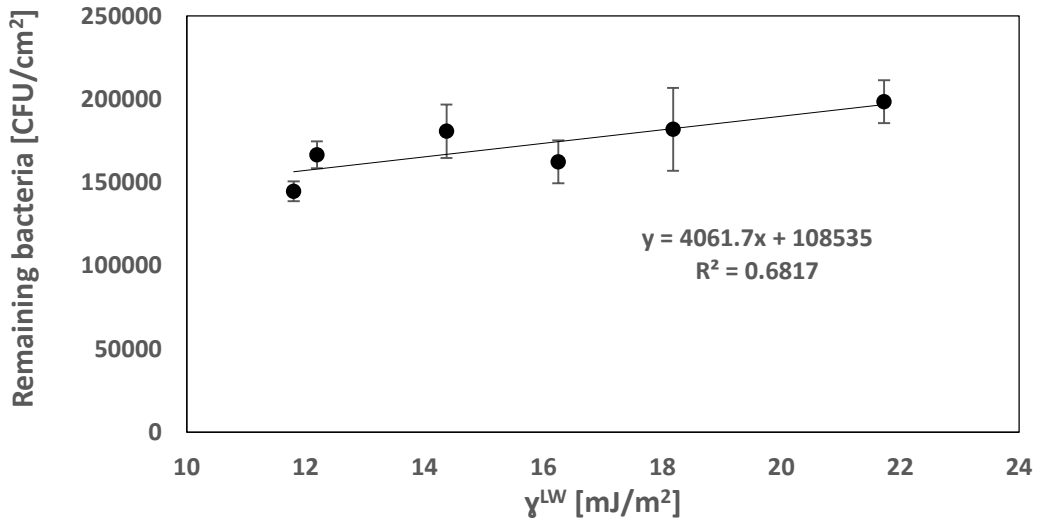

Figure 6.9 Effect of γ^{LW} of Ni-P-PTFE-ZrO_2 coatings on the remaining *Escherichia coli* cells

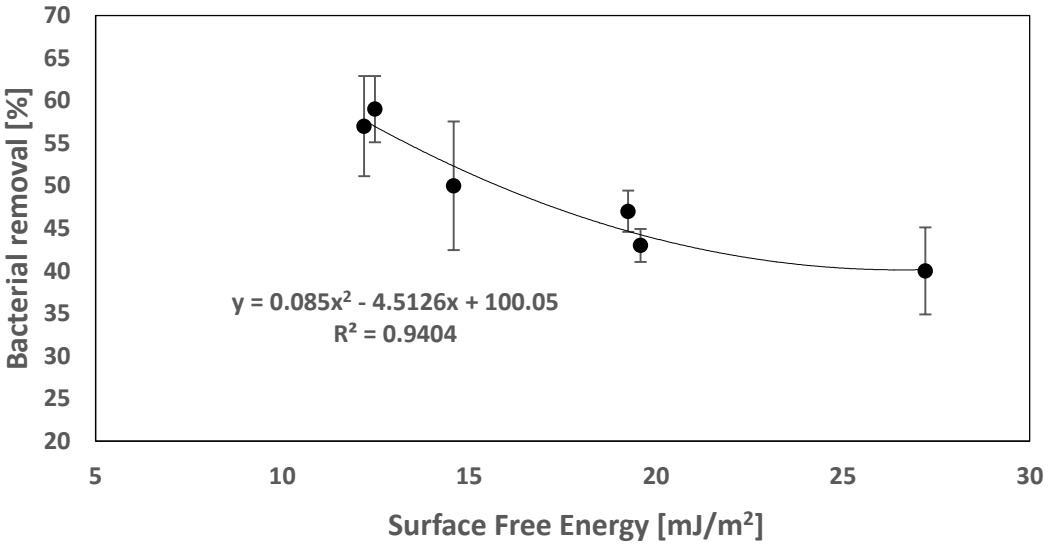

Figure 6.10 Effect of Surface Free Energy of Ni-P-PTFE-ZrO_2 coatings on *Escherichia coli* removal rate

Figure 6.10 and Figure 6.14 present the relationship between removal rate of *Escherichia coli* and *staphylococcus aureus* using a dipping process versus total surface free energy of Ni-P-

PTFE-ZrO_2 coatings, and according these two figures, the total surface free energy negatively affect the bacterial removal rate for both two types of bacteria. The correlation coefficient R^2 values for removal rate of *E. coli* and *S. aureus* versus surface free energy were 0.9404 and 0.8141, which means the correlation between bacterial removal rate and total surface free energy is quite strong.

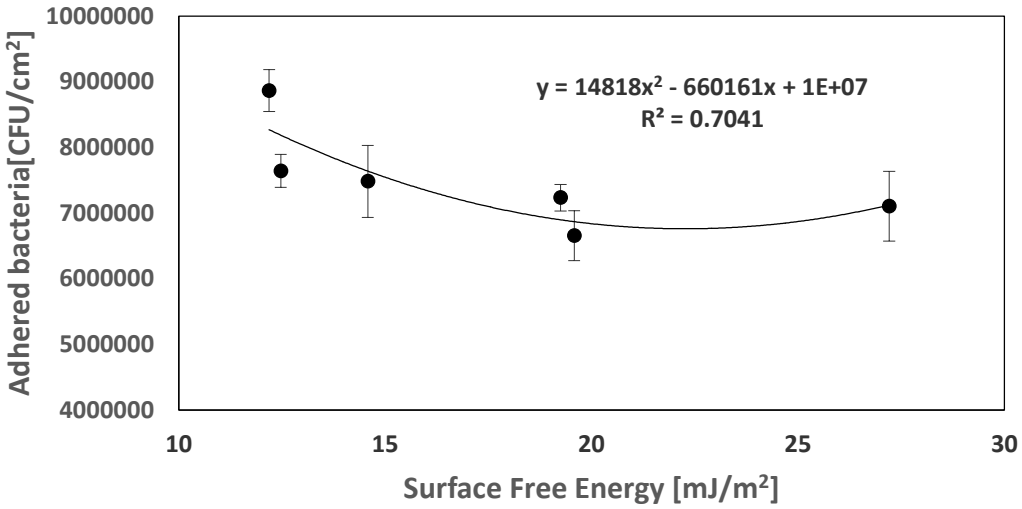

Figure 6.11 Effect of Surface Free Energy of Ni-P-PTFE-ZrO_2 coatings on the adhesion of *staphylococcus aureus*

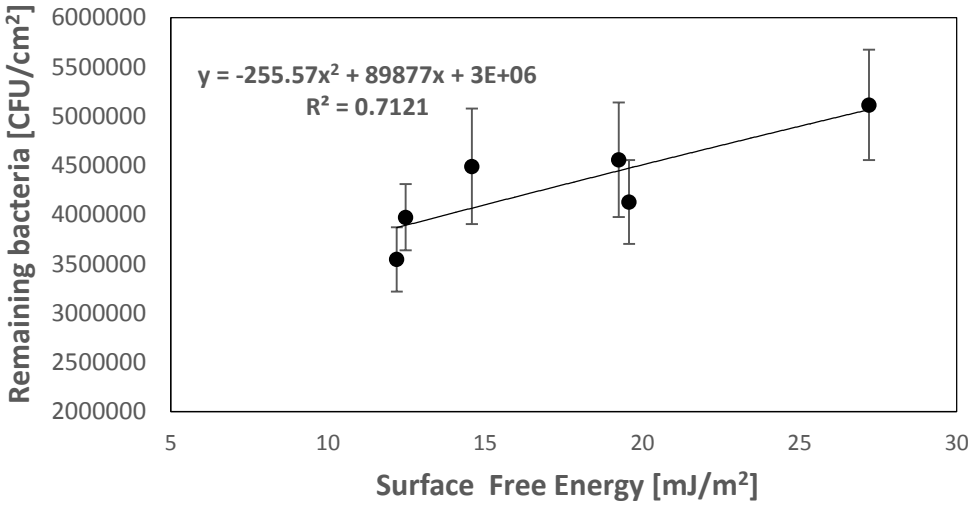

Figure 6.12 Effect of Surface Free Energy of Ni-P-PTFE-ZrO2 coatings on the remaining staphylococcus aureus cells

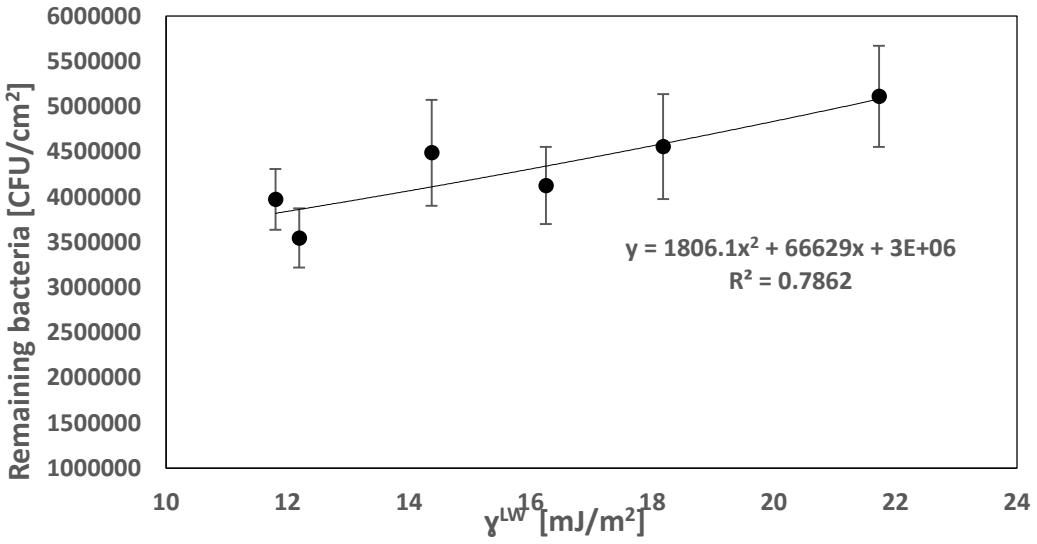

Figure 6.13 Effect of γ^{LW} of Ni-P-PTFE-ZrO_2 coatings on the remaining *Staphylococcus aureus*

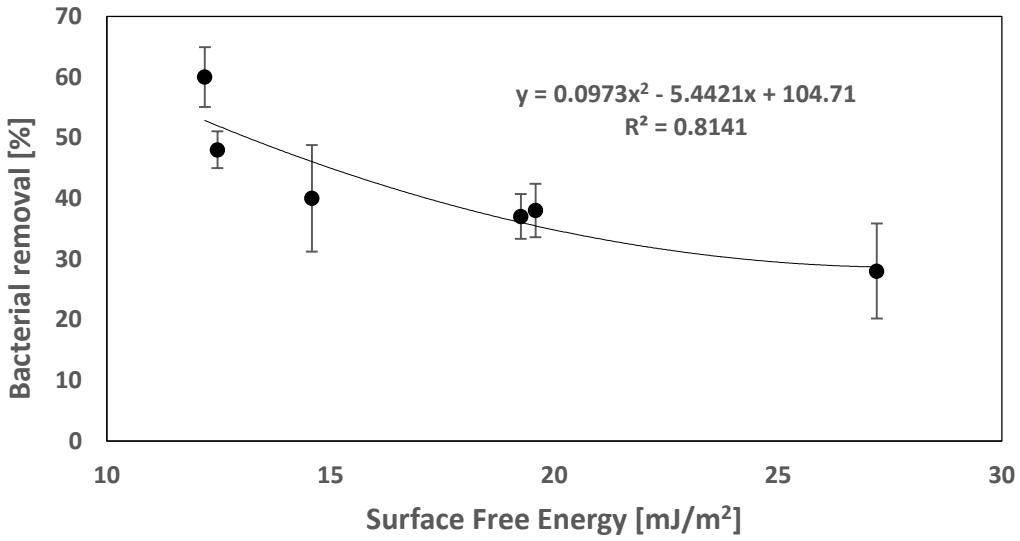

Figure 6.14 Effect of Surface Free Energy of Ni-P-PTFE-ZrO_2 coatings on *Staphylococcus aureus* removal rate

6.1.2 Ni-P-PTFE-ZrO_2-TiO_2 coatings

As we mentioned in literature review, TiO_2 material is widely used in the medical device markets, and its excellent properties such as antibacterial capability, biocompatibility, corrosion resistance and mechanical properties contribute to medical devices having higher safety and longer working life when implanted in human bodies. In recent years, some new coatings are developed by incorporating nanoparticle TiO_2 into other coatings which help to enhance the property of new coatings such as antibacteiral property, anticorrosion property, mechanical property and so on (Thomsen, Larsson et al. 1997, Depprich, Zipprich et al. 2008, Ionita, Grecu et al. 2011, Cui, Gao et al. 2012). Therefore, in this part, a new series of Ni-P-PTFE-ZrO_2-TiO_2 were developed by adding nanoparticle TiO_2 into Ni-P-PTFE-ZrO_2 coatings. And there are three different concentration of TiO_2 including 0.4 g/L, 0.8 g/L and 1.2 g/L, two different concentration of PTFE including 8ml/L and 12ml/L and three different concentration of ZrO_2 including 0.625 g/L, 1.25 g/L and 1.875 g/L, which were used to prepare 18 different coatings to see these coatings whether or not to have the capability of effectively resisting bacterial adhesion and removing adhered bacteria.

The bath composition and operating conditions for electroless Ni-P-PTFE-ZrO_2-TiO_2 nano-composite coatings is given in table 3.4. TiO_2 nano-powder was brought from Aldrich, and the particle size of TiO_2 is 25 nm. Detailed information of different coatings such as coating P1ZrLTiL-27 are shown in table 4.4 and experimental procedures of bacterial adhesion and removal are introduced in section 5.1.4, The assays of bacterial adhesion such as *Escherichia coli* and *Staphylococcus aureus* on the Ni-P-PTFE-ZrO_2-TiO_2 was investigated by immersing the coatings in the bacterial suspension of 10^6 cells/ml for 2h at 37 ^oC.

In this part, Figure 6.15 to Figure 6.26 show the result of assays of *Escherichia coli* and *Staphylococcus aureus* adhesion and removal on Ni-P-PTFE-ZrO_2-TiO_2 coatings.

6.1.2.1 Effect of ZrO_2 on Bacterial Adhesion and Removal

Figure 6.15 shows that the performance of Ni-P-PTFE-ZrO_2-TiO_2 (concentration of PTFE is 8ml/L), Ni-P and Ni-P-PTFE coatings (concentration of PTFE is 8ml/L) against *E. coli* adhesion. Compared with Ni-P and Ni-P-PTFE, except coating P1ZrMTiM and 15, the number of *E. coli* adhered on the Ni-P-PTFE-ZrO_2-TiO_2 coatings was 53.4-66.3% of Ni-P and 68.3%-86.1% Ni-P-PTFE coatings respectively.

While all Ni-P-PTFE-ZrO_2-TiO_2 coatings show much better capability of resisting *S. aureus* adhesion than *E. coli*. According to the figure 6.16, compared with Ni-P and Ni-P-PTFE coatings, the number of *S. aureus* adhered on the surface (CFU/cm^2) was 23.1-34.3% of Ni-P coating and 29.4-43.7% of Ni-P-PTFE coating respectively.

Figure 6.15 and 6.16 demonstrate that when Ni-P-PTFE-ZrO_2-TiO_2 coatings were prepared by 0.625g/L and 1.875g/L ZrO_2, they showed better capability of resisting bacterial adhesion than those prepared by 1.25g/L ZrO_2.

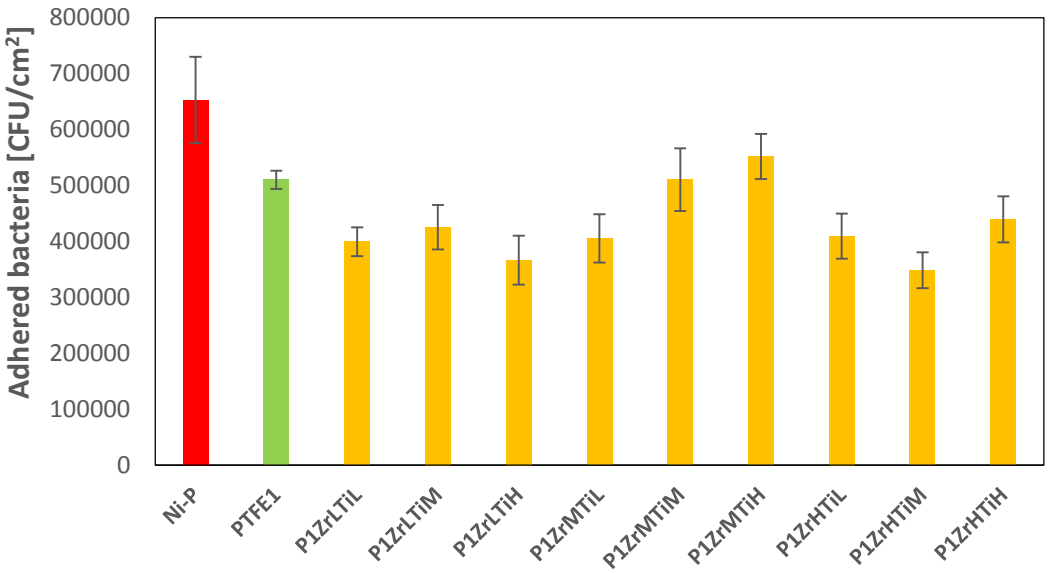

Figure 6.15 Adhesion of *Escherichia coli* on Ni-P-PTFE-ZrO_2-TiO_2 coatings (concentration of PTFE is 8ml/L)

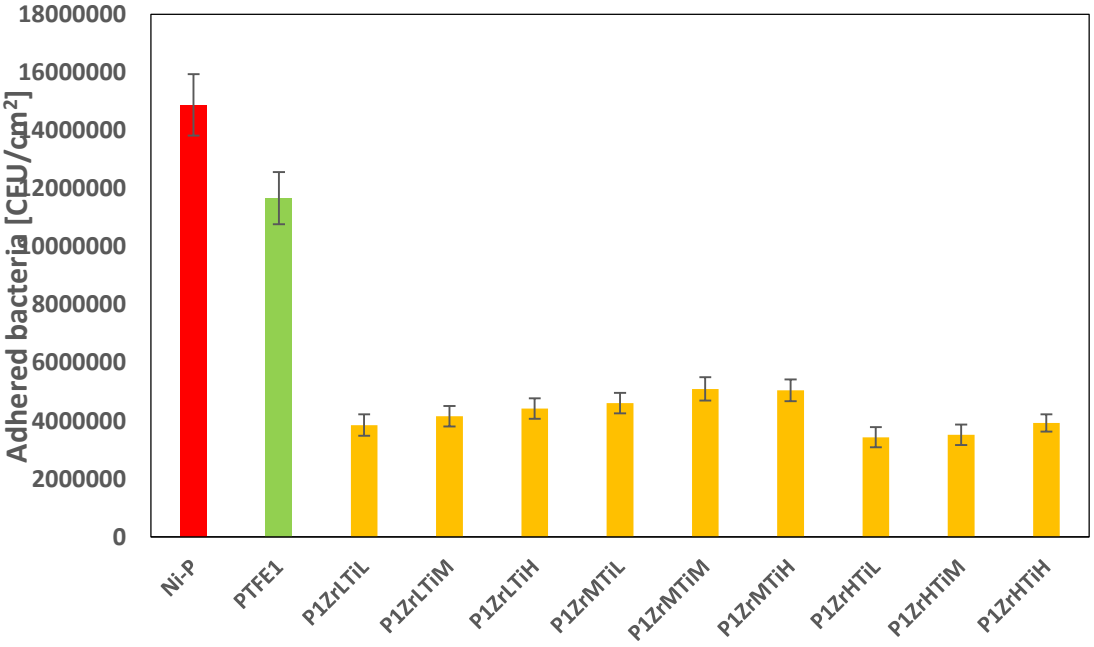

Figure 6.16 Adhesion of *Staphylococcus aureus* on Ni-P-PTFE-ZrO_2-TiO_2 coatings (concentration of PTFE is 8ml/L)

Figure 6.17 and Figure 6.18 show the result of assays of *E.coli* removal. It can be seen from Figure 6.17 that the number of remaining *Escherichia coli* cells on the Ni-P-PTFE-ZrO_2-TiO_2 coatings was 26.1-54.6% of Ni-P coating and 36.5-76.4% of Ni-P-PTFE coating using a dipping process. Coatings prepared by concentration of 0.625g/L ZrO_2 including coating P1ZrLTiL, 11 and 12, remain least number of bacteria on the surface of Ni-P-PTFE-ZrO_2-TiO_2 coatings. Figure 6.18 shows the removal percentage of *Escherichia coli* from Ni-P-PTFE-ZrO_2 coatings using a dipping process. And the removal percentage of *E. coli* is higher for coating P1ZrLTiL, 11 and 12 which were prepared by 0.625g/L ZrO_2. And removal percentage of these three coatings ranges from 60% to 65% which is much higher than Ni-P (18%) and Ni-P-PTFE (25%) coatings.

For assays of *S. aureus* removal, the results in the figure 6.19 and 6.20 show that Ni-P-PTFE-ZrO_2-TiO_2 coatings prepared by low concentration of ZrO_2 remain least number of bacteria on the coating using a dipping process. The remaining *S. aureus* cells on the Ni-P-PTFE-ZrO_2-TiO_2 coatings was 10.1-19.3% of Ni-P coating and 14.5-26.3% of Ni-P-PTFE coatings. The results of removal percentage of *S. aureus* from Ni-P-PTFE-ZrO_2-TiO_2 coatings show similar trend with that of *E. coli*. Coatings 10, 11 and 12 still show highest removal percentage between 59% and 66% compared with Ni-P coating (11%) and Ni-P-PTFE coating (22%).

In conclusion, among coatings 10 to 18, coatings 10, 11 and 12 prepared by low concentration of ZrO_2 (0.625g/L) show better capability of resisting *E.coli* and *S.aureus* adhesion and remain least bacteria on the surface and largest removal percentage in the *E.coli* and *S. aureus* removal assays.

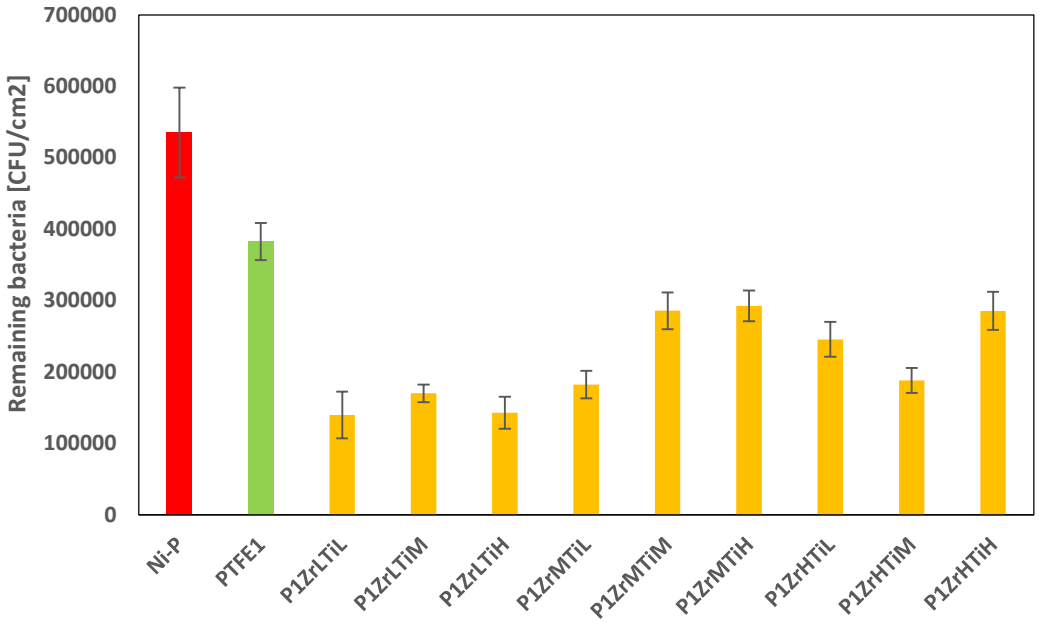

Figure 6.17 Remaining *Escherichia coli on* Ni-P-PTFE-ZrO_2-TiO_2 coatings after dipping process (concentration of PTFE is 8ml/L)

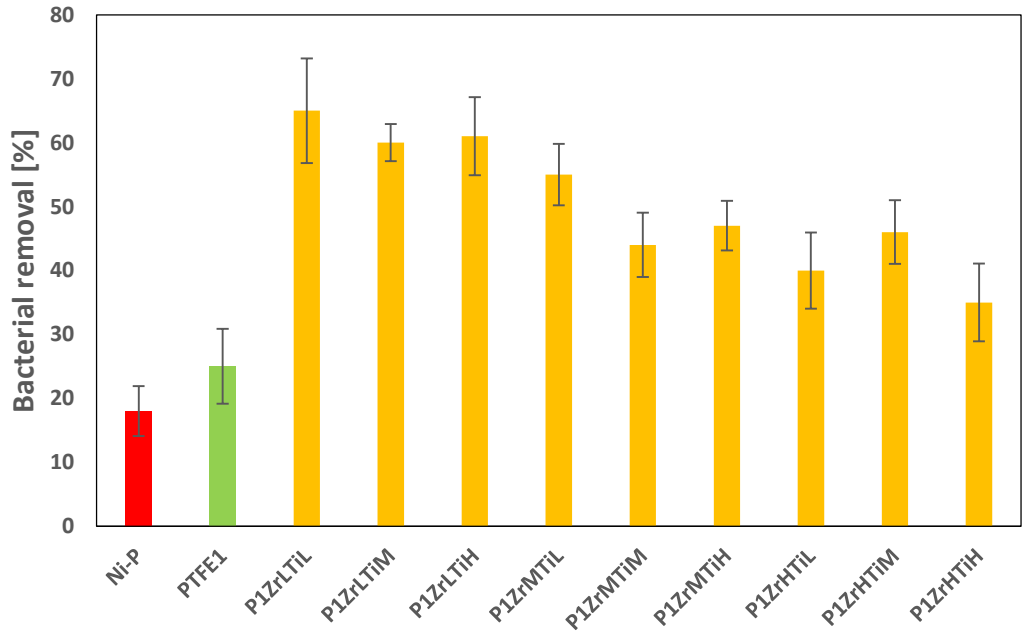

Figure 6.18 Removal percentage of *Escherichia coli from* Ni-P-PTFE-ZrO_2-TiO_2 coatings after dipping process (concentration of PTFE is 8ml/L)

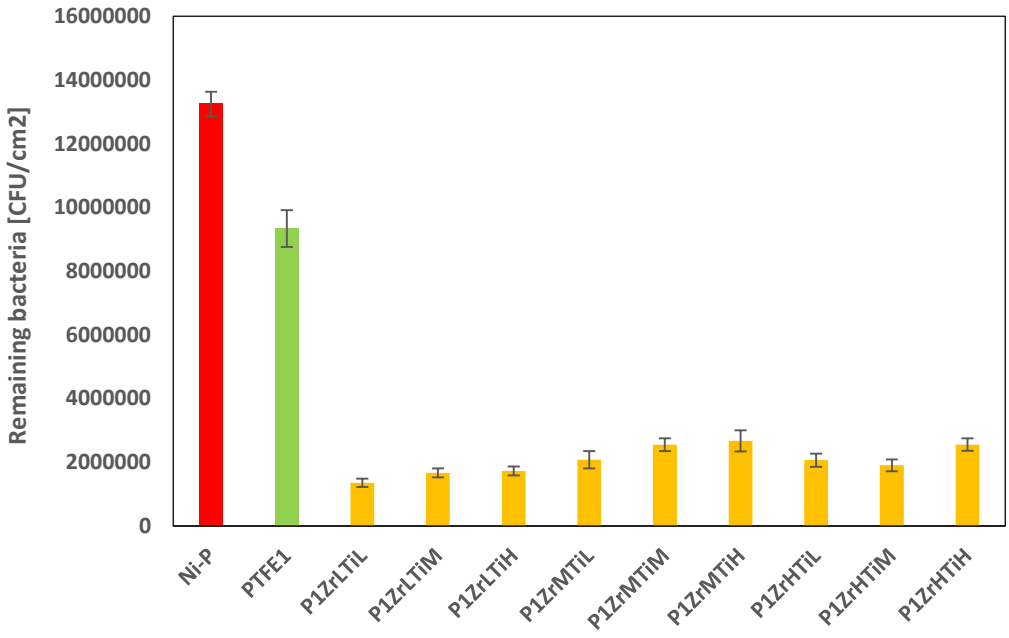

Figure 6.19 Remaining *Staphylococcus aureus on* Ni-P-PTFE-ZrO_2-TiO_2 coatings after dipping process (concentration of PTFE is 8ml/L)

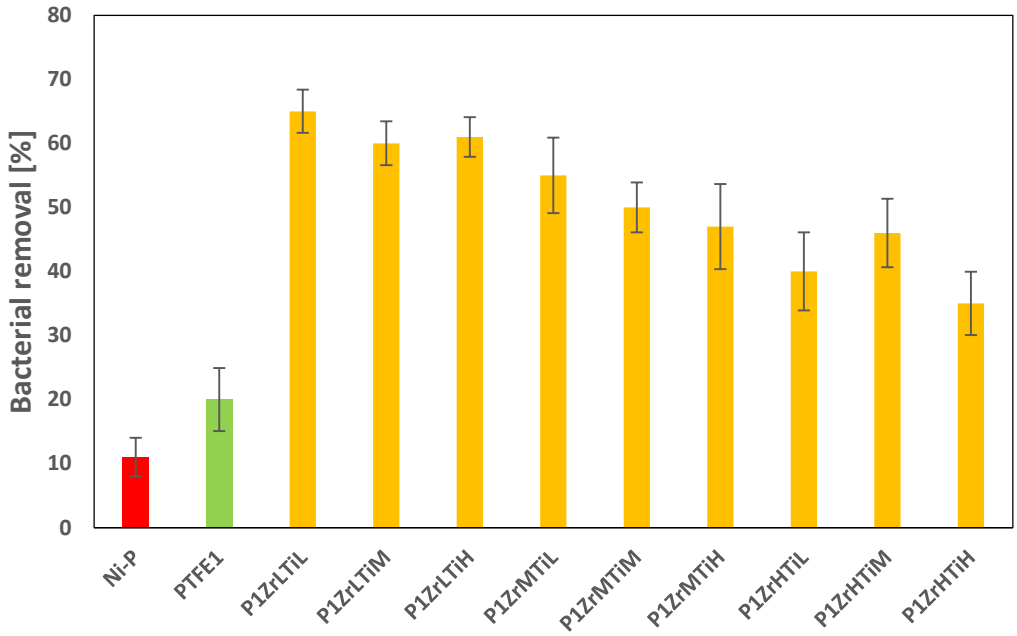

Figure 6.20 removal percentage of *Staphylococcus aureus from* Ni-P-PTFE-ZrO_2-TiO_2 coatings after dipping process (concentration of PTFE is 8ml/L)

Figure 6.21 shows that the results of Ni-P-PTFE-ZrO_2-TiO_2 (concentration of PTFE is 12ml/L) against *E. coli* adhesion. And most of the Ni-P-PTFE-ZrO_2-TiO_2 coatings show better capability

of resisting bacterial adhesion than that of Ni-P and Ni-P-PTFE coatings except coating P2ZrHTiM, the number of adhered *E. coli* was 33.1-60.7% of Ni-P coating and 46.6%-86.4% coating.

While for *S. aureus* adhesion assays, all Ni-P-PTFE-ZrO_2-TiO_2 coatings show much better property of resisting *S. aureus* adhesion compared with Ni-P and Ni-P-PTFE coatings. According to the figure 6.22, the number of *S. aureus* adhesion on the Ni-P-PTFE-ZrO_2-TiO_2 coatings (CFU/cm^2) was 21.2-44.3% of Ni-P coating and 30.6-63.8% of Ni-P-PTFE coating.

As it can be seen, figure 6.21 and figure 6.22 show that there exists some fluctuation of performance of Ni-P-PTFE-ZrO_2-TiO_2 coatings against *E. coli* and *S. aureus* adhesion. Ni-P-PTFE-ZrO_2-TiO_2 coatings such as coating P2ZrLTiL, 22 and 25, show better capability of resisting *E. coli* and *S. aureus* adhesion than others. They were prepared by 0.4g/L TiO_2 and different concentration of ZrO_2 including 0.625g/L 1.25g/L and 1.875g/L, which means that the addition of low concentration of TiO_2 have an enormous effect on resisting bacterial adhesion.

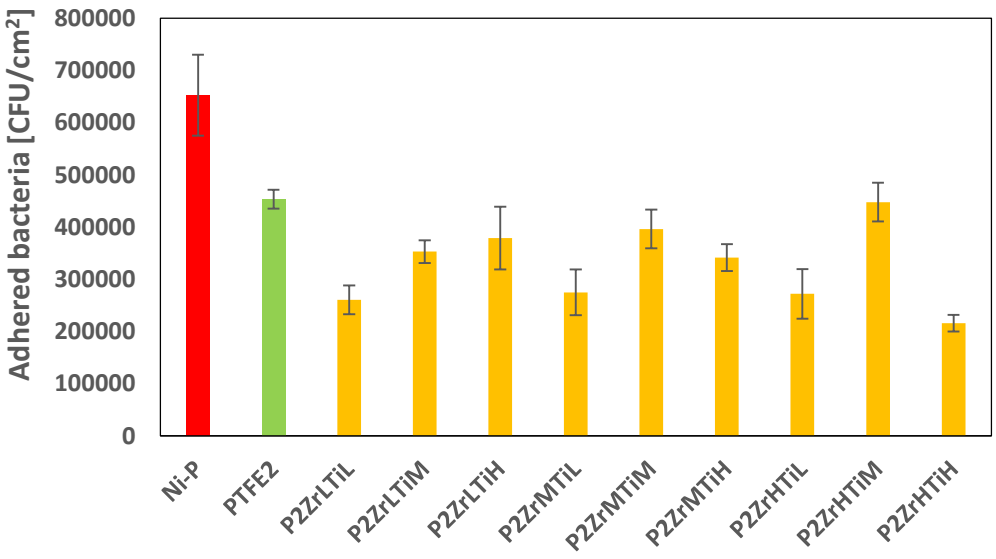

Figure 6.21 Adhesion of *Escherichia coli* on Ni-P-PTFE-ZrO_2-TiO_2 coatings (concentration of PTFE is 12ml/L)

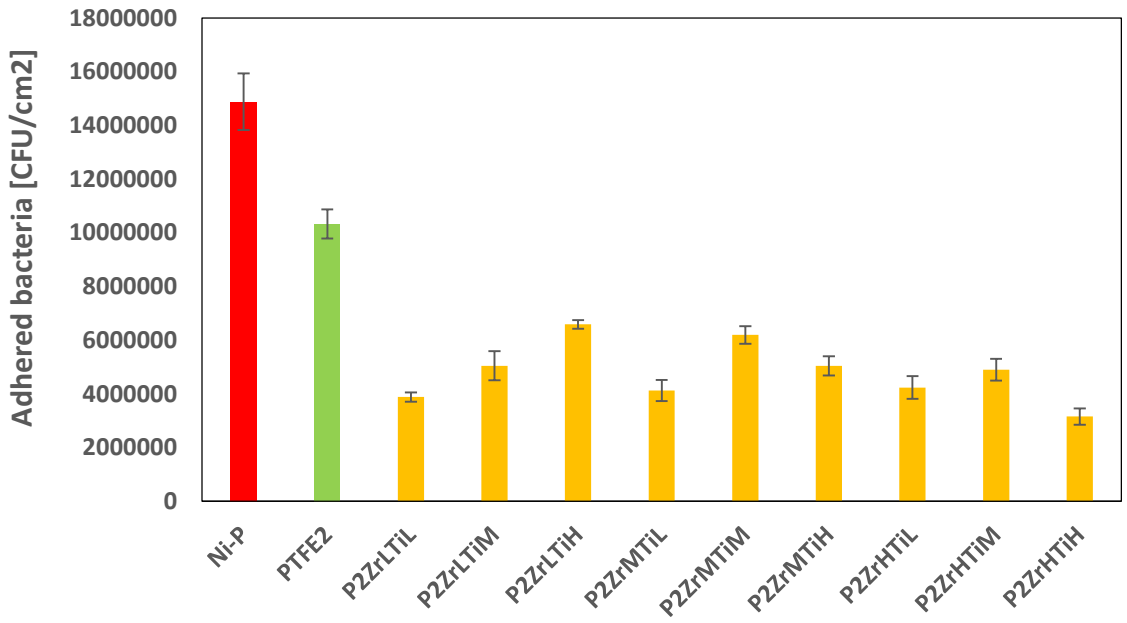

Figure 6.22 Adhesion of *Staphylococcus aureus* on Ni-P-PTFE-ZrO_2-TiO_2 coatings (concentration of PTFE is 12ml/L)

Figure 6.23 and Figure 6.24 show the results of assays of *E.coli* removal on Ni-P-PTFE-ZrO_2-TiO_2 coatings which is prepared by high concentration of PTFE (12ml/L). It can be seen from Figure 6.23 that the number of remaining *Escherichia coli* cells on the Ni-P-PTFE-ZrO_2-TiO_2 coatings using a dipping process was 14.8-30.5% of Ni-P coating and 14.8-50.0% of Ni-P-PTFE coating. The coating prepared by 0.625g/L ZrO_2 including coating P2ZrLTiL, 20 and 21, remained least number of bacteria on the surface of Ni-P-PTFE-ZrO_2-TiO_2 coatings.

Figure 6.24 shows the removal percentage of *Escherichia coli* from Ni-P-PTFE-ZrO_2-TiO_2 coatings using a dipping process. And the removal percentage of bacteria is higher for coating P2ZrLTiL, 20 and 21 than others, which were prepared by 0.625g/L ZrO_2. And removal percentage of these three coatings ranges from 68% to 72% which is much higher than Ni-P (18%) and Ni-P-PTFE (28%) coatings.

For assays of *S. aureus* removal, as it can be seen in Figure 6.25 and 6.26, coatings 19, 20, 22 and 23 prepared by low concentration of ZrO_2 (0.625g/L and 1.25g/L) and low concentration of TiO_2 (0.4g/L and 0.8g/L) remain less number of bacteria on the surface. The number of remaining *S. aureus* cells on the Ni-P-PTFE-ZrO_2-TiO_2 coatings using a dipping process is 13.2-22.4% of Ni-P coating and 22.0-36.3% of Ni-P-PTFE coatings. The results of removal percentage of *S. aureus* show similar trend with that of *E. coli*. Coatings 19, 20 and 21 still show highest removal percentage between 55%-65% compared with Ni-P coating (11%) and Ni-P-PTFE coating (23%).

In conclusion, among coatings 19 to 27, coatings 19 show great properties of resisting *E. coli* adhesion in the bacterial adhesion assays and coating P2ZrLTiL remain least bacteria on the surface and largest removal percentage in the bacterial removal assays. Which means Ni-P-PTFE-ZrO_2-TiO_2 coating prepared by 12ml/L PTFE, 0.625g/L ZrO_2 and 0.4g/L TiO_2 show best performance in the assays of bacterial adhesion and removal.

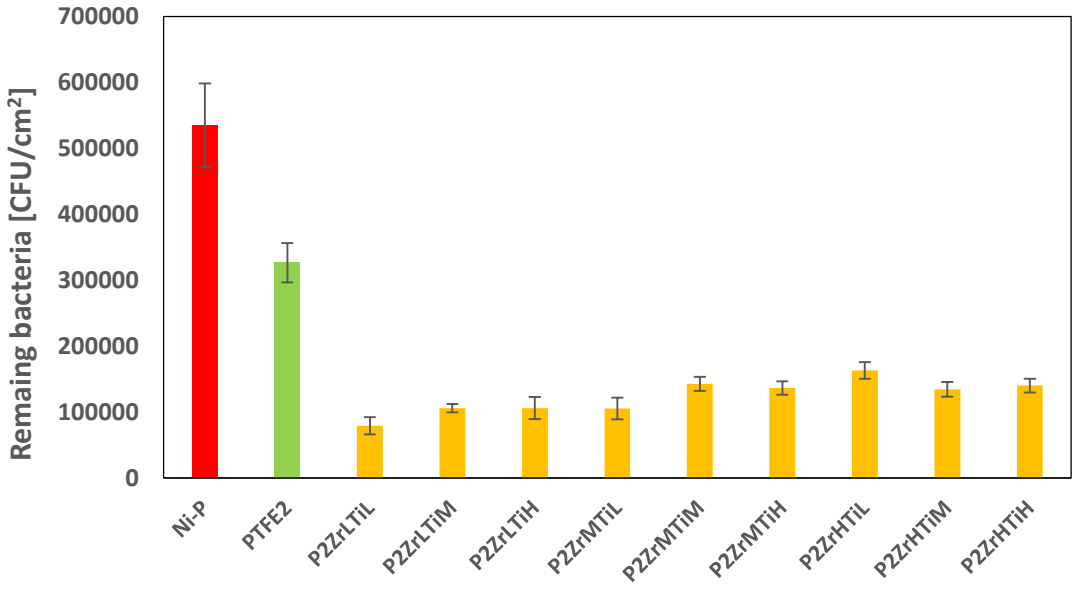

Figure 6.23 Remaining *Escherichia coli on* Ni-P-PTFE-ZrO_2-TiO_2 coatings after dipping process (concentration of PTFE is 12ml/L)

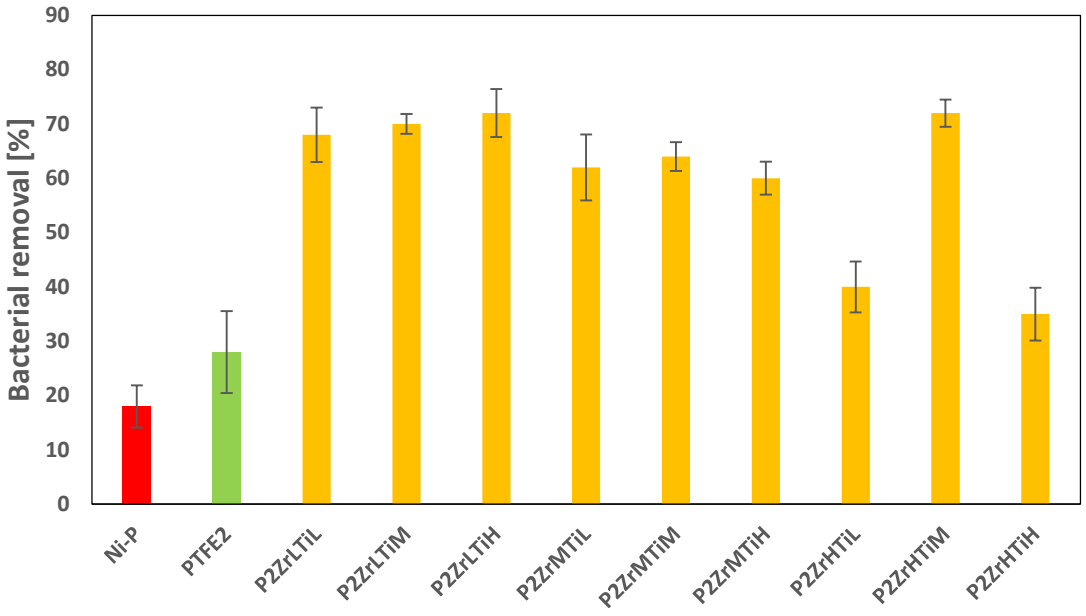

Figure 6.24 Removal percentage of *Escherichia coli from* Ni-P-PTFE-ZrO_2-TiO_2 coatings after dipping process (concentration of PTFE is 12ml/L)

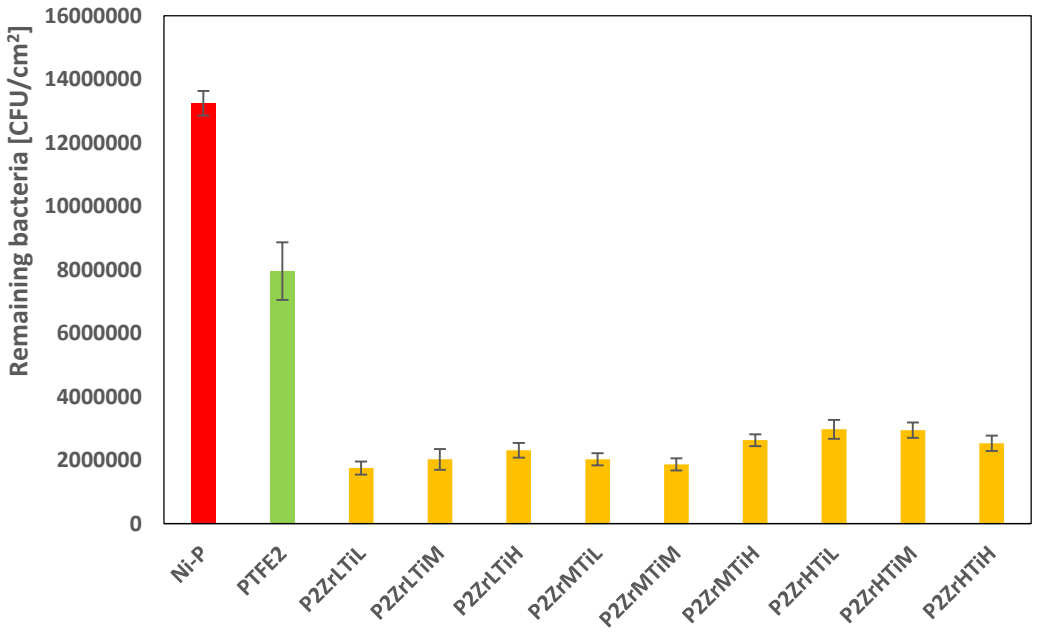

Figure 6.25 Remaining *Staphylococcus aureus on* Ni-P-PTFE-ZrO_2-TiO_2 coatings after dipping process (concentration of PTFE is 12ml/L)

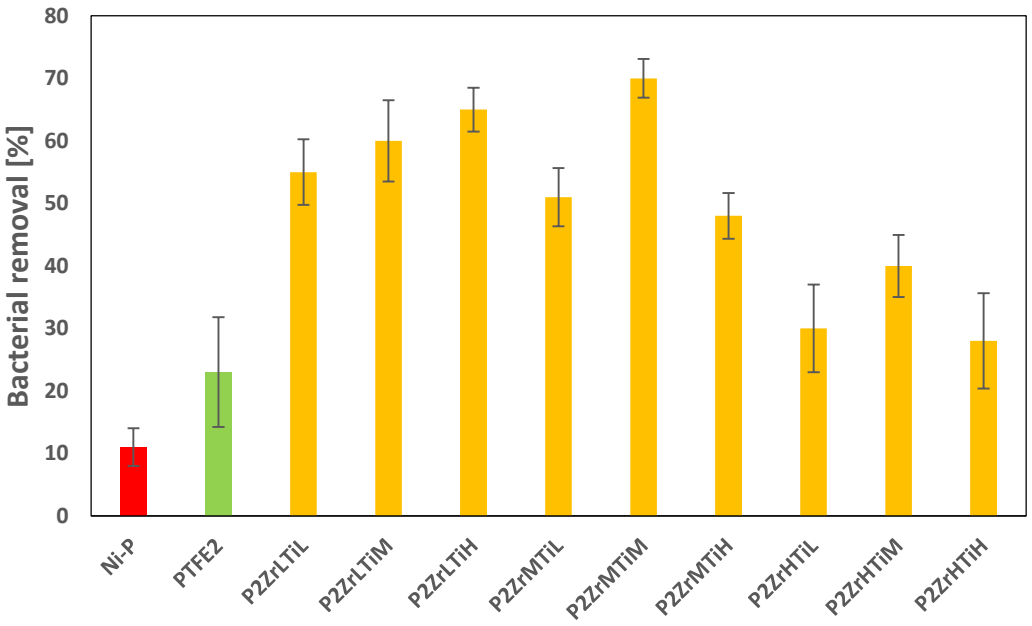

Figure 6.26 removal percentage of *Staphylococcus aureus from* Ni-P-PTFE-ZrO_2-TiO_2 coatings after dipping process (concentration of PTFE is 12ml/L)

6.1.2.2 Effect of TiO_2 on Bacterial Adhesion and Removal

Figure 6.27-6.38 compared the results of two different series of coatings including Ni-P-PTFE-ZrO_2 and Ni-P-PTFE-ZrO_2-TiO_2 in the assay of bacterial adhesion and removal. Effect of nanoparticle TiO_2 on the property of Ni-P-PTFE-ZrO_2-TiO_2 coatings against bacterial adhesion and reducing remaining bacteria are also demonstrated.

In the Figure 6.27-6.29, Ni-P-PTFE-ZrO_2 and Ni-P-PTFE-ZrO_2-TiO_2 coatings prepared by same concentration of PTFE (8ml/L) and same concentration of ZrO_2 are chosen to compare their capability of resisting bacterial adhesion and reducing adhered bacteria using a dipping process. From these figures, we can see that Ni-P-PTFE-ZrO_2 coatings show better capability than Ni-P-PTFE-ZrO_2-TiO_2 coatings in the assay of *E. coli* adhesion and removal. In the figure 6.27 only coating P1ZrHTiM have a little less number of *E. coli* on the surface than coating P1ZrH, and in

the figure 6.29 the removal percentage of coating P1ZrLTiL and P1ZrLTiH are slightly higher than coating P1ZrL. All of these illustrate that Ni-P-PTFE-ZrO_2-TiO_2 coatings prepared by 8ml/L PTFE, did not have better capability against *E. coli* adhesion and reducing the number of adhered bacteria using a dipping process than Ni-P-PTFE-ZrO_2 coatings.

However, in the assay of *S. aureus* adhesion and removal, the results is opposite. Ni-P-PTFE-ZrO_2-TiO_2 coatings have better capability of resisting *S. aureus* adhesion and remaining less *S. aureus* cells using a dipping process than Ni-P-PTFE-ZrO_2 coatings. These results can be seen in the Figure 6.33-6.35.

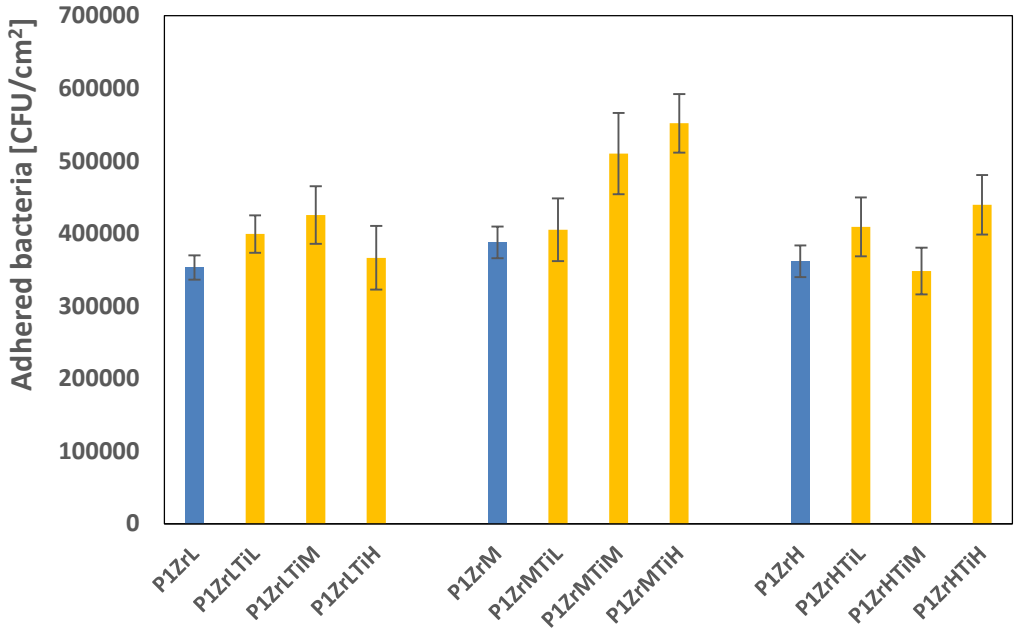

Figure 6.27 Comparison of Ni-P-PTFE-ZrO_2 and Ni-P-PTFE-ZrO_2-TiO_2 coatings (concentration of PTFE is 8ml/L) against *Escherichia coli* adhesion

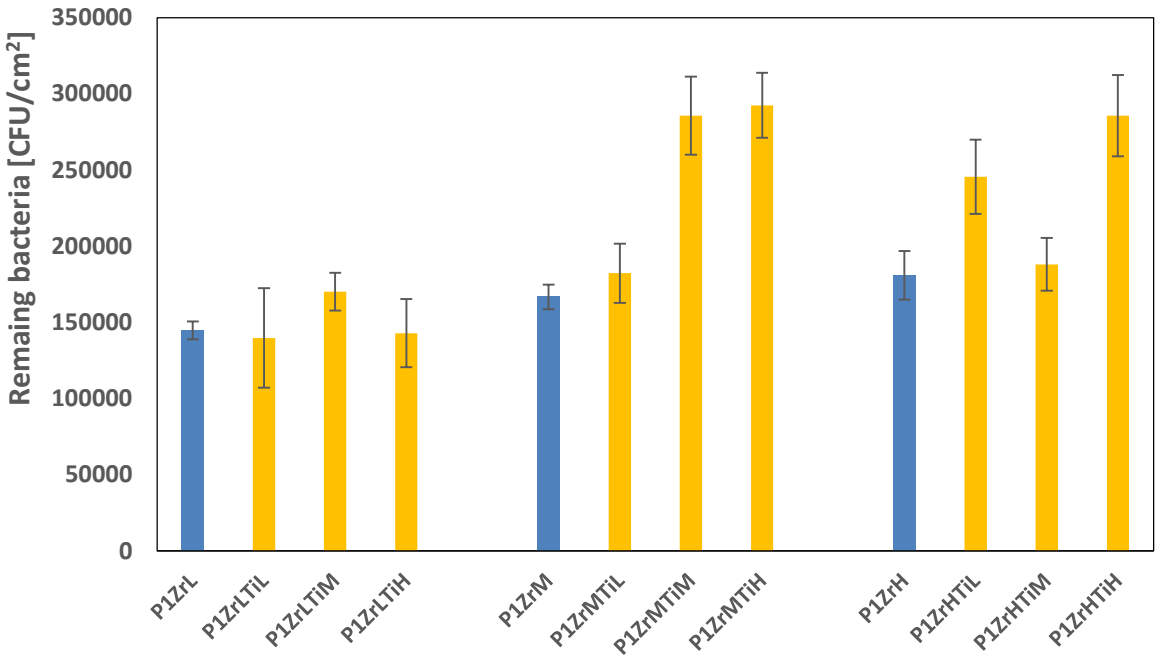

Figure 6.28 Comparison of remaining *Escherichia coli* on the Ni-P-PTFE-ZrO_2 and Ni-P-PTFE-ZrO_2-TiO_2 coatings (concentration of PTFE is 8ml/L)

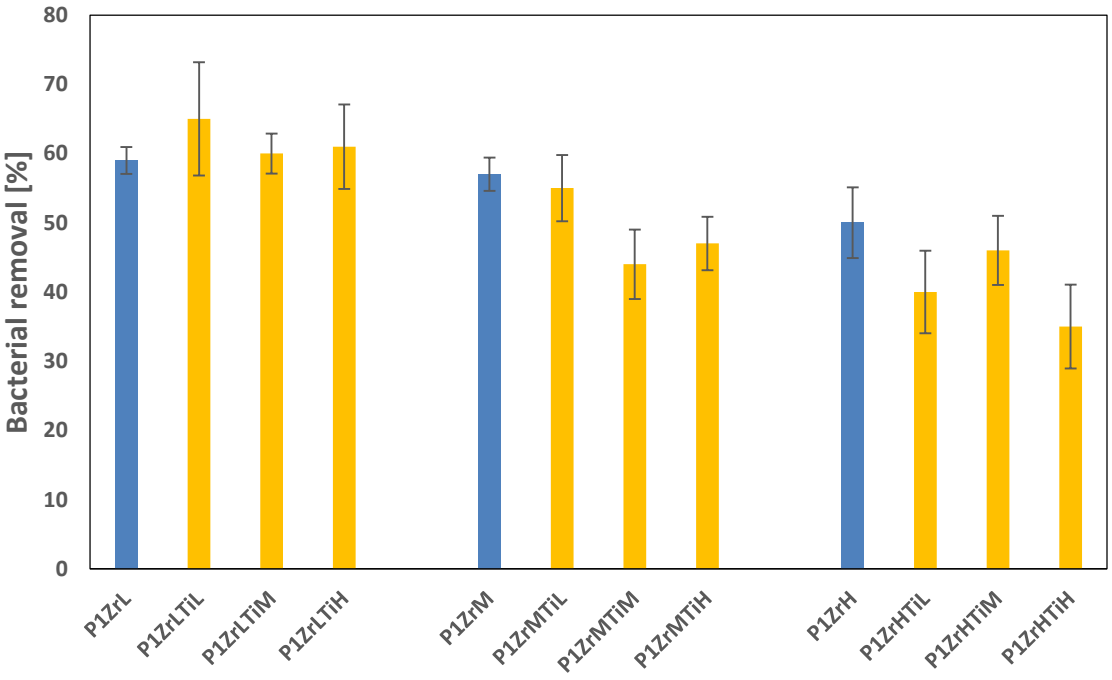

Figure 6.29 Comparison of removal percentage of *Escherichia coli from* Ni-P-PTFE-ZrO_2 and Ni-P-PTFE-ZrO_2-TiO_2 coatings (concentration of PTFE is 8ml/L)

Figure 6.30-6.32 compared the performance of Ni-P-PTFE-ZrO_2-TiO_2 and Ni-P-PTFE-ZrO_2 coatings prepared by high concentration of PTFE (12ml/L) and same concentration of ZrO_2 in the assay of *E. coli* adhesion and removal. According to these three figures, we can see that Ni-P-PTFE-ZrO_2-TiO_2 coatings show better performance than Ni-P-PTFE-ZrO_2 coatings, which means that addition of nanoparticle TiO_2 into Ni-P-PTFE-ZrO_2 plays an important role in enhancing the capability of resisting *E. coli* adhesion and reducing the strength of *E. coli* adhesion on the coatings.

Performances of Ni-P-PTFE-ZrO_2-TiO_2 and Ni-P-PTFE-ZrO_2 coatings in the assay of *S. aureus* adhesion and removal are shown in figure 6.36-6.38. These results are similar with that in the Figure 6.30-6.32. Addition of nanoparticle TiO_2 effectively enhance the capability of Ni-P-PTFE-ZrO_2-TiO_2 coatings to resist *S. aureus* adhesion and remove adhered *S. aureus* cells easily, which means that Ni-P-PTFE-ZrO_2-TiO_2 coatings have better capability of resisting *S. aureus* adhesion and remaining less *S. aureus* cells on the surfaces than Ni-P-PTFE-ZrO_2 coatings.

In conclusion, firstly, Ni-P-PTFE-ZrO_2-TiO_2 prepared by 8ml/L PTFE did not show better capability of resisting *E. coli* adhesion and reducing adhered *E. coli* using a dipping process than Ni-P-PTFE-ZrO_2 did. However, Ni-P-PTFE-ZrO_2-TiO_2 prepared by 8ml/L PTFE performed better in the assays of *S. aureus* adhesion and removal than Ni-P-PTFE-ZrO_2. Secondly, all Ni-P-PTFE-ZrO_2-TiO_2 prepared by 12ml/L PTFE have better capability of resisting bacterial adhesion and reducing adhered bacteria using a dipping process than Ni-P-PTFE-ZrO_2 did. Basically, addition of TiO_2 have significant effect on enhancing the capability of resisting bacterial adhesion and decreasing bacterial adhesive strength between bacteria and coatings.

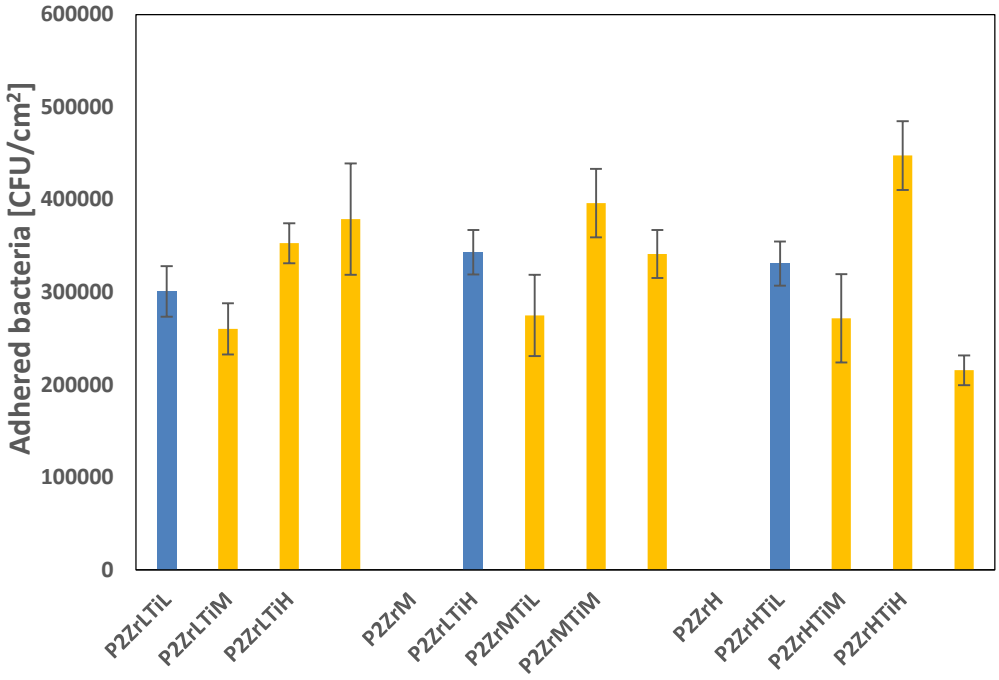

Figure 6.30 Comparison of Ni-P-PTFE-ZrO_2 and Ni-P-PTFE-ZrO_2-TiO_2 coatings (concentration of PTFE is 12ml/L) against *Escherichia coli* adhesion

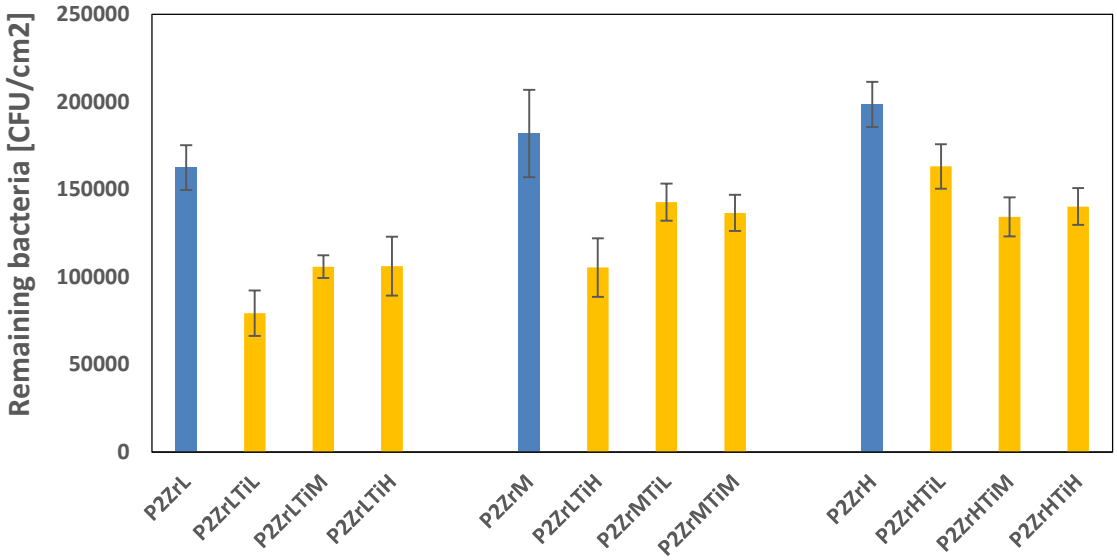

Figure 6.31 Comparison of remaining *Escherichia coli* on the Ni-P-PTFE-ZrO_2 and Ni-P-PTFE-ZrO_2-TiO_2 coatings (concentration of PTFE is 12ml/L)

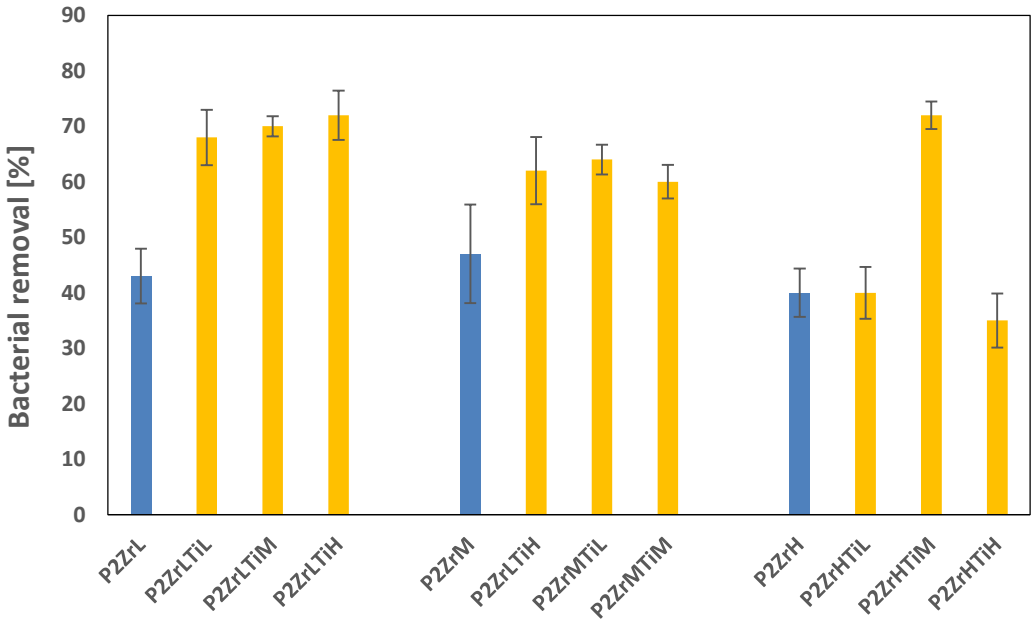

Figure 6.32 Comparison of removal percentage of *Escherichia coli from* Ni-P-PTFE-ZrO_2 and Ni-P-PTFE-ZrO_2-TiO_2 coatings (concentration of PTFE is 12ml/L)

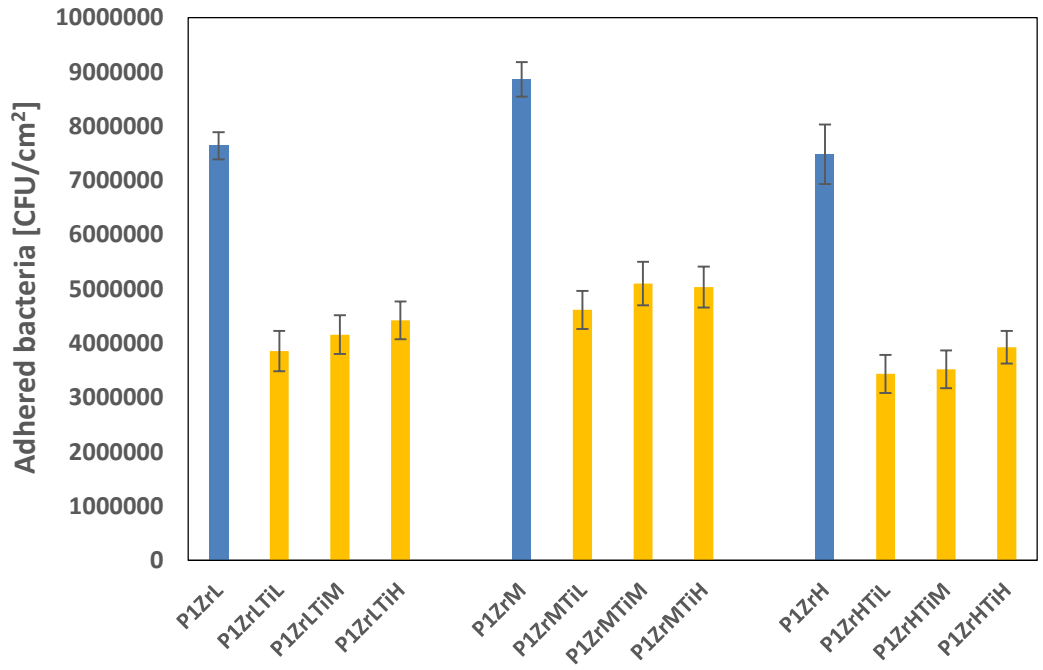

Figure 6.33 Comparison of Ni-P-PTFE-ZrO_2 and Ni-P-PTFE-ZrO_2-TiO_2 coatings (concentration of PTFE is 8ml/L) against *Staphylococcus aureus* adhesion

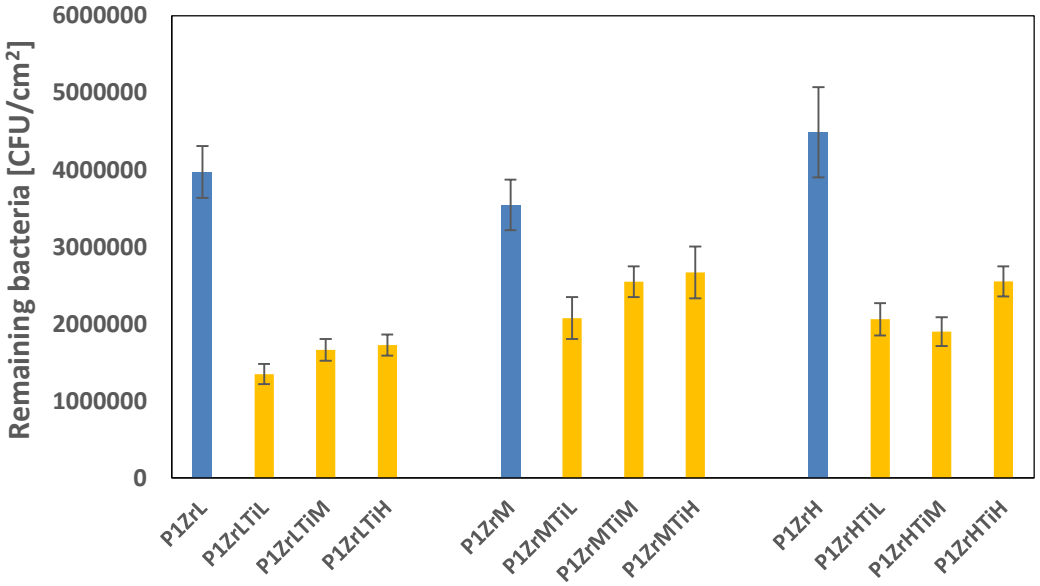

Figure 6.34 Comparison of remaining *Staphylococcus aureus* on the Ni-P-PTFE-ZrO_2 and Ni-P-PTFE-ZrO_2-TiO_2 coatings (concentration of PTFE is 8ml/L)

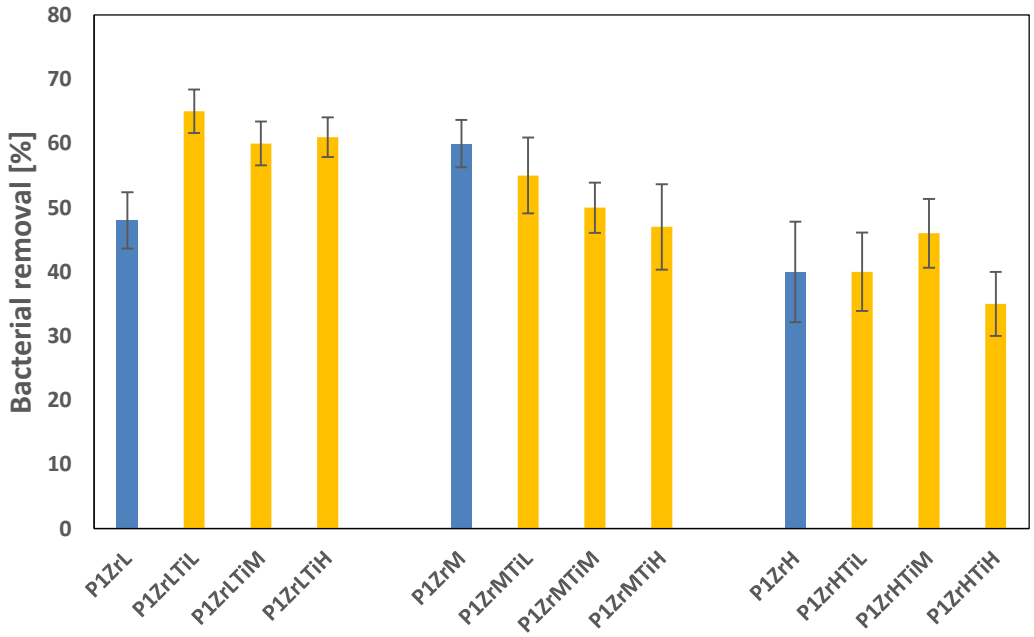

Figure 6.35 Comparison of removal percentage of *Staphylococcus aureus from* Ni-P-PTFE-ZrO_2 and Ni-P-PTFE-ZrO_2-TiO_2 coatings (concentration of PTFE is 8ml/L)

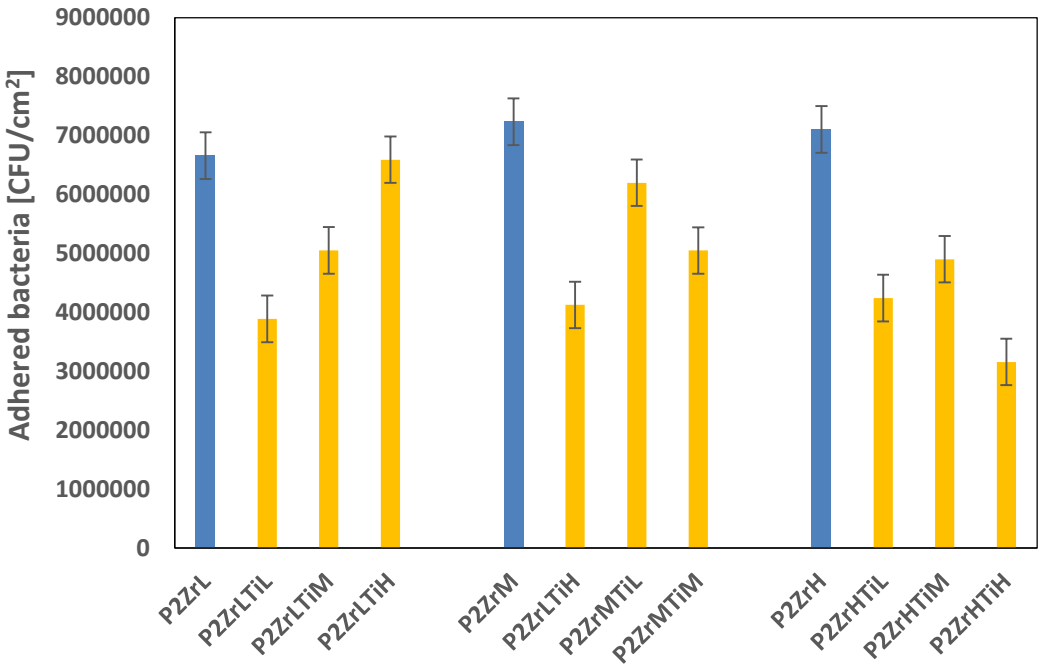

Figure 6.36 Comparison of Ni-P-PTFE-ZrO_2 and Ni-P-PTFE-ZrO_2-TiO_2 coatings (concentration of PTFE is 12ml/L) against *Staphylococcus aureus* adhesion

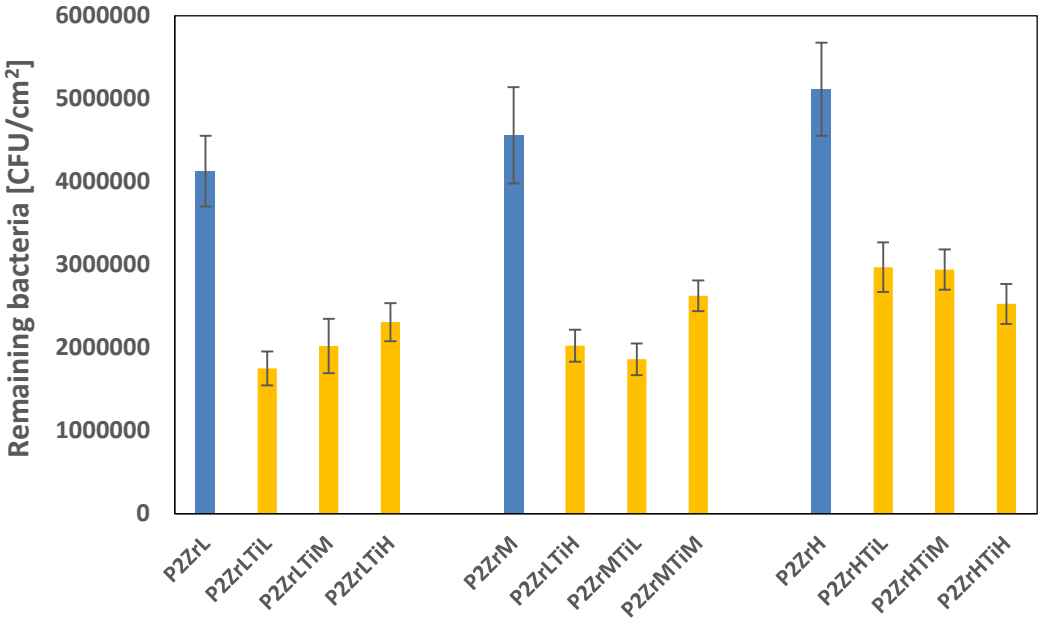

Figure 6.37 Comparison of remaining *Staphylococcus aureus* on the Ni-P-PTFE-ZrO_2 and Ni-P-PTFE-ZrO_2-TiO_2 coatings (concentration of PTFE is 12ml/L)

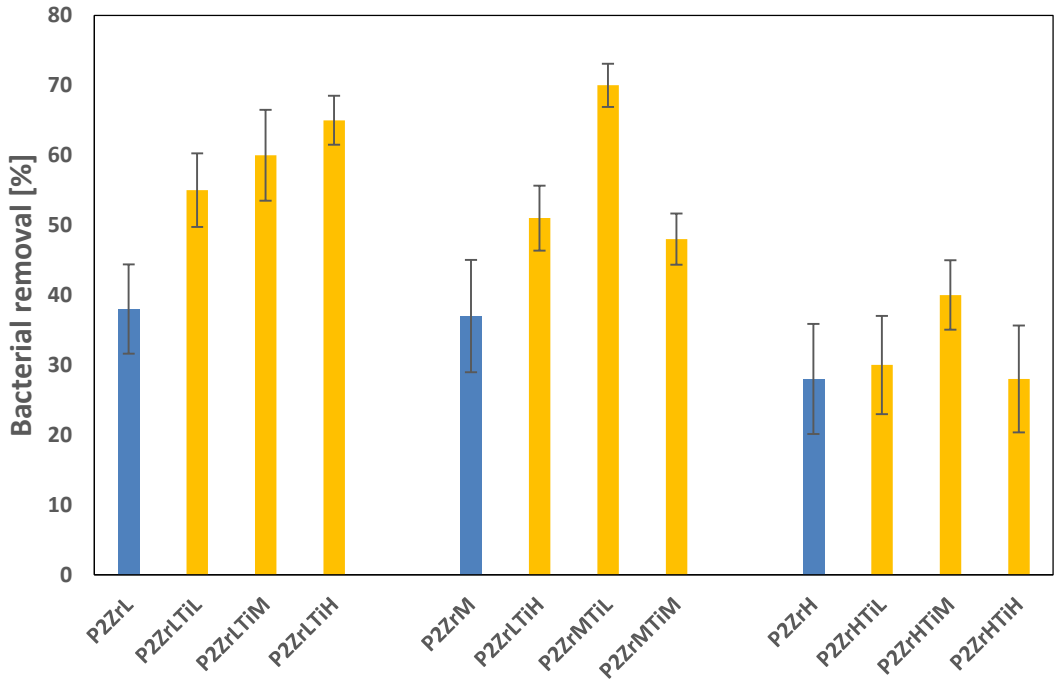

Figure 6.38 Comparison of removal percentage of *Staphylococcus aureus from* Ni-P-PTFE-ZrO_2 and Ni-P-PTFE-ZrO_2-TiO_2 coatings (concentration of PTFE is 12ml/L)

6.1.2.3 Effect of PTFE on Bacterial Adhesion and Removal

Figure 6.15, 6.17, 6.21 and 6.23 show the effect of PTFE on the performance of Ni-P-PTFE-ZrO_2-TiO_2 in the assay of *E. coli* adhesion and removal. According to Figure 6.15 and 6.21, Ni-P-PTFE-ZrO_2-TiO_2 coatings prepared by high concentration of PTFE (12ml/L) can resist adhesion of *E. coli* better than those prepared by low concentration (8ml/L), which is consistent with the effect of PTFE on performance of Ni-P-PTFE-ZrO_2 coatings in resisting *E. coli* adhesion.

The effect of PTFE on the performance of Ni-P-PTFE-ZrO_2-TiO_2 coatings in the assay of *E. coli* removal can be seen in figure 6.17 and 6.23. Ni-P-PTFE-ZrO_2-TiO_2 coatings prepared by low concentration of PTFE (8 ml/L) remain larger number of *E. coli* than those prepared by high concentration (12ml/L), according to table 3.4, Ni-P-PTFE-ZrO_2-TiO_2 coatings prepared by low

concentration of PTFE (8 ml/L) have larger value of total surface free energy (SFE) and its component such as γ^{LW} and γ^{-} than Ni-P-PTFE-ZrO_2-TiO_2 coatings prepared by high concentration of PTFE (12 ml/L), and according to correlation between SFE, γ^{LW} and γ^{-} vs. number of bacterial remaining on Ni-P-PTFE-ZrO_2-TiO_2 coatings in figure 6.41-6.45, we can conclude that maybe larger SFE, γ^{LW} make a lager contribution than γ^{-}, which leads to larger number of *E. coli* remaining on Ni-P-PTFE-ZrO_2-TiO_2 coatings prepared by 8ml/L PTFE.

However, from Figure 6.16, 6.19, 6.22 and 6.25, in the assay of *S. aureus* adhesion and removal, Ni-P-PTFE-ZrO_2-TiO_2 coatings prepared by low concentration of PTFE (8ml/L) can resist *S. aureus* adhesion better than those prepared by high concentration (12ml/L) and less *S. aureus* remain on the Ni-P-PTFE-ZrO_2-TiO_2 coatings prepared by low concentration of PTFE (8ml/L) than those prepared by high concentration (12ml/L). The results are opposite with that in the assay of *E. coli* adhesion and removal on Ni-P-PTFE-ZrO_2-TiO_2 coatings. The reason is that *S. aureus* has larger surface free energy component γ^{-} than *E. coli*, which lead to it is more sensitive to γ^{-} of Ni-P-PTFE-ZrO_2-TiO_2 coatings, since Ni-P-PTFE-ZrO_2-TiO_2 coatings prepared by low concentration of PTFE (8ml/L) have larger value of surface free energy component γ^{-}, which lead to the less *S. aureus* adhering and remaining on Ni-P-PTFE-ZrO_2-TiO_2 (8ml/L) coatings.

6.1.2.4 Effect of surface free energy of Ni-P-PTFE-ZrO_2-TiO_2 coatings on bacterial adhesion and removal

As shown in Figure 6.39 and 6.40, there exists a correlation between number of adhered bacteria and total surface free energy of Ni-P-PTFE-ZrO_2-TiO_2 coatings. According to Figure 6.39, when

the surface free energy of coatings was approximately 23 mJ/m^2, the number of *E. coli* attached to the coating reached to minimum. And similar results of relationship between *S. aureus* adhesion and surface free energy were obtained in Figure 6.40. There also exists an optimal surface free energy at about 25mJ/m^2, where the number of bacterial adhesion is minimal, which also verifies that surface free energy between 20 and 30mJ/m^2 is optimal to resist bacterial adhesion. It is consistent with the conclusion of the optimal surface free energy of Ni-P-PTFE-ZrO_2 coatings against *E. coli* and *S. aureus*. The correlation coefficient R^2 values for number of *E. coli* and *S. aureus* adhesion (CFU/cm^2) versus surface free energy were 0.7743 and 0.7736 respectively.

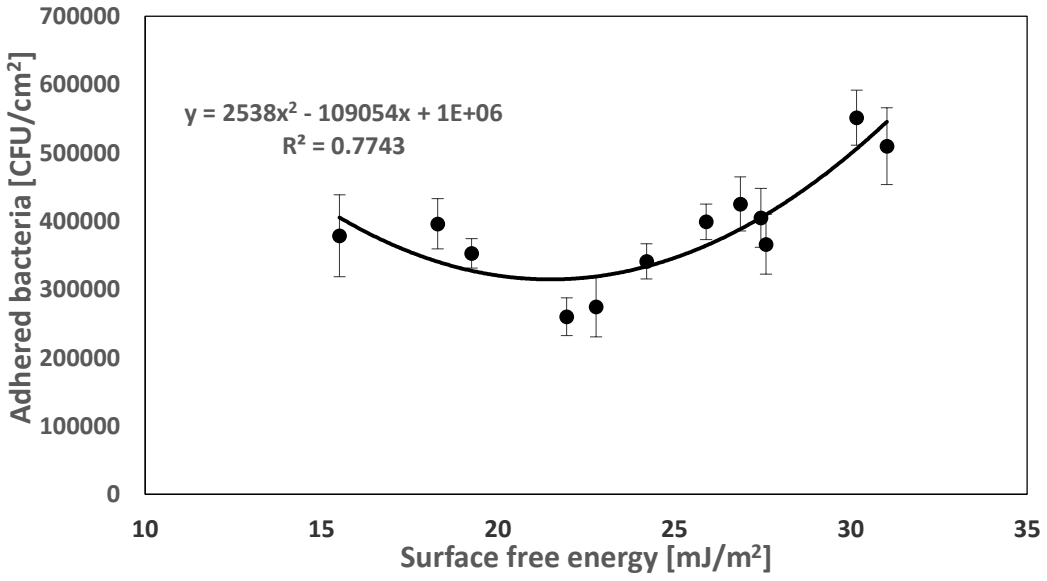

Figure 6.39 Effect of Surface Free Energy of Ni-P-PTFE-ZrO_2-TiO_2 coatings on the adhesion of *Escherichia coli*

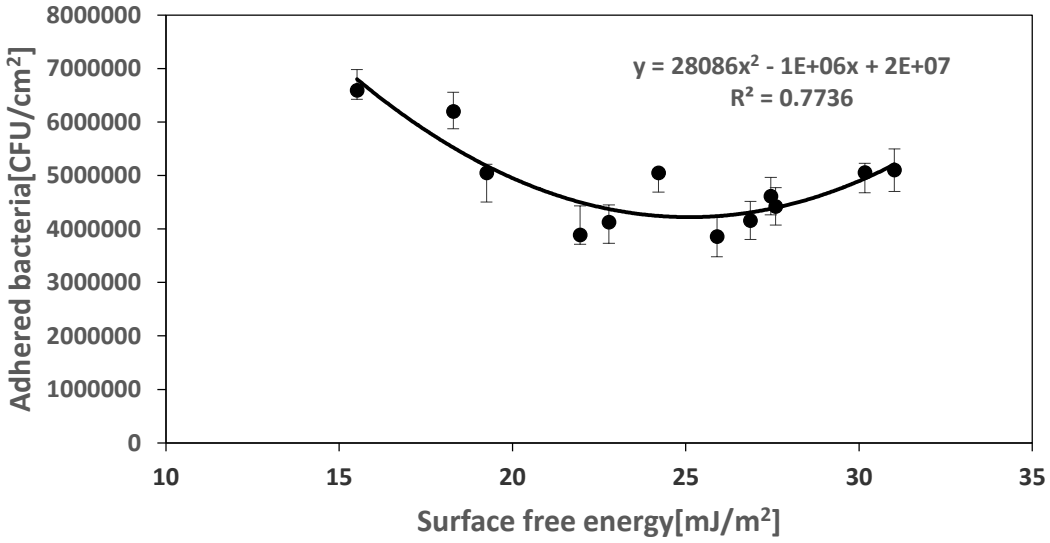

Figure 6.40 Effect of Surface Free Energy of Ni-P-PTFE-ZrO_2-TiO_2 coatings on the adhesion of *Staphylococcus aureus*

Figure6.41-6.60 show the relationship between surface free energy components such as total surface free energy (SFE), γ^{LW} and γ^{-} of Ni-P-PTFE-ZrO_2-TiO_2 coatings versus number of remaining bacteria (CFU/cm^2), removal percentage (%) in the assay of *E. coli* and *S. aureus* removal.

Figure 6.41, 6.46, 6.51 and 6.56 show the correlation between surface free energy of Ni-P-PTFE-ZrO_2-TiO_2 coatings and number of remaining bacteria including *E. coli* and *S. aureus* using a dipping process, Ni-P-PTFE-ZrO_2-TiO_2 coatings were classified into two different set of coatings according to different concentrations of PTFE (8ml/L and 12ml/L). These four figures all show that number of remaining *E. coli* cells and *S. aureus* cells on the Ni-P-PTFE-ZrO_2-TiO_2 coatings increased with surface free energy (SFE) of these coatings increasing. And according to these figures, we can conclude that when surface free energy of coatings are about 25 mJ/m^2, the strength of bacterial adhesion to the coatings was the weakest, which is consistent with the relationship between surface free energy of Ni-P-PTFE-ZrO_2 coatings and number of remaining

bacteria (CFU/cm^2). The correlation coefficient R^2 values of the figures mentioned above are 0.8026, 0.3195, 0.5999 and 0.41 respectively.

While Figure 6.42, 6.47, 6.52 and 6.57 show the correlation between surface free energy component γ^{LW} of Ni-P-PTFE-ZrO_2-TiO_2 coatings and number of remaining *E. coli* and *S. aureus*. Similar with the relationship of SFE and number of remaining bacteria, number of remaining bacteria including *E. coli* and *S. aureus* increases with γ^{LW} increasing. The correlation coefficient R^2 values of the figures mentioned above are 0.5378, 0.5895, 0.4592 and 0.6059 respectively.

However, Figure 6.43, 6.48, 6.53 and 6.58 show the number of remaining bacteria on the Ni-P-PTFE-ZrO_2-TiO_2 coatings decreased with surface free energy component γ^- of Ni-P-PTFE-ZrO_2-TiO_2 coatings increasing, which is opposite correlation compared with relationship between remaining bacteria vs γ^{LW} and remaining bacteria vs surface free energy. The correlation coefficient R^2 values of the figures mentioned above are from 0.2667 to 0.5642.

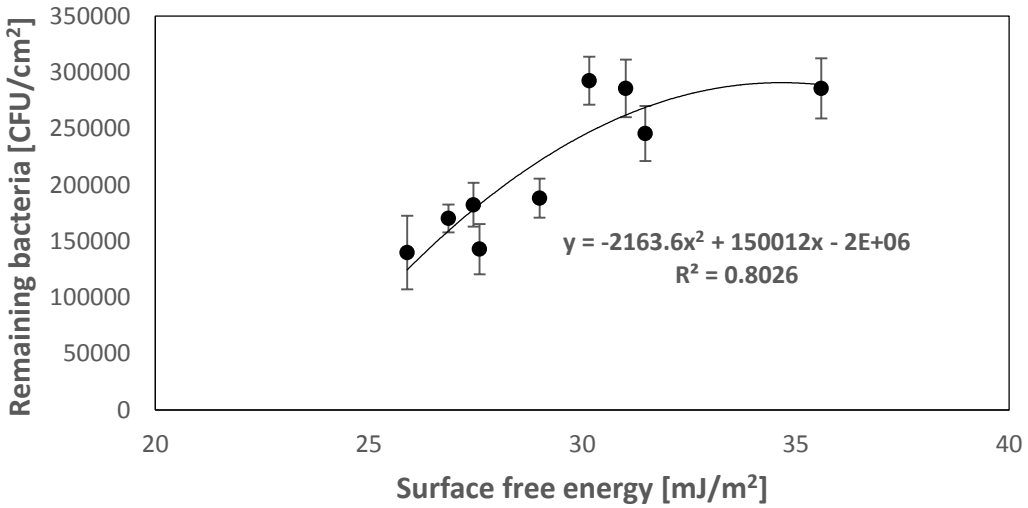

Figure 6.41 Effect of Surface Free Energy of Ni-P-PTFE-ZrO_2-TiO_2 coatings on the remaining *Escherichia coli* (concentration of PTFE=8ml/L)

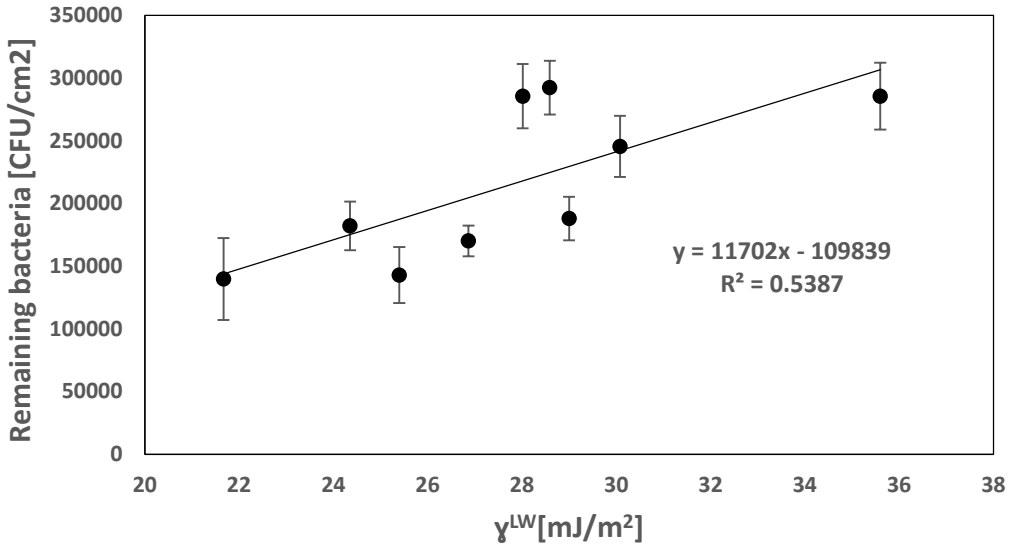

Figure 6.42 Effect of γ^{LW} of Ni-P-PTFE-ZrO_2-TiO_2 coatings on the remaining *Escherichia coli* (concentration of PTFE=8ml/L)

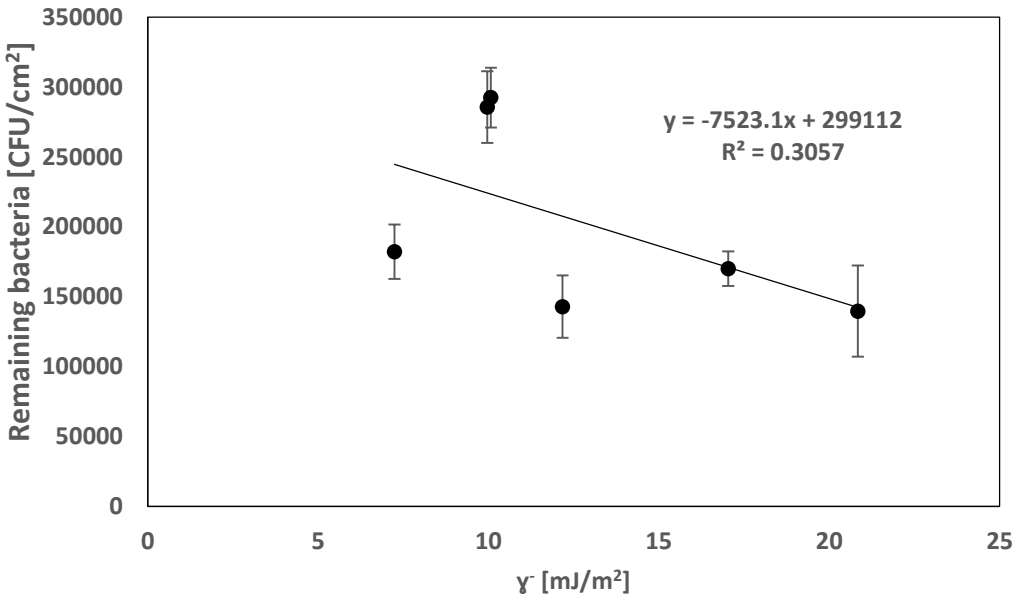

Figure 6.43 Effect of γ^- of Ni-P-PTFE-ZrO_2-TiO_2 coatings on the remaining *Escherichia coli* (concentration of PTFE=8ml/L)

The relationship between removal rate of bacteria and surface free energy of Ni-P-PTFE-ZrO_2-TiO_2 coatings are also investigated. From Figure 6.44, 6.49, 6.54 and 6.59, multinomial regression analysis of these data revealed that percentage of bacterial removal was negatively correlated with surface free energy and the correlation coefficient R^2 illustrate that there is strong relationship between surface free energy and bacterial removal (%).The correlation coefficient R^2 values of the figures mentioned above are 0.9443, 0.875, 0.8852 and 0.9402 respectively.

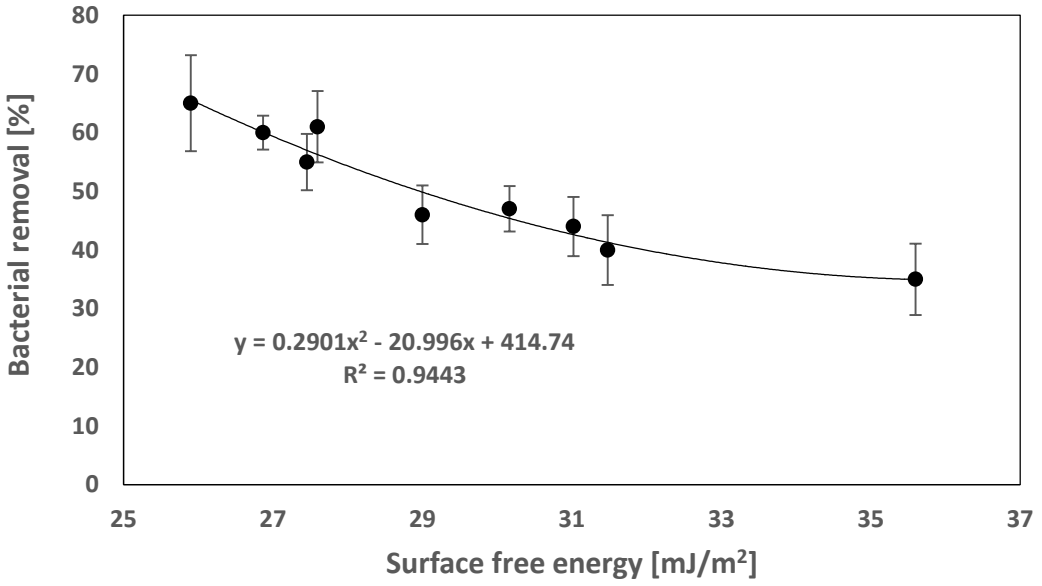

Figure 6.44 Effect of Surface Free Energy of Ni-P-PTFE-ZrO_2-TiO_2 coatings on *Escherichia coli* removal rate (concentration of PTFE=8ml/L)

Similar correlation between γ^{LW} of Ni-P-PTFE-ZrO_2-TiO_2 coatings and bacterial removal rate are shown in Figure 6.45, 6.50, 6.55 and 6.60. According these four figures, the surface free energy component γ^{LW} negatively affect the bacterial removal rate for both two bacteria. The correlation coefficient R^2 values for removal rate of both *E. coli* and *S. aureus* and surface free

energy were 0.8075, 06601, 0.8417 and 0.8535, which means the correlation between bacterial removal rate and surface free energy component γ^{LW} is quite strong.

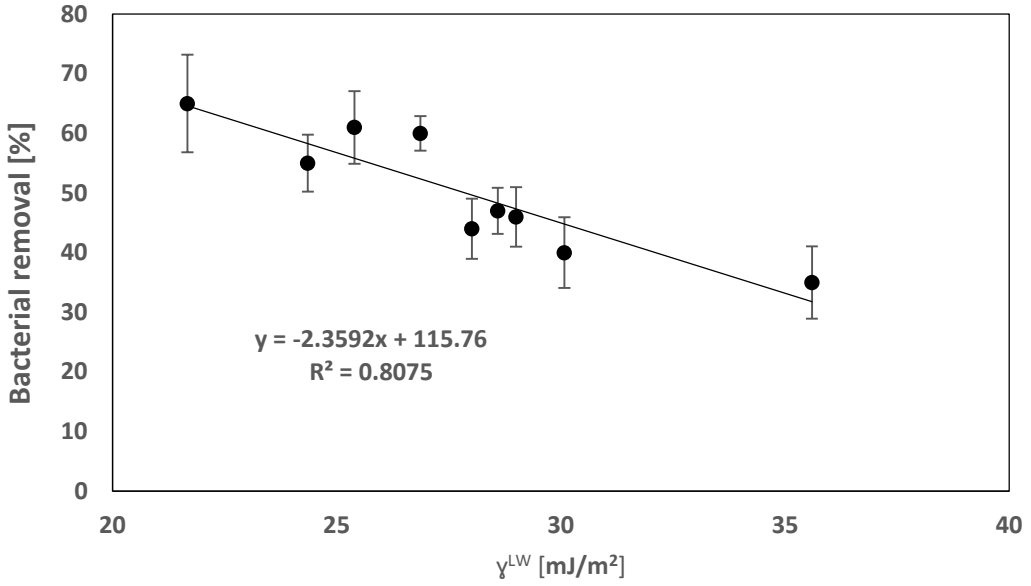

Figure 6.45 Effect of γ^{LW} of Ni-P-PTFE-ZrO_2-TiO_2 coatings on *Escherichia coli* removal rate (concentration of PTFE=8ml/L)

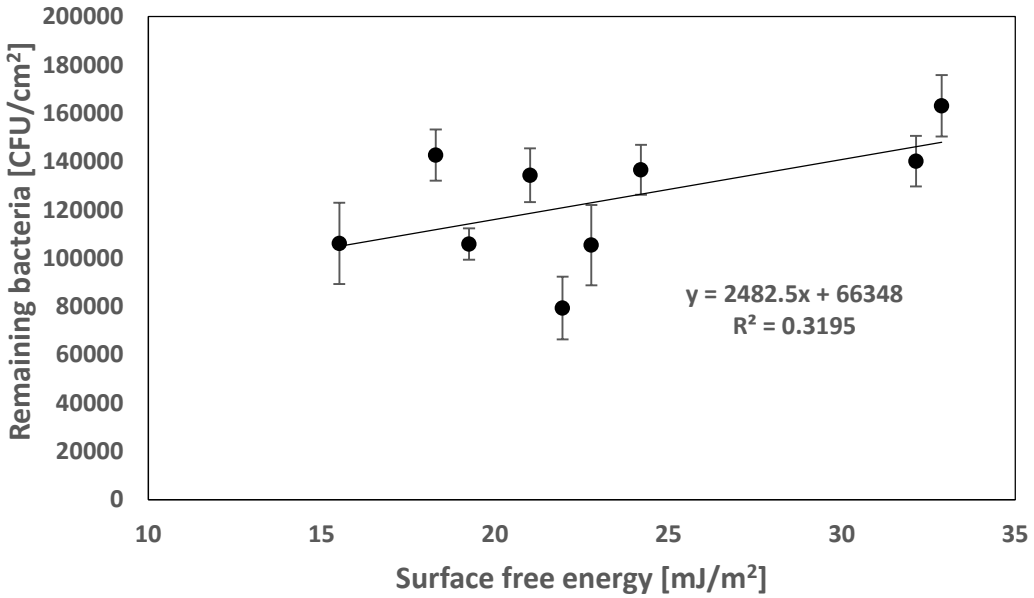

Figure 6.46 Effect of Surface Free Energy of Ni-P-PTFE-ZrO_2-TiO_2 coatings on the remaining *Escherichia coli* (concentration of PTFE=12ml/L)

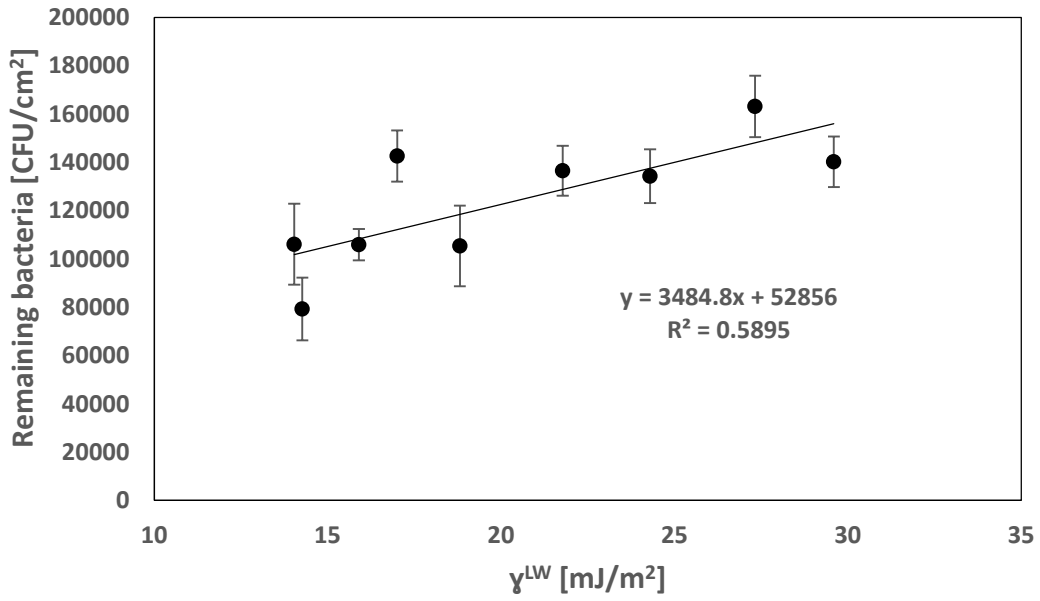

Figure 6.47 Effect of γ^{LW} of Ni-P-PTFE-ZrO_2-TiO_2 coatings on the remaining *Escherichia coli* (concentration of PTFE=12ml/L)

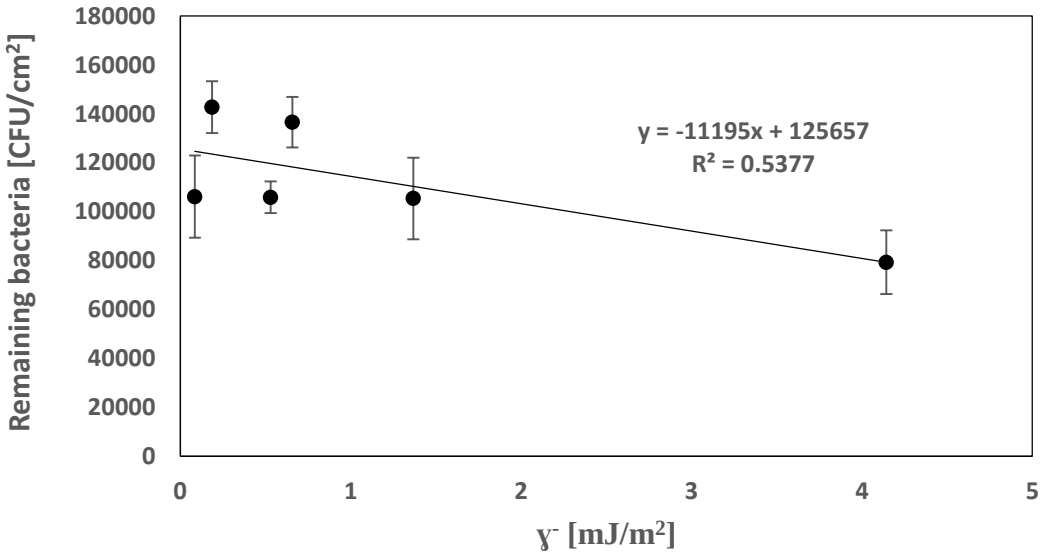

Figure 6.48 Effect of γ^- of Ni-P-PTFE-ZrO_2-TiO_2 coatings on the remaining *Escherichia coli* (concentration of PTFE=12ml/L)

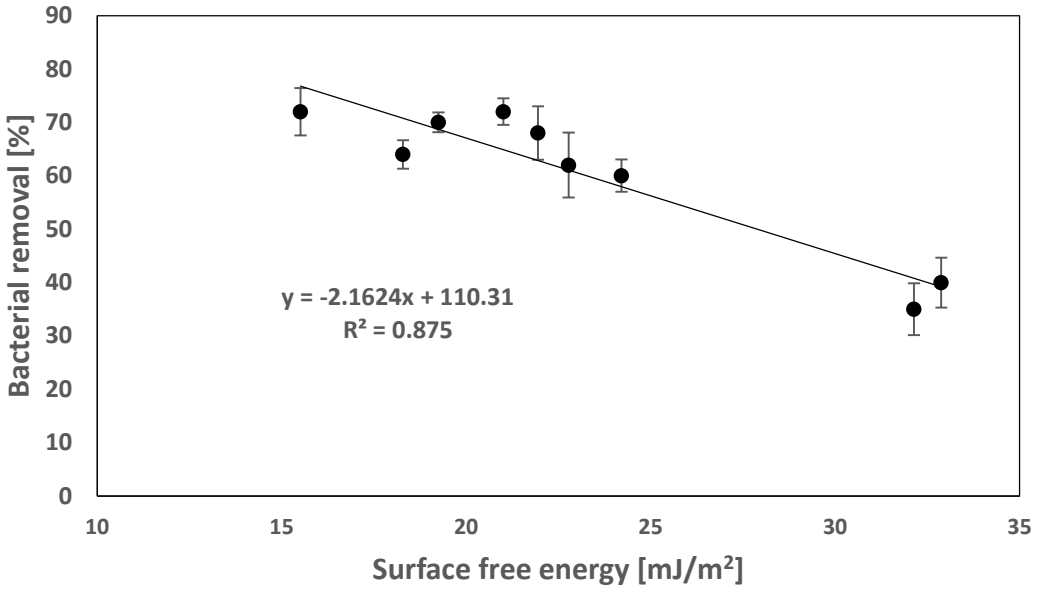

Figure 6.49 Effect of Surface Free Energy of Ni-P-PTFE-ZrO_2-TiO_2 coatings on *Escherichia coli* removal rate (concentration of PTFE=12ml/L)

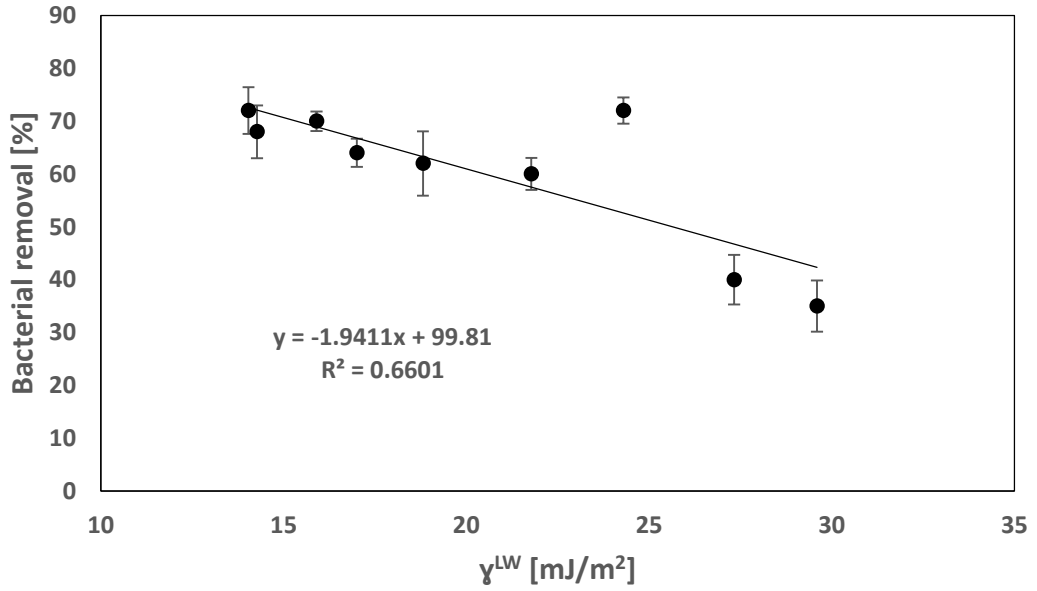

Figure 6.50 Effect of γ^{LW} of Ni-P-PTFE-ZrO_2-TiO_2 coatings on *Escherichia coli* removal rate (concentration of PTFE=12ml/L)

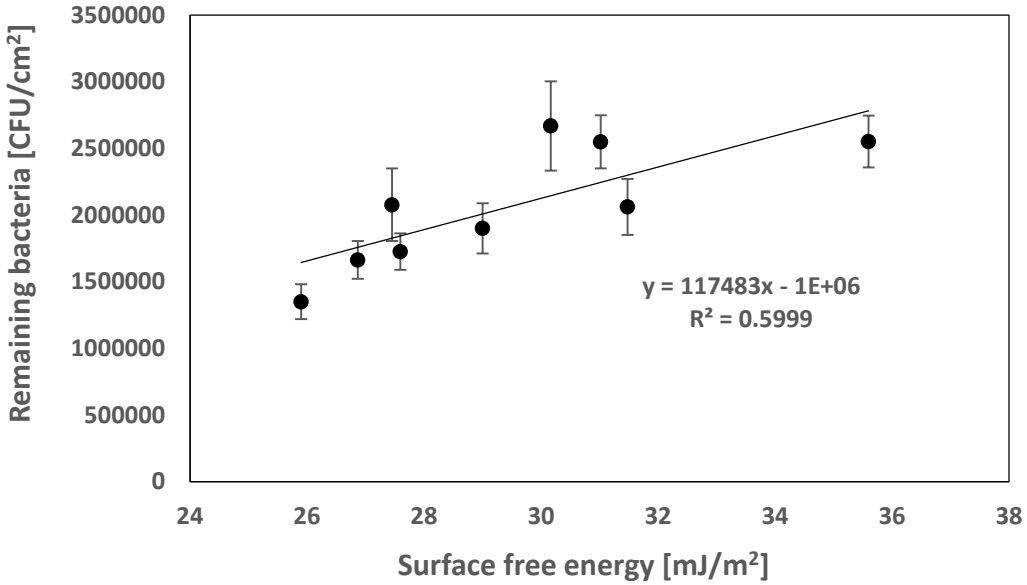

Figure 6.51 Effect of Surface Free Energy of Ni-P-PTFE-ZrO_2-TiO_2 coatings on the remaining *staphylococcus aureus* (concentration of PTFE=8ml/L)

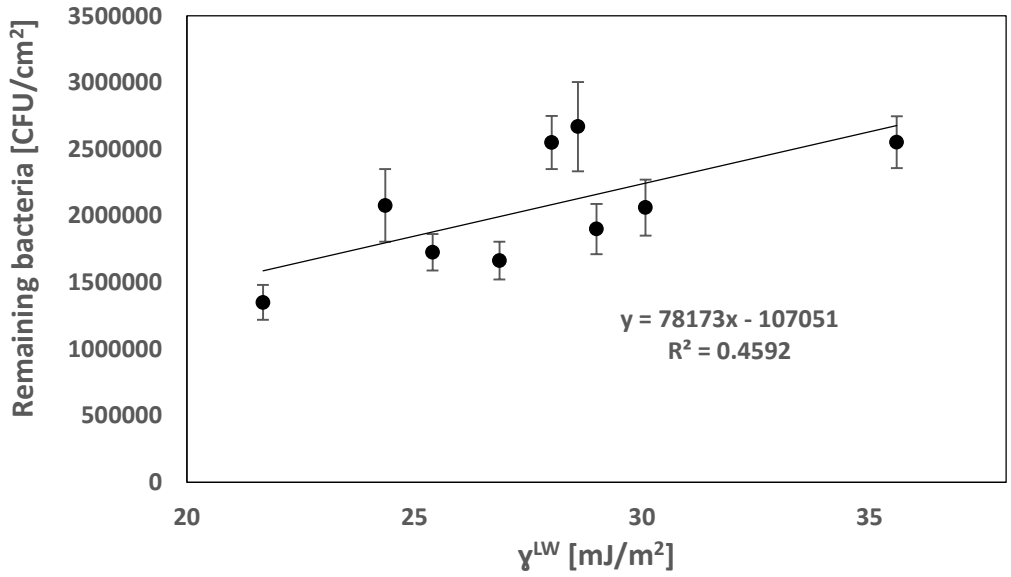

Figure 6.52 Effect of γ^{LW} of Ni-P-PTFE-ZrO_2-TiO_2 coatings on the remaining *staphylococcus aureus* (concentration of PTFE=8ml/L)

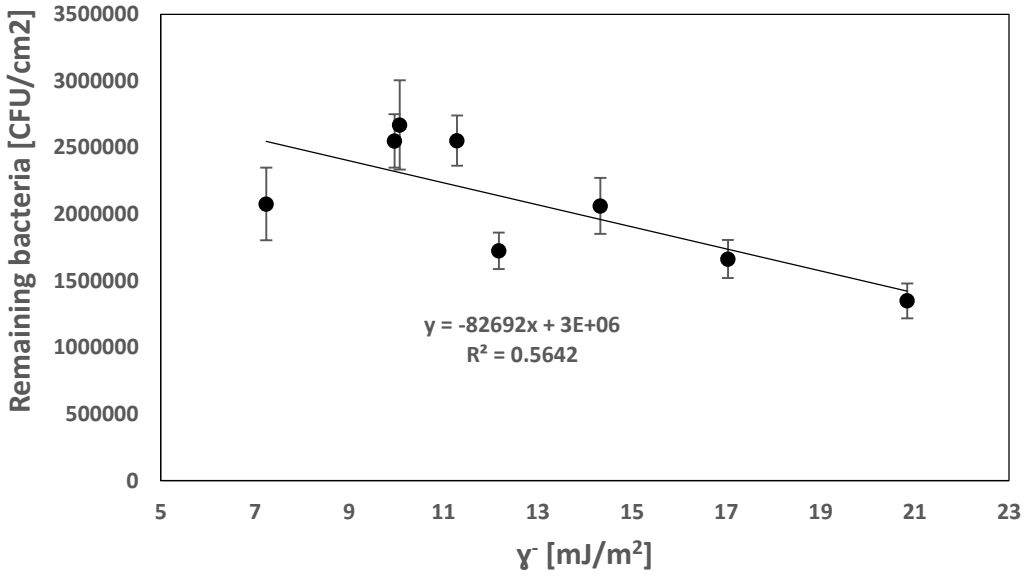

Figure 6.53 Effect of γ^- of Ni-P-PTFE-ZrO_2-TiO_2 coatings on the remaining *staphylococcus aureus* (concentration of PTFE=8ml/L)

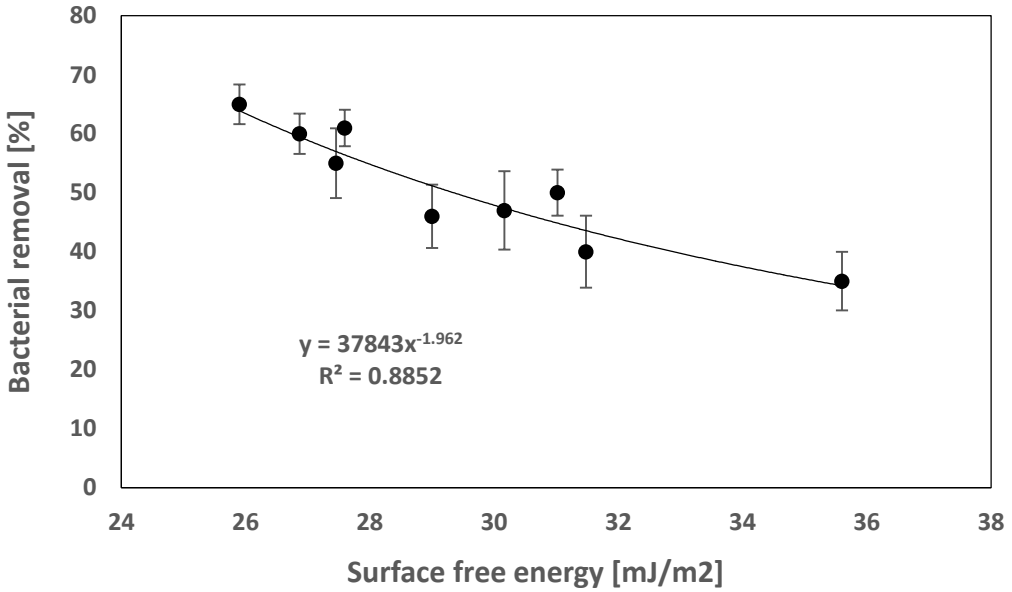

Figure 6.54 Effect of Surface Free Energy of Ni-P-PTFE-ZrO_2-TiO_2 coatings on *staphylococcus aureus* removal rate (concentration of PTFE=8ml/L)

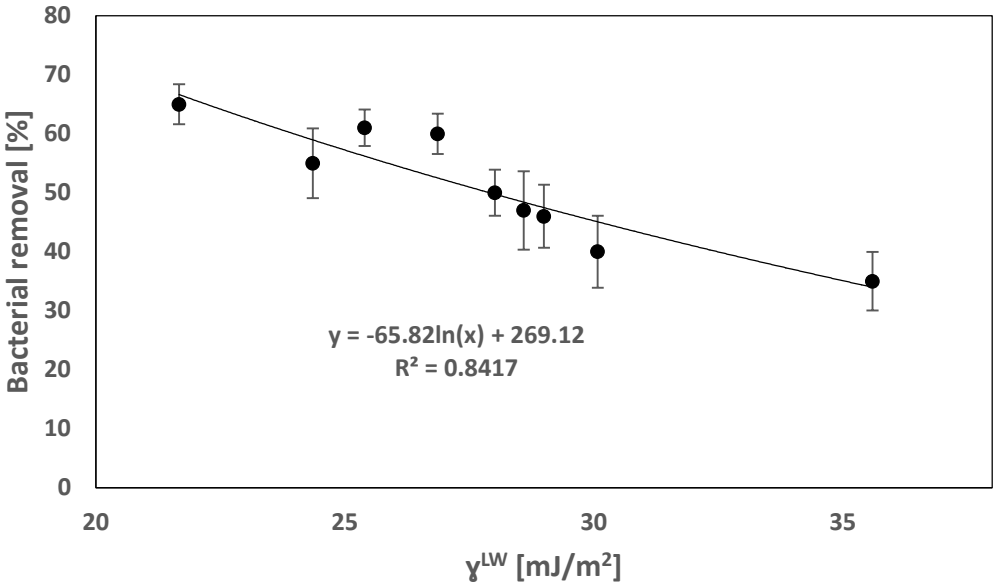

Figure 6.55 Effect of γ^{LW} of Ni-P-PTFE-ZrO_2-TiO_2 coatings on *staphylococcus aureus* removal rate (concentration of PTFE=8ml/L)

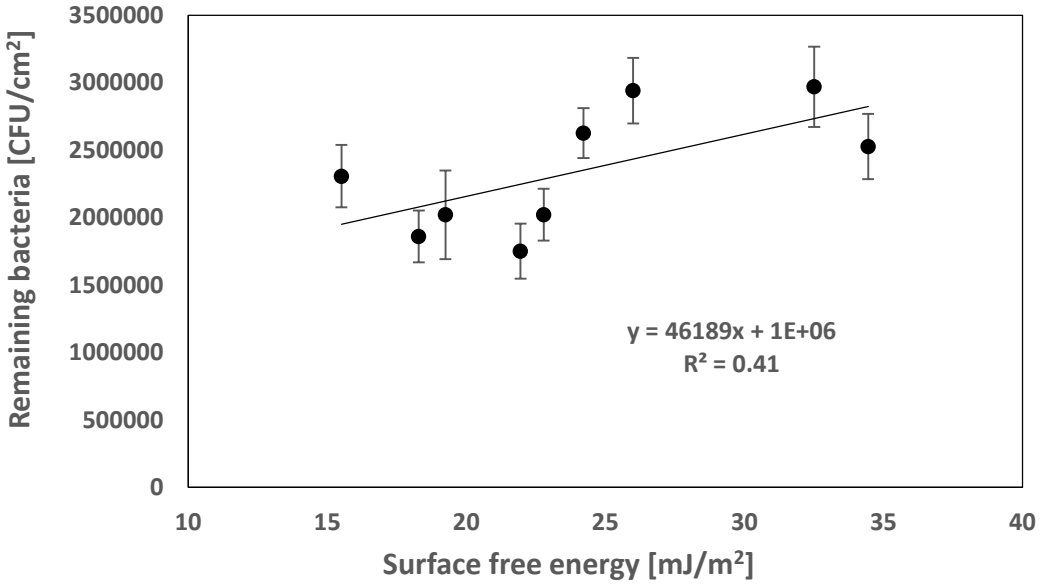

Figure 6.56 Effect of Surface Free Energy of Ni-P-PTFE-ZrO_2-TiO_2 coatings on the remaining *staphylococcus aureus* (concentration of PTFE=12ml/L)

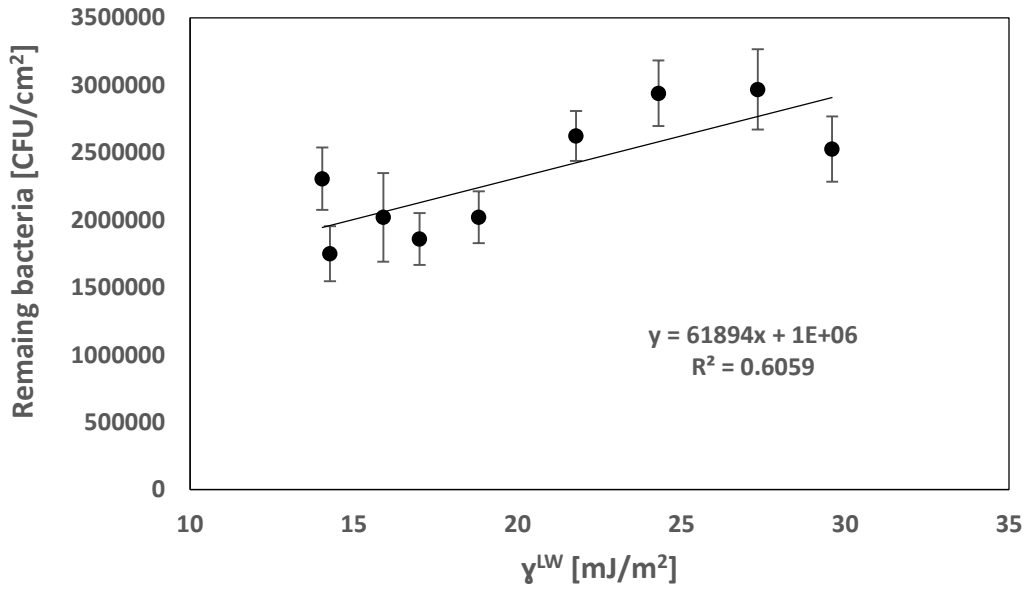

Figure 6.57 Effect of γ^{LW} of Ni-P-PTFE-ZrO_2-TiO_2 coatings on the remaining *staphylococcus aureus* (concentration of PTFE=12ml/L)

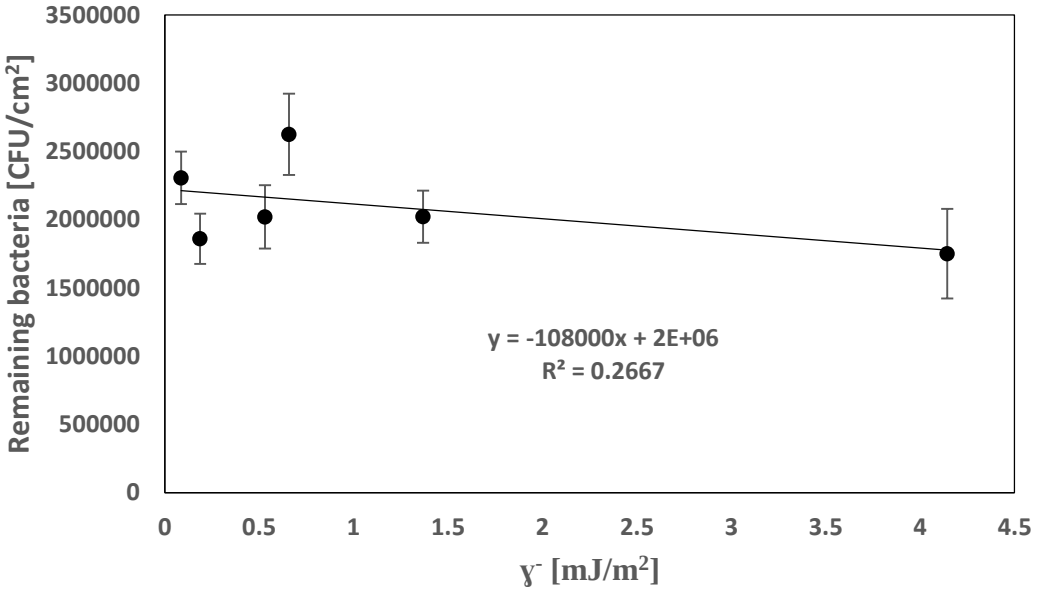

Figure 6.58 Effect of γ^- of Ni-P-PTFE-ZrO_2-TiO_2 coatings on the remaining *staphylococcus aureus* (concentration of PTFE=12ml/L)

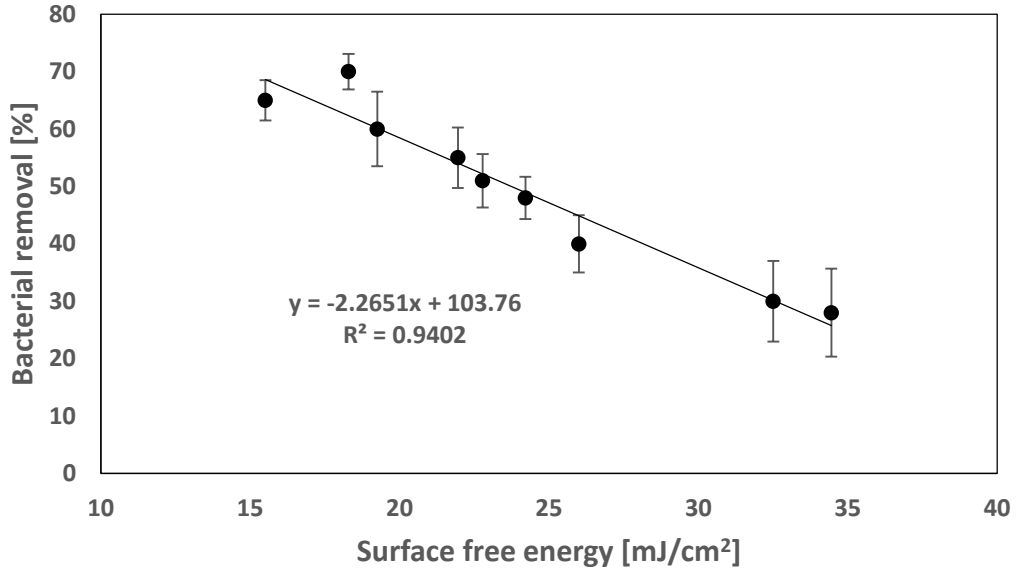

Figure 6.59 Effect of Surface Free Energy of Ni-P-PTFE-ZrO_2-TiO_2 coatings on *staphylococcus aureus* removal rate (concentration of PTFE=12ml/L)

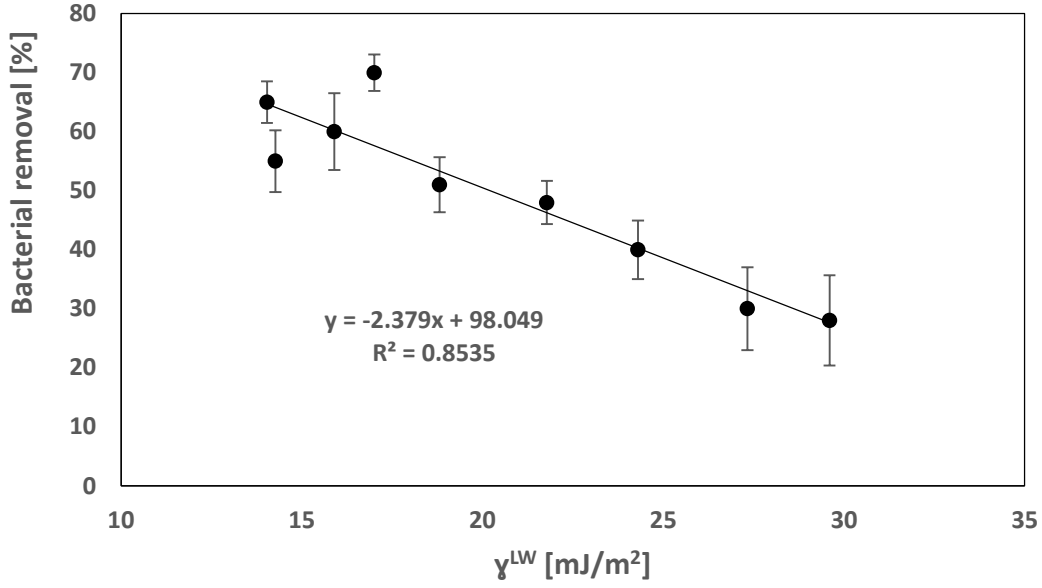

Figure 6.60 Effect of γ^{LW} of Ni-P-PTFE-ZrO_2-TiO_2 coatings on *staphylococcus aureus* removal rate (concentration of PTFE=12ml/L)

6.2 Anticorrosion Performance of Ni-P-PTFE Based Coatings

In this assay, anticorrosive property of Ni-P, Ni-P-PTFE and a series of Ni-P-PTFE based coatings such as Ni-P-PTFE-ZrO_2 and Ni-P-PTFE-ZrO_2-TiO_2 coatings are tested by measuring the open circuit potential and anodic, cathodic tafel plots by CS300 Electrochemistry Workstation to evaluate the anticorrosive performances of coatings above. Different coupons are tested in two different solutions respectively, including 0.9% and 3.5% NaCl solutions.

6.2.1 Measurement of the open circuit potential

6.2.1.1 Ni-P-PTFE-ZrO_2 coatings

The open circuit potential can be used as a criterion for the corrosion behaviour. It is a parameter which is used to show the thermodynamical tendency of a material to electrochemical oxidation in a corrosive medium. And it usually shows a relatively stable value after a period of time immersing in a corrosive solution. In this study, the open circuit potential of coatings are tested by immersing them in the 0.9% NaCl and 3.5% NaCl respectively.

Figure 6.61 and 6.62 show the open circuit potential of Ni-P-PTFE-ZrO_2 coatings in 0.9% NaCl solution and 3.5% NaCl solution respectively. It can be seen from figures 6.61 and figure 6.62 that the open circuit potential tends to be stable after varing with time at intial measurement. For the test of the open circuit potential in 0.9% NaCl, Ni-P-PTFE(8ml/L) shows the highest potential followed by coatings P1ZrH, P1ZrM, P2ZrL and Ni-P, which means Ni-P-PTFE-ZrO_2 coatings did not have better thermodynamically stability than Ni-P-PTFE coating, but had better thermodynamically stability than Ni-P coating.

However, when coupons were in the 3.5% NaCl solution, coating P2ZrL presents highest corrosion potential, followed by coating P2ZrM and coating P2ZrH,which means that Ni-P-PTFE-ZrO_2 coatings prepared by 12ml/L of PTFE and low concentration of ZrO_2 (0.625g/L) is more themodynamically stable. Ni-P coating and Ni-P-PTFE coating were in the middle position. While that Ni-P-PTFE-ZrO_2 coatings 5 and 6 present lowest corrosion potential.

In conclusion, Ni-P-PTFE-ZrO_2 coatings prepared by 12 ml/L of PTFE show better thermodynamically stabilility than Ni-P and Ni-P-PTFE coatings in the 3.5% NaCl solution. While in the 0.9% NaCl solution, both Ni-P-PTFE and Ni-P-PTFE-ZrO_2 coatings prepared by 8ml/L PTFE show better thermodynamically stability.

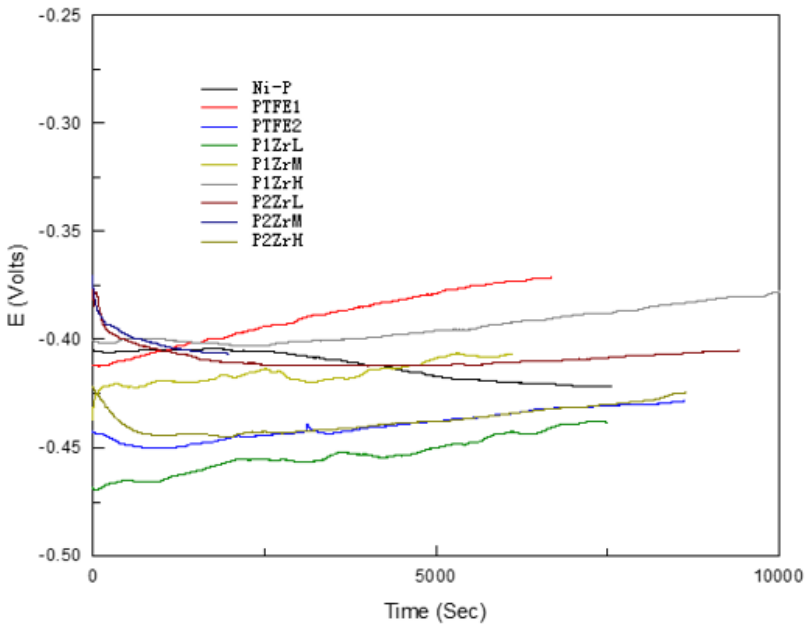

Figure 6.61 the open circuit potential of Ni-P-PTFE-ZrO_2 coatings in 0.9% NaCl solution

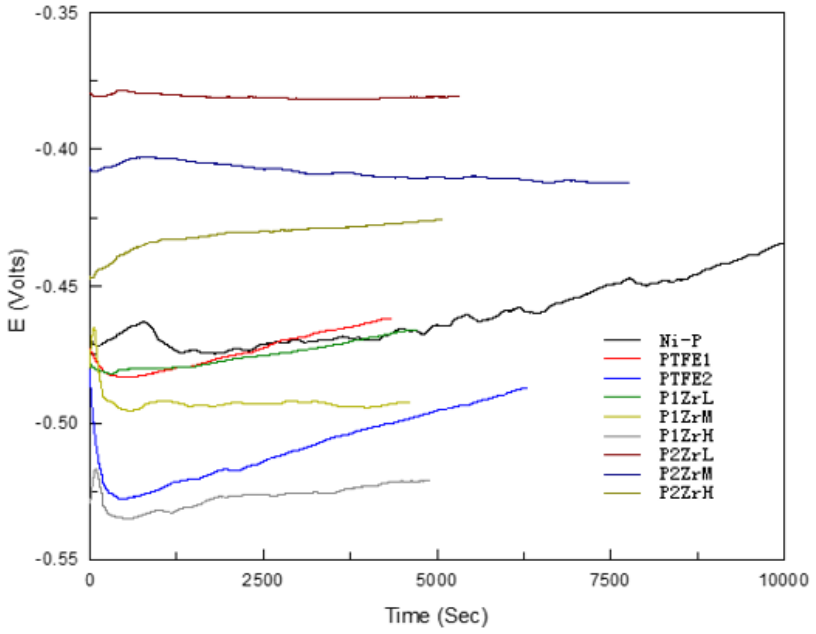

Figure 6.62 the open circuit potential of Ni-P-PTFE-ZrO_2 coatings in 3.5% NaCl solution

6.2.1.2 Ni-P-PTFE-ZrO_2-TiO_2 coatings

Figure 6.63-6.66 show the open circuit potential of Ni-P-PTFE-ZrO_2-TiO_2 coatings in 0.9% NaCl solution and 3.5% NaCl solution respectively. For Ni-P-PTFE-ZrO_2-TiO_2 coatings prepared by 8ml/L of PTFE, they did not show higher corrosion potential than Ni-P-PTFE and Ni-P coating in 0.9% NaCl solution except coating P1ZrHTiH, whose corrosion potential is higher than Ni-P coating but lower than Ni-P-PTFE coating, which is shown in figure 6.63.

While from figure 6.64, we can see that when coupons above were immersed in 3.5% NaCl solution, Ni-P-PTFE-ZrO_2-TiO_2 coatings prepared by low concentration of ZrO_2 such as coating P1ZrMTiM, P1ZrMTiH, P1ZrMTiL, P1ZrHTiH and P1ZrHTiL show higher corrosion potential

than Ni-P and Ni-P-PTFE coatings which means that these Ni-P-PTFE-ZrO_2-TiO_2 coatings have better thermodynamically stability than Ni-P and Ni-P-PTFE coatings.

Figure 6.65 and 6.66 show the open circuit potential of Ni-P-PTFE-ZrO_2-TiO_2 coatings prepared by 12ml/L of PTFE in 0.9% NaCl solution and 3.5% NaCl solution respectively. According to figure 6.65, coating P2ZrMTiL and P2ZrHTiL show higher corrosion potential than Ni-P, Ni-P-PTFE and other Ni-P-PTFE-ZrO_2-TiO_2 coatings in 0.9% NaCl solution. Compared with assays in 0.9% NaCl solution, figure 6.66 show that all Ni-P-PTFE-ZrO_2-TiO_2 coatings have higher corrosion potential than Ni-P and Ni-P-PTFE coatings in 3.5% NaCl solution. And among these Ni-P-PTFE-ZrO_2-TiO_2 coatings, coatings P2ZrLTiL, P2ZrLTiM and P2ZrMTiL show higher thermodynamical stability than other coatings

In conclusion, Ni-P-PTFE-ZrO_2-TiO_2 coatings show better thermodynamical stability than Ni-P and Ni-P-PTFE coatings in the 3.5% NaCl solution. While when coupons immersed in the 0.9% NaCl solutions, only two coatings P2ZrMTiL and P2ZrHTiL show higher corrosion potential than Ni-P and Ni-P-PTFE coatings.

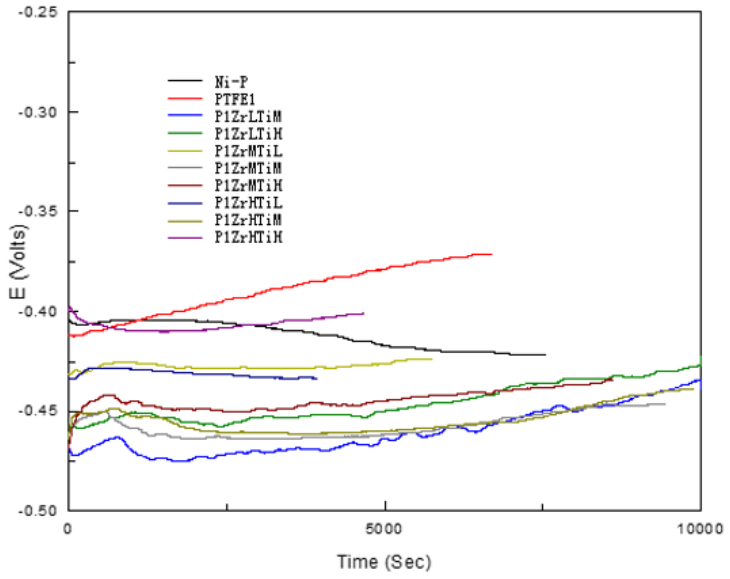

Figure 6.63 the open circuit potential of Ni-P-PTFE-ZrO_2-TiO_2 (8ml/L PTFE) coatings in 0.9% NaCl solution

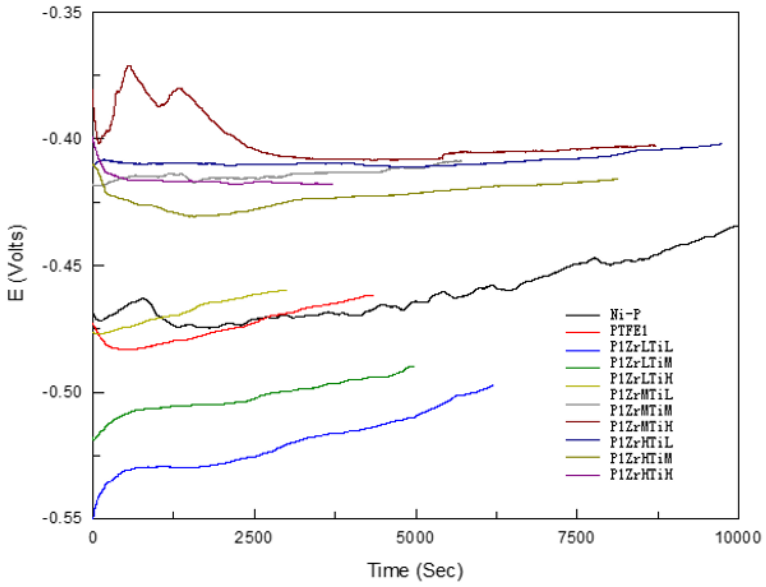

Figure 6.64 the open circuit potential of Ni-P-PTFE-ZrO2-TiO2 (8ml/L PTFE) coatings in 3.5% NaCl solution

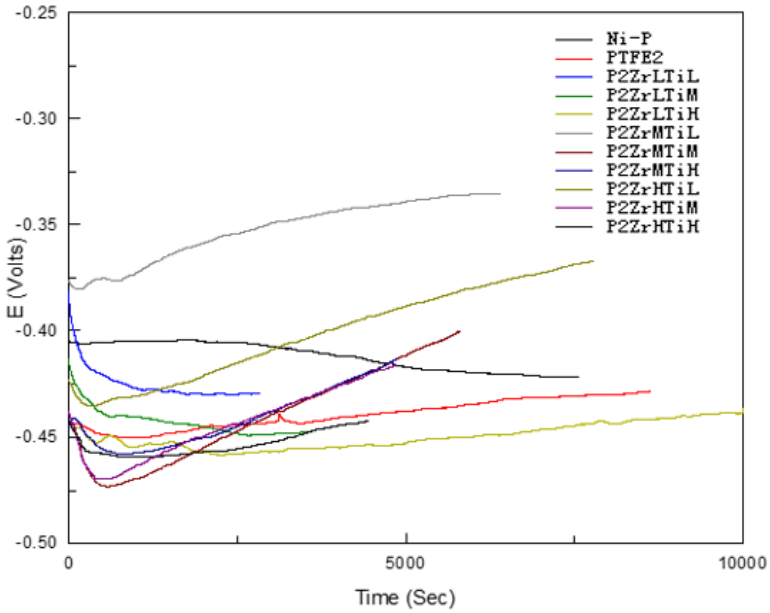

Figure 6.65 the open circuit potential of Ni-P-PTFE-ZrO_2-TiO_2 (12ml/L PTFE) coatings in 0.9% NaCl solution

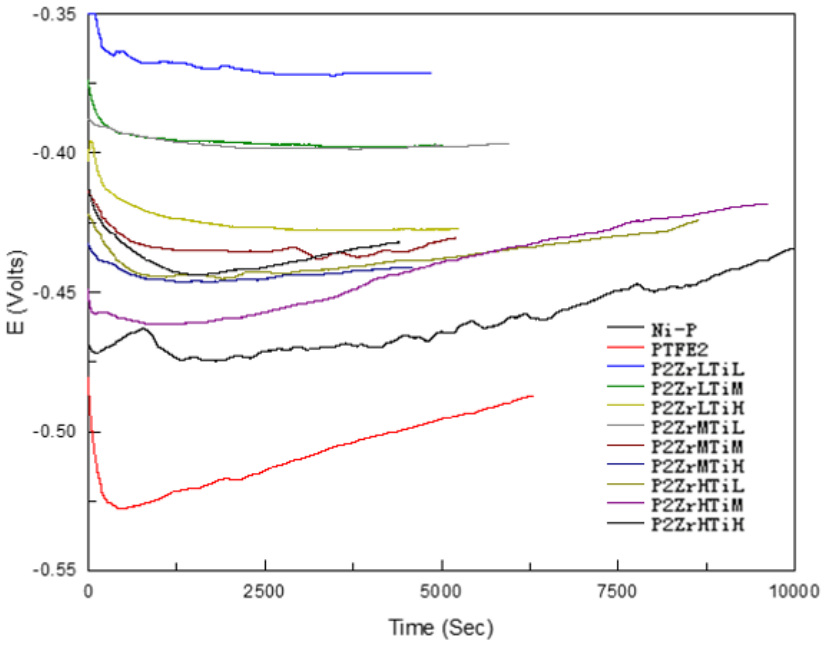

Figure 6.66 the open circuit potential of Ni-P-PTFE-ZrO_2-TiO_2 (12ml/L PTFE) coatings in 3.5% NaCl solution

6.2.2 Measurement of Potentiodynamic Polarization Tafel Plots

Potentiodynamic polarization tafel plots of the coatings were generated by corrtest software and according to the tafel plots, the corrosion potential (E_{corr}), polarization resistance (R_p), corrosion current density (I_{corr}), and corrosion rate (CR) can be obtained.

In this study, the plot was generated in a single scan by beginning the scan from -500mv and scanning continuously to +500 mV at a scan rate of 1 mV/s and the resulting tafel curve was a plot of the applied potential vs. the logarithm of the measured current.

6.2.2.1 Ni-P-PTFE-ZrO_2 coatings

Figure 6.67 and Figure 6.68 show the tafel plots of Ni-P, Ni-P-PTFE, and Ni-P-PTFE-ZrO_2 coatings prepared by three different concentration of ZrO_2 including 0.625 g/L, 1.25 g/L and 1.875 g/L and two different concentration of PTFE including 8ml/L and 12ml/L to test their anticorrosive property in 0.9% NaCl solution and 3.5% NaCl solution. And table 6.1, 6.2, 6.4 and 6.5 show the value of polarization resistance (R_p), corrosion current density (I_{corr}), corrosion rate (CR) and corrosion potential (E_{corr}) of the coatings mentioned above. It can be seen table 6.1 and 6.2 that Ni-P-PTFE-ZrO_2 coatings except coating P2ZrH, have much larger polarization resistance (ranging from 21.75 kΩ cm^2 to 42.80 kΩ cm^2) than Ni-P and Ni-P-PTFE coatings (ranging from 13.90 kΩ cm^2 to 18.89 kΩ cm^2), and corrosion current density (ranging from 5.000E-7 Amp/cm^2 to 8.770E-7 Amp/cm^2) and corrosion rate (from 0.00533mm/a to 0.00935 mm/a) of Ni-P-PTFE-ZrO_2 coatings are lower than Ni-P and Ni-P-PTFE coatings whose corrosion current density range from 1.460E-6 Amp/cm^2 to 2.310E-6 Amp/cm^2 and corrosion rate range from 0.0156mm/a to 0.0246 mm/a in 0.9% NaCl solution, while for the anticorrosive behaviours of Ni-P-PTFE-ZrO_2 coatings in 3.5 % NaCl solution, similar as their anticorrosive

behaviour in the 0.9% NaCl solution, Ni-P-PTFE-ZrO_2 coatings show much better corrosion resistance property than Ni-P, and Ni-P-PTFE coatings, and the statistics can be seen in the table 6.4 and6.5.

From table 6.1, 6.2, 6.4 and 6.5, we can also find out the effect of concentration of ZrO_2 on anticorrosive property, coatings P1ZrL, P1ZrM, P2ZrL and P2ZrM prepared by low and medium concentration of ZrO_2 (0.625g/L and 1.25g/L) show a better anticorrosive property. They have lower corrosion rate and corrosion current density but higher polarization resistance than those prepared by high concentration of ZrO_2 (coatings P1ZrH and P2ZrH).

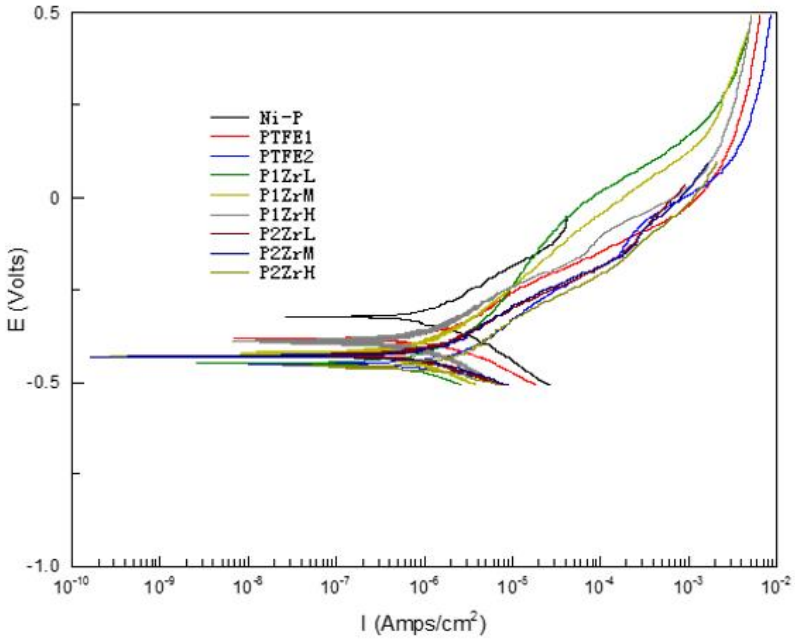

Figure 6.67 polarization tafel plots of Ni-P-PTFE-ZrO_2 coatings in 0.9% NaCl solution

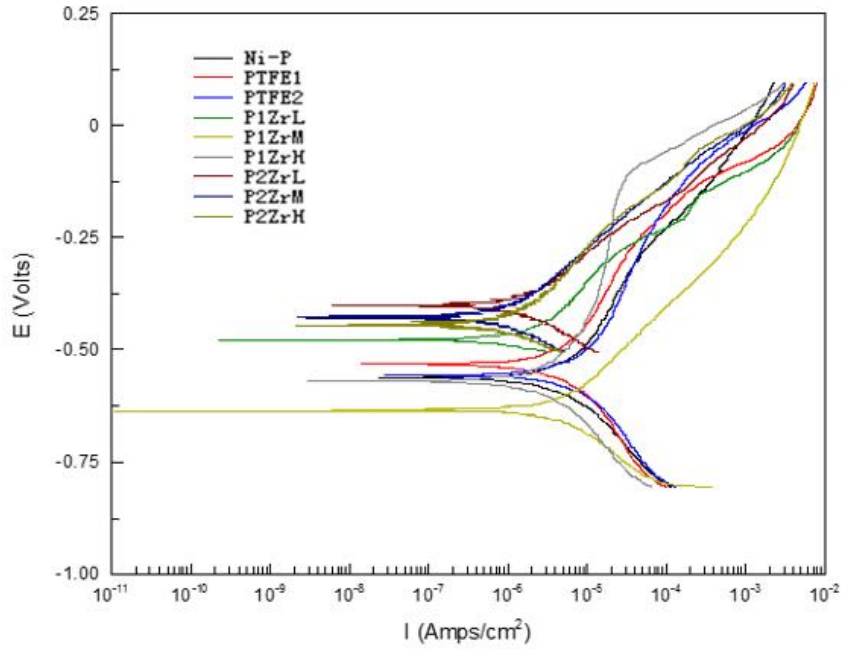

Figure 6.68 polarization tafel plots of Ni-P-PTFE-ZrO_2 coatings in 3.5% NaCl solution

6.2.2.2 Ni-P-PTFE-ZrO_2-TiO_2 coatings

In this study, a series of Ni-P-PTFE-ZrO_2-TiO_2 coatings prepared by three different concentration of ZrO_2, including 0.625 g/L, 1.25 g/L and 1.875 g/L, three different concentration of TiO_2 including 0.4 g/L, 0.8 g/L and 1.2 g/L and two different concentration of PTFE including 8ml/L and 12ml/L were tested to evaluate anticorrosive behaviour of these coatings. Figure 6.69 to Figure 6.72 present the tafel plots of Ni-P-PTFE-ZrO_2-TiO_2 coatings mentioned above in 0.9% and 3.5% NaCl solution, and the tafel plots of Ni-P and Ni-P-PTFE coatings are also shown in these figures. Table 6.3 and 6.6 show the value of the corrosion potential (E_{corr}), polarization resistance (R_p), corrosion current density (I_{corr}), and corrosion rate (CR) of Ni-P-PTFE-ZrO_2-TiO_2 coatings in 0.9% NaCl and 3.5% NaCl solution which is analysed by corrtest software.

6.2.2.2.1 Effect of ZrO_2 on Anticorrosion Behaviour of Ni-P-PTFE-ZrO_2-TiO_2 Coatings

Figure 6.69 and Figure 6.70 show the tafel plots of Ni-P-PTFE-ZrO_2-TiO_2 prepared by 8ml/L of PTFE in 0.9% NaCl and 3.5% NaCl solution respectively. According to figure 6.69 and table 6.3, we can see that compared with Ni-P and Ni-P-PTFE coating, Ni-P-PTFE-ZrO_2-TiO_2 show better anticorrosive property in 0.9% NaCl solution. For corrosion current density (I_{corr}), they are much lower ranging from 1.010E-6 Amp/cm^2 to 4.410E-7 Amp/cm^2 than that of Ni-P (2.310E-6 Amp/cm^2) and Ni-P-PTFE (1.460E-6 Amp/cm^2) coatings; for corrosion rate (CR), they are also much lower ranging from 0.00470mm/a to 0.0119mm/a compared with Ni-P (0.0246 mm/a) and PTFE (0.0156mm/a); for polarization resistance (R_p), Ni-P-PTFE-ZrO_2-TiO_2 coatings show higher corrosive resistance ranging from 16.99 kΩ cm^2 to 46.16 kΩ cm^2 than Ni-P (18.89 kΩ cm^2) and Ni-P-PTFE (18.30 kΩ cm^2) coatings. Coating P1ZrLTiL to P1ZrMTiH prepared by 0.625 g/L and 1.25g/L ZrO_2 show a better anticorrosive property than other Ni-P-PTFE-ZrO_2-TiO_2 coatings, which means coatings prepared by low and medium concentration of ZrO_2 have better corrosive resistance in 0.9g/L NaCl solution.

While for anticorrosive test of Ni-P-PTFE-ZrO_2-TiO_2 coatings in 3.5% NaCl solution, there are similar results as anticorrosive test in 0.9% NaCl solution. Ni-P-PTFE-ZrO_2-TiO_2 coatings show much better corrosion resistance property than Ni-P, and Ni-P-PTFE coatings, and the statistics can be seen in the table 6.6. However, coating P1ZrHTiL, P1ZrHTiMand P1ZrHTiH prepare by 1.875g/L ZrO_2 show a better anticorrosive property than other Ni-P-PTFE-ZrO_2-TiO_2 coatings, which means coatings prepared by high concentration of ZrO_2 have better corrosive resistance in 3.5 g/L NaCl solution.

Compared with figure 6.69 and figure 6.70, figure 6.71 and figure 6.72 show the tafel plots of Ni-P-PTFE-ZrO_2-TiO_2 coatings prepared by 12ml/L of PTFE in 0.9% NaCl and 3.5% NaCl

solution respectively. From table 6.1, 6.3, 6.4 and 6.6, we can see that Ni-P-PTFE-ZrO_2-TiO_2 coatings still show better anticorrosive property than Ni-P coatings and Ni-P-PTFE coatings in 0.9% NaCl and 3.5% NaCl solution respectively. Statistics from table 6.1, 6.3, 6.4 and 6.6 demonstrate that Ni-P-PTFE-ZrO_2-TiO_2 coatings prepared by 12ml/L of PTFE have lower corrosion current density (I_{corr}) and corrosion rate (CR) but higher polarization resistance (R_p) than Ni-P coatings and Ni-P-PTFE coatings in 0.9% NaCl and 3.5% NaCl solution respectively, which has the similar conclusion as Ni-P-PTFE-ZrO_2-TiO_2 coatings prepared by 8ml/L of PTFE.

Ni-P-PTFE-ZrO_2-TiO_2 (12ml/L PTFE) coatings P2ZrLTiL to P2ZrLTiH prepared by 0.625g/L ZrO_2 show better anticorrosive property than other Ni-P-PTFE-ZrO_2-TiO_2 coatings in 0.9% NaCl solution. However coating P2ZrHTiL prepared by high concentration of ZrO_2 (1.875g/L) and 1.2g/L TiO_2, show better anticorrosive property than other Ni-P-PTFE-ZrO_2-TiO_2 coatings, which means coatings prepared by high concentration of ZrO_2 have better corrosive resistance in 3.5 % NaCl solution.

6.2.2.2.2 Effect of PTFE on Anticorrosion Behaviour of Ni-P-PTFE-ZrO_2-TiO_2 Coatings

There are differences between two sets of Ni-P-PTFE-ZrO_2-TiO_2 coatings which were prepared by different concentration of PTFE including 8ml/L of PTFE and 12ml/L of PTFE. And the effect of PTFE on anticorrosive property of Ni-P-PTFE-ZrO_2-TiO_2 can be obtained by the analysis of statistics from table 6.3 and 6.6. For anticorrosive assays in 0.9% NaCl solution, Ni-P-PTFE-ZrO_2-TiO_2 coatings prepared by 8ml/L of PTFE have better anticorrosive property than those prepared by 12ml/L of PTFE. For example each coating prepared by same concentration of ZrO_2 and TiO_2 but 8ml/L PTFE has lower corrosion current density (I_{corr}) and corrosion rate (CR) but higher polarization resistance (R_p) than that prepared by 12 ml/L PTFE.

However, when the anticorrosive assays were conducted in 3.5% NaCl solution, most of Ni-P-PTFE-ZrO_2-TiO_2 coatings prepared by 12ml/L of PTFE have lower corrosion current density (I_{corr}) and corrosion rate (CR) than those prepared by 8ml/L of PTFE, which means that Ni-P-PTFE-ZrO_2-TiO_2 coatings prepared by 12ml/L of PTFE have better anticorrosive property in 3.5% NaCl solution.

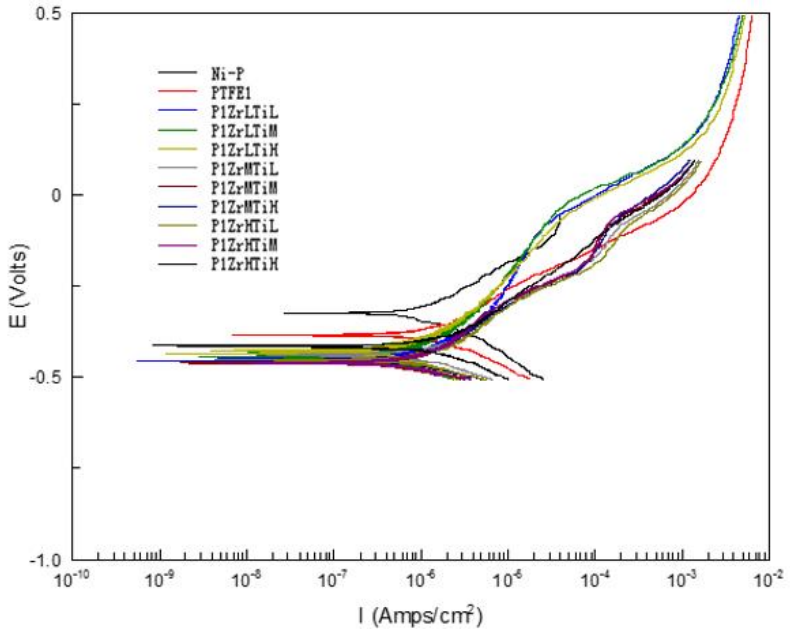

Figure 6.69 polarization tafel plots of Ni-P-PTFE-ZrO_2-TiO_2 (8ml/L) coatings in 0.9% NaCl solution

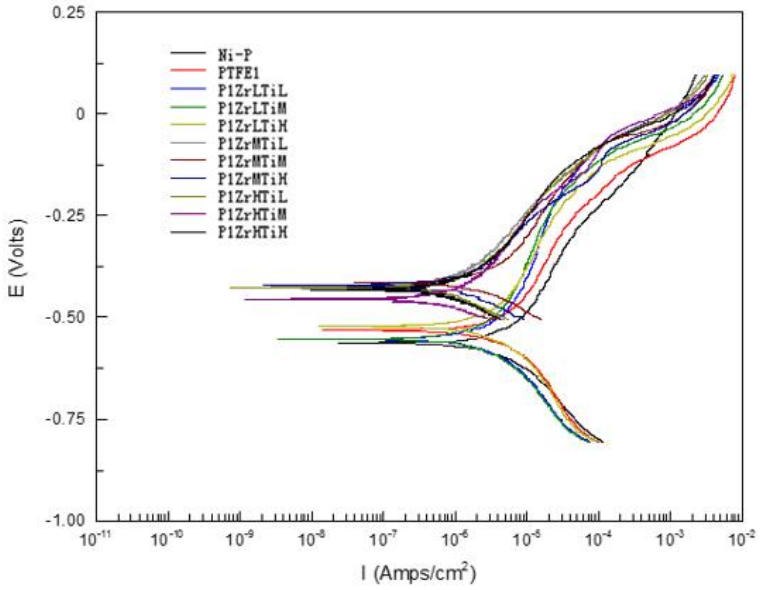

Figure 6.70 polarization tafel plots of Ni-P-PTFE-ZrO2-TiO2 (8ml/L PTFE) coatings in 3.5% NaCl solution

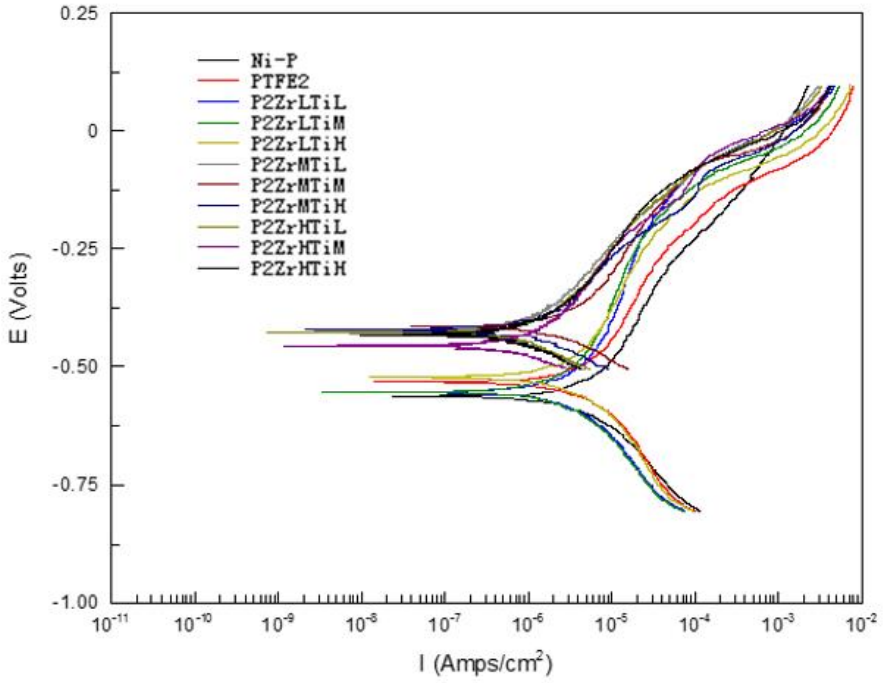

Figure 6.71 polarization tafel plots of Ni-P-PTFE-ZrO_2-TiO_2 (12ml/L PTFE) coatings in 0.9% NaCl solution

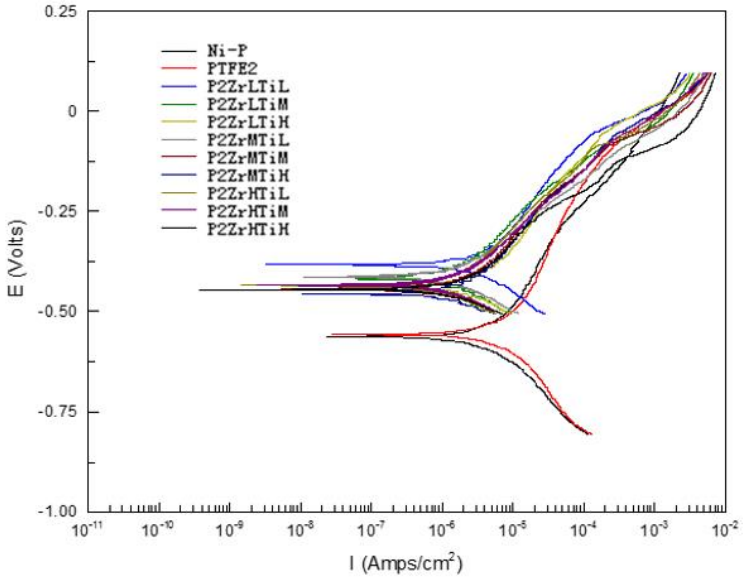

Figure 6.72 polarization tafel plots of Ni-P-PTFE-ZrO_2-TiO_2 (12ml/L PTFE) coatings in 3.5% NaCl solution

6.2.2.2.3 Effect of TiO_2 on Anticorrosion Behaviour of Ni-P-PTFE-ZrO_2-TiO_2 Coatings

Figure 6.73-6.84 show the comparison of anticorrosive property between Ni-P-PTFE-ZrO_2 coatings and Ni-P-PTFE-ZrO_2-TiO_2 coatings and the effect of addition of TiO_2 on anticorrosive property of Ni-P-PTFE-ZrO_2-TiO_2 coatings in both 0.9% of NaCl and 3.5% of NaCl solution respectively.

According to table 6.2 and 6.3, we can conclude that for anticorrosive assays in 0.9% of NaCl solution, compared with Ni-P-PTFE-ZrO_2 coatings 4 and 7, Ni-P-PTFE-ZrO_2-TiO_2 coatings such as coating P1ZrLTiL, P1ZrLTiM, P1ZrLTiH and P2ZrLTiL, P2ZrLTiM, P2ZrLTiH prepared by same concentration of PTFE and ZrO_2, but adding different concentration of TiO_2 enhance its anticorrosive property. For example, corrosion current density (I_{corr}) of coating P1ZrL is 6.990E-

7 Amp/cm^2; corrosion rate (CR) is 0.00852mm/a; polarization resistance (R_p) is 31.77 kΩ cm^2. However when TiO_2 was added, corrosion current density (I_{corr}) of Ni-P-PTFE-ZrO_2-TiO_2 coatings such as coating P1ZrLTiL, P1ZrLTiM and P1ZrLTiH range from 4.410E-7 Amp/cm^2 to 5.360E-7 Amp/cm^2; corrosion rate (CR) of coatings range from 0.00471 mm/a to 0.00572 mm/a; polarization resistance (R_p) of coatings range from 32.15 kΩ cm^2 to 46.16 kΩ cm^2, which all show that Ni-P-PTFE-ZrO_2-TiO_2 coatings have better anticorrosive property than corresponding Ni-P-PTFE-ZrO_2 coating.

While for anticorrosive assays in 3.5 % of NaCl solution, compared with Ni-P-PTFE-ZrO_2 coatings 5, 6 and 7, Ni-P-PTFE-ZrO_2-TiO_2 coatings such as coating P1ZrMTiL, P1ZrMTiM, P1ZrMTiH; P1ZrHTiL, P1ZrHTiM, P1ZrHTiH and P2ZrLTiL, P2ZrLTiM, P2ZrLTiH prepared by same concentration of PTFE and ZrO_2, but adding different concentration of TiO_2 enhance its anticorrosive property, and table 6.5 and 6.6 show the detailed value of corrosion current density, corrosion rate (CR) and polarization resistance of all the coatings mentioned above.

For Ni-P-PTFE-ZrO_2 coating P1ZrM, it shows best anticorrosive property in the 0.9% of NaCl solution than other Ni-P-PTFE-ZrO_2 coatings. However, the corresponding Ni-P-PTFE-ZrO_2-TiO_2 coatings such as P2ZrMTiL, P2ZrLTiM and P2ZrLTiH did not show better anticorrosive property than coating P1ZrM. For Ni-P-PTFE-ZrO_2 coating P2ZrM, it shows best anticorrosive property in the 3.5% of NaCl solution. However, the corresponding Ni-P-PTFE-ZrO_2-TiO_2 coatings such as coating P2ZrMTiL, P2ZrMTiM and P2ZrMTiH also did not show better anticorrosive property than coating P2ZrM.

The effect of TiO_2 on anticorrosive property of Ni-P-PTFE-ZrO_2-TiO_2 coatings in both 0.9% of NaCl and 3.5% of NaCl solution also can be seen in the table 6.3 and 6.6. Almost every Ni-P-PTFE-ZrO_2-TiO_2 coatings show better anticorrosive property when the coating was prepared by

0.8g/L of TiO_2 than those prepared by the same concentration of ZrO_2 and PTFE but different concentration of TiO_2 such as 0.4g/L of TiO_2 and 1.2g/L of TiO_2 in the anticorrosive assays in the 0.9% and 3.5% NaCl solution.

For example, for anticorrosive assay in the 0.9% NaCl solution, corrosion current density (I_{corr}) of coating P1ZrLTiM is 4.410E-7 Amp/cm^2; corrosion rate (CR) is 0.00471 mm/a; polarization resistance (R_p) is 43.70 kΩ cm^2. However corrosion current density (I_{corr}) of coatings P1ZrLTiL and P1ZrLTiH are 5.360E-7 Amp/cm^2 and 4.500E-7 Amp/cm^2; corrosion rate (CR) are 0.00572 mm/a and 0.00480 mm/a; polarization resistance (R_p) of coatings are 32.15 kΩ cm^2 and 46.16 kΩ cm^2, which show that Ni-P-PTFE-ZrO_2-TiO_2 coatings prepared by 0.8g/L of TiO_2 have better anticorrosive property.

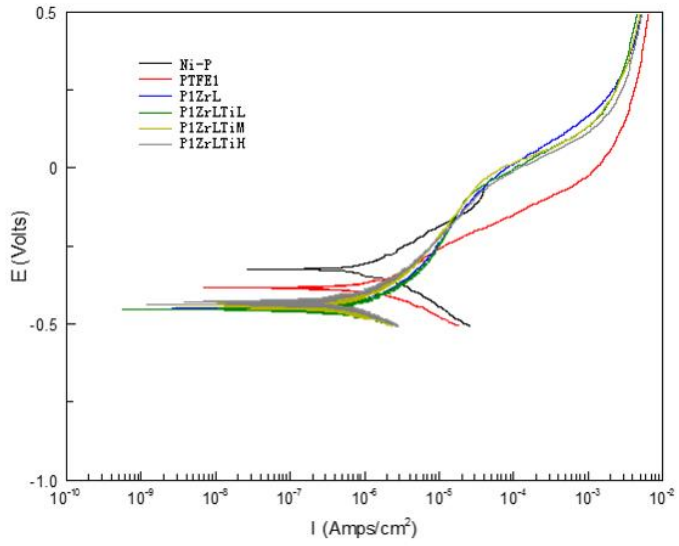

Figure 6.73 polarization tafel plots of Ni-P-PTFE-ZrO_2 vs. Ni-P-PTFE-ZrO_2-TiO_2 (8ml/L PTFE) coatings in 0.9% NaCl solution

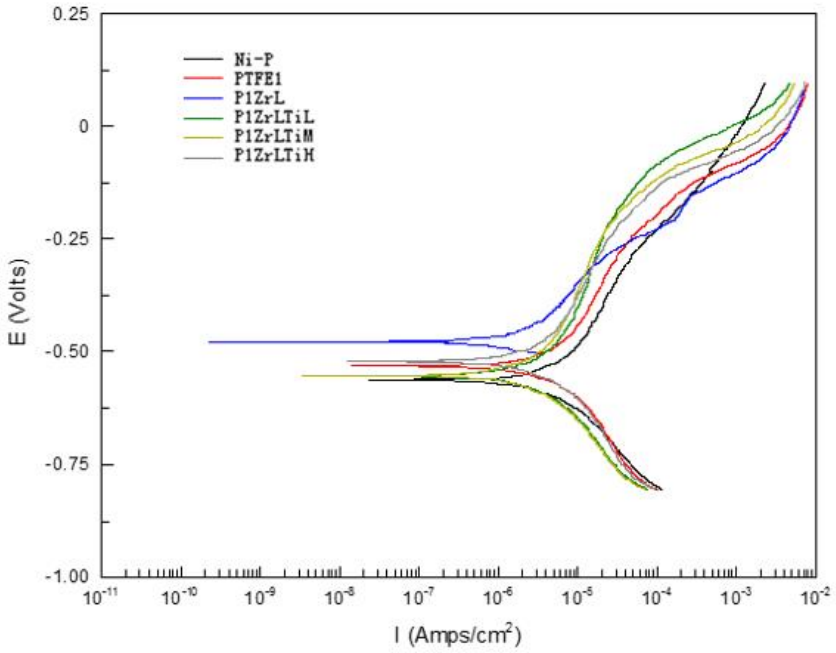

Figure 6.74 polarization tafel plots of Ni-P-PTFE-ZrO_2 vs. Ni-P-PTFE-ZrO_2-TiO_2 (8ml/L PTFE) coatings in 3.5% NaCl solution

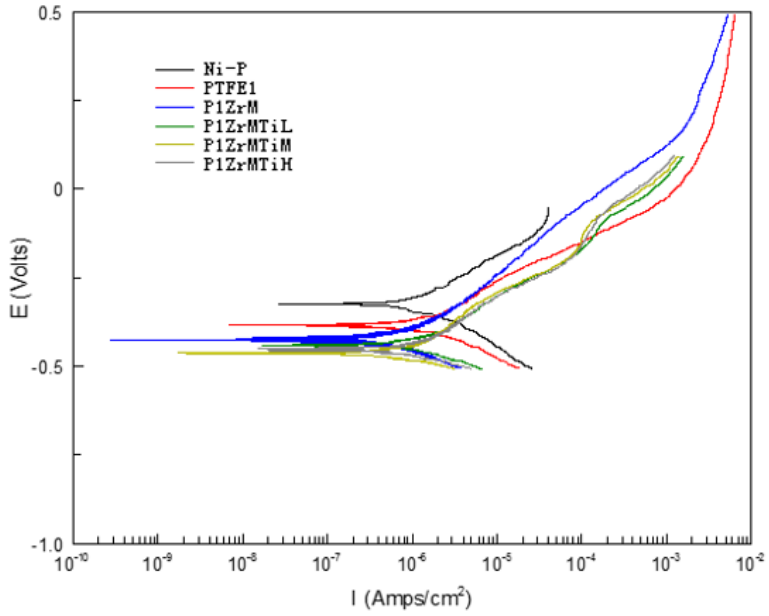

Figure 6.75 polarization tafel plots of Ni-P-PTFE-ZrO_2 vs. Ni-P-PTFE-ZrO_2-TiO_2 (8ml/L PTFE) coatings in 0.9 % NaCl solution

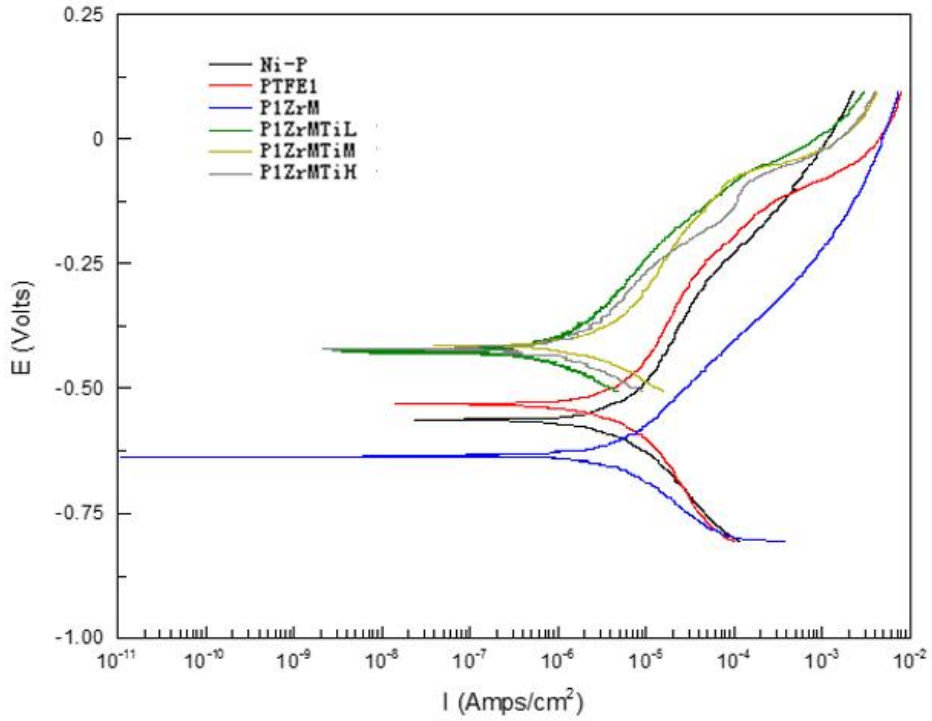

Figure 6.76 polarization tafel plots of Ni-P-PTFE-ZrO_2 vs. Ni-P-PTFE-ZrO_2-TiO_2 (8ml/L PTFE) coatings in 3.5 % NaCl solution

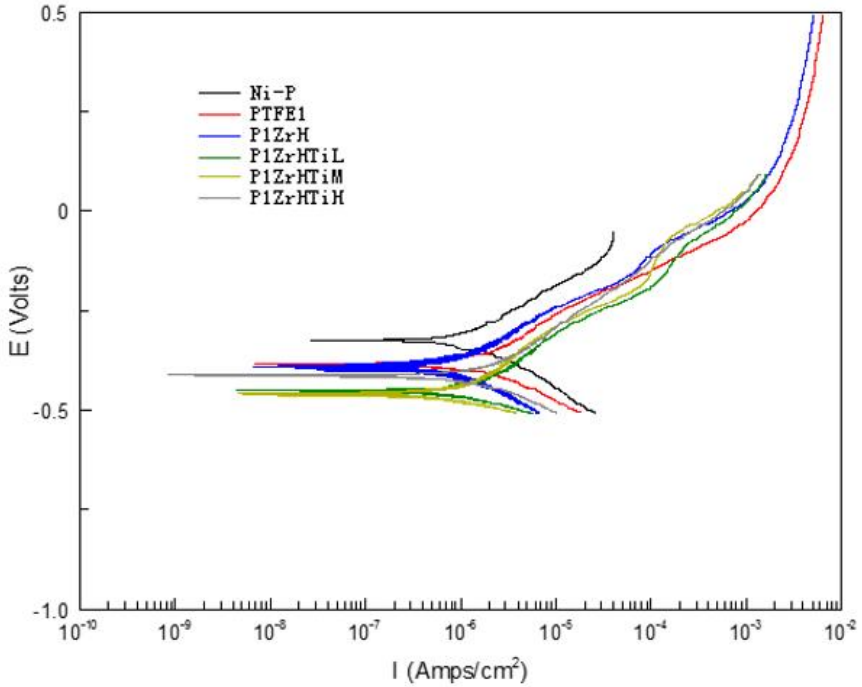

Figure 6.77 polarization tafel plots of Ni-P-PTFE-ZrO_2 vs. Ni-P-PTFE-ZrO_2-TiO_2 (8ml/L PTFE) coatings in 0.9 % NaCl solution

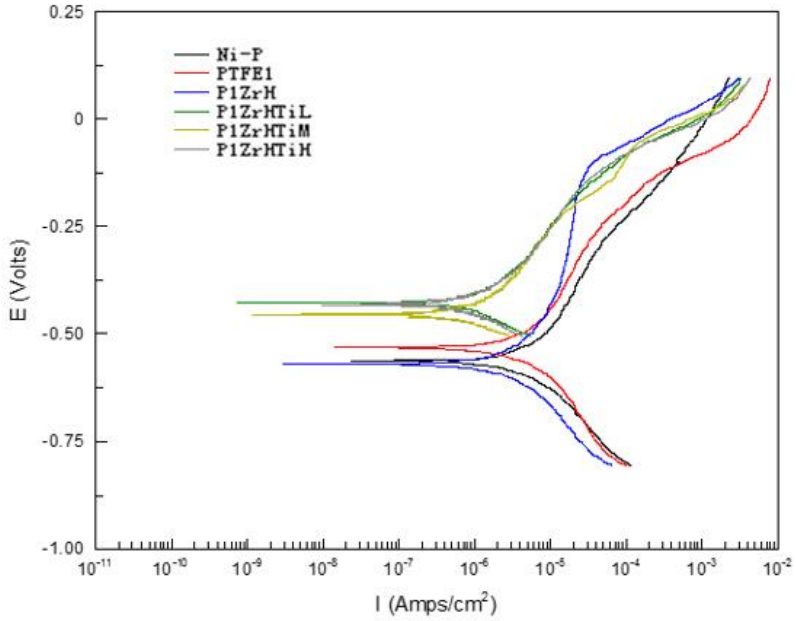

Figure 6.78 polarization tafel plots of Ni-P-PTFE-ZrO_2 vs. Ni-P-PTFE-ZrO_2-TiO_2 (8ml/L PTFE) coatings in 3.5 % NaCl solution

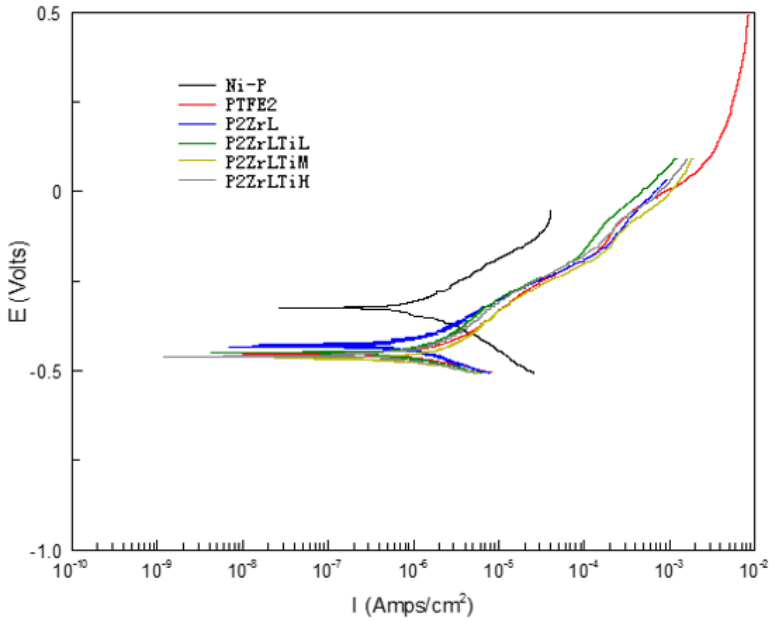

Figure 6.79 polarization tafel plots of Ni-P-PTFE-ZrO_2 vs. Ni-P-PTFE-ZrO_2-TiO_2 (12ml/L PTFE) coatings in 0.9 % NaCl solution

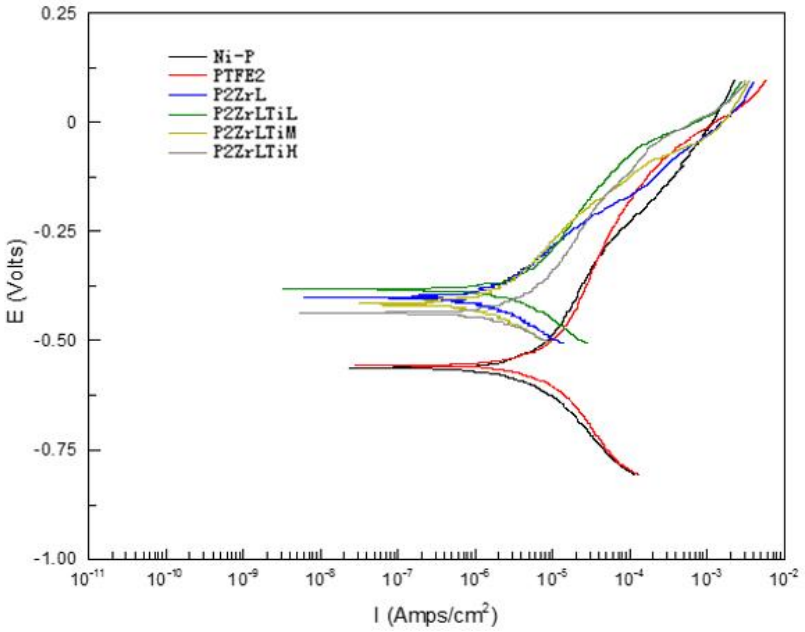

Figure 6.80 polarization tafel plots of Ni-P-PTFE-ZrO_2 vs. Ni-P-PTFE-ZrO_2-TiO_2 (12ml/L PTFE) coatings in 3.5 % NaCl solution

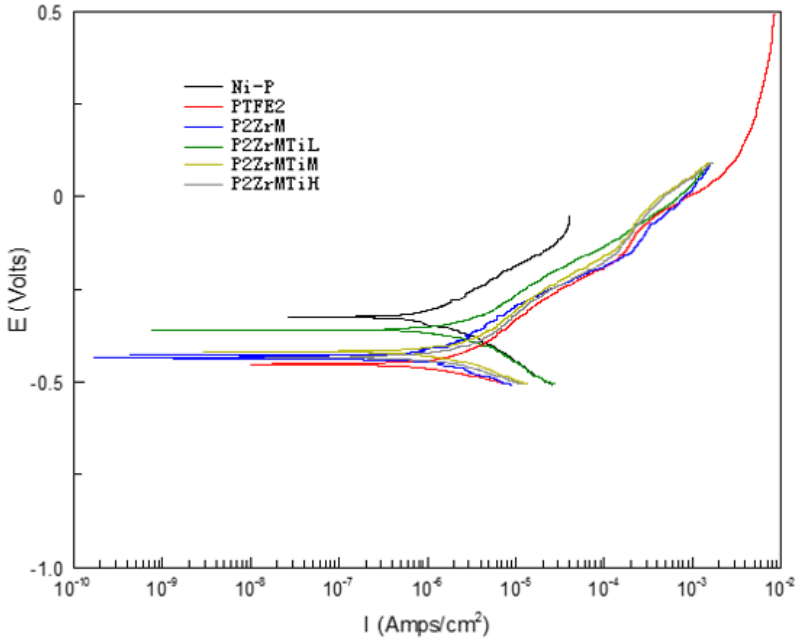

Figure 6.81 polarization tafel plots of Ni-P-PTFE-ZrO_2 vs. Ni-P-PTFE-ZrO_2-TiO_2 (12ml/L PTFE) coatings in 0.9 % NaCl solution

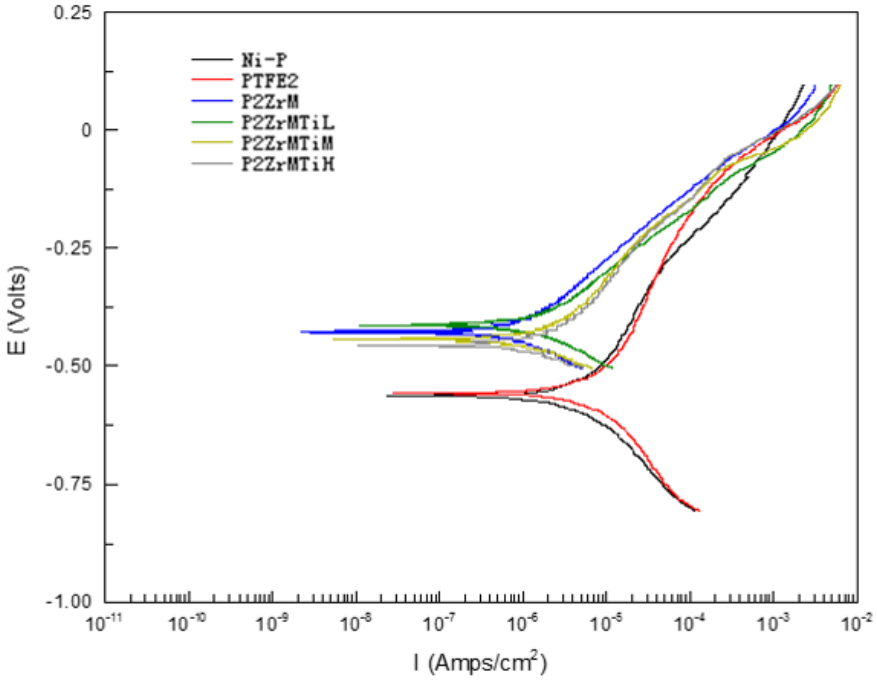

Figure 6.82 polarization tafel plots of Ni-P-PTFE-ZrO_2 vs. Ni-P-PTFE-ZrO_2-TiO_2 (12ml/L PTFE) coatings in 3.5 % NaCl solution

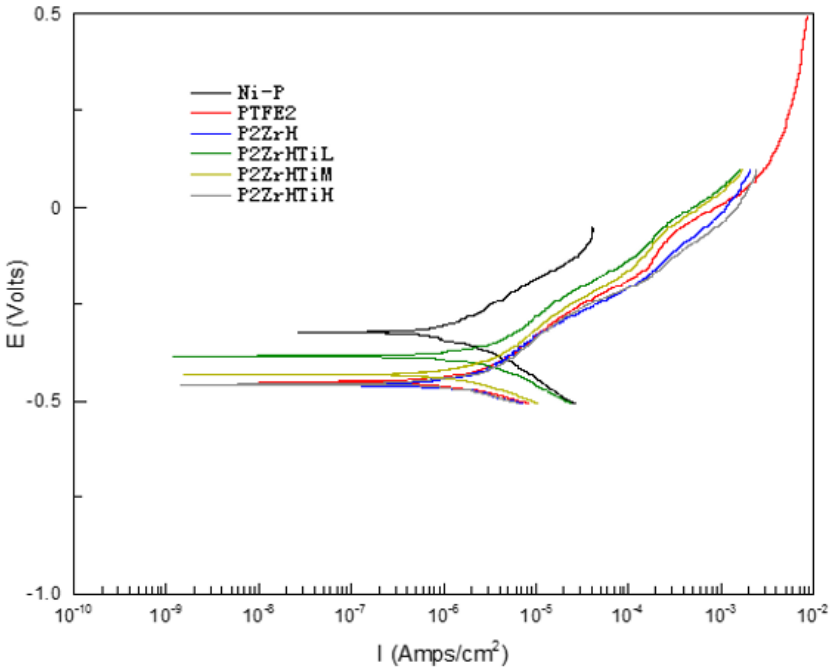

Figure 6.83 polarization tafel plots of Ni-P-PTFE-ZrO_2 vs. Ni-P-PTFE-ZrO_2-TiO_2 (12ml/L PTFE) coatings in 0.9 % NaCl solution

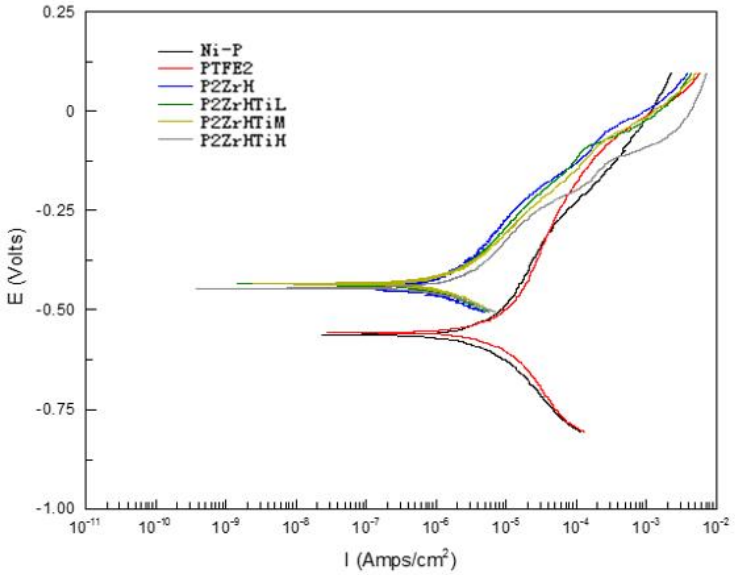

Figure 6.84 polarization tafel plots of Ni-P-PTFE-ZrO_2 vs. Ni-P-PTFE-ZrO_2-TiO_2 (12ml/L PTFE) coatings in 3.5 % NaCl solution

Table 6.1 Results of potentiodynamic polarization plots of Ni-P and Ni-P-PTFE coatings in 0.9% NaCl solution

Name	chemistry			Ba (mV)	Bc (mV)	Icorr (Amp/cm2)	Ecorr (v)	Corrosion rate (mm/a)	Rp (KΩ cm2)
	Ni-P &Ni-P-PTFE								
	$NiSO_4$ (g/L)	NaH_2PO_2 (g/L)	PTFE (ml/L)						
Ni-P	25	15	0	238.33	173.73	2.310E-6	-0.325	0.0246	18.89
PTFE1	25	15	8	143.33	108.40	1.460E-6	-0.382	0.0156	18.30
PTFE2	25	15	12	153.73	80.06	1.650E-6	-0.452	0.0176	13.90

Table 6.2 Results of potentiodynamic polarization plots of Ni-P-PTFE-ZrO2 coatings in 0.9% solution

Name	chemistry			Ba (mV)	Bc (mV)	Icorr (Amp/cm2)	Ecorr (v)	Corrosion rate (mm/a)	Rp (KΩ cm2)
	Ni-P-PTFE-ZrO_2-TiO_2								
	PTFE (ml/L)	ZrO_2 (g/L)	TiO_2 (g/L)						
P1ZrL	8	0.625	0	134.5	103.39	6.990E-7	-0.449	0.00852	31.77
P1ZrM	8	1.250	0	112.82	86.49	5.000E-7	-0.427	0.00533	42.80
P1ZrH	8	1.875	0	146.83	126.84	8.767E-7	-0.393	0.00935	33.83
P2ZrL	12	0.625	0	96.00	-71.04	6.140E-7	−0.431	0.00766	24.69
P2ZrM	12	1.250	0	105.57	-75.29	8.773E-7	-0.430	0.00935	21.75
P2ZrH	12	1.875	0	76.605	45.12	9.861E-7	-0.457	0.01052	12.57

Table 6.3 Results of potentiodynamic polarization plots of Ni-P-PTFE-ZrO_2-TiO_2 coatings in 0.9% NaCl solution

Name	chemistry			Ba (mV)	Bc (mV)	Icorr (Amp/cm2)	Ecorr (V)	Corrosion rate (mm/a)	Rp (KΩcm2)
	Ni-P-PTFE-ZrO_2-TiO_2								
	PTFE (ml/L)	ZrO_2 (g/L)	TiO_2 (g/L)						
P1ZrLTiL	8	0.625	0.4	110.04	62.07	5.360E-7	-0.460	0.00572	32.15
P1ZrLTiM	8	0.625	0.8	110.96	73.96	4.410E-7	-0.448	0.00471	43.70
P1ZrLTiH	8	0.625	1.2	98.10	96.51	4.500E-7	-0.428	0.00480	46.16
P1ZrMTiL	8	1.250	0.4	76.10	58.69	6.242E-7	-0.439	0.00670	22.91
P1ZrMTiM	8	1.250	0.8	81.36	48.33	4.759E-7	-0.465	0.00510	26.59
P1ZrMTiH	8	1.250	1.2	84.06	50.08	5.909E-7	-0.456	0.00630	23.06
P1ZrHTiL	8	1.875	0.4	70.16	53.34	6.183E-7	-0.452	0.00660	21.14
P1ZrHTiM	8	1.875	0.8	128.01	74.39	1.009E-6	-0.459	0.0107	20.25
P1ZrHTiH	8	1.875	1.2	108.40	80.37	1.114E-6	-0.471	0.0119	16.99
P2ZrLTiL	12	0.625	0.4	79.35	54.29	6.025E-7	-0.451	0.00749	19.92
P2ZrLTiM	12	0.625	0.8	46.8	36.62	5.690E-7	-0.464	0.00607	15.98
P2ZrLTiH	12	0.625	1.2	96.12	53.65	6.289E-7	0.4604	0.00780	20.40
P2ZrMTiL	12	1.250	0.4	131.91	98.64	1.908E-6	-0.364	0.0203	12.84
P2ZrMTiM	12	1.250	0.8	164.51	98.59	1.990E-6	-0.426	0.0210	13.45
P2ZrMTiH	12	1.250	1.2	152.32	81.81	1.840E-6	-0.439	0.0195	12.56
P2ZrHTiL	12	1.875	0.4	196.22	144.03	3.350E-6	-0.384	0.0357	10.77
P2ZrHTiM	12	1.875	0.8	115.27	81.35	1.410E-6	-0.434	0.0150	14.69
P2ZrHTiM	12	1.875	1.2	118.45	63.042	1.613E-6	-0.458	0.0172	11.08

Table 6.4 Results of potentiodynamic polarization plots of Ni-P and Ni-P-PTFE coatings in 3.5% NaCl solution

Name	chemistry			Ba (mV)	Bc (mV)	Icorr (Amp/cm2)	Ecorr (v)	Corrosion rate (mm/a)	Rp (KΩ cm2)
	Ni-P &Ni-P-PTFE								
	NiSO4 (g/L)	NaH_2PO_2 (g/L)	PTFE (ml/L)						
Ni-P	25	15	0	310.24	-179.72	5.499E-6	-0.576	0.0587	8.98
PTFE1	25	15	8	308.45	-246.06	5.346E-6	-0.527	0.0570	11.14
PTFE2	25	15	12	378.45	-245.28	8.724E-6	-0.561	0.0931	6.37

Table 6.5 Results of potentiodynamic polarization plots of Ni-P-PTFE-ZrO_2 coatings in 3.5% NaCl solution

Name	chemistry			Ba (mV)	Bc (mV)	Icorr (Amp/cm2)	Ecorr (v)	Corrosion rate (mm/a)	Rp (KΩ cm2)
	Ni-P-PTFE-ZrO_2-TiO_2								
	PTFE (ml/L)	ZrO_2 (g/L)	TiO_2 (g/L)						
P1ZrL	8	0.625	0	85.55	-32.60	6.952E-7	-0.486	0.00848	12.89
P1ZrM	8	1.250	0	172.30	-136.69	4.478E-6	-0.637	0.0478	6.35
P1ZrH	8	1.875	0	299.34	-182.71	3.205E-6	-0.578	0.0342	15.37
P2ZrL	12	0.625	0	113.12	88.54	9.390E-7	−0. 401	0.0100	22.97
P2ZrM	12	1.250	0	119.48	85.80	6.280E-7	-0.427	0.00675	34.31
P2ZrH	12	1.875	0	112.05	68.06	6.690E-7	-0.447	0.00723	26.12

Table 6.6 Results of potentiodynamic polarization plots of Ni-P-PTFE-ZrO_2-TiO_2 coatings in 3.5% NaCl solution

Name	chemistry			Ba (mV)	Bc (mV)	Icorr (Amp/cm2)	Ecorr (V)	Corrosion rate (mm/a)	Rp (KΩcm2)
	Ni-P-PTFE-ZrO_2-TiO_2								
	PTFE (ml/L)	ZrO_2 (g/L)	TiO_2 (g/L)						
P1ZrLTiL	8	0.625	0.4	289.88	181.92	3.031E-6	-0.554	0.0323	16.01
P1ZrLTiM	8	0.625	0.8	340.04	-164.96	2.755E-6	-0.561	0.0294	16.43
P1ZrLTiH	8	0.625	1.2	353.49	-211.97	3.169E-6	-0.546	0.0338	18.16
P1ZrMTiL	8	1.250	0.4	130.63	-79.50	6.168E-7	-0.433	0.00662	34.57
P1ZrMTiM	8	1.250	0.8	298.81	163.42	4.582E-6	-0.414	0.0489	10.01
P1ZrMTiH	8	1.250	1.2	111.95	-89.55	9.601E-7	-0.419	0.0102	22.50
P1ZrHTiL	8	1.875	0.4	204.92	150.75	1.571E-6	-0.426	0.0168	24.00
P1ZrHTiM	8	1.875	0.8	222.51	138.74	1.415E-6	-0.454	0.0151	26.18
P1ZrHTiH	8	1.875	1.2	126.61	-90.30	6.313E-7	-0.436	0.00784	31.13
P2ZrLTiL	12	0.625	0.4	144.75	104.84	2.010E-6	-0.382	0.0214	13.13
P2ZrLTiM	12	0.625	0.8	132.29	84.60	1.040E-6	-0.420	0.0111	21.54
P2ZrLTiH	12	0.625	1.2	155.91	112.20	2.277E-6	-0.437	0.0243	12.44
P2ZrMTiL	12	1.250	0.4	143.27	110.09	1.681E-6	-0.413	0.0179	16.08
P2ZrMTiM	12	1.250	0.8	113.73	-63.79	1.021E-6	-0.453	0.0109	16.33
P2ZrMTiH	12	1.250	1.2	182.97	100.35	2.018E-6	-0.457	0.0215	13.94
P2ZrHTiL	12	1.875	0.4	116.96	-80.34	8.773E-7	-0.441	0.00936	23.65
P2ZrHTiM	12	1.875	0.8	131.00	91.92	1.121E-6	-0.434	0.0120	20.92
P2ZrHTiM	12	1.875	1.2	185.70	122.39	2.338E-6	-0.446	0.0249	13.70

7 Modelling of interaction energies

As mentioned above, bacterial adhesion on the surface of implanted medical devices leads to medical device-associated infections which is the main reason to lead to failure of implantations of medical device, and in order to prevent the failure of implantation, a wide range of methods was tried to reduce medical device-associated infections. Although there are a great number of coatings or material presenting an excellent property to resist adhesion of some kind of bacteria effectively, it is still very significant to find out a theory or a model to build up a relationship of complex interplay between bacteria and surfaces, which can give an explanation that why some bacteria prefer to adhere on some kinds of surfaces or why some coatings have the capability of resisting bacterial adhesion effectively. Considering that different kinds of bacteria and coatings have their own unique physical and chemical properties, and the complex physicochemical reactions between bacteria and coatings have an enormous effect on bacterial attraction and repulsion, scientists have always tried to find out a model to accurately predict bacterial adhesive behaviours. And this kind of model will give certain instruction to synthesize some coating with certain physicochemical property to resist adhesion of one bacteria or some bacteria with similar physicochemical properties. Basically, there are two theoretical approaches have been used including thermodynamic approach and extended DLVO theory.

7.1 Extend DLVO theory

Firstly, one of the theories applied to describe the behaviour of bacterial adhesion is Derjaguin-Landau-verwey-overbeek (DLVO) theory, which was firstly built up to describe the interaction between a colloidal particle and a surface. DLVO theory was the first theory to describe the behaviour of bacterial adhesion due to the size of bacteria ranging from 0.5-2 μm, which is

similar as colloidal particles. The classic DLVO theory express that the behaviour of bacterial adhesion is dominated by two interactions including attractive LifshiZ-Van de Walls force (LW) and repulsive electrostatic force (EL) (Hermansson 1999) which can be expressed as followed:

$$\Delta E_{132}^{TOT} = \Delta E_{132}^{LW} + \Delta E_{132}^{EL} \quad (7.1)$$

However, DLVO theory was found to be not good enough to express the process of bacteria attaching to the substratum, because in the classic DLVO theory, the surface of colloidal particles and substratum are assumed to be chemically inert. The real interations between bacteria and substratum is different because surfaces of bacteria and substratum are chemically active and there are hydrogen and chemical bonds involved in the bacterial adhesion. Therefore, Van Oss (2005) suggested another two terms called Lewis acid-base (AB) and Brownian motion interaction (Br) to be added to the classic DLVO theory, The Lewis acid-base (AB) interactions is to account for hydrogen bonding when bacteria approach to the surface of substratum around 5nm which is called short-range interaction as mentioned before. The essence of the AB interactions are based on electron-donating (γ^-) and electron-accepting (γ^+) interactions between polar moieties in aqueous solutions and the polar interactions could be attractive or repulsive which depends on the hydrophilicity and hydrophobicity of bacteria and substratum. Besides the AB interactions have much more effect on bacterial adhesion when bacteria and substratum have a closed contact (less than 5 nm) and the AB interactions may be up to 10-100 orders of magnitude greater than the EL and LW interactions, which explained the reason that the classic DLVO theory sometimes cannot predict the actual bacterial adhesion. And another term the Brownian motion interactions (Br) are kinetic energy of onward motion by any molecule suspended in liquid. Therefore, bacterial adhesion is described as a balance between attractive LW force, repulsive electrostatic force, AB interaction force and Br force. The total interaction

energy ΔG_{132}^{TOT} between a particle 1 and a solid surface 2 in liquid 3 can be written as the sum of these corresponding interaction terms:

$$\Delta G_{132}^{TOT} = \Delta G_{132}^{LW} + \Delta G_{132}^{EL} + \Delta G_{132}^{AB} + \Delta G^{Br} \quad (7.2)$$

The balance between all possible interactions determine whether or not the particle or bacterium prefer to attach on the surface, and adhesion is favoured if ΔG_{132}^{TOT} is negative (Oliveira 1997, Azeredo, Visser et al. (1999)).

7.1.1 Lifshitz-van der Waals Interaction

The Lifshiz-van der Waals (LW) interaction can be described by following equations, when bacteria 1 and substratum are immersed in liquid 3.

$$\Delta G_{132}^{LW} = -\frac{A_{132} \cdot R}{6H} \quad (7.3)$$

$$A_{132} = (\sqrt{A_{11}} - \sqrt{A_{33}})(\sqrt{A_{22}} - \sqrt{A_{33}}) \quad (7.4)$$

Where A is the Hamaker constant; R is the radius of the cell and the cell is assumed to be spherical; H is the distance of separation between the cell and the substratum. Hamaker constant A for different interacting material such as bacteria, substratum and liquid, can be calculated by following equation, which is related to Surface free energy component γ_i^{LW} of correspondent material (Van Oss 2005).

$$A_{ii} = 24\pi H_0^2 \cdot \gamma_i^{LW} \quad (7.5)$$

Where H_0 is the minimum equilibrium distance between two interacting entities such as bacteria and substratum, which is equal to 0.157 nm (Van Oss 2005). Finally, the ΔG_{132}^{LW} can be expressed as:

$$\Delta G_{132}^{LW} = -\frac{24\pi H_0^2(\sqrt{\gamma_1^{LW}} - \sqrt{\gamma_3^{LW}})(\sqrt{\gamma_2^{LW}} - \sqrt{\gamma_3^{LW}})R}{6H} \quad (7.6)$$

7.1.2 Electrostatic Double-Layer Interaction

The electrostatic double layer interaction ΔG_{132}^{EL} can be seen as following equation(Bos, Van der Mei et al. 1999):

$$\Delta G_{132}^{EL} = \pi\varepsilon R(\zeta_1^2 + \zeta_2^2)[\frac{2\zeta_1\zeta_2}{\zeta_1^2 + \zeta_2^2}\ln\frac{1+\exp(-\kappa H)}{1-\exp(-\kappa H)} + \ln\{1-\exp(-2\kappa H)\}] \quad (7.7)$$

$\varepsilon = \varepsilon_0\varepsilon_r$ is the electrical permittivity of the solution; ε_0 is the permittivity under vacuum of 8.85×10^{-12} J m^{-2} V^{-2}; ε_r is the relative dielectric permittivity of water (78.54 for water at 25 ^{o}C); κ is the Debye-Hückel parameter ($1/\kappa$ = 1.1 nm); $\zeta 1$ and $\zeta 2$ are the zeta potentials of the substrate and bacteria, respectively. ζ_1 was assumed to be 40mV, while ζ_2 was taken as -36mV (Wang, Sodagari et al. 2011) and -5mV (Bruinsma, Van der Mei et al. 2001) for *E. coli* and *S. aureus* respectively.

7.1.3 Lewis Acid-Base Interation Energy

The acid-base interaction energy ΔG_{132}^{AB} between bacteria cell and solid surfaces can be calculated according to the following equation(Van Oss 2005):

$$\Delta G_{132}^{AB} = 2\pi R\lambda \Delta G_{123(H_0)}^{AB} \exp(\frac{H_0 - H}{\lambda}) \quad (7.8)$$

$$\Delta G_{132(H_0)}^{AB} = 2[\sqrt{\gamma_3^+}(\sqrt{\gamma_1^-} + \sqrt{\gamma_2^-} - \sqrt{\gamma_3^-}) + \sqrt{\gamma_3^-}(\sqrt{\gamma_1^+} + \sqrt{\gamma_2^+} - \sqrt{\gamma_3^+}) - \sqrt{\gamma_1^+\gamma_2^-} - \sqrt{\gamma_1^-\gamma_2^+}] \quad (7.9)$$

Where λ is correlation length of the molecules of the liquid medium, which is in the range of 0.2-1.0 nm. It was taken as 0.6 nm in water (Davalos-Pantoja, Ortega-Vinuesa et al. 2000). γ^+, and γ^- are the electron-acceptor, and electron-donator components of surface energy respectively, which can be calculated using contact angle data; R is radius of bacterium, which was taken as 0.7 μm (Wang, Sodagari et al. 2011) and 0.4 μm (Harris, Foster et al. 2002) for *E. coli* and *S. aureus* respectively and table 7.1 show contact angle and surface free energy component of *E. coli* and *S. aureu* ; H is the separation distance between the bacteria and the substratum which was assumed to be around 4 nm(Liu and Zhao 2005); H_0 is the minimum equilibrium distance, which is equal to 0.157 nm.

Table 7.1 parameters of *E. coli* and *S. aureus*

name	Contact angle, θ			Surface free energy (mJ/m^2)				
	θ^{di}	θ^{eg}	θ^{w}	γ^{LW}	γ^+	γ^-	γ^{AB}	γ^{TOT}
Escherichia coli ATCC 25922	46.45	28.25	71.2	22.2	7.7	25.4	28.05	50.25
Staphylococcus aureus ATCC 25923	26.45	30.4	59.45	28.85	2.4	51.3	21.9	57.5

7.1.4 Brownian Motion

For all suspended particle, regardless of their size, they usually are considered to have same average translational kinetic energy (Van Oss 2005), which can be expressed as:

$$\Delta G^{Br} = 0.414 \times 10^{-20} J = 1kT \quad (7.10)$$

Where k is Boltzmann' s constant (1.381×10^{-23} J/K) and T is the absolute temperature in degree K (T=300K) .

7.2 LW-AB approach of the thermodynamic theory

Thermodynamic approach has also been used to describe bacterial attachment to solid surfaces, and in order to calculate the Gibbs adhesion energy for bacterial adhesion, interfacial free energy of the interacting surfaces are involved, which can be expressed by the following equation:

$$\Delta G_{adh} = \gamma_{sm} - \gamma_{sl} - \gamma_{ml} \quad (7.11)$$

Where ΔG_{adh} is the change of Gibbs adhesion energy for bacterial adhesion and γ_{sm}, γ_{sl}, and γ_{ml} are the interfacial free energies of the solid–microorganism, solid–liquid, and microorganism–liquid interfaces, respectively. From the equation (7.11) we can conclude that the change from interfacial free energies of solid–liquid, and microorganism–liquid to a new solid-microorganism will decide the value of ΔG_{adh}, and the behaviours of bacterial adhesion will be thermodynamically unfavourable if

$$\Delta G_{adh} > 0 \quad (7.12)$$

And the different components including γ_{sm}, γ_{sl}, and γ_{ml} can be calculated by van Oss Acid-Base Approach (Van Oss 2005), which can be expressed as follows:

$$\gamma_{SB} = \gamma_S + \gamma_B - 2\left(\sqrt{\gamma_S^{LW}\gamma_B^{LW}} + \sqrt{\gamma_S^{+}}\right) \quad (7.13)$$

Besides, ΔG_{adh} also can be expressed by a similar way as XDLVO theory, which consist of ΔG^{AB} and ΔG^{LW} as the following equation:

$$\Delta G_{adh} = \Delta G_{d_0}^{AB} + \Delta G_{d_0}^{LW} \quad (7.14)$$

In the equation 7.14, ΔG_{adh} can be divided into two components including $\Delta G_{d_0}^{AB}$ and $\Delta G_{d_0}^{LW}$, and d_0 means that the separation distance between bacteria and coatings immersed in liquid tends to zero. Polar interactions AB and apolar interactions LW are considered to play a key role in bacterial adhesion.

Although there are two equations to express the change of Gibbs adhesion energy, the final equation for the ΔG_{adh} is the same, which can be expressed as:

$$\Delta G_{Adh}=2(\sqrt{\gamma_S^{LW}\gamma_L^{LW}}+\sqrt{\gamma_S^{+}\gamma_L^{-}}+\sqrt{\gamma_S^{-}\gamma_L^{+}}+\sqrt{\gamma_B^{LW}\gamma_L^{LW}}+\sqrt{\gamma_B^{+}\gamma_L^{-}}+\sqrt{\gamma_B^{-}\gamma_L^{+}}-\sqrt{\gamma_S^{LW}\gamma_B^{LW}}-\sqrt{\gamma_S^{-}\gamma_B^{+}}-\gamma_L) \quad (7.15)$$

Although XDLVO theory and thermodynamic approach can both be used to predict behaviours of bacterial adhesion and instruct the development of coatings, there are some differences between these two methods. In spite the fact that XDLVO theory considered more interactions than thermodynamic approach, such as electrostatic interactions and Brownian motion. For XDLVO theory, the behaviours of bacterial adhesion can be described as a process that bacteria approach to the substratum, while for thermodynamic approach, it is not applicable if the bacteria does not contact with the substratum to form a new cell-substratum interface. However, it is almost impossible to know the percentage of the bacteria that are actually in contact with the substratum in most situations, which is one of drawbacks of thermodynamic approach. And In this study, XDLVO theory were used to explain behaviour of bacterial attachment to the coatings.

7.3 Modelling of Interaction Energy Between Bacteria and Coatings

7.3.1 Ni-P-PTFE-ZrO_2 coatings

The total interaction energy ΔG_{132}^{TOT} between bacteria (*E. coli* and *S. aureus*, whose parameter can be seen in table 7.1) and Ni-P-PTFE-ZrO_2 coatings (includingcoating P1ZrL-coating9, which can be seen in table 4.2) in water was calculated using the extended DLVO theory. Figure7.1 and 7.2 show that there exist good correlations between number of adhered bacteria (*E. coli* and *S. aureus*) and total interaction energy ΔG_{132}^{TOT}. From these two figures, we can see that the number of adhered bacteria decreased with ΔG_{132}^{TOT} increasing, which is consistent with the extended DLVO theory. And it also explained why less number of bacteria including *E. coli* and *S. aureus* adhered on coating Ni-P-PTFE-ZrO_2 4 and 7, which were prepared by low concentration of ZrO_2 than other Ni-P-PTFE-ZrO_2 coatings.

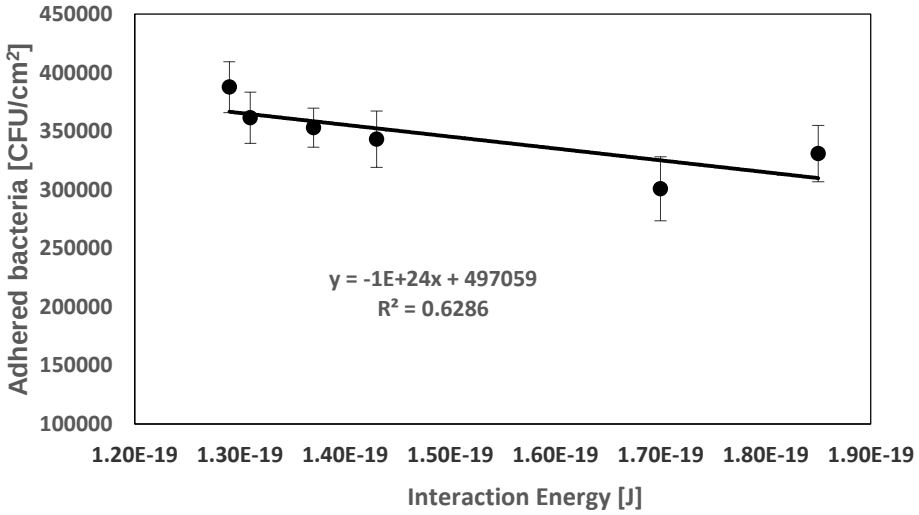

Figure 7.1 Effect of ΔG_{132}^{TOT} on *E. coli* adhesion

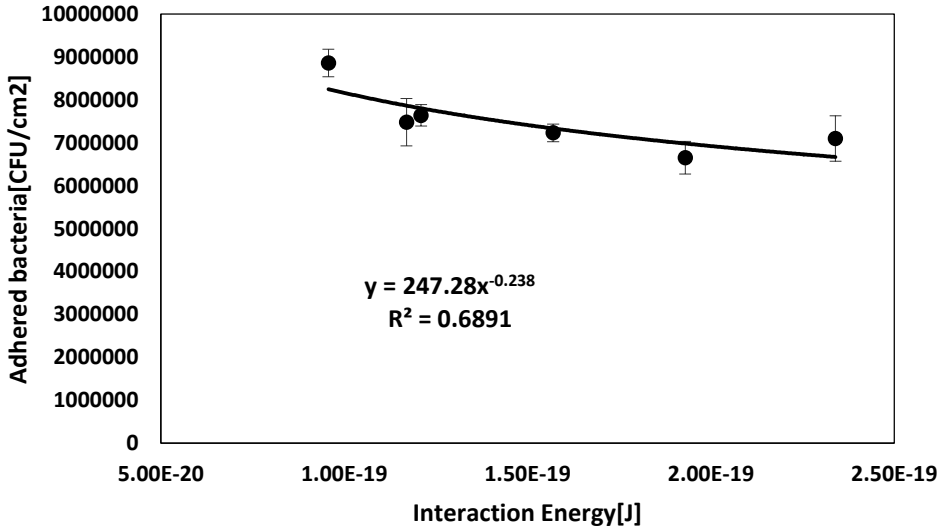

Figure7.2 Effect of ΔG_{132}^{TOT} on *S. aureus* adhesion

7.3.2 Ni-P-PTFE-ZrO_2-TiO_2 coatings

Figure 7.3-7.6 presents the effect of the total interaction energies ΔG_{132}^{TOT} between bacteria and Ni-P-PTFE-ZrO_2-TiO_2 coatings on the adhesion of *E. coli* and *S. aureus*. Figure 7.3 and 7.4, plot the number of adhered bacteria on different Ni-P-PTFE-ZrO_2-TiO_2 coatings prepared by 8ml/L PTFE as a function of the total interaction energies ΔG_{132}^{TOT} between two bacteria and coating P1ZrLTiL-18 in water. They show that with the total interaction energies ΔG_{132}^{TOT} increasing, the number of adhered bacteria decreased.

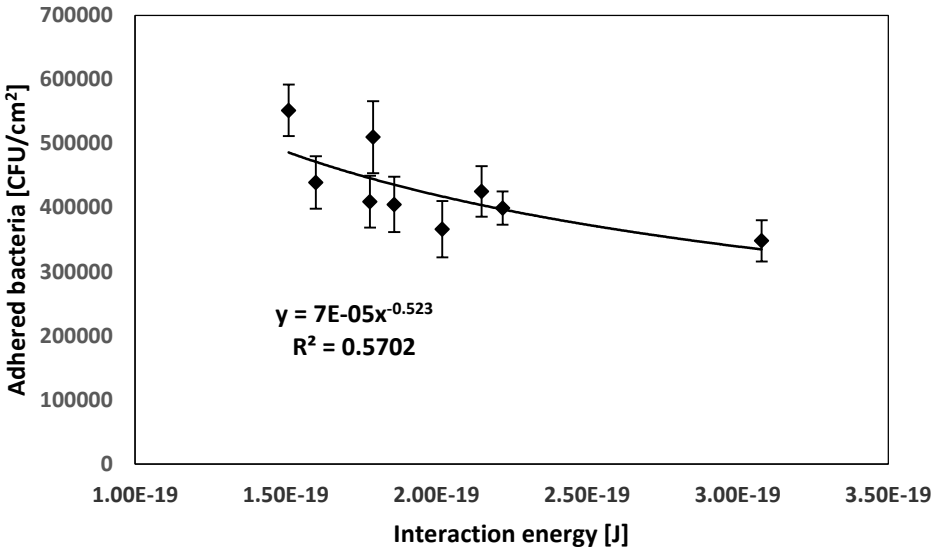

Figure 7.3 Effect of ΔG_{132}^{TOT} on *E.coli* adhesion

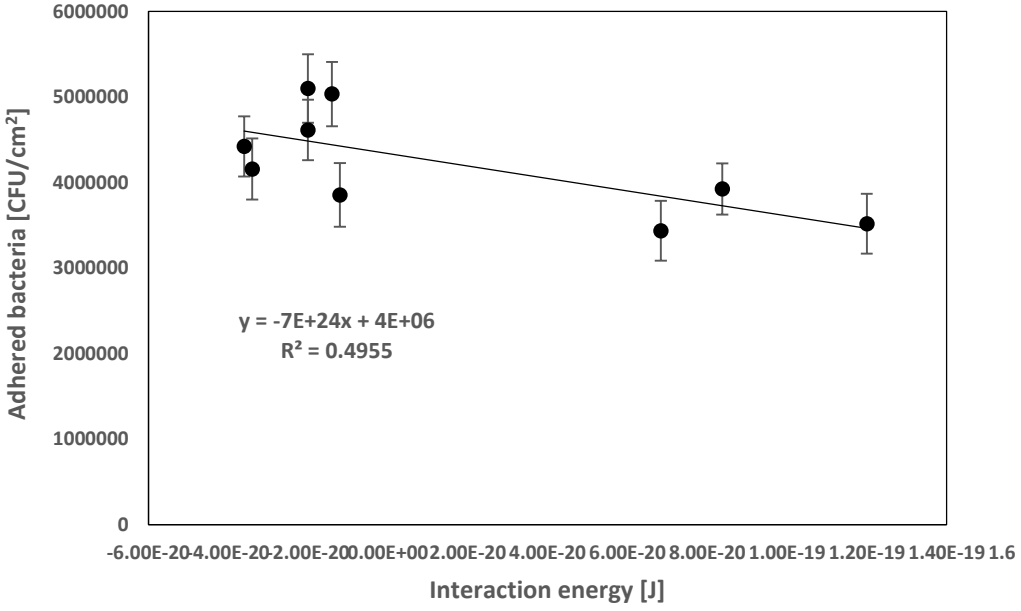

Figure 7.4 Effect of ΔG_{132}^{TOT} on *S. aureus* adhesion

While from figure 7.5 and 7.6, we can see that number of adhered bacteria on different Ni-P-PTFE-ZrO_2-TiO_2 coatings prepared by 12ml/L PTFE as a function of the total interaction energy

ΔG_{132}^{TOT} of adhesion between bacterial strains including *E. coli* and *S. aureus* and Ni-P-PTFE-ZrO_2-TiO_2 coatings (coating19-coating27) were plotted. Similar trend as figures above, the number of adhered bacteria decreased with ΔG_{132}^{TOT} increasing.

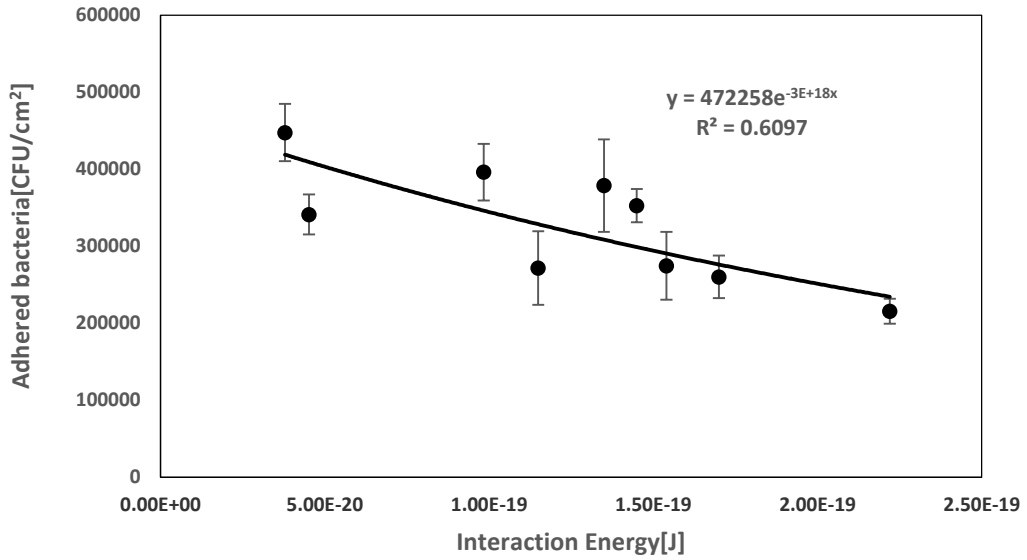

Figure 7.5 Effect of ΔG_{132}^{TOT} on *E.coli* adhesion

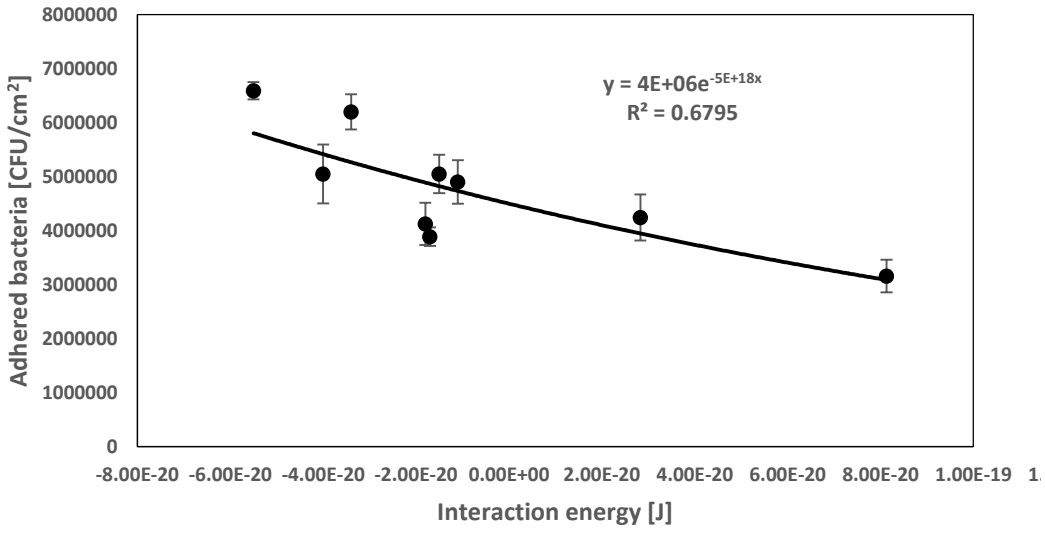

Figure 7.6 Effect of ΔG_{132}^{TOT} on *S. aureus* adhesion

Besides, from figure 7.3-7.6, we can see total interaction energy ΔG_{132}^{TOT} between *E. coli* and all Ni-P-PTFE-ZrO2-TiO2 coatings ranges from 3.79E-20 to 3.08E-19. While total interaction energy ΔG_{132}^{TOT} between *S. aureus* and all Ni-P-PTFE-ZrO_2-TiO_2 coatings ranges from-5.50E-20 to 1.20E-19, which is lower than total interaction energy ΔG_{132}^{TOT} between *E. coli* and Ni-P-PTFE-ZrO_2-TiO_2 coatings. According to XDLVO theory, adhered bacterial number was negatively correlated with ΔG_{132}^{TOT}. This explained why the number of S. aureus adhered on Ni-P-PTFE-ZrO_2-TiO_2 coatings is larger than that of *E. coli* did.

Overall, for Ni-P-PTFE-ZrO_2-TiO_2 coatings, figure 7.3-7.6 show good correlation between the interaction energy and number of adhered bacteria and explained the reason why Ni-P-PTFE-ZrO_2-TiO_2 prepared by lower concentration of TiO_2 show better capability of resisting bacterial adhesion.

Chapter 8

8 Conclusions and Future Work

8.1 conclusion

In literature review part, it shows that bacterial adhesion onto the surface and subsequent formation of a biofilm can lead to the failure of surgery or implantation of medical devices and corrosion behaviour of implanted medical devices in human bodies also will cause adverse tissue responses and postimplantation complications due to the release of metal ions or particles from the medical devices. And a great number of strategies or methods were used to synthesize and develop the coating to prevent bacterial adhesion and resist corrosion behaviour by providing barrier coatings.

In this thesis, two new novel Ni-P-PTFE based coatings were developed including Ni-P-PTFE-ZrO_2 and Ni-P-PTFE-ZrO_2-TiO_2 coatings by using electroless plating technique, which were designed for the purpose of preventing bacterial adhesion and resisting corrosion behaviour effectively.

8.1.1 Ni-P-PTFE-ZrO_2 coatings

1. Ni-P-PTFE-ZrO_2 coatings show better capability of resisting bacterial adhesion and removing adhered bacteria using a dipping process than Ni-P and Ni-P-PTFE coatings.

2. For the assay of bacterial adhesion, Ni-P-PTFE-ZrO_2 coatings (coating 4 and 7) prepared by low concentration of ZrO_2 (0.625g/L) have better capability of resisting bacterial adhesion such as *E. coli* and *S. aureus* adhesion. Compared with Ni-P and Ni-P-PTFE coatings, the number of *E.coli* adhesion on the Ni-P-PTFE-ZrO_2 coatings (CFU/cm^2) was 54.1% -59.4% of Ni-P coating,

and 66.4%-76.0% of Ni-P-PTFE coatings. While, the number of *S. aureus* adhesion on the Ni-P-PTFE-ZrO_2 coatings was 44.7% - 51.3% of Ni-P coating, and 64.1% -76.0% of Ni-P-PTFE coatings.

3. Ni-P-PTFE-ZrO_2 coating prepared by high concentration of PTFE (12ml/L) can resist adhesion of *E. coli* and *S. aureus* better than that prepared by low concentration (8ml/L), which might be explained by the effect of surface free energy and surface free energy component γ^-.on bacterial adhesion.

4. For the assay of bacterial removal, Ni-P-PTFE-ZrO_2 coating (coating 4) prepared by 8ml/L PTFE and 0.625g/L ZrO_2 remains least number of *E. coli*. The remaining number of bacteria using a dipping process on thecoating P1ZrL was 26.0%, 36.8% and 44.3% of Ni-P coating, and Ni-P-PTFE coatings prepared by low (8ml/L) and high (12ml/L) concentration of PTFE respectively.coating P1ZrL still has the highest the removal percentage of *E. coli*, which is 59%. While for assay of *S. aureus* removal, Ni-P-PTFE-ZrO_2 coating (Coating 5) prepared by 8ml/L PTFE and 1.25 g/L ZrO_2 shows better results than other coatings. The remaining number of bacteria on thecoating P1ZrM were 26.8%, 38.0% and 44.6% of Ni-P coating, and Ni-P-PTFE coatings prepared by low (8ml/L) and high (12ml/L) concentration of PTFE respectively. Besides, the removal rate ofcoating P1ZrM is as high as 60%. Overall, Ni-P-PTFE-ZrO_2 coatings prepared by low concentration of ZrO_2 performed better in the assay of bacterial removal.

5. Effect of PTFE on assay of bacterial removal is opposite with that on assay of bacterial adhesion. Less number of bacteria remains on Ni-P-PTFE-ZrO_2 coatings which is prepared by low concentration of PTFE (8ml/L) using a dipping process, the reason for this result can be explained that less total surface free energy and surface free energy component γ^{LW} may have

more effect on strength of bacterial adhesion than γ^-, which lead to less bacterial remaining on Ni-P-PTFE-ZrO_2 coatings (8ml/L) than Ni-P-PTFE-ZrO_2 coatings (12ml/L).

6. In the assay of bacterial adhesion and removal, surface free energy of Ni-P-PTFE-ZrO_2 coatings between 20 and 30mJ/m^2 is optimal to resist bacterial adhesion. The number of remaining *Escherichia coli* and *staphylococcus aureus* increases with values of γ^{LW} increasing. Remaining bacterial number (CFU/cm^2) was positively correlated with total surface free energy, which means that the strength of adhered bacteria to the coatings increased with total surface free energy increasing. The total surface free energy negatively affect the bacterial removal rate for both two types of bacteria.

7. XDLVO theory was used and demonstrate that the Ni-P-PTFE-ZrO_2 coating, which had better capability of resisting bacterial adhesion than others, have larger total interaction energy between bacteria and Ni-P-PTFE-ZrO_2 coatings in water.

8. For anticorrosion assays, Ni-P-PTFE-ZrO_2 coatings 4, 5, 7 and 8 prepared by low and medium concentration of ZrO_2 (0.625g/L and 1.25g/L) show a better anticorrosive property. They have lower corrosion rate and corrosion current density but higher polarization resistance than Ni-P, Ni-P-PTFE than those prepared by high concentration of ZrO_2 (coatings 6 and 9) in the 0.9% and 3.5% NaCl solution.

9. Ni-P-PTFE-ZrO_2 coatings prepared by 12 ml/L of PTFE show better thermodynamically stabilility than Ni-P and Ni-P-PTFE coatings in the 3.5% NaCl solution. While in the 0.9% NaCl solution, both Ni-P-PTFE and Ni-P-PTFE-ZrO_2 coatings prepared by 8ml/L PTFE show better thermodynamically stability.

8.1.2 Ni-P-PTFE-ZrO_2-TiO_2 coatings

1. Ni-P-PTFE-ZrO_2-TiO_2 coatings show better capability of resisting bacterial adhesion and removing adhered bacteria using a dipping process than Ni-P and Ni-P-PTFE coatings

2. Ni-P-PTFE-ZrO_2-TiO_2 (8ml/L) coatings prepared by 0.625g/L and 1.875g/L ZrO_2, show better capability of resisting *E.coli* and *S. aureus* adhesion compared with those prepared by 1.25g/L ZrO_2. While Ni-P-PTFE-ZrO_2-TiO_2 (12ml/L)coatings prepared by 0.4g/L TiO_2 and different concentration of ZrO_2 including 0.625g/L 1.25g/L and 1.875g/L show better property of resisting *E.coli* and *S.aureus* adhesion than others, which means that the addition of low concentration of TiO_2 have an enormous effect on resisting bacterial adhesion

3. For assays of *E.coli* and *S. aureus* removal, Ni-P-PTFE-ZrO_2-TiO_2 (prepared by 8ml/L PTFE) coatings 10, 11 and 12 prepared by low concentration of ZrO_2 (0.625g/L) remain least number of bacteria on the surface and largest removal percentage in the bacterial removal assays. While Ni-P-PTFE-ZrO_2-TiO_2 (prepared by 12ml/L PTFE) coating P2ZrLTiL prepared by 0.625g/L ZrO_2 and 0.4g/L TiO_2 remain least bacteria on the surface and largest removal percentage in the bacterial removal assays.

4. In the assay of bacterial adhesion and removal. surface free energy of Ni-P-PTFE-ZrO_2 coatings between 20 and 30mJ/m^2 is optimal to resist bacterial adhesion. The number of remaining bacteria such as *Escherichia coli* and *staphylococcus aureus* increased with values of γ^{LW} increasing. Remaining bacterial number (CFU/cm^2) was positively correlated with total surface free energy. And the remaining bacteria on the Ni-P-PTFE-ZrO_2-TiO_2 coatings decreased with surface free energy component γ^- increasing. The total surface free energy and γ^{LW} both negatively affect the bacterial removal rate for both two types of bacteria.

5. When the performance of Ni-P-PTFE-ZrO_2-TiO_2 coatings was compared with Ni-P-PTFE-ZrO_2 coatings in the assays of bacterial adhesion, Ni-P-PTFE-ZrO_2-TiO_2 prepared by 8ml/L PTFE did not show better capability of resisting *E. coli* adhesion and reducing adhered *E. coli* using a dipping process than Ni-P-PTFE-ZrO_2 did. However, Ni-P-PTFE-ZrO_2-TiO_2 prepared by 8ml/L PTFE performed better in the assays of *S. aureus* adhesion and removal than Ni-P-PTFE-ZrO_2. While all Ni-P-PTFE-ZrO_2-TiO_2 prepared by 12ml/L PTFE have better capability of resisting bacterial adhesion and reducing adhered bacteria using a dipping process than Ni-P-PTFE-ZrO_2 did. Overall, addition of TiO_2 have significant effect on enhancing the capability of resisting bacterial adhesion and decreasing the adhesive strength between bacteria and coatings.

6. XDLVO theory was used and demonstrate that the Ni-P-PTFE-ZrO_2-TiO_2 coating, which had better capability of resisting bacterial adhesion and reducing adhered bacteria using a dipping process, has larger total interaction energy between bacteria and Ni-P-PTFE-ZrO_2-TiO_2 coatings in water.

7. Ni-P-PTFE-ZrO_2-TiO_2 coatings show lower corrosion current density (I_{corr}) and corrosion rate (CR) but higher polarization resistance (R_p) than Ni-P coatings and Ni-P-PTFE coatings in 0.9% NaCl and 3.5% NaCl solution respectively, which means coatings Ni-P-PTFE-ZrO_2-TiO_2 have better anticorrosion property in 0.9% and 3.5% NaCl solution than Ni-P and Ni-P-PTFE coatings.

8. Ni-P-PTFE-ZrO_2-TiO_2 (prepared by 8ml/L PTFE) coatings 10 to 15 prepared by 0.625 g/L and 1.25g/L ZrO_2 show a better anticorrosive property than other Ni-P-PTFE-ZrO_2-TiO_2 coatings in 0.9g/L NaCl solution, which means coatings prepared by low and medium concentration of ZrO_2 have better corrosive resistance in 0.9g/L NaCl solution. However, coating P1ZrHTiL, 17 and 18 prepare by 1.875g/L ZrO_2 show a better anticorrosive property than other Ni-P-PTFE-ZrO_2-TiO_2

coatings, which means coatings prepared by high concentration of ZrO_2 have better corrosive resistance in 3.5 g/L NaCl solution.

9. Ni-P-PTFE-ZrO_2-TiO_2 (prepared by 12ml/L PTFE) coatings 19-22 prepared by 0.625g/L ZrO_2 show a better anticorrosive property than other Ni-P-PTFE-ZrO_2-TiO_2 coatings in 0.9g/L NaCl solution. However coating P2ZrHTiL prepared by high concentration of ZrO_2 (1.875g/L) and 1.25g/L TiO_2, show a better anticorrosive property than other Ni-P-PTFE-ZrO_2-TiO_2 coatings in 3.5g/L NaCl solution, which means coatings prepared by high concentration of ZrO_2 have better corrosive resistance in 3.5 g/L NaCl solution.

10. Effect of PTFE on anticorrosive property of Ni-P-PTFE-ZrO_2-TiO_2 is significant in different solutions. Ni-P-PTFE-ZrO_2-TiO_2 coatings prepared by 8ml/L of PTFE have better anticorrosive property than those prepared by 12ml/L of PTFE in 0.9% NaCl solution. However, Ni-P-PTFE-ZrO_2-TiO_2 coatings prepared by 12ml/L of PTFE have better anticorrosive property in 3.5% NaCl solution.

11. Almost every Ni-P-PTFE-ZrO_2-TiO_2 coatings show better anticorrosive property when the coating was prepared by 0.8g/L of TiO_2 than those prepared by the same concentration of ZrO_2 and PTFE but different concentration of TiO_2 such as 0.4g/L of TiO_2 and 1.2g/L of TiO_2 in the anticorrosive assays in the 0.9% and 3.5% NaCl solution.

12. Ni-P-PTFE-ZrO_2-TiO_2 coatings show better thermodynamical stability than Ni-P and Ni-P-PTFE coatings in the 3.5% NaCl solution. While when coupons immersed in the 0.9% NaCl solutions, only two coatings 22 and 25 show higher corrosion potential than Ni-P and Ni-P-PTFE coatings.

8.2 Future Work

As demonstrated in this thesis, two types of novel Ni-P-PTFE based coatings including Ni-P-PTFE-ZrO_2 and Ni-P-PTFE-ZrO_2-TiO_2 were developed and they both show great capability of resisting bacterial adhesion under static condition. However, a lot of assays still need to be conducted to evaluate the property of these two novel coatings. In the future, firstly, we will focus on the evaluation of their capability of resisting bacterial adhesion under dynamic condition and try to find out a mathematical model or theory which could explain and accurately predict the bacterial adhesion under dynamic condition. Secondly, biocompatibility of the coating should be evaluated, which is significant property to be used as an implanted medical devices. For example, I could examine the toxicity of the coating to osteoblast or fibroblast cells, and then further test in vivo could be conducted by implanting coatings into animals such as rabbit. Thirdly, although PTFE and ZrO_2 have proved that they could improve the wear coefficient, for Ni-P-PTFE-ZrO_2 and Ni-P-PTFE-ZrO_2-TiO_2 coatings, wear resistance of the coating still need to be evaluated.

Besides, roughness of the coatings should be paid more attention. Roughness not only play a key role in bacterial adhesion, but also have a significant effect on biocompatibility. During the preparation of Ni-P-PTFE-ZrO_2 and Ni-P-PTFE-ZrO_2-TiO_2 coatings, aggregation of nanoparticle of TiO_2 and ZrO_2 have a significant effect on property of coatings especially roughness of the coating. Therefore, surface modification of nanoparticle TiO_2 and ZrO_2 and choose better surfactant also need to be investigated in the future.

9 REFERENCE

Abey, S., et al. (2011). Electrochemical behavior of dental implants (CpTi): influence of pH of artificial saliva. J Oral Implantol(November).

Abu-Lail, N. I. and T. A. Camesano (2006). The effect of solvent polarity on the molecular surface properties and adhesion of Escherichia coli. Colloids and Surfaces B: Biointerfaces **51**(1): 62-70.

Aita, H., et al. (2009). The effect of ultraviolet functionalization of titanium on integration with bone. Biomaterials **30**(6): 1015-1025.

Al-Radha, A. S., et al. (2012). Surface properties of titanium and zirconia dental implant materials and their effect on bacterial adhesion. J Dent **40**(2): 146-153.

Albers, C. E., et al. (2013). In vitro cytotoxicity of silver nanoparticles on osteoblasts and osteoclasts at antibacterial concentrations. Nanotoxicology **7**(1): 30-36.

Ali, S., et al. (1993). Mechanisms of polymer degradation in implantable devices: I. Poly (caprolactone). Biomaterials **14**(9): 648-656.

Alibakhshi, E., et al. (2013). Corrosion inhibition by lithium zinc phosphate pigment. Corrosion Science **77**: 222-229.

Alt, V., et al. (2006). The effects of combined gentamicin–hydroxyapatite coating for cementless joint prostheses on the reduction of infection rates in a rabbit infection prophylaxis model. Biomaterials **27**(26): 4627-4634.

An, Y. H. and R. J. Friedman (1998). Concise review of mechanisms of bacterial adhesion to biomaterial surfaces. Journal of biomedical materials research(43): 338-348.

Anselme, K., et al. (2010). The interaction of cells and bacteria with surfaces structured at the nanometre scale. Acta Biomater **6**(10): 3824-3846.

Aoyagi, S., et al. (2007). Novel chitosan wound dressing loaded with minocycline for the treatment of severe burn wounds. International journal of pharmaceutics **330**(1): 138-145.

Azeredo, J., et al. (1999). Exopolymers in bacterial adhesion: interpretation in terms of DLVO and XDLVO theories. Colloids and Surfaces B: Biointerfaces **14**(1): 141-148.

Bahloul, W., et al. (2012). Structural characterisation and antibacterial activity of PP/TiO2 nanocomposites prepared by an in situ sol–gel method. Materials Chemistry and Physics **134**(1): 399-406.

Bangham, D. and R. Razouk (1937). Adsorption and the wettability of solid surfaces. Transactions of the Faraday Society **33**: 1459-1463.

Barbour, M. and G. Rees (2005). The role of erosion, abrasion and attrition in tooth wear. The Journal of clinical dentistry **17**(4): 88-93.

Barthlott, W. and C. Neinhuis (1997). Purity of the sacred lotus, or escape from contamination in biological surfaces. Planta **202**(1): 1-8.

Biggs, M. J., et al. (2009). The use of nanoscale topography to modulate the dynamics of adhesion formation in primary osteoblasts and ERK/MAPK signalling in STRO-1+ enriched skeletal stem cells. Biomaterials **30**(28): 5094-5103.

Blättler, T., et al. (2006). Nanopatterns with biological functions. Journal of nanoscience and nanotechnology **6**(8): 2237-2264.

Blaiszik, B., et al. (2010). Self-healing polymers and composites. Annual Review of Materials Research **40**: 179-211.

Bos, R., et al. (1999). Physico-chemistry of initial microbial adhesive interactions–its mechanisms and methods for study. FEMS microbiology reviews **23**(2): 179-230.

Braydich-Stolle, L., et al. (2005). In vitro cytotoxicity of nanoparticles in mammalian germline stem cells. Toxicological sciences **88**(2): 412-419.

Brenner, A. and G. E. Riddell (1946). Nickel plating on steel by chemical reduction. J. Res. NBS **37**(1): 31-34.

Bruinsma, G., et al. (2001). Bacterial adhesion to surface hydrophilic and hydrophobic contact lenses. Biomaterials **22**(24): 3217-3224.

Buchholz, H. and H. Engelbrecht (1970). Über die Depotwirkung einiger Antibiotika bei Vermischung mit dem kunstharz Palacos. Chirurg **41**(11): 511-515.

Buczynski, B. W., et al. (2003). Bacterial adhesion to zirconium surfaces. Colloids and Surfaces B: Biointerfaces **30**(1-2): 167-175.

Campoccia, D., et al. (2006). The significance of infection related to orthopedic devices and issues of antibiotic resistance. Biomaterials **27**(11): 2331-2339.

Campoccia, D., et al. (2013). A review of the biomaterials technologies for infection-resistant surfaces. Biomaterials **34**(34): 8533-8554.

Campoccia, D., et al. (2013). A review of the clinical implications of anti-infective biomaterials and infection-resistant surfaces. Biomaterials **34**(33): 8018-8029.

Campoccia, D., et al. (2010). Antibiotic-loaded biomaterials and the risks for the spread of antibiotic resistance following their prophylactic and therapeutic clinical use. Biomaterials **31**(25): 6363-6377.

Castellano, J. J., et al. (2007). Comparative evaluation of silver‐containing antimicrobial dressings and drugs. International Wound Journal **4**(2): 114-122.

Chai, F., et al. (2007). Antibacterial activation of hydroxyapatite (HA) with controlled porosity by different antibiotics. Biomolecular engineering **24**(5): 510-514.

Chaiban, G., et al. (2005). A rapid method of impregnating endotracheal tubes and urinary catheters with gendine: a novel antiseptic agent. J Antimicrob Chemother **55**(1): 51-56.

Charville, G. W., et al. (2008). Reduced bacterial adhesion to fibrinogen-coated substrates via nitric oxide release. Biomaterials **29**(30): 4039-4044.

Chaudhury, M. K. (1996). Interfacial interaction between low-energy surfaces. Materials Science and Engineering: R: Reports **16**(3): 97-159.

Chen, W., et al. (2006). In vitro anti-bacterial and biological properties of magnetron co-sputtered silver-containing hydroxyapatite coating. Biomaterials **27**(32): 5512-5517.

Chen, Y.-M., et al. (2014). Effectiveness of silver-impregnated central venous catheters for preventing catheter-related blood stream infections: a meta-analysis. International Journal of Infectious Diseases **29**: 279-286.

Chevalier, J., et al. (2004). Critical effect of cubic phase on aging in 3mol% yttria-stabilized zirconia ceramics for hip replacement prosthesis. Biomaterials **25**(24): 5539-5545.

Choi, H. W., et al. (2008). Effects of plastic strain of diamond-like carbon coated stainless steel on the corrosion behavior in simulated body fluid environment. Surface and Coatings Technology **202**(12): 2632-2637.

Cucarella, C., et al. (2001). Bap, a Staphylococcus aureus surface protein involved in biofilm formation. J Bacteriol **183**(9): 2888-2896.

Cui, C. X., et al. (2012). Microstructure and antibacterial property of in situ TiO(2) nanotube layers/titanium biocomposites. J Mech Behav Biomed Mater **8**: 178-183.

Daghighi, S., et al. (2013). Infection resistance of degradable versus non-degradable biomaterials: an assessment of the potential mechanisms. Biomaterials **34**(33): 8013-8017.

Dalby, M., et al. (2004). Cell response to nano-islands produced by polymer demixing: a brief review. IEE Proceedings-Nanobiotechnology, IET.

Davalos-Pantoja, L., et al. (2000). A comparative study between the adsorption of IgY and IgG on latex particles. Journal of Biomaterials Science, Polymer Edition **11**(6): 657-673.

Davies, D. G. (2000). Physiological events in biofilm formation. SYMPOSIA-SOCIETY FOR GENERAL MICROBIOLOGY, Cambridge; Cambridge University Press; 1999.

de Leon, A. and R. C. Advincula (2015). Conducting Polymers with Superhydrophobic Effects as Anticorrosion Coating. 409-430.

Dearnaley, G. and J. H. Arps (2005). Biomedical applications of diamond-like carbon (DLC) coatings: A review. Surface and Coatings Technology **200**(7): 2518-2524.

Depprich, R., et al. (2008). Osseointegration of zirconia implants compared with titanium: an in vivo study. Head Face Med **4**: 30.

Domenech, S., et al. (2003). Electroless plating of nickel–phosphorous on surface-modified poly (ethylene terephthalate) films. Applied Surface Science **220**(1): 238-250.

Dong, D., et al. (2009). Preparation and properties of electroless Ni–P–SiO 2 composite coatings. Applied Surface Science **255**(15): 7051-7055.

Duan, K., et al. (2005). Electrolytic deposition of calcium etidronate drug coating on titanium substrate. Journal of Biomedical Materials Research Part B: Applied Biomaterials **72**(1): 43-51.

Elek, S. D. and P. Conen (1957). The virulence of Staphylococcus pyogenes for man. A study of the problems of wound infection. British journal of experimental pathology **38**(6): 573.

Fadlallah, S. A., et al. (2014). An overview of NiTi shape memory alloy: Corrosion resistance and antibacterial inhibition for dental application. Journal of Alloys and Compounds **583**: 455-464.

Fowkes, F., et al. (1980). Contact angles and the equilibrium spreading pressures of liquids on hydrophobic solids. J Colloid Interface Sci **78**(1): 200-206.

Fowkes, F. M. (1962). Determination of interfacial tensions, contact angles, and dispersion forces in surfaces by assuming additivity of intermolecular interactions in surfaces. The Journal of Physical Chemistry **66**(2): 382-382.

Fowkes, F. M. (1964). Attractive forces at interfaces. Industrial & Engineering Chemistry **56**(12): 40-52.
Gao, J., et al. (2009). Mimicking biological structured surfaces by phase-separation micromolding. Langmuir **25**(8): 4365-4369.

Gao, R., et al. (2007). Study of the corrosion resistance of electroless Ni-P deposits in a sodium chloride medium. Journal of Ocean University of China **6**(4): 349-354.

GAO, W., et al. (2012). High temperature oxidation protection using nanocrystalline coatings. Corrosion Protection and Control Using Nanomaterials: 146.

Garrett, T. R., et al. (2008). Bacterial adhesion and biofilms on surfaces. Progress in Natural Science **18**(9): 1049-1056.

Giamarellos-Bourboulis, E. J. (2000). Carrier systems for the local delivery of antibiotics in bone infections. Drugs **59**(6): 1223-1232.

Girifalco, L. and R. Good (1957). A theory for the estimation of surface and interfacial energies. I. Derivation and application to interfacial tension. The Journal of Physical Chemistry **61**(7): 904-909.
Good, R. J. (1992). Contact angle, wetting, and adhesion: a critical review. Journal of adhesion science and technology **6**(12): 1269-1302.

Grari, O., et al. (2015). Effects of high frequency ultrasound irradiation on incorporation of SiO2 particles within polypyrrole films. Ultrason Sonochem **22**: 220-226.

Gu, J., et al. (2012). Preparation and thermal properties of Poly(2,3-dimethylaniline)/ZrO2 composite. Thermochimica Acta **549**: 13-16.

Guzman, M., et al. (2012). Synthesis and antibacterial activity of silver nanoparticles against gram-positive and gram-negative bacteria. Nanomedicine **8**(1): 37-45.

Hajipour, M. J., et al. (2012). Antibacterial properties of nanoparticles. Trends Biotechnol **30**(10): 499-511.

Hajipour, M. J., et al. (2012). Antibacterial properties of nanoparticles. Trends Biotechnol **30**(10): 499-511.

Hall-Stoodley, L. and P. Stoodley (2002). Developmental regulation of microbial biofilms. Current Opinion in Biotechnology **13**(3): 228-233.

Harris, L., et al. (2002). An introduction to Staphylococcus aureus, and techniques for identifying and quantifying S. aureus adhesins in relation to adhesion to biomaterials: review. Eur Cell Mater **4**(3).

Harris, L. G. and R. G. Richards (2006). Staphylococci and implant surfaces: a review. Injury **37 Suppl 2**: S3-14.

Harvey, J. N., et al. (1999). Oxidation properties of the early transition-metal dioxide cations MO 2+(M= Ti, V, Zr, Nb) in the gas-phase. International journal of mass spectrometry **182**: 85-97.

Hasan, J., et al. (2013). Antibacterial surfaces: the quest for a new generation of biomaterials. Trends Biotechnol **31**(5): 295-304.

Hauert, R. (2003). A review of modified DLC coatings for biological applications. Diamond and Related Materials **12**(3): 583-589.

Hench, L. L. (1991). Bioceramics: from concept to clinic. Journal of the American Ceramic Society **74**(7): 1487-1510.

Hermansson, M. (1999). The DLVO theory in microbial adhesion. Colloids and Surfaces B: Biointerfaces **14**(1): 105-119.

Hofacker, S., et al. (2002). Sol–gel: a new tool for coatings chemistry. Progress in Organic Coatings **45**(2): 159-164.

Hori, K. and S. Matsumoto (2010). Bacterial adhesion: From mechanism to control. Biochemical Engineering Journal **48**(3): 424-434.

Hou, L., et al. (2014). In vitro and in vivo studies on biodegradable magnesium alloy. Progress in Natural Science: Materials International **24**(5): 466-471.

Hu, H., et al. (2012). Antibacterial activity and increased bone marrow stem cell functions of Zn-incorporated TiO2 coatings on titanium. Acta Biomater **8**(2): 904-915.

Huang, H., et al. (2008). Protein-mediated assembly of nanodiamond hydrogels into a biocompatible and biofunctional multilayer nanofilm. ACS nano **2**(2): 203-212.

Huber, M., et al. (2009). Presence of corrosion products and hypersensitivity-associated reactions in periprosthetic tissue after aseptic loosening of total hip replacements with metal bearing surfaces. Acta Biomater **5**(1): 172-180.

Ingham, E. and J. Fisher (2000). Biological reactions to wear debris in total joint replacement. Proceedings of the Institution of Mechanical Engineers, Part H: Journal of Engineering in Medicine **214**(1): 21-37.

Ionita, D., et al. (2011). Modifying the TiAlZr biomaterial surface with coating, for a better anticorrosive and antibacterial performance. Applied Surface Science **257**(21): 9164-9168.

Ivanova, E. P., et al. (2012). Natural bactericidal surfaces: mechanical rupture of Pseudomonas aeruginosa cells by cicada wings. Small **8**(16): 2489-2494.

Jelinek, M., et al. (2015). Chromium-doped DLC for implants prepared by laser-magnetron deposition. Materials Science and Engineering: C **46**: 381-386.

Jum'ah, A. A., et al. (2012). Zirconia Implants The New Arrival in the Armoury of Successful Aesthetic Implant Dentistry. Smile Dent J **7**(2): 02-16.

Katsikogianni, M. and Y. Missirlis (2004). Concise review of mechanisms of bacterial adhesion to biomaterials and of techniques used in estimating bacteria-material interactions. Eur Cell Mater **8**(3).

Kawahara, K., et al. (2000). Antibacterial effect of silver-zeolite on oral bacteria under anaerobic conditions. Dental materials **16**(6): 452-455.

Kelley, S. C. and D. F. Untereker (2013). Evaluating the corrosion performance of metal medical device welds. 178-210.

Kim, J. S., et al. (2007). Antimicrobial effects of silver nanoparticles. Nanomedicine: Nanotechnology, Biology and Medicine **3**(1): 95-101.

Komaromy, A. Z., et al. (2012). Arrays of nano-structured surfaces to probe the adhesion and viability of bacteria. Microelectronic Engineering **91**: 39-43.

Kreuer, K. (2003). Proton-conducting oxides. Annual Review of Materials Research **33**(1): 333-359.
Lam, R., et al. (2008). Nanodiamond-embedded microfilm devices for localized chemotherapeutic elution. ACS nano **2**(10): 2095-2102.

Lara, H. H., et al. (2011). Silver nanoparticles are broad-spectrum bactericidal and virucidal compounds. J Nanobiotechnology **9**: 30.

Li, Z., et al. (2013). Synthesis and anticorrosion performance of poly (2, 3-dimethylaniline)–TiO 2 Composite. Progress in Organic Coatings **76**(9): 1161-1167.

Liu, C. and Q. Zhao (2011). Influence of surface-energy components of Ni–P–TiO2–PTFE nanocomposite coatings on bacterial adhesion. Langmuir **27**(15): 9512-9519.

Liu, J., et al. (2015). Graphene dip coatings: An effective anticorrosion barrier on aluminum. Applied Surface Science **327**: 241-245.

Liu, K. and L. Jiang (2011). Bio-inspired design of multiscale structures for function integration. Nano Today **6**(2): 155-175.

Liu, X., et al. (2004). Surface modification of titanium, titanium alloys, and related materials for biomedical applications. Materials Science and Engineering: R: Reports **47**(3): 49-121.

Liu, Y. and G. Li (2012). A new method for producing "Lotus Effect" on a biomimetic shark skin. J Colloid Interface Sci **388**(1): 235-242.

Liu, Y. and Q. Zhao (2005). Influence of surface energy of modified surfaces on bacterial adhesion. Biophysical chemistry **117**(1): 39-45.

Ma, J., et al. (2011). Nanostructure on taro leaves resists fouling by colloids and bacteria under submerged conditions. Langmuir **27**(16): 10035-10040.

Mack, D., et al. (2004). Mechanisms of biofilm formation in Staphylococcus epidermidis and Staphylococcus aureus: functional molecules, regulatory circuits, and adaptive responses. Int J Med Microbiol **294**(2-3): 203-212.

Mallory, G. (1974). Influence of the Electroless Plating Bath on the Corro-sion Resistance of the Deposits. Plating **61**(11): 1005-1014.

Marciano, F. R., et al. (2009). Antibacterial activity of DLC films containing TiO 2 nanoparticles. J Colloid Interface Sci **340**(1): 87-92.

Marshall, K. (1986). Adsorption and adhesion processes in microbial growth at interfaces. Adv Colloid Interface Sci **25**: 59-86.

Martins, V. C., et al. (1998). The controlled release of antibiotic by hydroxyapatite: anionic collagen composites. Artificial organs **22**(3): 215-221.

Masse, A., et al. (2000). Prevention of pin track infection in external fixation with silver coated pins: clinical and microbiological results. Journal of biomedical materials research **53**(5): 600-604.

Mathew, M. T., et al. (2012). Influence of pH on the tribocorrosion behavior of CpTi in the oral environment: synergistic interactions of wear and corrosion. J Biomed Mater Res B Appl Biomater **100**(6): 1662-1671.

Mathew, M. T., et al. (2014). Tribocorrosion and oral and maxillofacial surgical devices. Br J Oral Maxillofac Surg **52**(5): 396-400.

Mercuri, L. G. (2007). A rationale for total alloplastic temporomandibular joint reconstruction in the management of idiopathic/progressive condylar resorption. Journal of oral and maxillofacial surgery **65**(8): 1600-1609.

Meslemani, D. and R. M. Kellman (2012). Recent advances in fixation of the craniomaxillofacial skeleton. Current opinion in otolaryngology & head and neck surgery **20**(4): 304-309.

Mills, A. and S. Le Hunte (1997). An overview of semiconductor photocatalysis. Journal of photochemistry and photobiology A: Chemistry **108**(1): 1-35.

Monds, R. D. and G. A. O'Toole (2009). The developmental model of microbial biofilms: ten years of a paradigm up for review. Trends Microbiol **17**(2): 73-87.

Montanaro, L., et al. (2011). Scenery of Staphylococcus implant infections in orthopedics. Future Microbiology **6**(11): 1329-1349.

Muñoz, M. C., et al. (2006). Adhesion at metal–ZrO2 interfaces. Surface Science Reports **61**(7): 303-344.

Nishino, J. and Y. Kanno (2008). An influence of concentration of polyvinylpyrrolidone on the morphology of silver metal formed from AgNO 3 aqueous solution. Journal of Nanomaterials **2008**: 2.

Oliveira, R. (1997). Understanding adhesion: a means for preventing fouling. Experimental Thermal and Fluid Science **14**(4): 316-322.

Palmer, J., et al. (2007). Bacterial cell attachment, the beginning of a biofilm. J Ind Microbiol Biotechnol **34**(9): 577-588.

Peng, L., et al. (2009). Long-term small molecule and protein elution from TiO2 nanotubes. Nano letters **9**(5): 1932-1936.

Percival, S. L., et al. (2011). Introduction to biofilms. Biofilms and Veterinary Medicine, Springer**:** 41-68.

Pezzotti, G. and K. Yamamoto (2014). Artificial hip joints: The biomaterials challenge. J Mech Behav Biomed Mater **31**: 3-20.

Piconi, C., et al. (2003). Alumina and zirconia ceramics in joint replacements. Journal of Applied Biomaterials & Biomechanics **1**(1): 19-32.

Prabu, P., et al. (2006). Preparation and drug release activity of scaffolds containing collagen and poly (caprolactone). Journal of Biomedical Materials Research Part A **79**(1): 153-158.

Puckett, S. D., et al. (2010). The relationship between the nanostructure of titanium surfaces and bacterial attachment. Biomaterials **31**(4): 706-713.

Ragaseema, V. M., et al. (2012). The antithrombotic and antimicrobial properties of PEG-protected silver nanoparticle coated surfaces. Biomaterials **33**(11): 3083-3092.

Rai, M., et al. (2009). Silver nanoparticles as a new generation of antimicrobials. Biotechnol Adv **27**(1): 76-83.

Raspe, R. E., et al. (1954). (Baron Munchausen's Narrative of His Marvellous Travels and Campaigns in Russia), De Roos.

Ratner, B. D., et al. (2004). Biomaterials science: a multidisciplinary endeavor. Biomaterials science: an introduction to materials in medicine: 1-9.

Reclaru, L., et al. (2014). New generation super alloy candidates for medical applications: corrosion behavior, cation release and biological evaluation. Mater Sci Eng C Mater Biol Appl **45**: 411-420.

Riedel, R. and I.-W. Chen (2011). Ceramics Science and Technology, Materials and Properties, John Wiley & Sons.

Rocha, L. A., et al. (2013). Bio-tribocorrosion in dental applications. 223-249.

Rojas, I. A., et al. (2000). Polyurethane coatings release bioactive antibodies to reduce bacterial adhesion. Journal of controlled release **63**(1): 175-189.

Rosenthal, V. D., et al. (2014). International Nosocomial Infection Control Consortiu (INICC) report, data summary of 43 countries for 2007-2012. Device-associated module. American journal of infection control **42**(9): 942-956.

Rossi, S., et al. (2007). Wound dressings based on chitosans and hyaluronic acid for the release of chlorhexidine diacetate in skin ulcer therapy. Pharmaceutical development and technology **12**(4): 415-422.

RYU, J. and P. SHROTRIYA (2013). Synergistic mechanisms of bio-tribocorrosion in medical implants. Bio-Tribocorrosion in Biomaterials and Medical Implants: 25.

Ryu, J. J. and P. Shrotriya (2013). Synergistic mechanisms of bio-tribocorrosion in medical implants. 25-44.

Sørensen, P. A., et al. (2009). Anticorrosive coatings: a review. Journal of Coatings Technology and Research **6**(2): 135-176.

Sahoo, P. and S. K. Das (2011). Tribology of electroless nickel coatings – A review. Materials & Design **32**(4): 1760-1775.

Sargeant, A. and T. Goswami (2006). Hip implants: Paper V. Physiological effects. Materials & Design **27**(4): 287-307.

Sargeant, A. and T. Goswami (2007). Hip implants – Paper VI – Ion concentrations. Materials & Design **28**(1): 155-171.

Scarano, A., et al. (2004). Bacterial adhesion on commercially pure titanium and zirconium oxide disks: an in vivo human study. Journal of Periodontology **75**(2): 292-296.

Schaefer, K. and A. Miszczyk (2013). Improvement of electrochemical action of zinc-rich paints by addition of nanoparticulate zinc. Corrosion Science **66**: 380-391.

Schalamon, J., et al. (2007). Pin tract infection with external fixation of pediatric fractures. J Pediatr Surg **42**(9): 1584-1587.

Schwarz, F. P., et al. (2011). Antibacterial properties of silver containing diamond like carbon coatings produced by ion induced polymer densification. Surface and Coatings Technology **205**(20): 4850-4854.

Seok, S. I., et al. (2006). Preparation of corrosion protective coatings on galvanized iron from aqueous inorganic–organic hybrid sols by sol–gel method. Surface and Coatings Technology **200**(11): 3468-3472.

Shanmugasundaram, N., et al. (2006). Design and delivery of silver sulfadiazine from alginate microspheres‐impregnated collagen scaffold. Journal of Biomedical Materials Research Part B: Applied Biomaterials **77**(2): 378-388.

Shao, W. and Q. Zhao (2010). Effect of corrosion rate and surface energy of silver coatings on bacterial adhesion. Colloids Surf B Biointerfaces **76**(1): 98-103.

Shao, W. and Q. Zhao (2010). Influence of reducers on nanostructure and surface energy of silver coatings and bacterial adhesion. Surface and Coatings Technology **204**(8): 1288-1294.

Shipilov, S. A. and I. Le May (2006). Structural integrity of aging buried pipelines having cathodic protection. Engineering Failure Analysis **13**(7): 1159-1176.

Silverman, L. M. (1949). An investigation of gelatin sponge with thrombin and penicillin in the treatment of oral surgical wounds. Oral Surgery, Oral Medicine, Oral Pathology **2**(2): 260-288.

Simões, M., et al. (2010). A review of current and emergent biofilm control strategies. LWT - Food Science and Technology **43**(4): 573-583.

Simchi, A., et al. (2011). Recent progress in inorganic and composite coatings with bactericidal capability for orthopaedic applications. Nanomedicine **7**(1): 22-39.

Sims, J. M. (1869). Ovariotomy: pedicle secured by silver-wire ligatures: cure. British medical journal **1**(432): 326.

Sims, M. and M. Saleh (2000). External fixation–the incidence of pin site infection: a prospective audit. Journal of Orthopaedic Nursing **4**(2): 59-63.

Sonawane, S. H., et al. (2012). Improved active anticorrosion coatings using layer-by-layer assembled ZnO nanocontainers with benzotriazole. Chemical Engineering Journal **189-190**: 464-472.

Song, J., et al. (2011). Bacterial adhesion inhibition of the quaternary ammonium functionalized silica nanoparticles. Colloids and Surfaces B: Biointerfaces **82**(2): 651-656.

Srinivasan, K., et al. (2010). Studies on development of electroless Ni–B bath for corrosion resistance and wear resistance applications. Surface Engineering **26**(3): 153-158.

Stigter, M., et al. (2004). Incorporation of different antibiotics into carbonated hydroxyapatite coatings on titanium implants, release and antibiotic efficacy. Journal of controlled release **99**(1): 127-137.

Su, X., et al. (2010). Modification of diamond-like carbon coatings with fluorine to reduce biofouling adhesion. Surface and Coatings Technology **204**(15): 2454-2458.

Sudagar, J., et al. (2013). Electroless nickel, alloy, composite and nano coatings – A critical review. Journal of Alloys and Compounds **571**: 183-204.

Teupe, C., et al. (1992). Ciprofloxacin-impregnated poly-L-lactic acid drug carrier. Archives of orthopaedic and trauma surgery **112**(1): 33-35.

Thomsen, P., et al. (1997). Structure of the interface between rabbit cortical bone and implants of gold, zirconium and titanium. Journal of Materials Science: Materials in Medicine **8**(11): 653-665.

Treccani, L., et al. (2013). Functionalized ceramics for biomedical, biotechnological and environmental applications. Acta Biomater **9**(7): 7115-7150.

Tsuneda, S., et al. (2004). Significance of cell electrokinetic properties determined by soft-particle analysis in bacterial adhesion onto a solid surface. J Colloid Interface Sci **279**(2): 410-417.

Ubbink, J. and P. Schär-Zammaretti (2007). Colloidal properties and specific interactions of bacterial surfaces. Current Opinion in Colloid & Interface Science **12**(4): 263-270.

Urban, R. M., et al. (2000). Dissemination of Wear Particles to the Liver, Spleen, and Abdominal Lymph Nodes of Patients with Hip or Knee Replacement*. The Journal of Bone & Joint Surgery **82**(4): 457-457.

Valero Vidal, C. and A. Igual Muñoz (2013). Influence of protein adsorption on corrosion of biomedical alloys. 187-219.

Van Oss, C. (1993). Acid—base interfacial interactions in aqueous media. Colloids and Surfaces A: Physicochemical and Engineering Aspects **78**: 1-49.

Van Oss, C. (2005). Interfacial Forces in Aqueous Media. 1994. New York: Marcel Decker Inc.

Van Oss, C., et al. (1987). The mechanism of partition in aqueous media. Separation Science and Technology **22**(6): 1515-1526.

Van Oss, C., et al. (1986). The role of van der Waals forces and hydrogen bonds in “hydrophobic interactions” between biopolymers and low energy surfaces. J Colloid Interface Sci **111**(2): 378-390.

Van Oss, C. J. (2006). Interfacial forces in aqueous media, CRC press.

Van Oss, C. J., et al. (1988). Interfacial Lifshitz-van der Waals and polar interactions in macroscopic systems. Chemical Reviews **88**(6): 927-941.

Veenstra, G., et al. (1996). Ultrastructural organization and regulation of a biomaterial adhesin of Staphylococcus epidermidis. Journal of Bacteriology **178**(2): 537-541.

Veselý, D. and A. Kalendova (2008). Anticorrosion efficiency of ZnxMgyAl2O4 core–shell spinels in organic coatings. Progress in Organic Coatings **62**(1): 5-20.

von Eiff, C., et al. (2005). Infections associated with medical devices. Drugs **65**(2): 179-214
.
Walker, J. and P. Marsh (2004). A review of biofilms and their role in microbial contamination of dental unit water systems (DUWS). International biodeterioration & biodegradation **54**(2): 87-98.

Wang, H., et al. (2011). Initial bacterial attachment in slow flowing systems: effects of cell and substrate surface properties. Colloids and Surfaces B: Biointerfaces **87**(2): 415-422.

Wang, W. C., et al. (2004). Nanoporous Ultra - Low - κ Films Prepared from Fluorinated Polyimide with Grafted Poly (acrylic acid) Side Chains. Advanced Materials **16**(1): 54-57.

Wen, G., et al. (2006). Effect of spreading solvents on Langmuir monolayers and Langmuir–Blodgett films of PS-b-P2VP. Polymer **47**(26): 8575-8582.

Wen, H.-C., et al. (2007). Observation of growth of human fibroblasts on silver nanoparticles. Journal of Physics: Conference Series, IOP Publishing.

Wu, J. J., et al. (2012). The synthesis of nano-silver/polypropylene plastics for antibacterial application. Current Applied Physics **12**: S89-S95.

Wu, P. and D. W. Grainger (2006). Drug/device combinations for local drug therapies and infection prophylaxis. Biomaterials **27**(11): 2450-2467.

Wu, R., et al. (2015). Recent progress in synthesis, properties and potential applications of SiC nanomaterials. Progress in Materials Science **72**: 1-60.

Wu, Y., et al. (2011). Differential response of Staphylococci and osteoblasts to varying titanium surface roughness. Biomaterials **32**(4): 951-960.

Xu, L.-C. and C. A. Siedlecki (2012). Submicron-textured biomaterial surface reduces staphylococcal bacterial adhesion and biofilm formation. Acta Biomater **8**(1): 72-81.

Xu, Q., et al. (2007). Encapsulation and release of a hydrophobic drug from hydroxyapatite coated liposomes. Biomaterials **28**(16): 2687-2694.

Yan, Y., et al. (2010). Electrochemical instrumentation of a hip simulator: a new tool for assessing the role of corrosion in metal-on-metal hip joints. Proceedings of the Institution of Mechanical Engineers, Part H: Journal of Engineering in Medicine **224**(11): 1267-1273.

Young, T. (1805). An essay on the cohesion of fluids. Philosophical Transactions of the Royal Society of London: 65-87.

Zhao, L., et al. (2010). The influence of hierarchical hybrid micro/nano-textured titanium surface with titania nanotubes on osteoblast functions. Biomaterials **31**(19): 5072-5082.

Zhao, L., et al. (2011). Antibacterial nano-structured titania coating incorporated with silver nanoparticles. Biomaterials **32**(24): 5706-5716.

Zhao, Q. (2004). Effect of surface free energy of graded NI–P–PTFE coatings on bacterial adhesion. Surface and Coatings Technology **185**(2): 199-204.

Zhao, Q. and Y. Liu (2005). Electroless Ni–Cu–P–PTFE composite coatings and their anticorrosion properties. Surface and Coatings Technology **200**(7): 2510-2514.

Zhao, Q., et al. (2002). Graded Ni–P–PTFE coatings and their potential applications. Surface and Coatings Technology **155**(2): 279-284.

Zhao, Q., et al. (2005). Development and evaluation of electroless Ag-PTFE composite coatings with anti-microbial and anti-corrosion properties. Applied Surface Science **252**(5): 1620-1627.

Zhao, Q., et al. (2007). Evaluation of bacterial adhesion on Si-doped diamond-like carbon films. Applied Surface Science **253**(17): 7254-7259.

Zhao, Q., et al. (2008). Reduction of bacterial adhesion on ion-implanted stainless steel surfaces. Medical engineering & physics **30**(3): 341-349.

Zilberman, M. and J. J. Elsner (2008). Antibiotic-eluting medical devices for various applications. J Control Release **130**(3): 202-215.